BEYOND WATER DEPTH: THE ENVIRONMENTAL CONTROLS ON MARINE BENTHIC INVERTEBRATE ASSEMBLAGES IN THE MODERN AND FOSSIL RECORD

by

GARETT MATTINGLY BROWN

(Under the Direction of Steven M. Holland)

ABSTRACT

Water depth is the most common environmental gradient correlated with community composition of marine benthic invertebrates in the modern and fossil record. It is a complex gradient comprising of other environmental gradients such as temperature, substrate, water pressure, shear stress, salinity, light penetration, nutrients, and oxygen. However, the frequency of each covarying gradient is currently unknown for the fossil record, as well as the frequencies of gradients not correlated with water depth. This dissertation conducts an extensive literature review of modern and ancient studies and fieldwork in modern and ancient carbonate environments to accomplish two goals. First, it quantifies the frequency of environmental gradients identified in ancient settings and compares those frequencies and amounts of explained variance to gradients in the modern. Second, it combines detailed faunal and lithological data in the modern and ancient to test for gradients that covary with water depth as well as any additional gradients not correlated with water depth. The literature review focuses on studies that use multivariate ordinations to interpret environmental gradients in benthic invertebrate

assemblages and compares frequencies among ordination axes to interpret each gradient's relative impact on assemblage variation in the modern and ancient. The modern study tests for environmental gradients controlling the molluscan death assemblage of the shallow subtidal of San Salvador Island, The Bahamas. Sampling is restricted to a 4.2 m depth range and vegetation density, grainsize distribution, and physical and chemical oceanographic data were collected for each assemblage. The ancient study tests for environmental gradients controlling the Mississippian benthic invertebrate assemblage of the lower Madison Group in Montana. Sampling collected lithological specimens in conjunction with faunal counts, providing quantitative lithologic data for every sample. The results of this dissertation underline the predominance of the water-depth gradient, but it also identifies substrate and wave energy as the covarying gradients that commonly impact assemblage compositions. Additionally, it demonstrates that substrate gradients that are not correlated with water depth are equally important to assemblage variation. Furthermore, it emphasizes how closely spaced, replicate sampling of lithological data in conjunction with faunal data can highlight sources of environmental variation controlling fossil community compositions.

INDEX WORDS: Gradient analysis, multivariate ordinations, carbonate ramps, benthic invertebrates, Mississippian

BEYOND WATER DEPTH: THE ENVIRONMENTAL CONTROLS ON MARINE BENTHIC INVERTEBRATE ASSEMBLAGES IN THE MODERN AND FOSSIL RECORD

by

GARETT MATTINGLY BROWN

B.S., The University of South Florida, 2014

M.S., The Pennsylvania State University, 2016

A Dissertation Submitted to the Graduate Faculty of The University of Georgia in Partial Fulfillment of the Requirements for the Degree

DOCTOR OF PHILOSOPHY

ATHENS, GEORGIA

2020

BEYOND WATER DEPTH: THE ENVIRONMENTAL CONTROLS ON MARINE BENTHIC INVERTEBRATE ASSEMBLAGES IN THE MODERN AND FOSSIL RECORD

by

GARETT MATTINGLY BROWN

Major Professor:	Steven M. Holland
Committee:	Susan T. Goldstein
	James E. Byers
	Michal Kowalewski
	Mark E. Patzkowsky

Electronic Version Approved:

Ron Walcott
Interim Dean of the Graduate School
The University of Georgia
May 2020

DEDICATION

To my wife, Jessica, who provided unlimited love and support while I accomplished my dream.

ACKNOWLEDGEMENTS

First and foremost, I want to thank my advisor Dr. Steven Holland for his endless guidance, advice, and support. Steve had me design my own dissertation project, without any restrictions as to questions or study area. From this experience, I learned how to properly conduct paleobiological studies from the ground up and gained a greater appreciation on effective mentoring methods. These past four years have been full of growing pains, but thanks to Steve's patience, constructive criticism, and sound advice, I have become a better researcher, writer, and person. I will carry the lessons I learned from Steve everywhere I go and remember them when it is my turn to advise students of my own.

I also want to thank my committee members Dr. Susan Goldstein and Dr. James Byers at the University of Georgia, Dr. Michal Kowalewski at the Florida Museum of Natural History, and Dr. Mark Patzkowsky at the Pennsylvania State University. Sue constantly kept my project focused at all times by reminding me that I need to be very careful in my word choice while being explicit when writing or presenting. Without our many conversations, my communication skills would be nowhere near where they are today. Jeb brought a much-needed modern viewpoint to this project that taught me how to better frame my work for a wider audience. From Jeb, I learned how to take a moment, collect my thoughts, and imagine the viewpoint of my audience before I begin speaking. This has not only helped when presenting my research at conferences, but it has also improved my lecturing skills in the classroom. Michal was indispensable in fine-tuning

my research on San Salvador Island during the Taphonomic and Ecological Processes in Tropical Environments field course, yet I am most thankful for his candor and kindness as we discussed my future career goals. These discussions helped me to understand more what I want after my degree, how I want my family to be just as important as academia, and how best to pursue my future goals, and for that I am extremely grateful. Mark's familiarity with the Lodgepole Formation and stratigraphic paleobiology in general was crucial in interpreting my stratigraphic data and contextualizing the faunal patterns I observed.

I would like to thank my co-author Ekaterina Larina for the hard work she put in while we worked on San Salvador Island. When I severely injured my right ankle and could not walk for a week, she pulled double duty and collected not only the samples for our paper, but for her other project as well. I would also like to thank the rest of the participants of the 2017 Taphonomic and Ecological Processes in Tropical Environments field course who also helped in data collection, as well as Dr. Troy Dexter and the staff of the Gerace Research Centre for their assistance with site access and logistical support while on San Salvador Island.

I greatly appreciate Trez Rice and Joshua Slattery for their field assistance in Montana. Trez brought an infectious level of optimism and eagerness that helped to make the long days bearable, especially as I struggled with running my first independent field season. Josh helped me out of a tight corner and volunteered to be my field partner last minute when it seemed like everyone would have been unavailable. I would also like to thank Dr. Bruce Douglas, Mark Toensing, and the rest of the faculty and staff at the Indiana University Judson Mead Geological Field Station for food, housing, logistical

support and assistance with accessing field sites on private lands. I would also like to thank David Bobbit from the Forest Service for the assistance in getting the collecting permits for my samples in Montana.

I also thank the multiple funding sources that facilitated this dissertation: The Gilles and Bernadette Allard Geology Award and Mirriam Watts-Wheeler Fund from the Department of Geology at UGA, the Wyoming Geological Association, the Gulf Coast Association of Geological Societies, the Tobacco Roots Geological Society, the Geological Society of America Student Research Grant, and the Charles J. Vitaliano Grant-In-Aid from the Indiana University Judson Mead Geological Field Station.

This dissertation would not have been possible without the friends I made at UGA. Chris Smith, Kelly Cronin, Kelsey Warden, and Pedro Monarrez all provided endless support—from lending an ear on a rough day to providing advice on navigating a PhD or job searches. Pedro deserves more gratitude and credit than I can put into words. As the senior lab member, he became my second mentor here at UGA and a sounding board for all my ideas before I began implementing anything. Most importantly he became one of my greatest supporters during a time when I felt all alone. Bonding over fossils, Pokémon, and tacos, I met one of my greatest friends in Pedro.

Finally, I would like to thank my entire family who have cheered me on from the sidelines and seeing me through to the finish line. Their words of encouragement and understanding over these last four years helped most when it seemed overwhelming. Last but not least, I want to thank my wife Jessica for joining me on this grand adventure and having faith that our love for each other would carry us through as we journey together into the unknown.

TABLE OF CONTENTS

Page

LIST OF TABLES

Page

LIST OF FIGURES

Page

CHAPTER 1

INTRODUCTION

Marine Environmental Gradients

The Gleasonian model of ecology argues that species distributions and community structure are primarily controlled by environmental gradients (Gleason, 1926). For a given environmental parameter, a species typically has an optimum where the species has its greatest abundance and a range over which it can survive, albeit in lower abundances (Whittaker, 1956; 1960; 1967; 1973). Species abundances change along these environmental gradients, which causes community composition to also change along those gradients.

Environmental gradients are described as resource, direct, indirect, and complex gradients (Austin, 1980; Austin et al., 1984). Resource gradients reflect materials directly consumed by organisms such as nutrients, oxygen, and water (Austin et al., 1984; Patzkowsky and Holland, 2012). Direct gradients are those that impact survival and morphology of organisms but are not controlled by substances that are consumed (Austin, 1980), such as substrate, water pressure, water chemistry, and shear stress (Patzkowsky and Holland, 2012). Indirect gradients are those that do not directly impact the survival or morphology of organisms, (Austin, 1980; Austin et al., 1984), such as elevation in the terrestrial realm and water depth in the marine realm. Complex gradients are indirect gradients that covary with direct and resource gradients (Whitaker, 1956; Whitaker, 1960, Austin et al., 1984, Patzkowsky and Holland, 2012).

The water-depth gradient in the most common environmental gradient correlated with variation in community composition of marine benthic invertebrates in the modern and ancient record. Water depth is not a variable that directly controls this variation, but rather it is a complex gradient comprising of other environmental gradients (sensu Whitaker, 1956). The covarying resource gradients include nutrients and oxygen, and the covarying direct gradients include temperature, substrate, water pressure, shear stress, salinity, and light penetration (Tait and Dipper, 1998; Patzkowsky and Holland, 2012). It is far more likely that species are responding to one or more of these covarying environmental parameters that contribute to the water-depth gradient than they are to water depth itself.

In ancient settings, determining the role of environmental variables with respect to assemblage variation and their correlation with water depth is more difficult. Compared to the direct measurements used in modern studies, the nature of the fossil and stratigraphic records often allows only for indirect measurements of environmental variables. Examination of the lithological data (i.e., grain size, grain composition, bioturbation levels, and biogenic structures) as well as the ecological characteristics of assemblages (i.e., life mode and feeding ecology) indicate that substrate and wave-energy gradients commonly covary with water depth in the ancient record (Cisne and Rabe, 1978; Lafferty et al., 1994; Patzkowsky, 1995; Holland et al., 2001; Webber, 2002; Novack-Gotshall and Miller, 2003; Scarponi and Kowalewski, 2004; McMullen et al., 2014; Scarponi et al., 2014; Zuschin et al., 2014). Evaluating these same lithological and faunal characteristics has also identified substrate and wave-energy gradients that are uncorrelated with water depth (Holland et al., 2001; Olszewski and Patzkowsky, 2001;

Scarponi and Kowalewski, 2004; Tomašových, 2006; Redman et al., 2007; Bush and Brame, 2010; Perera and Stigall, 2018). The relative frequencies of other environmental gradients are currently unknown for the fossil record.

Purpose of Study

The purpose of this dissertation is to identify the environmental gradients that most commonly affect the community composition of ancient benthic marine invertebrates. This dissertation conducts an extensive literature review of modern and ancient studies as well as fieldwork in modern and ancient carbonate environments to identify these environmental gradients. This dissertation has two primary goals. First, it quantifies the frequency of environmental gradients identified in ancient settings and compare those frequencies and amount of explained variance to gradients in the modern. Second, it will attempt to devise sampling and analytical methods that combine detailed faunal and lithological data to identify gradients that covary with water depth as well as any additional independent gradients controlling modern and ancient assemblages.

In the first chapter of this dissertation, I review the results from a comparable number of modern and ancient studies on environmental gradient analysis and marine benthic invertebrate communities. The frequency of which these gradients have been identified and contributions made to explain the variation in benthic assemblages has not been tabulated nor directly compared between the modern and ancient. Doing so provides a sense of which variables can be identified, how often they are identified, and the differences in identification between the modern and ancient. This chapter will focus on studies that use multivariate ordinations such as principal components analysis (PCA), correspondence analysis (CA), detrended correspondence analysis (DCA), canonical

correspondence analysis (CCA), and nonmetric multidimensional scaling (NMS) to interpret gradients controlling benthic communities. Authors' interpretations of environmental gradients will be tabulated for each axis of ordination to compare frequencies of identification between not only the modern and ancient, but also among ordination axes to interpret their respective impacts on assemblage variation. The data and R code used for this chapter as well as tables containing authors' results of gradient analyses are in Appendix A.

The second chapter is a modern field-based study to test which environmental variables are controlling variation in assemblages when water depth is constrained to an individual depositional environment. The shallow subtidal of San Salvador Island, The Bahamas was selected because it contains a wide variety of environments such as seagrass meadows, open sand flats, protected lagoons, and patch reefs. The molluscan death assemblage was sampled from these environments in conjunction with sedimentological (sediment composition, grain size, bioturbation intensity) and oceanographic data (water depth, temperature, wave intensity, dissolved oxygen levels). By constraining sampling to a narrow depth range in the shallow subtidal (1–5 m), water depth is not expected to correlate with assemblage variation. Rather, other environmental gradients, such as substrate or wave energy, are expected to explain the greatest amount of variation in the molluscan death assemblage on San Salvador Island. The data and R code used for this chapter are in Appendix B as well as the Mendeley Data Repository https://data.mendeley.com/datasets/sn75nhwpkf/1.

Finally, the third chapter is a field-based study of a Mississippian carbonate ramp combining faunal and lithological data to test for environmental gradients controlling

assemblage variation in the lower Madison Group of Montana. Closely spaced, replicate samples of faunal and lithological data are used to minimize the impact of heterogeneity in the fossil and lithologic records and strengthen the interpretation of ancient gradients. Water depth is expected to be the primary gradient, but the goal of this study is to determine if this replicate sampling method can identify specific covarying gradients as well as additional uncorrelated gradients. The collection of replicate lithological samples in conjunction with faunal data directly links lithological data to each assemblage, potentially expanding the number of environmental gradients that can be identified in the fossil record. Locality locations, data, R code, and monograph of species for this chapter are in Appendix C.

CHAPTER 2

ENVIRONMENTAL GRADIENTS AND COMMUNITY VARIATION OF MARINE BENTHIC COMMUNITIES IN THE MODERN AND FOSSIL RECORD[1]

[1] Brown, G.M. Submitted to Palaeontology

ABSTRACT

Modern ecological studies can directly measure environmental variables when sampling marine benthic invertebrate communities and can determine their relative impacts on assemblage compositions. However, the relative frequencies and strengths of environmental gradients controlling variation in fossil benthic communities are uncertain. This study reviews the results of previously published modern (n = 46) and ancient (n = 48) multivariate ordinations of benthic marine communities to identify the most common environmental gradients associated with assemblage composition, their frequency in the modern and fossil records, and the amounts of variation explained by each ordination axis. In modern and ancient studies, water depth and substrate variations are the most common gradient associated with assemblage variation. In the modern, these are followed by temperature, salinity, and pollution, and in ancient assemblages by geologic age, geography, and life habit. Reported eigenvalues and relative inertia indicate axis 2 typically explains about half of the variation compared to axis 1 in both modern and ancient ordinations, whereas higher axes explain substantially less and are often uninterpretable. This indicates most ordinations need to examine gradients along the first two axes of ordination to explain the majority of variation in assemblage data. Tabulating and ranking the gradients correlated with variation in benthic marine assemblages provides direction for future investigations to gradient analysis in the fossil record. Although water depth is the most common gradient, there is great potential for recognizing other gradients in the fossil record through closely spaced, replicate sampling and interpretation of higher axes of ordination.

INTRODUCTION

The Gleasonian model of ecology argues that species distributions and community structure are primarily controlled by environmental gradients (Gleason, 1926). For a given environmental parameter, a species typically has an optimum where the species has its greatest abundance and a range over which it can survive, albeit in lower abundances (Whittaker, 1956; 1960; 1967; 1973). Species abundances change along these environmental gradients, causing community composition to change along those gradients. A water-depth gradient (usually equivalent to an onshore–offshore gradient) is the environmental gradient most commonly associated with variation in assemblage compositions for modern and ancient marine benthic communities (see Patzkowsky and Holland, 2012 for review). Water depth is a complex gradient (sensu Whittaker, 1956; 1960) comprising many covarying environmental parameters such as substrate type, vegetation, sunlight penetration, nutrient availability, oxygenation, shear stress, pressure, salinity, and temperature (Tait and Dipper, 1998). The composition of benthic invertebrate communities reflects the response of species to these variables, giving rise to this complex gradient correlated with water depth.

A singular environmental gradient does not encompass all variation in community composition, and environmental variables uncorrelated with water depth also influence benthic community composition. Modern studies are able to directly measure many of these environmental factors to test for their role. The nature of the fossil records, however, often allows only indirect measurements of environmental variables. In both cases, this raises several questions. First, what are the most common environmental gradients correlated with the composition of benthic invertebrate assemblages in both the

modern and the fossil record? Second, what are the sampling, environmental and ecological conditions in which these gradients are recognized? Third, what are the relative strengths of these gradients in the fossil record compared to the modern?

One commonly used method for investigating environmental gradients in modern and ancient communities is multivariate ordination, such as non-metric multidimensional scaling (Kruskal, 1964a;1964b; Minchin, 1987; Shi, 1993; McCune and Grace, 2002), detrended correspondence analysis (Hill and Gauch, 1980; Legendre and Legendre, 1980; Minchin, 1987; Shi, 1993), and principal components analysis (Goodall, 1954; Shi, 1993; McCune and Grace, 2002). Here, I examine the results of published ordinations of modern and fossil marine benthic assemblages to identify the types and the frequencies of environmental gradients. I also assess how the various gradients are identified for modern and fossil ordinations along multiple axes of ordination. Finally, I compare the strengths of gradients along ordination axes to determine their relative impact on community compositions in the modern and fossil records.

Examining gradients correlated with modern assemblages provides guidance into how fossil communities may have responded to environmental parameters. Identifying the most common sources of variation in the modern provides clues as to which variables should be targeted for ecological studies in ancient settings. When combined with the currently published sources of variation in fossil ordinations, it provides a list of environmental gradients and how they can be identified in the fossil record.

BACKGROUND ON GRADIENTS AND ORDINATIONS

Environmental Gradients

Environmental gradients are described as resource, direct, indirect, and complex gradients (Austin, 1980; Austin et al., 1984). Resource gradients reflect materials directly consumed by organisms such as nutrients, oxygen, and water (Austin et al., 1984; Patzkowsky and Holland, 2012). Direct gradients are those that impact survival and morphology of organisms but are not controlled by substances that are consumed (Austin, 1980), such as substrate, water pressure, water chemistry, and shear stress (Patzkowsky and Holland, 2012). Indirect gradients are those that do not directly impact the survival or morphology of organisms, (Austin, 1980; Austin et al., 1984), such as elevation in the terrestrial realm and water depth in the marine realm. Complex gradients are indirect gradients that covary with direct and resource gradients (Whitaker, 1956; Whitaker, 1960, Austin et al., 1984, Patzkowsky and Holland, 2012). In the marine realm, water depth is a complex gradient as organisms are not responding to directly, but rather are responding to covarying environmental gradients such as substrate type, vegetation, sunlight penetration, nutrient availability, oxygenation, shear stress, salinity, and temperature (Tait and Dipper, 1998).

Common Ordination Techniques

Ordinations are indirect gradient analyses that analyze and plot samples with respect to the covariation and similarity of assemblage compositions. They are often used to reconstruct patterns of community variation, generally related to underlying environmental gradients. Samples that are more similar will plot close to one another within the ordination space, whereas samples that are dissimilar will plot further apart.

Several ordination methods have been used, including principal components analysis, detrended correspondence analysis, canonical correspondence analysis, and nonmetric multidimensional scaling.

Principal component analysis (PCA) is an eigenvector approach that displays sample and variable data within the ordination space (Goodall, 1954; McCune and Grace, 2002). Samples are ordinated in a multivariate space with major axis regression and are rotated such that the greatest amount of variance is oriented along principal component 1 (PC1; Goodall, 1954; McCune and Grace, 2002). Additional axes are orthogonal to one another and reflect decreasing amounts of explained variance. Although PCA has been used on ecological datasets in the past (Goodall, 1954), it is no longer acceptable to ordinate ecological datasets with PCA as ecological variables (i.e., species data) do not follow the linear relationship PCA requires, resulting in severe distortions (Kessell and Whittaker, 1976; Kenkel and Orlóci, 1986; Minchin, 1987). It is most commonly used in modern analyses to ordinate environmental data separately from species data, and then compared to the distribution of samples and taxa in other multivariate methods such as cluster analysis and nonmetric multidimensional scaling to indirectly infer environmental gradients (see Llewellyn and Messing, 1993; Netto et al., 1999; Bremner et al., 2006; Barros et al. 2008; Mariano and Barros, 2015 for examples).

Detrended correspondence analysis (DCA) is a different eigenvector approach that modifies a correspondence analysis (CA) to display samples and species within the ordination space (Hill and Gauch, 1980). Environmental gradients can be inferred from the distribution of samples and taxa within the ordination space by overlaying external environmental or taxonomic information onto the ordination. Unlike the PCA, DCA does

not require linear relationships between variables and can accept ecological datasets (Hill and Gauch, 1980, McCune and Grace, 2002). DCA is calculated from a CA, which is a weighted averaging technique that weights sample distances to one another using similarities between species and weighting the species locations by the position of samples (Hill, 1973; Hill and Gauch, 1980). Unfortunately, CA produces an "arch" effect, where samples from the endpoints of a gradient with shared taxonomic absences are shown as more similar than they really are (Hill and Gauch, 1980). DCA flattens this arch by segmenting axis 1 of the CA and adjusting those segments along axis 2 such that the mean axis 2 score of each segment is zero (Hill and Gauch 1980, McCune and Grace 2002). The position of samples along each axis is also rescaled with respect to their species scores to eliminate the compression and extension of sample distributions caused by the CA arch (Hill and Gauch, 1980; McCune and Grace, 2002). The distortion along higher axes and the rescaling methods utilized in DCA has drawn much criticism (Pielou, 1984; Legendre and Legendre, 1998; McCune and Grace, 2002), which has decreased the usage of DCA in modern studies. However, DCA is still commonly used as it is useful for identifying the ecological gradients in fossil assemblages (Patzkowsky and Holland, 2012).

Canonical correspondence analysis (CCA) is a constrained ordination where a CA of species data is constrained by a multiple linear regression of environmental data (ter Braak, 1986; McCune and Grace, 2002). CCA plots samples and species within the ordination space and overlays environmental variables as vectors. The direction and length of a vector signifies the strength of correlation an environmental variable with each axis. Additionally, CCA calculates axis loadings for each environmental gradient to

identify the contribution of each environmental variable to each axis (ter Braak, 1986; McCune and Grace, 2002). As a result, the distribution of samples and taxa along each axis can be directly correlated with the measured environmental variables (ter Braak, 1986; McCune and Grace, 2002).

Nonmetric multidimensional scaling (NMS) is an ordination method commonly used in modern and ancient studies. It differs from other ordination techniques in that it takes a numerical and iterative approach instead of using eigenvalues to calculate similarity between samples (Kruskal, 1964a;1964b). NMS is a flexible technique that can analyze ecological as well as environmental datasets (McCune and Grace, 2002). NMS works by optimizing the goodness of fit (i.e., stress) between the original similarity matrix and the reduced dimension similarity matrix over a specified number of axes (Kruskal, 1964a, 1964b; McCune and Grace, 2002). One drawback to NMS is it produces a cloud of points with an arbitrary orientation in the ordination space. This cloud can be rotated in any direction and the axes cannot be ranked in terms of explained variance as in eigenanalysis methods (Kenkel and Burchill, 1990; McCune and Grace, 2002; Clarke and Gorley, 2015). This can be remedied by rotating the NMS cloud with PCA such that the most variance in the dataset now lay along axis 1, and subsequent amounts of variation will be on higher order axes (Clarke and Gorley, 2015; Oksanen, 2019).

Calculating Percent Variance in Ordinations

The amount of variance explained by an axis of ordination is calculated in several ways. Eigenanalysis based ordination methods such as PCA directly calculate the variance explained along each axis of ordination as the eigenvalues. PC 1 will have the

largest eigenvalue, with subsequent axes having progressively smaller eigenvalues (Goodall, 1954; McCune and Grace, 2002; Clapham, 2011; Legendre and Birks, 2012).

Eigenvalues calculated by a CA, DCA, or CCA differ from PCA eigenvalues in that they represent the "inertia" of each axis. Inertia is equivalent to the strength of the gradient along each axis but is not strictly percent variance explained (Legendre and Birks, 2012). Inertia can be used to calculate "relative inertia", which is similar to the percent variance explained in PCA eigenvalues. Relative inertia is calculated by dividing the eigenvalue of an axis by the sum of eigenvalues for all axes in the ordination (Økland, 1999). Relative inertia may not be appropriate for CA as higher order axes are quadratic distortions of the previous axis, because the second axis may not truly be independent of the first (McCune and Grace, 2002). Relative inertia may also not be appropriate for DCA. The detrending and rescaling used on the higher axes to remove the horseshoe effect and quadratic distortion of the CA alters the distribution of samples along these higher axes such that the eigenvalues no longer accurately represented sample distributions (Økland, 1999). The many complications associated with eigenvalues and relative inertia from CA and DCA limit their functionality and are no longer encouraged within ecological analyses (Økland, 1999, McCune and Grace, 2002). Relative inertia should be reported for all CCA as it represents the amount of variance explained by the constrained axes within the ordination (ter Braak, 1986, McCune and Grace, 2002).

An after-the-fact approach to explained variance can be used on ordinations that previously relied on relative inertia (i.e., CA, DCA, CCA) or that do not use an eigenvector approach (i.e., NMS; McCune and Grace, 2002). In this method, the Pearson correlation between distances in the ordination space and distances in the original data

produces an r^2 value equivalent to percent variance represented along the axes of ordination (McCune and Grace, 2002). Distance measures in the ordination space will vary by ordination technique (see McCune and Grace, 2002 for suggestions). Obtaining the explained variance for each axis requires calculating the Pearson correlation coefficient by incrementally adding axes in the ordination space matrix until it encompasses all axes. The percent variance explained for an individual axis is calculated by taking the difference between r^2_n and r^2_{n-1} where n is the number of axes used (McCune and Grace, 2002). For the first axis of ordination, r^2_1 represents the value of percent variance explained by the first axis, as there are no ordination scores for when the number of axes equal 0. For the second axis of ordination, r^2_2 is the correlation between the species-abundance distance matrix with the distance matrix of ordination scores of the first and second axes. Δr^2_2 is the difference in r^2_2 and r^2_1 and represents the percent variance explained by gradients along the second axis (McCune and Grace, 2002).

METHODS

Here, ordination results from modern studies (46 ordinations in 33 studies) and ancient studies (48 ordinations in 32 studies) are used to evaluate the relative frequency of reported environmental controls on the composition of marine benthic communities. Ancient studies were selected by searching for paleoecological studies with ordinations of benthic macroinvertebrates. While not exhaustive, this search examined work published through August of 2019 from the journals of *Paleobiology*; *Palaios*; *Palaeogeography, Palaeoclimatology, Palaeoecology*; *Lethaia*; *Geological Society of London Special Papers*; *Geological Society of America Bulletin*; and *Geology*. Modern studies were selected via a *Google Scholar* search using the keywords “marine benthic

invertebrates", "gradient analysis", and "ordinations", until the number of ordinations was comparable to the ancient studies. Studies that used data from previous works were excluded from this review to avoid duplicating results. Studies in this analysis were selected based on whether they: 1) incorporate entirely new data without using older datasets; 2) add a substantial amount of new data to older datasets; and 3) analyze old datasets that were previously un-ordinated.

For each study, I recorded the macroinvertebrate groups studied, the geographic location of the study, the age of the study interval (modern vs geologic age), the duration of study interval (i.e., collection times for modern studies and geologic range for ancient studies), and the number of ordinations (Supplementary Table 2.1 and 2.2). For each ordination, I recorded the type of ordination used, how many axes the authors examined, and the authors' interpretation of environmental gradients for each ordination axis (Supplementary Table 2.1 and 2.2).

The authors' interpretations were tabulated and grouped into categories. For the modern studies, categories included: 1) the complex water-depth gradient (axes that include depth and/or covarying variables); 2) substrate (i.e., grainsize, sorting, and substrate firmness); 3) seafloor vegetation (i.e., density, diversity, leaf surface area, plant volume); 4) salinity; 5) pollution (i.e., trace metal contaminants); 6) temperature; 7) geography (i.e., latitude longitude, or location); 8) wave energy; 9) nutrients; 10) pH; 11) time; 12) turbidity; 13) taxa ecology (i.e., diversity, life habit of taxa); 14) shelf patchiness (i.e., unknown variation in the seafloor); 15) oxygenation. For the ancient studies, categories included: 1) the complex water-depth gradient (axes that include depth, change in depositional environment, and/or covarying variables); 2) geographic

separation of samples; 3) time; 4) substrate (grainsize, composition, firmness); 5) wave energy; 6) oxygen gradients (oxygen stable isotope or lithologic proxies); 7) nutrients (carbon and nitrogen stable isotopes); 8) salinity; 9) temperature; 10) taxa ecology (life habit, motility, feeding modes); and 11) turbidity.

Once tabulated, the occurrence frequency of each category was calculated for each axis of ordination against the total number of gradients identified along each axis. These frequencies are then compared among axes for both the modern and ancient studies to identify the most common environmental gradients as well as their relative level of contribution to assemblage variation. Frequencies of gradients are also compared between the modern and ancient ordinations to assess differences between the two records of marine invertebrates.

I also recorded the variation explained by each ordination axis (i.e., eigenvalue or relative inertia), if reported by the authors. Range and median values of percent variance were compared across each axis to assess the relative decrease in gradient strength along subsequent axes.

RESULTS

Ordination Types

Modern Studies.—Forty-six ordinations from thirty-three modern studies were examined (Figure 2.1). Nonmetric multidimensional scaling (NMS) is the most common ordination method (22 ordinations), followed by principal components analysis (PCA; 12 ordinations). Less common ordinations include canonical correspondence analysis (CCA; 4 ordinations), detrended correspondence analysis (DCA; 2 ordinations), and principal

coordinates analysis (PCO; 2 ordinations). Partial PCA, partial redundancy analysis, polar ordination, and reciprocal averaging (RA) are used only once.

Ancient Studies.—Forty-eight ordinations from thirty-two ancient studies were examined (Figure 2.1). DCA is the most common ordination (21 ordinations), followed by NMS (13 ordinations) and CCA (10 ordinations). Polar ordination is less common (3 ordinations), and PCA is used only once.

Taxonomic Groups

Modern Studies.—Species examined in modern studies were grouped into eleven taxonomic groups. Gastropods are most commonly examined (22 studies), followed by bivalves (19 studies). Common groups also include echinoderms (i.e., sea stars, brittle stars, echinoids; 13 studies), crustaceans (i.e., crabs, lobsters, shrimp; 12 studies), and polychaete worms (11 studies). Less common groups include bryozoans, corals, and other non-polychaete "worms" (5 studies). The least common groups include sponges (4 studies), non-crustacean arthropods (4 studies), and ostracodes (3 studies). Five studies did not report which benthic invertebrates were included in their analyses.

Ancient Studies.—Species examined in ancient studies were grouped into eleven taxonomic groups. Bivalves are the most commonly examined group (25 studies, followed by gastropods (22 studies) and brachiopods (19 studies). Less common taxonomic groups include bryozoans (9 studies), trilobites (7 studies), crinoids (7 studies), ostracodes (4 studies), and echinoderms (i.e., sea stars, brittle stars, echinoids; 4 studies). The least common groups include rugose corals (2 studies), shelled cephalopods (i.e., ammonites and nautiloids; 2 studies), and sponges (1 study). One study did not report which benthic invertebrates were included in their analyses.

All Modern Ordinations

Potential Gradients.—A total of eighteen potential environmental gradients were examined by the thirty-three modern studies (Figure 2.3). Water depth is most common gradient included in analyses (25 studies), followed closely by variation in substrate (23 studies). These gradients are then followed by salinity and temperature (11 studies), nutrients (8 studies), vegetation and geography (7 studies), and taxonomic gradients (i.e., diversity and life habit), latitude and wave energy (6 studies). Less common gradients include pollution and time (4 studies), longitude and oxygenation (3 studies), turbidity and pH (2 studies), and shelf patchiness and topography (1 study).

Axis 1.—Forty-five environmental gradients were identified along axis 1 in the forty-six modern ordinations. Water depth is the most common gradient identified along the first axis of ordination (17 ordinations; 37.8 % of axis 1 gradients; Table 2.1; Figures 2.4 and 2.6). The most common gradients along axis 1 where water depth is correlated with axis 2 are variations in substrate (8 ordinations; 17.7% of axis 1 gradients) and vegetation (6 ordinations; 13.3% of axis 1 gradients). These gradients are then followed by salinity and pollution (3 ordinations, 6.7% of axis 1 gradients), wave energy and life habit of taxa (2 ordinations, 4.4% of axis 1 gradients), and nutrient levels, temperature, shelf patchiness, and turbidity (1 ordination, 2.2% of axis 1 gradients; Table 2.1; Figures 2.4 and 2.6).

Axis 2.—Twenty-eight environmental gradients were identified along axis 2 of the forty-five modern ordinations. Substrate is the most common gradient identified along axis 2 (6 ordinations; 20.0% of axis 2 gradients; Table 2.1, Figures 2.4 and 2.6). This is followed by water depth (4 ordinations; 13.3% of Axis 2 gradients) temperature, salinity, and latitude (3 ordinations; 10.0% of axis 2 gradients) and pollution and life habit (2

ordinations; 6.7% of axis 2 gradients). Vegetation, nutrients, wave energy, turbidity, shelf patchiness, pH, and time are all rarely reported, with each reported only once along axis 2 (3.3% of axis 2 gradients; Table 2.1; Figures 2.4 and 2.6).

Axis 3.— Only four modern studies explore axis 3 or higher of ordinations. Water depth, substrate, and life habit of taxa were each identified only once (Table 2.1).

All Ancient Ordinations

Potential Gradients.— A total of eleven potential environmental gradients were examined by the thirty-two ancient studies (Figure 2.3). Water depth and lithology are the two most common gradients examined (29 studies), followed closely by time (28 studies). Other common gradients include taxa ecology (14 studies) and geography (12 studies). Less common gradients include salinity (3 studies), oxygen and wave energy (2 studies), and nutrients, temperature and turbidity (1 study).

Axis 1.— Fifty-four gradients were identified along axis 1 of the forty-eight ancient ordinations. Water depth is the most common gradient identified along axis 1 (19 studies, 35.2% of axis 1 gradients; Table 2.2, Figures 2.5 and 2.6). The second most common gradient is the duration of the study interval (12 studies, 22.2% of axis 1 gradients). These are followed by substrate (8 studies; 14.8% of axis 1 gradients), geography (5 studies; 9.3% of axis 1 gradients), oxygen (4 studies; 7.4% of axis 1 gradients), life habit of taxa and salinity (2 studies; 3.7% of axis 1 gradients), and turbidity and nutrients (1 study; 1.9% of axis 1 gradients; Table 2.2; Figures 2.5 and 2.6).

Axis 2.— Twenty-six gradients are identified along axis 2 of the forty-five ancient ordinations. Substrate is the most common gradient identified along axis 2 (6 studies, 19.4% of axis 2 gradients; Table 2.2, Figures 2.5 and 2.6). The second most common

gradients identified along axis 2 are water depth, time, and taxonomic gradients (5 studies; 16.1% of axis 2 gradients). These gradients are followed by wave energy, and geography (3 studies; 9.7% of axis 2 gradients), nutrient level (2 studies; 6.5% axis 2 of gradients), and salinity and temperature (1 study; 3.2% of axis 2 gradients; Table 2.2; Figures 2.5 and 2.6).

Axis 3.—Only five ancient studies explore axis 3 or higher of their ordination space. Substrate, time, and salinity were each identified once along axis 3, and 3 was left uninterpreted in two ordinations.

Modern Gradients Weighted by Ordination Sample Size

Axis 1.—Frequency of identification was also calculated using the number of modern ordinations examining each gradient (Figure 2.7). Shelf patchiness was identified along axis 1 in the only ordination that included it. Vegetation (86% of 7 ordinations), pollution (75% of 4 ordinations), and water depth (0.68% of 25 ordinations) are the next most identified gradients along axis 1 in ordinations that included them. These are followed by turbidity (50 % of 2 ordinations), substrate (35% of 23 ordinations), taxa ecology and wave energy (33% of 6 ordinations), and salinity (27% of 11 ordinations). Nutrients (12% of 8 ordinations) and temperature (9% of 11 ordinations) are the least commonly identified gradients along axis 1 in ordinations that included them. Geography (7 ordinations), latitude (6 ordinations), time (4 ordinations), longitude (3 ordinations), oxygenation (3 ordinations), pH (2 ordinations), and shelf topography (1 ordination) were not identified along axis 1.

Axis 2.—Shelf patchiness was identified along axis 2 in the only ordination that included it. Latitude (6 ordinations), pollution (4 ordinations), turbidity (2 ordinations) and pH (2

ordinations) are identified along axis 2 in 50% of ordinations that included them. Less commonly identified gradients along axis 2 include taxa ecology (33% of 6 ordinations), salinity and temperature (27% of 11 ordinations), substrate (26% of 23 ordinations), time (25% of 4 ordinations), wave energy (17% of 6 ordinations),water depth (16% of 25 ordinations), vegetation (14% of 7 ordinations), and nutrients (12% of 8 ordinations). Geography (7 ordinations), latitude (6 ordinations), oxygenation (3 ordinations), and shelf topography (1 ordination) were not identified along axis 2.

Ancient Gradients Weighted by Ordination Sample Size

Axis 1.—Frequency of identification was also calculated using only the number of ancient ordinations examining each gradient (Figure 2.7). Oxygenation (4 ordinations) and turbidity (1 ordination) were identified along axis 1 in all ordinations that included them. Salinity (67% of 3 ordinations) and water depth (66% of 29 ordinations) are the next most common gradients identified along axis 1 in ancient ordinations. These are followed by time (43% of 28 ordinations), geographic location (42% of 12 ordinations), nutrients (33% of 3 ordinations), lithology (28% of 29 ordinations), and taxa ecology (14% of 14 ordinations). Wave energy (3 ordinations) and temperature (1 ordination) were not identified along axis 1 in the ancient ordinations.

Axis 2.— Wave energy (3 ordinations) and temperature (1 ordination) were identified along axis 2 in all ordinations that included them. Nutrient gradients (67% of 3 ordinations) are the next most common along axis 1 in ancient ordinations. This is followed by taxa ecology (36% of 14 ordinations), salinity (33% of 3 ordinations), geographic location (25% of 12 ordinations) lithology (21% of 29 ordinations), time (18% of 28 ordinations), and water depth (17% of 29 ordinations).

Percent Variance Explained

Modern Studies.—The percent variance explained along axis 1 was reported for 19 of the 46 ordinations, either as eigenvalues or relative inertia. Percent variance was reported from twelve PCAs, two DCAs, four CCAs, and one redundancy analysis. The amount of variation explained by axis 1 ranges from 8–86.7% with a median value of 41.0% (Figure 2.8). The percent variance explained along axis 2 was reported for 18 of the 46 ordinations, either as eigenvalues or relative inertia. Percent variance was reported from twelve PCAs, two DCAs, three CCAs, and one redundancy analysis. The amount of variation explained axis 2 ranges from 4.1–31.5% with a median value of 19.9% (Figure 2.8). Percent variation explained in these three ordinations is reported from PCAs and ranges from 7.8% to 12.0% variation explained (Figure 2.8).

Ancient Studies.—The percent variation explained along axis 1 was reported for 13 of the 45 ordinations. Nine are reported from correspondence analyses, three from DCAs, and one PCA. Percent variance ranges from 4.6–61.9% with a median value of 16.4% (Figure 2.8). The percent variation explained along axis 2 was reported for 13 of the 45 ordinations. Nine are reported from correspondence analyses, three from DCAs, and one PCA. Percent explained variation ranges from 4.4–27.8% with a median value of 10.4% (Figure 2.8). Four ordinations reported percent variation explained along axis 3, which ranges from 4.3–15.1% with a median value of 5.2% (Figure 2.8).

DISCUSSION

Ordinations Used in the Modern Compared to the Ancient

NMS is commonly used in the modern and ancient studies examined (Figure 2.1), which is likely because of the technique's flexibility with different types of data and its preservation of rank-order distances among samples regardless of data standardizations, transformations, or distance metrics (Clarke, 1993; McCune and Grace, 2002). While NMS produces a cloud of data that can be rotated in any orientation, most ancient and several modern studies commonly orient the cloud such that most variation lays along the first axis of ordination. Many modern studies did not plot axes within their ordination space (Seiderer and Newell, 1999; Anderson et al., 2006; Kuklinski et al., 2006; Olabarria, 2006; Aldea et al., 2008; Barros et al., 2008; Smale, 2008; Konar et al., 2009; McClain et al., 2010; Williams et al., 2010), but the longest axis of the point cloud correlates with their interpretation of environmental gradients explaining the the most variation in their faunal datasets.

PCA is commonly used in many of the modern studies examined, but it was used only once in the ancient studies (Figure 2.1). Few analyzed species data using PCA, as this method tends to infer the absence of species as a shared similarity among samples that are otherwise dissimilar. Rather, many of these studies ordinated environmental data collected alongside the faunal data, and compare the sample distributions within the ordination space to the sample distribution in cluster analyses and NMS on the faunal data (Llewellyn and Messing, 1993; Netto et al., 1999; Bremner et al., 2006; McKinney and Hageman, 2006; Barros et al., 2008; Bolam et al., 2008; Mariano and Barros, 2015). Comparing the PCA results of the environmental data to other multivariate methods on

the faunal data often identify similar patterns in sample distribution, which can be used to infer primary gradients in these modern studies.

DCA is the most common ordination in the ancient studies examined, but it is rarely used in the modern studies (Figure 2.1). Some have argued that DCA is an unfavorable ordination technique because the detrending, rescaling, and quadratic distortions of higher axes makes interpretations of environmental gradients difficult (Pielou, 1984; Legendre and Legendre, 1998; McCune and Grace, 2002), although modeling studies show that its performance is equivalent to NMS (Patzkowsky and Holland, 2012). However, DCA is still used in ecological studies as it is useful in identifying gradients controlling fossil assemblage compositions (Patzkowsky and Holland, 2012).

Taxonomic Groups examined in the Modern Compared to the Ancient

Bivalves and gastropods are the most common benthic invertebrates in the modern and ancient studies (Figure 2.2). Although they originated in the Cambrian, bivalves and gastropods diversified after the End Permian Mass Extinction and dominate the marine benthic invertebrate record from the Mesozoic through the recent. They are abundant in modern marine ecosystems and contribute a large percentage of shell material to modern death assemblages. Presumably, ancient bivalves and gastropods responded to environmental gradients similarly to their modern relatives, and results of gradient analyses should be comparable between the modern and ancient mollusks.

Bryozoans and ostracodes are common in both the modern and ancient studies examined. (Fig. 2.2). Bryozoans are common in modern marine ecosystems, are a large component of Paleozoic benthic assemblages, and have good preservation potential in the

fossil record. Ostracodes are also common in modern marine ecosystems and have an excellent fossil record as their calcified carapace increases their preservation potential relative to other arthropods.

Several taxonomic groups are unique to the ancient studies examined (Figure 2.2). Many of these groups were greatly impacted by the End Permian Mass Extinction. Brachiopods were abundant during the Paleozoic, but the mass extinction reduced their diversity to a handful of lineages. Modern brachiopod responses to environmental variables as analogues for ancient brachiopods should be used with caution. Modern brachiopods are distantly related to many of the extinct Paleozoic lineages and possibly have different life habits. Crinoids were also abundant during the Paleozoic but lost much diversity after the End Permian Mass Extinction. Both modern and Paleozoic crinoids are upper-level epifaunal suspension feeders with similar life habits, indicating modern crinoids may be adequate analogues for crinoid response to environmental gradients in the Paleozoic. Trilobites and rugose corals became extinct as a result of the mass extinction and their modern arthropod or anthozoan relatives may not be good analogues for their responses to environmental gradients.

Some taxonomic groups included in the modern studies are rare or absent in the ancient studies as the result of poor preservation potential or disarticulation. Polychaetes, “worms”, and crustaceans are unique to the modern studies examined (Figure 2.2) as they have low preservation potential in the fossil record. Body fossils of polychaetes and other “worms” are occasionally found in the fossil record. However, most evidence for them in ancient communities is commonly inferred from preserved traces and burrows, making polychaetes and other “worms” difficult to quantify for gradient analyses. Crustaceans

and other arthropods are found in the fossil record, but their chitinous carapaces have a lower preservation potential than the calcite or aragonite shells of other invertebrates. Sponges and echinoderms such as sea stars, brittle stars, sea urchins, and echinoids are common in the modern studies but are rare in the ancient studies (Figure. 2.2). While represented in the fossil record since the Paleozoic, sponges often disarticulate into individual spicules and echinoderms fragment along skeletal plates, which makes quantifying the number of individuals difficult for ancient gradient analyses.

These soft-bodied or easily fragmented taxa are a large component of modern studies, and their inclusion in ordinations may lead to different interpretations of gradient analyses than studies that include only fauna with good preservation potential. Modern studies can perform a second ordination without these soft-bodied taxa to better simulate ancient benthic communities. Procrustes analysis can test the similarity between ordinations that include and omit soft-bodied taxa to determine their influence on gradient analyses (Gower, 1971; Podani, 191; Schneider and Borlund, 2006). If the Procrustes analysis determines a similarity between the two ordinations and there are no major changes in the distribution of samples along axes, this implies soft-bodied taxa are responding similarly to environmental gradients as their hard-bodied cohorts and modern and ancient gradient results can be compared more directly.

Variables Examined in the Modern Compared to the Ancient

More variables are examined in the modern studies of benthic macroinvertebrates than in ancient studies (Figure 2.3). Modern studies can directly measure a wider variety of variables, whereas the ancient record is limited to fewer variables with indirect measurements. Common environmental variables shared between modern and ancient

studies include the complex water-depth gradient, substrate variations, community variation associated with geographic location, and taxa ecology gradients. Temporal gradients, while commonly included in ancient studies (28 studies), is rarely examined in modern studies (4 studies). Time is integral to include with ancient studies as sampling vertically through a geologic section samples progressively younger fossil assemblages, and many ancient studies sample assemblages across millions of years (e.g., Tuckey and Anstey, 1989; Patzkowsky, 1995; Holland et al., 2001; Olszewski and Patzkowsky, 2001; Clapham and James, 2008; Olszewski and Erwin, 2009; Hendy, 2013; McMullen et al., 2014; Balseiro, 2016; Danise and Holland, 2017). While sampling duration in the modern varied from months to decades, time was only considered when decadal (Smith et al., 2001; Ferguson and Miller, 2007) or seasonal changes (Barros et al., 2008; 2012) were hypothesized to be important. Salinity, temperature, nutrient level, and oxygen level gradients are commonly examined in modern studies, as this data is easily collected alongside the faunal data via probes or stations. Salinity, temperature, nutrients, and oxygenation are rarely considered in ancient studies as the geochemical proxies commonly used to indirectly measure them (i.e., $\delta^{18}O$, $\delta^{13}C$) are subject to alteration after burial and only well-preserved samples will reflect the environmental conditions.

Modern Ordinations

Despite the larger pool of environmental variables in the modern, ordination results of the studies examined only found fourteen of the eighteen variables to be associated with modern assemblage variations. These variables include water depth, substrate, vegetation, salinity, pollution, taxa ecologies, wave energy, temperature, nutrients, shelf patchiness, turbidity, latitude, pH and time (Table 2.1, Figure 2.4).

The complex gradient of water depth and correlated variables is the most common gradient identified in modern studies (37.8% of gradients on axis 1 and 14.3% on axis 2; Table 2.1; Figures 2.4 and 2.6). Often, water depth is the only variable reported to correlate with axis 1. Assemblage compositions are commonly documented to change with water depth alone along axis 1 (Springer and Flessa, 1996; Sumida and Pires-Vanin, 1997; Olabarria, 2006; Aldea et al., 2008; Smale, 2008; Konar et al., 2009; McClain et al, 2010; Compton et al., 2013; Webber and Zuschin, 2013; Tyler and Kowalewski, 2014). This pattern is observable across multiple scales, including shallow, nearshore transects spanning intertidal zones through shallow-subtidal environments ((0–-10s of m water depth; Springer and Flessa, 1996; Smale, 2008; Konar et al., 2009; Webber and Zuschin, 2013; Tyler and Kowalewski, 2014), along the shelf-slope break (50–100 m water depth; Sumida and Pires-Vanin, 1997), and deep-sea transects (100s to 1000s m water depth; Olabarria, 2006; Aldea et al., 2008; McClain et al., 2010; Compton et al., 2013). When other variables are included, substrate most commonly covaries with water depth along axis 1 of ordinations (Netto et al., 1999; Van Hoey et al., 2004; Fernandez et al, 2007; Barros et al., 2008; Blanchard et al., 2013). Grain size commonly decreases along axis 1 with increasing water depth (Van Hoey et al., 2004; Fernandez et al., 2007; Barros et al., 2008; Blanchard et al., 2013), and grain sorting (Netto et al., 1999) also varies with depth along axis 1. Other environmental variables along axis 1 that covary with increasing water depth include nutrient levels (Netto et al., 1999; Fernandez et al., 2007; Blanchard et al, 2013), temperature (Williams et al., 2010; Compton et al., 2013), and oxygen (Williams et al., 2010).

No study identifies only water depth variation along axis 2. Rather, water depth covaries with other variables such as grain size (Smith et al., 2001; Blanchard et al., 2013), grain sorting (Bolam et al., 2008), substrate hardness (Bremner et al., 2006), nutrient levels (Blanchard et al., 2013), or wave shear stress (Bolam et al., 2008). When this happens, axis 1 gradients typically reflect substrate (Bolam et al., 2008), salinity (Bremner et al., 2006, Bolam et al., 2008), temperature (Bremner et al., 2006), tidal energy (Bolam et al., 2008), or pollution (Smith et al., 2001).

Water depth is not identified as a gradient in fourteen studies. Most commonly, water depth is absent in studies examining assemblages over narrow depth ranges either in the shallow nearshore or deep-water environment (Miller, 1988; Llewellyn and Messing, 1993; Seiderer and Newell, 1999; Smith et al., 2001; Anderson et al., 2008; Ferguson and Miller, 2007; Ferguson, 2008; Reich, 2014; Casebolt and Kowalewski, 2018). Additionally, assemblages covering large latitudinal distances (30° or more latitudinal change) do not ordinate along a water-depth gradient (Kuklinski et al., 2006; Anderson et al., 2008). For some of these fourteen studies however, patterns in assemblage variation with the identified gradients appear to correlate with water depth. Vegetation density (Miller, 1988; Ferguson and Miller, 2007) and grain size (Long and Poiner, 1994) both decrease with increasing water depths along onshore-offshore transects, but water-depth was not included in the gradient analyses. Salinity, trace metal levels, and percent fine-grained substrates all correlate with distance from estuary mouths (Barros et al., 2008; Barros et al., 2012; Mariano and Barros, 2015), but these may also be linked to water depth as depth increases with distance from the estuary mouth. Finally, onshore-offshore change in taxonomic ecologies and life habits (i.e., epifaunal to

infaunal, carnivore and scavengers to deposit and detrital feeders) in nearshore waters (McKinney and Hageman, 2006) indicate potential water-depth and substrate gradients, but such environmental variables were not included in their analysis. Thus, water depth is likely reflected on axis 1 more often than is reported.

Sediment and substrate variations independent of water depth are the next most common gradients (17.7% of gradients on axis 1 and 20.0% of gradients of axis 2; Table 2.1; Figures 2.4 and 2.6). Communities found in coarse-grained gravel and sandy substrates differ in composition from those found in fine-grained, muddy substrates (Long and Poiner, 1994; Netto et al., 1999; Seiderer and Newell, 1999; Van Hoey et al., 2004; Barros et al., 2008; Bolam et al., 2008; Barros et al., 2012; Mariano and Barros, 2015). Feeding strategies of benthic taxa also differ on fine-grained and coarse-grained substrates (Long and Poiner, 1994; Seiderer and Newell, 1999). Substrate firmness (Springer and Flessa, 1996) and percent of coarse sediment (Llewellyn and Messing, 1993; Seiderer and Newell, 1999) have been linked to greater percentages of attached and epifaunal taxa. While these types of substrate factors can covary with depth, these studies show that substrate-correlated gradient can be independent of water depth when examining assemblages within narrow depth ranges (Llewellyn and Messing, 1993; Springer and Flessa, 1996; Netto et al., 1999; Seiderer and Newell, 1999; Barros et al., 2008; Barros et al., 2012; Mariano and Barros, 2015). These substrate gradients can covary with other physical parameters, such as wave energy or tidal stress (Netto et al., 1999; Bolam et al., 2008) or proximity to sediment supply (Llewellyn and Messing, 1993; Barros et al., 2008; Barros et al., 2012; Mariano and Barros, 2015).

Seafloor vegetation gradients are also common in modern studies (13.3% of axis 1 gradients and 3.3% of axis 2 gradients; Table 2.1; Figures 2.4 and 2.6). Vegetation density, vegetation volume, and seagrass species abundance all have an impact on benthic communities (Moore, 1974; Miller, 1988; Anderson et al., 2006; Ferguson and Miller, 2007; Ferguson, 2008; Reich, 2014). For example, tropical shallow-subtidal communities within densely vegetated seagrass beds have a higher abundance and species richness of epifaunal, grazing gastropods (e.g., *Smaragdia viridis*, *Eulithidium thalassicola*, *Tegula fasciata*, and multiple species from the genus *Cerithium*) and chemosymbiotic bivalves (e.g., species from the genera *Lucina*, *Divaricella*, and *Codakia*) than non-vegetated areas (Miller, 1988; Ferguson and Miller, 2007; Reich, 2014; Casebolt and Kowalewski, 2018). Vegetated sites rich in wide-bladed seagrasses, such as *Thalassia*, can host a greater diversity of large grazing gastropods, whereas vegetated sites rich in narrow-bladed seagrasses, such as *Halodule*, can support only smaller micrograzing gastropods (Ferguson, 2008). The volume of kelp holdfasts can also impact the diversity of benthic assemblages, with smaller holdfasts supporting a more diverse community than larger holdfasts (Moore, 1974; Anderson et al., 2006).

Salinity gradients are typically identified in areas with substantial freshwater input or areas that experience intense evaporation (6.7% of axis 1 gradients, and 10.0% of axis 2 gradients; Table 2.1; Figures 2.4 and 2.6). Changes in benthic assemblages and salinity correlate with distance from estuary mouths, reflecting the amount of freshwater input (Bremner et al. 2006; Barros et al., 2008; Bolam et al., 2008). Restricted seaways can vary in salinity, which affects diversity, feeding ecology, and community structure (Bremner et al., 2006). Assemblages from tidal pools are also sensitive to salinity, which

can vary based on rates of evaporation, the size of the tidal pools, and overall connectivity to open-marine conditions (Netto et al., 1999).

Pollution gradients are identifiable in areas near human activity (6.7% of axis 1 and axis 2 gradients; Table 2.1; Figures 2.4 and 2.6). Species abundances respond to levels of introduced contaminant trace metals (Smith et al., 2001; Barros et al., 2008; 2012). Pollution caused by human sewage can be difficult to directly correlate with benthic assemblage change, but it may indirectly impact community structure by disrupting nutrient levels in the environment (Moore, 1974).

Temperature gradients, while rare on axis 1 (2.2% of axis 1 gradients, Table 2.1; Figures 2.4 and 2.6), are occasionally identified along axis 2 (10.0% of axis 2 gradients). Bottom-water temperature can vary at a given depth as the result of seafloor topography, geomorphology, and water-mass mixing, which affects the species composition and ecological structure of offshore communities (Fernandez et al., 2007; Compton et al. 2013). Temperature is also correlated with assemblage composition of tidal pool communities, although temperature may form a complex gradient with salinity, pool volume, evaporation rate, and connection to ocean water (Netto et al., 1999).

Latitudinal gradients (10.0% of axis 2 gradients; Table 2.1; Figures 2.4 and 2.6) driving community changes are identifiable in studies of broad geographic context (1000s of km; Kuklinski et al., 2006). They are also identifiable at smaller scales in temperate and polar climates (1–10s of km; Bremner et al., 2006; Smale, 2008; Blanchard et al., 2013). Latitude is a complex gradient, but the covarying environmental variables differ based on spatial scale and geographic location. Water temperature commonly covaries with latitude in studies of both broad geographic (Kuklinski et al., 2006) and small

geographic ranges (Bremner et al., 2006; Smale, 2008; Blanchard et al., 2013). Increased physical disturbance from either storms or wave energy (Kuklinski et al., 2006) and by ocean currents (Smale, 2008) has also been correlated with latitude and also impact benthic assemblages at in temperate and polar communities.

Using all modern ordinations to calculate the frequency of identification for environmental variables may emphasize those variables most often sampled. For example, water depth and substrate were identified most frequently in part because they were included in the majority of ordinations (Figures 2.3 and 2.6). Using only the ordinations that include an environmental variable to calculate frequency of identification may better reflect the potential contribution of that variable to assemblage compositions.

When the frequency for water depth is calculated using only the ordinations that included it, water depth is the fourth most common gradient along axis 1 after shelf patchiness, vegetation, and pollution (Figure 2.7). Water depth is identified on axis 1 in 68% of the 25 ordinations that include it, and along axis 2 for 17% of those ordinations. This high frequency along axis 1 and the large difference in identification between axis 1 and axis 2 further emphasizes the predominance of water depth as the primary gradient of variation in community composition of modern benthic invertebrates.

Substrate is the sixth most common gradient along axis 1 following turbidity (Figure 2.7). Substrate is identified on axis 1 in 35% of the 23 ordination that include it and along axis 2 in 26% of those ordinations (Figure 2.7). This moderate frequency of identification over a large sample size demonstrates that substrate is a common primary gradient and secondary gradient controlling the composition of modern benthic communities.

Several environmental variables have a higher frequency of identification when calculated using only the number of ordinations that included them (Figure 2.7). Vegetation and pollution are identified along axis 1 in the majority of ordinations that include them, which demonstrates the large impact both of these environmental variables have when present in marine environments. Wave energy, taxa ecology, and salinity, which are uncommon when comparing all 46 ordinations (Figure 2.6), are just as common as substrate gradients along axis 1 and axis 2 when calculated using this approach (Figure 2.7). Latitude, pH, and temperature, which are uncommon when comparing all 46 ordinations (Figure 2.6) but are identified along axis 2 in 27% of the ordinations that include them (Figure 2.7), suggesting these variables may be important secondary gradients in modern communities. While these higher frequencies of identification imply that their impact is greater than what the comparison of all ordinations indicates, these variables are included in less than ten ordinations and greater sampling of ordinations including them is needed to support the patterns shown here.

Ancient Ordinations

The spatial scales analyzed in ancient marine studies must be considered carefully, as studies examining a large spatial range may find geographic distance to be the predominant gradient describing differences in assemblage rather than basin-scale environmental factors. Spatial scales in the fossil studies examined range from less than 1 km (Redman et al., 2007) to greater than 1000 km (Kowalewski et al., 2002). Community variation associated with geographic location is most commonly identified when distances between samples are 100s of kilometers or greater (9.2% of axis 1 gradients, 9.7% of axis 2 gradients; Table 2.2; Figures 2.5 and 2.6). This can reflect biogeographic

provinces at the continental scale (Kowalewski et al., 2002) or the geographic distance in large basins despite similar environmental conditions (Olszewski and Erwin, 2009). Studies with distances on the order of 10 to 100 kilometers typically identify basin-scale gradients pertaining to environmental variables such as water depth, substrate, or wave energy (e.g., Cisne and Rabe, 1978; Patzkowsky, 1995; Holland et al., 2001; Scarponi and Kowalewski, 2004; Hendy, 2013). Geographic gradients may still be identified at the 10–100 km scale, but they tend to covary with water depth (e.g., Lafferty et al., 1994; Layou, 2009). At spatial scales less than 1 km, water depth is difficult to distinguish, and gradients may represent more localized environmental and faunal heterogeneity (Redman et al., 2007).

The temporal scale analyzed in the ancient marine studies must also be carefully considered, as studies spanning a large temporal duration may find time (i.e., evolutionary turnover) to be the predominant control on community composition rather than environmental factors. Temporal scales in the studies examined ranged from 10 k.y. to 35 m.y., and temporal gradients were identified frequently (22.2% of axis 1 gradients, 16.1% of axis 2 gradients; Table 2.2; Figures 2.5 and 2.6). Temporal gradients are common for fossil assemblages spanning tens of millions of years (Erwin, 1989; Tuckey and Anstey, 1989; Clapham and James, 2008; Olszewski and Erwin, 2009; Dineen et al., 2013; Balseiro, 2016; Danise and Holland, 2017). Occasionally, studies spanning shorter durations (100s k.y. to millions of years) can be distinguished in localities with well-resolved, high-resolution sequence stratigraphic framework (Novack-Gottshall and Miller, 2003; Holland and Patzkowsky, 2004; Scarponi and Kowalewski, 2004; Layou, 2009; Fall and Olszewski, 2010). These temporal gradients may correlate with periods of

extinction or significant, localized community change, such as the distinction between latest Ordovician (Hirnantian) and Silurian bryozoans (Tuckey and Anstey, 1989) , pre-Richmondian (Late Ordovician) and Richmondian fauna (Novack-Gottshall and Miller, 2003), and pre-glacial and post-glacial fauna in the Late Carboniferous (Dineen et al., 2013; Balseiro, 2016). All of these provide clues about community restructuring during ecological turnover.

Water depth is the most common environmental gradient associated with benthic community structure in ancient studies (35.2% of axis 1 gradients and 16.1% of axis 2 gradients; Table 2.2; Figures 2.5 and 2.6). Unlike in modern studies, ancient studies do not have the ability to measure an exact value for water depth. Rather, changes in water depth are estimated from the onshore-offshore position of the interpreted depositional environment. Depositional environments are recognized by the sediment grain size, sediment compositions, bedding, sedimentary structures, and trace fossils preserved in the lithologic record. These characteristics are compared with modern environments in which they co-occur, providing an estimate of onshore-offshore position for the ancient depositional system. As offshore communities typically differ from those closer to shore, ancient communities are inferred to be responding to the complex water-depth gradient (Cisne and Rabe, 1978; Erwin, 1989; Lafferty et al., 1994; Patzkowsky, 1995; Holland et al., 2001; Olszewski and Patzkowsky, 2001; Webber, 2002; Novack-Gottshall and Miller, 2003; Holland and Patzkowsky, 2004; Webber, 2005; Clapham and James, 2008; Layou, 2009; Bush and Brame, 2010; Hendy, 2013; Belanger and Garcia, 2014; McMullen et al., 2014; Scarponi et al., 2014; Zuschin et al., 2014; Balsiero, 2016; Danise and Holland, 2017) Occasionally, water-depth gradients in ancient, but relatively young settings can be

identified using the water-depth preferences for modern relatives of taxa (Tomašových, 2006; Hendy, 2013), although this is only useful for fossil groups with good representation in the modern (e.g., gastropods and bivalves).

Similar to modern studies, substrate variation is the second most common gradient recognized in ancient studies (14.8% of Axis 1 gradients and 19.4% of Axis 2 gradients; Figures 2.5 and 2.6). Substrate variation can be reflected in several ways. Fossil assemblages can vary with grain size and composition, with assemblages from coarse-grained sediments differing from those in fine-grained sediments (Redman et al., 2007; Bush and Brame, 2010). In addition, assemblages from siliciclastic environments differ from those in carbonate environments (Erwin, 1989; Tuckey and Anstey, 1989; Lebold and Kammer, 2006; Foster et al., 2015; Danise and Holland, 2017). Furthermore, fossil assemblages differ based on whether the environment contained only soft substrates with predominantly burrowing, infaunal organisms or included hard substrates on which epifaunal encrusting organisms could attach (Holland et al., 2001; Tomašových, 2006; Perera and Stigall, 2018). Substrate and lithology typically change with respect to water depth in the fossil record, but fine-resolution sampling of assemblages from within a limited spatial and temporal context (i.e., on the order of kilometers and tens of thousands of years; Redman et al., 2007; Perera and Stigall, 2018) and examining the life modes and feeding habits of taxa (Tomašových, 2006; Redman et al., 2007; Perera and Stigall, 2018) can identify lithologic variation that is water-depth independent.

Wave-energy gradients are occasionally identified along axis 2 of ancient ordinations when water depth is identified on axis 1 (11.5% of axis 2 gradients; Table 2.2, Figures 2.5 and 2.6). While sedimentary structures and grain sizes provide lithologic

evidence of energy in a depositional environment, these characteristics also tend to covary with water depth. Combining the lithological evidence with taxonomic morphology, such as shell durability, ribbing, and spinosity (Bush and Brame, 2010), or with the wave-energy tolerances of modern relatives (Scarponi and Kowalewski, 2004; Zuschin et al., 2014) can help identify potential wave-energy gradients.

When examining assemblages from the same depositional environment or limited temporal range (Olszewski and Patzkowsky, 2001; Lebold and Kammer, 2006; Belanger and Garcia, 2014), oxygen gradients are occasionally along axis 1 of ancient ordinations when water depth is identified along axis 2 (7.4% of axis 1 gradients; Table 2.2; Figures 2.5 and 2.6). $\delta^{18}O$ isotope data collected from well-preserved mollusks or co-occurring benthic foraminifera can be used as proxies for oxygenation and analyzed within the ordination space (Belanger and Garcia, 2014). Lithological characteristics such as sediment color, laminated bedding, and bioturbation levels can be used to infer oxygenation levels (Lebold and Kammer, 2006). Taxonomic information such as life modes and ecological guilds, if well-resolved, can be used to infer oxygen gradients within nearshore communities (Olszewski and Patzkowsky, 2001).

Other ocean chemistry gradients are less commonly identified as independent of water depth in ancient settings. Nutrient gradients (1.9% of axis 1 gradients, 6.5% of axis 2 gradients; Table 2.2; Figures 2.5 and 2.6) can be identified using $\delta^{13}C$ isotope data collected from well-preserved mollusks or co-occurring benthic foraminifera as proxies for nutrient levels (Belanger and Garcia, 2014) or well-resolved taxonomic information, such as life modes and ecological guilds (Tomašových, 2006). Salinity gradients (3.7% of axis 1 gradients; 3.2% of axis 2 gradients) can be identified in more recent fossil

assemblages with limited depth ranges by examining the salinity tolerances of modern taxa (Scarponi and Kowalewski, 2004; Amorosi et al., 2014) and ecological guild associations (Lebold and Kammer, 2006). Temperature gradients are rarely identified in ancient ordinations (3.2% of axis 2 gradients) but may be inferred from $\delta^{18}O$ isotope data collected from well-preserved mollusks or co-occurring benthic foraminifera (Belanger and Garcia, 2014).

Some ordinations of ancient systems examined the distribution of fossil taxa within the ordination space and identified gradients related to taxa ecology that were not directly tied to a specific environmental gradient (3.7% of axis 1 gradients, 16.1% of axis 2 gradients; Table 2.2; Figures 2.5 and 2.6). Such taxa ecology gradients included feeding modes (i.e., carnivore, detritivore, suspension feeder; Kowalewski et al., 2002), and motility (i.e., attached, sessile, free moving; Kowalewski et al., 2002; Dineen et al., 2013; Hendy, 2013. Taxa diversity gradients can also be identified in ordinations, where high diversity or high-evenness samples are distinct from low diversity or low-evenness samples (Erwin, 1989). It is likely that these taxonomic gradients represent environmental gradients such as substrate, wave energy, or nutrient levels as identified in other studies using taxa distributions (Holland et al., 2001; Olszewski and Patzkowsky, 2001; Scarponi and Kowalewski, 2004; Tomašových, 2006; Redman et al., 2007; Bush and Brame, 2010; Zuschin et al., 2014; Perera and Stigall, 2018) or they may represent another undefined complex gradient.

Water depth, lithology, and time are identified as the most common gradients when comparing all 48 ancient ordination results in part because they are included in most ordinations (Figures 2.3 and 2.6). These three variables are easy to include in

ancient studies as they can all be derived from the stratigraphic record. Water depth, and lithology are interpreted using grain composition, grain size, and sedimentary structures, while time is interpreted using biostratigraphy or position within a stratigraphic column. Taxa ecology and geographic location are also common gradients in ancient ordinations partly because they are also commonly included variables, while the remaining chemical and physical gradients are rare at least partly because they were included in less than 5 ordinations (Figures 2.3 and 2.6). Using only the number of ancient ordinations that includes each gradient to calculate frequency reveals patterns of identification similar to the modern studies.

When calculating frequency for water depth using only the ordinations that include it, water depth becomes the fourth most common variables along axis 1 after turbidity, oxygen, and salinity (Figure 2.7). Water depth is identified along axis 1 in 66% of the 29 ancient ordinations that included it and along axis 2 in 17% of ordinations, which is comparable to its frequency in the modern ordinations. Such high frequency of identification over a large sample size further emphasizes that the complex water-depth gradient is the most common primary gradient impacting the composition benthic communities in the modern and ancient records.

Lithology is the seventh most common variable along axis 1 after time and geographic location (Figure 2.7). Lithology is identified along axis 1 in 28% of the 29 ancient ordinations that include it and along axis 2 in 21% of those ordinations (Figure 2.7). As with substrate in the modern, this moderate frequency of identification across a large sample size emphasizes that lithology is a common primary and secondary gradient

controlling the composition of ancient benthic communities even when accounting for sample size.

Other physical and chemical gradients are more frequently recognized when calculated as a percentage of the ancient ordinations that include them (Figure 2.7). Oxygenation, turbidity, and salinity are common along axis 1, with oxygenation and turbidity identified along axis 1 in all ordinations that include them. Wave energy, temperature, and nutrients are common along axis 2, with wave energy and temperature identified in along axis 2 in all their ordinations. Such high frequencies of identification suggest that these physical and chemical gradients are just as important in controlling the composition of ancient benthic communities as they are in the modern. However, these gradients are included in less than 5 ordinations, with turbidity and temperature included only once (Figure 2.3). Greater sampling and inclusion of such variables in ancient ordinations is needed to verify the patterns seen here.

Identifying Additional Gradients in the Fossil Record that are Common in the Modern

Closely spaced and replicate sampling of faunal data and environmental data is necessary for identifying additional gradients that are independent of water depth in ancient settings. High-density, replicate sampling within depositional environments (i.e., shoreface, shallow subtidal, deep subtidal, offshore, etc.) will capture greater variability in fossil benthic assemblages (Bennington, 2003; Webber, 2005) even when ordinating assemblages from very small (e.g., less than 1 km) to much larger (e.g., 10s of km) spatial areas (see Webber, 2005; Redman et al., 2007; Perera and Stigall, 2018 for examples). Collecting environmental data with each sample as descriptively as the stratigraphic record allows will highlight the environmental variable in greater detail,

similar to the modern ordination studies. Such environmental data can be either qualitative or quantitative, though this will affect the choice of ordination method, and should draw from multiple lines of lithologic evidence, information on taxa ecologies, or geochemical proxies derived from the sediment or the skeletal material. The exact type of environmental data collected will vary as certain parameters, such as skeletal morphologies and geochemical proxies, will be affected by preservation potential and alteration after burial.

Several environmental parameters are common in modern ordinations and are likely to be preserved in the stratigraphic record. Identifying them in ancient marine settings will require collecting specific types of data

Variations in substrate type and consistency are one of the most common gradients identified in both the modern and the ancient. Field observations of lithologic composition and grain size should be included within the environmental datasets for ordinations, but this can be expanded upon. For faunal samples from unconsolidated sediments, sieving the sediments will collect data on exact grain sizes such as the amount of muds, sands, and coarse fragments, as well as mean grain sizes and sorting. Thin sections can be made for more consolidated lithologic samples, and point counts of thin sections can quantify the amount of different grain compositions such as lithic fragments, quartz, skeletal fragments, and mud. Trace fossils can provide information on the type of substrate. For example, the configuration of certain burrows such as *Ophiomorpha* or *Thalassinoides* will indicate non-cohesive or cohesive substrates respectively, *Glossifungites* reflects firm but non-lithified substrates, and *Trypanites* and other types of borings indicating hard substrates (Pemberton et al., 1992; Bromley, 1996). The

ecologies of taxa within the faunal assemblage may provide clues as to the substrate as well. Greater percentages of epifaunal, encrusting or attaching taxa may indicate hard substrates while a greater percentage of infaunal to semi-infaunal taxa indicates softer substrates (Tomašových, 2006; Redman et al., 2007; Perera and Stigall, 2018). The faunal assemblage can also be used to determine if seagrass or other marine vegetation was present. While seagrass has a poor preservation potential and appears sparsely in the fossil record (see Reich et al., 2015), the presence of certain species of mollusks (Daley, 2002; James and Bone, 2007; Zuschin et al., 2007; Reuter et al., 2012; Reich, 2014, Reich et al., 2014) as well as the co-occurrence of epiphytic foraminifera (Brasier, 1975; Cann and Clarke, 1993; Reuter et al., 2010; O'Connell et al., 2012) are suggestive of seagrass in the past.

Temperature is commonly inferred indirectly measured using $\delta^{18}O$ isotopic ratios from benthic foraminifera tests, benthic invertebrate shells, or carbonate sediment grains (Anderson and Arthur, 1983; Wefer and Berger, 1991). Carbonate shells and grains that precipitate in isotopic equilibrium with seawater will record higher amounts of $\delta^{18}O$ during colder periods, and lesser amounts during warmer periods (Epstein et al., 1953; O'Neil et al., 1969). If an organism imparts a vital effect and precipitates a carbonate shell in disequilibrium with seawater, the $\delta^{18}O$ values will not accurately reflect temperature (Wefer and Berger, 1991). However, many taxonomic groups have been investigated, and corrections can be made for taxa that predictably offset $\delta^{18}O$ (Wefer and Berger, 1991). $\delta^{18}O$ measurements are also influenced by salinity as increases in salinity also increases $\delta^{18}O$ values (Epstein and Mayeda, 1953; Railsback et al., 1989), which may lead to interpretations of colder temperatures. Mg/Ca ratios can be compared with

$\delta^{18}O$ to support the inferred paleotemperatures and potentially disentangle the effects of salinity, although this method is also problematic as Mg/Ca ratios can also be affected by salinity (see Katz et al., 2010 for review). While Mg/Ca ratios are commonly used for foraminiferal assemblages (Ferguson et al., 2008; Katz et al., 2010, Hönisch et al., 2013), it has been applied in other low-Mg calcite taxa such as belemnites (Rosales et al., 2004).

Oxygenation is also difficult to quantify in the stratigraphic record and is typically treated qualitatively. Trace-fossil abundance is the most common proxy for oxygenation as the presence of infaunal, multicellular life necessitates oxygen (Allison et al., 1995; Boyer and Droser, 2011). Ichnofabric indices (Droser and Bottjer, 1986; Taylor and Goldring, 1993; Miller and Smail, 1997) allow semi-quantitatively assessment of bioturbation intensity. While less common for invertebrate ichnofossils, grid-based estimations provide another metric to quantify bioturbation intensity, especially along bedding planes (Pemberton and Frey, 1984; Heard and Pickering, 2008; Marenco and Bottjer, 2010). Sediment color serves as a qualitative proxy for redox state, where darker sediments (i.e., blacks and greens) typically indicate reducing conditions and lighter sediments (i.e., tans and reds) indicate oxidizing conditions (Berner, 1981; Maynard, 1982). Molybdenum isotopic composition of carbonate sediments has been suggested as a quantitative proxy for redox state and oxygenation (Voegelin et al., 2010; Dickson et al., 2012; Westermann et al., 2014), although this method can be compromised depending on concentrations of sulfides in the water at time of fractionation (see Westermann et al., 2014 for review).

Nutrient levels and productivity are also gradients common in modern ordinations that may be identifiable in the fossil record. They are typically quantified using

geochemical proxies. $\delta^{13}C$ values of benthic foraminifera is the most common proxy for ancient productivity levels (see Katz et al., 2010 and references therein) and these values can be applied to any co-occurring marine benthic assemblage (see Belanger and Garcia, 2014 for example). $\Delta^{13}C$ values between epifaunal and infaunal benthic foraminifera or between planktonic and benthic foraminifera has also been suggested as a suitable proxy for productivity (Katz et al., 2010). Additionally, the relative abundance of benthic and infaunal foraminifera that co-occur with the invertebrate assemblage maybe used as a proxy for productivity. High relative abundances of benthic and infaunal foraminifera compared to planktonic and epifaunal foraminifera respectively indicate high-productivity conditions (Katz et al., 2010).

Variance Explained by Ordination Axes

Most ordination techniques portion variance such that the predominant source of variation in assemblages is represented the first axis of ordination with less variation explained on each subsequent axis (Figure 2.8). In the modern ordinations examined, percent variance and relative inertia values for the first axis range from 8.0–86.7% with a median value of 41.0% (Figure 2.8). In ancient ordinations, explained variance along the first axis ranges from 4.6–61.9% with a median value of 16.4% (Figure 2.8). Eigenvalues for the second axis of ordination explain less variation, but occasionally can still account for a large amount of variation in assemblages, in some cases nearly equivalent to the first axis (Figure 2.8). In the modern ordinations examined, percent variance and relative inertia values for the second axis ranges from 4.1–31.5 % with a median value of 19.9%, while the variation along the second axis ranges from 4.4–27.8% with a median value of 10.4% in the ancient ordinations examined (Figure 2.8). Given this substantial decrease

in variance explained and identifiable gradients on higher order axes, an essential question is determining how many ordination axes should be considered when identifying environmental gradients.

There are three approaches that can be used to determine the number of ordination axes that should be investigated. First, since most variation in the modern and ancient ordinations appear to be explained by the first two axes, ordinations can focus on the distribution of samples and species along the first two axes to infer environmental gradients. The downside to this approach is it potentially ignores additional, meaningful gradients if significant amounts of variance are still explained by higher axes of ordination. Second, environmental gradients can be examined along any axes with percent variance values greater than a predetermined threshold. Based on the previous studies examined here, a value of 10% variance explained may be a reasonable threshold for ancient ordinations. Alternatively, this threshold can also be calculated from the expected percent variance explained by one axis if all axes explain variation equally (Legendre and Legendre, 1998). For example, if PCA or CCA calculates 7 axes of ordination, the threshold can be set to 14.3% variance explained. Any axis with values less than the threshold percentage can be ignored. Third, distributions of samples and species can be examined along all axes up to where the percent variance explained produces diminishing returns (Legendre and Legendre, 1998; McCune and Grace, 2002). This approach will typically include the first and second axes of ordinations (Figure 2.8) but may demonstrate that the third axis occasionally needs to be explored for potential gradients.

CONCLUSIONS

The complex water-depth gradient is the most common gradient associated with assemblage variation in benthic marine invertebrates in modern studies. Variations in substrate type (i.e., composition, grain size, hard vs. soft substrates) are the second most common environmental gradients, suggesting substrate contributes to a large amount of variation in modern benthic community structure. Other gradients such as vegetation density, salinity, temperature, and pollution are less commonly identified along orthogonal axes to water depth or when sampling within narrow depth ranges, demonstrating the strong correlation between water depth and assemblage composition.

Similar to modern marine systems, the complex water-depth gradient is also the most common gradient associated with benthic invertebrate communities in ancient settings. Variations in substrate and lithology (i.e., composition, grain size, and substrate hardness) are the second most common environmental gradients when water depth is correlated along an orthogonal axis, implying that substrate also contributes a large amount of variation to ancient community structure similar to modern communities. Sedimentological, taxonomic, and geochemical proxies may be used to temperature and nutrient gradients, but this is contingent on the preservation of the fossil material and may only be applicable in few cases.

The amount of variance explained in ancient ordinations is generally small compared to modern ordinations, with much variance left unexplained. In modern ordinations, axis 1 and 2 explain about 41.0% and 19.9% of variance in assemblage composition; ancient ordinations explain about half as much variance. Closely spaced, replicate sampling of fossil assemblages and environmental data are needed to identify detailed environmental gradients in ancient marine settings. Exploring ancient benthic

invertebrate assemblages for these additional gradients will identify potential environmental mechanisms for the heterogenic nature of fossil assemblages.

TABLES

Table 2.1 Frequency of identified gradients along the first two axes of modern ordinations.

Gradient	Axis 1 (45 gradients)	Axis 2 (30 gradients)
Water depth	37.8%	13.3%
Substrate	17.8%	20.0%
Vegetation	13.3%	3.3%
Salinity	6.7%	10.0%
Pollution	6.7%	6.7%
Life habit	4.4%	6.7%
Wave energy	4.4%	3.3%
Temperature	2.2%	10.0%
Nutrients	2.2%	3.3%
Turbidity	2.2%	3.3%
Shelf patchiness	2.2%	3.3%
Latitude	–	10.0%
pH	–	3.3%
Time	–	3.3%

Table 2.2: Frequency of identified gradients along the first two axes of ancient ordinations.

Gradients	Axis 1 (54 gradients)	Axis 2 (31 gradients)
Water depth	35.2%	16.1%
Time	22.2%	16.1%
Substrate	14.8%	19.4%
Geography	9.3%	9.7%
Oxygen	7.4%	–
Taxa ecology	3.7%	16.1%
Salinity	3.7%	3.2%
Turbidity	1.9%	–
Nutrients	1.9%	6.5%
Wave energy	–	9.7%
Temperature	–	3.2%

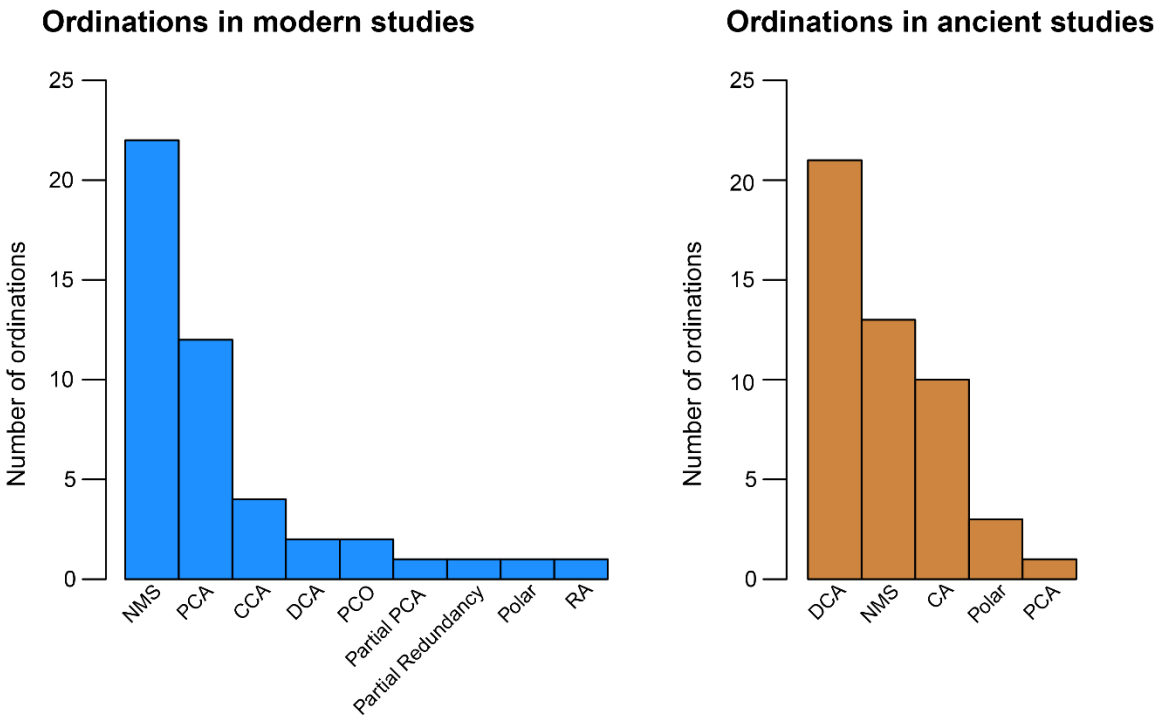

Figure 2.1: Frequency of ordinations used by modern and ancient studies.

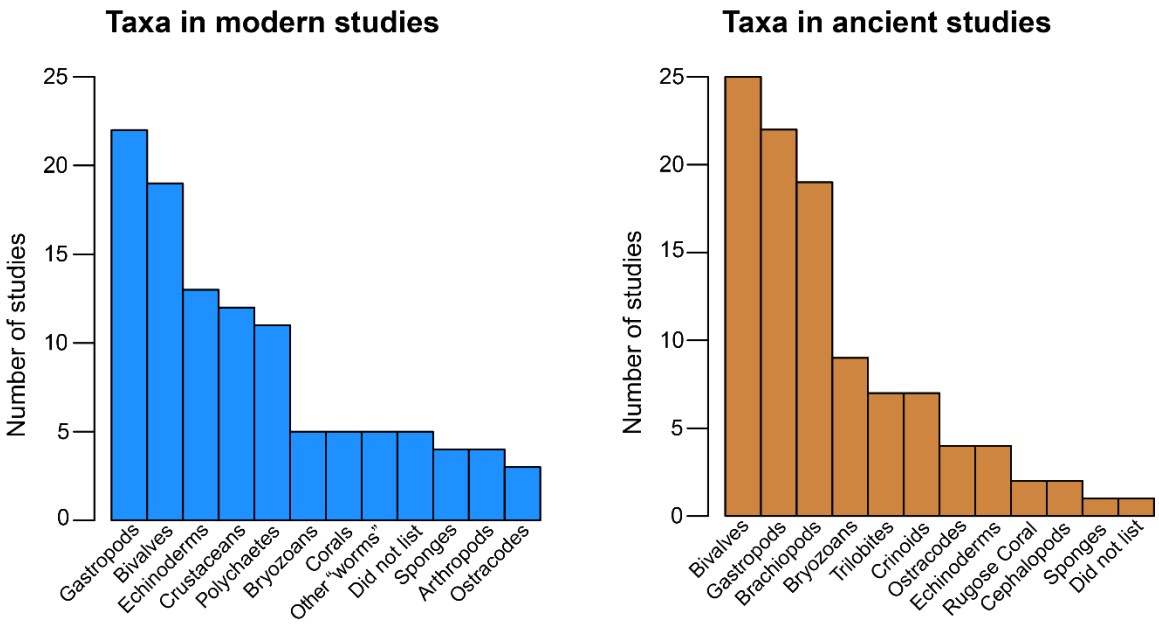

Figure 2.2: Taxonomic groups studied in the ancient and modern studies.

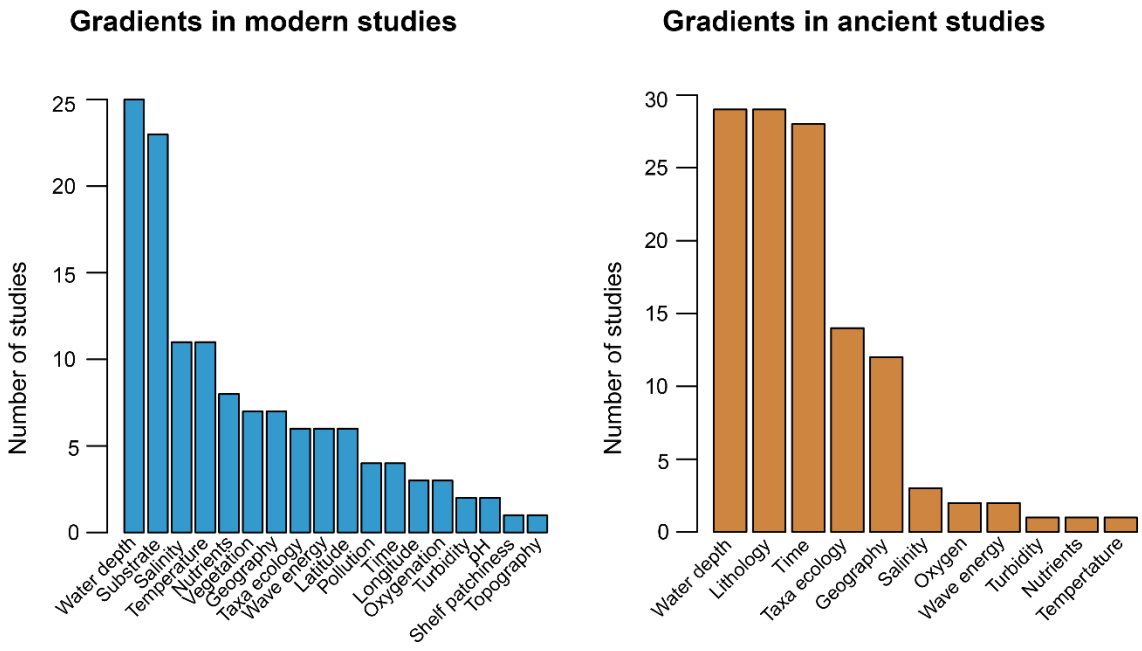

Figure 2.3: Frequency of the various environmental gradients considered by modern and ancient studies.

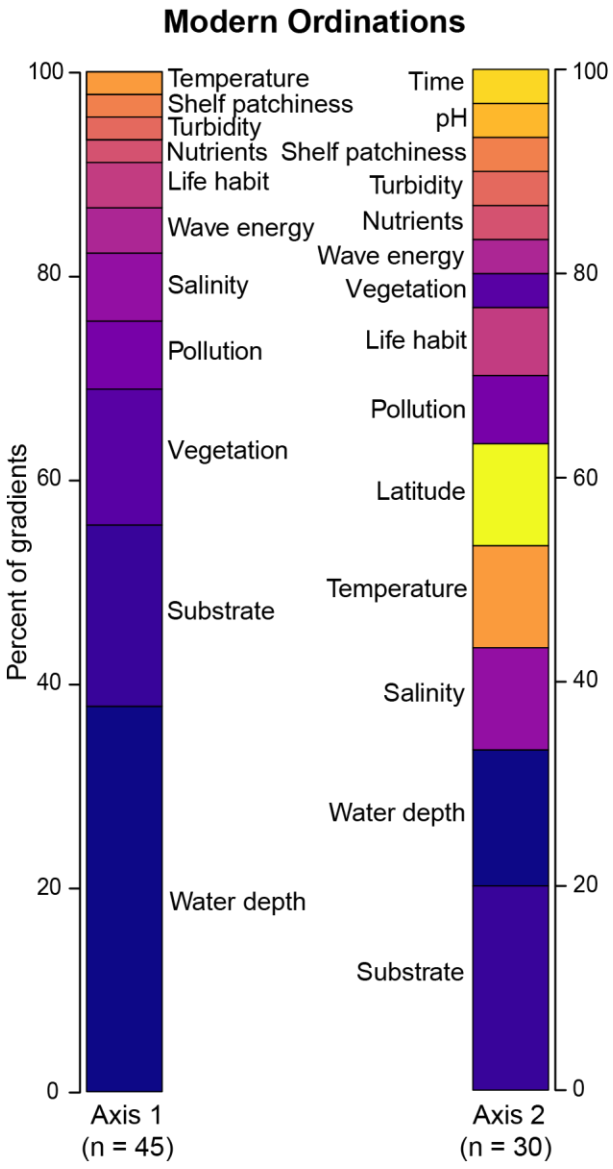

Figure 2.4: Reported results of gradients along each axis of ordination for modern marine benthic invertebrates. n represents the total number of gradients identified along each axis.

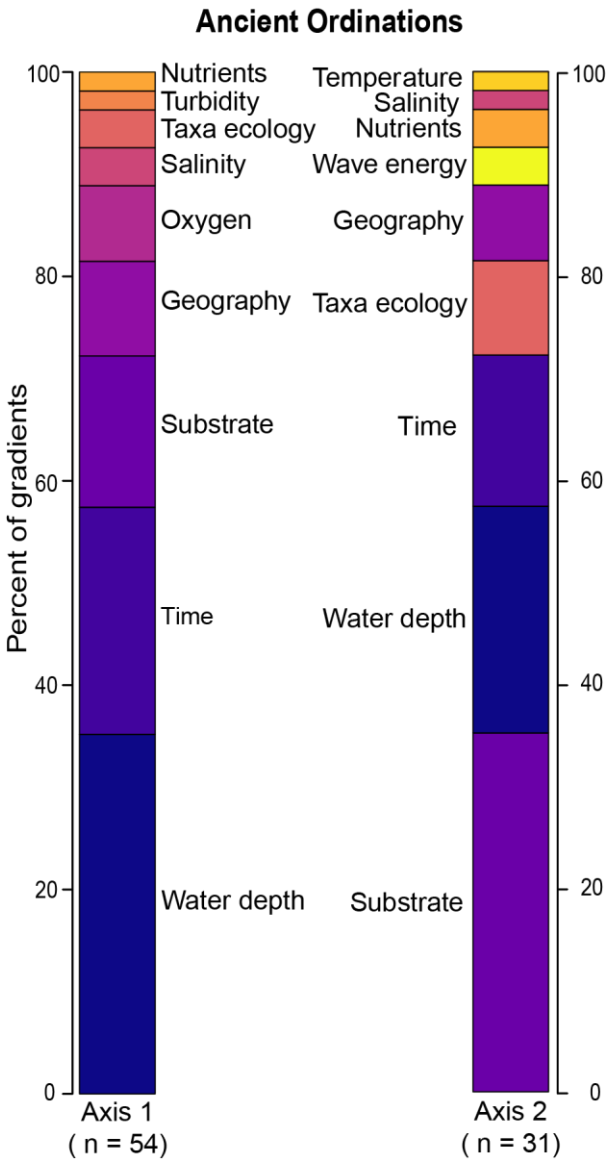

Figure 2.5: Reported results of gradients along each axis of ordination for ancient marine benthic invertebrates. Taxa ecology includes life habits and diversity gradients. n represents the total number of gradients identified along each axis.

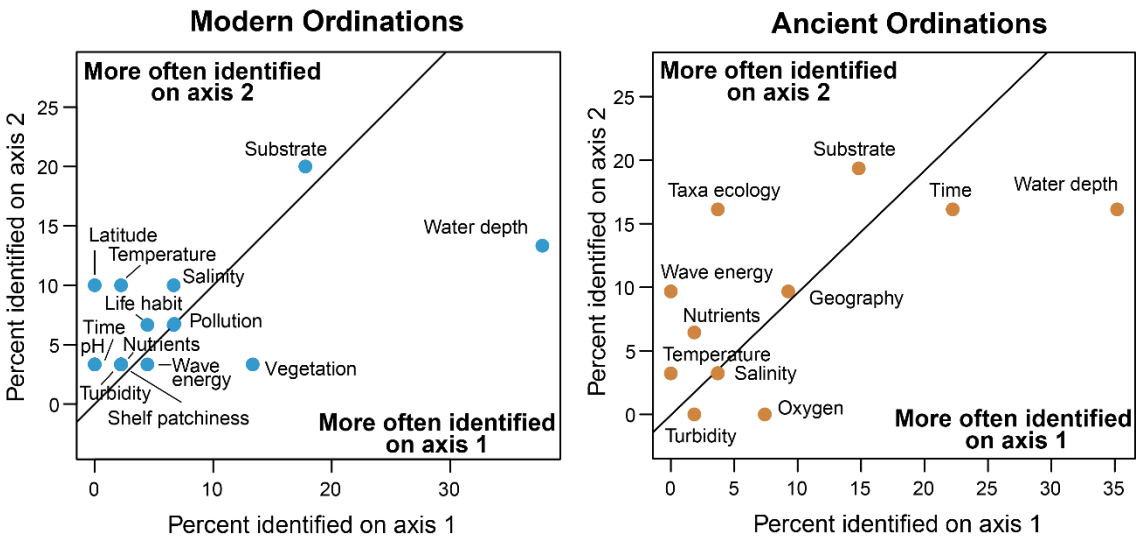

Figure 2.6: Comparison of gradient distributions along Axis 1 and Axis 2 across all ordinations in modern and ancient studies. Percent identification reflects the number of times a gradient was identified across all ordinations.

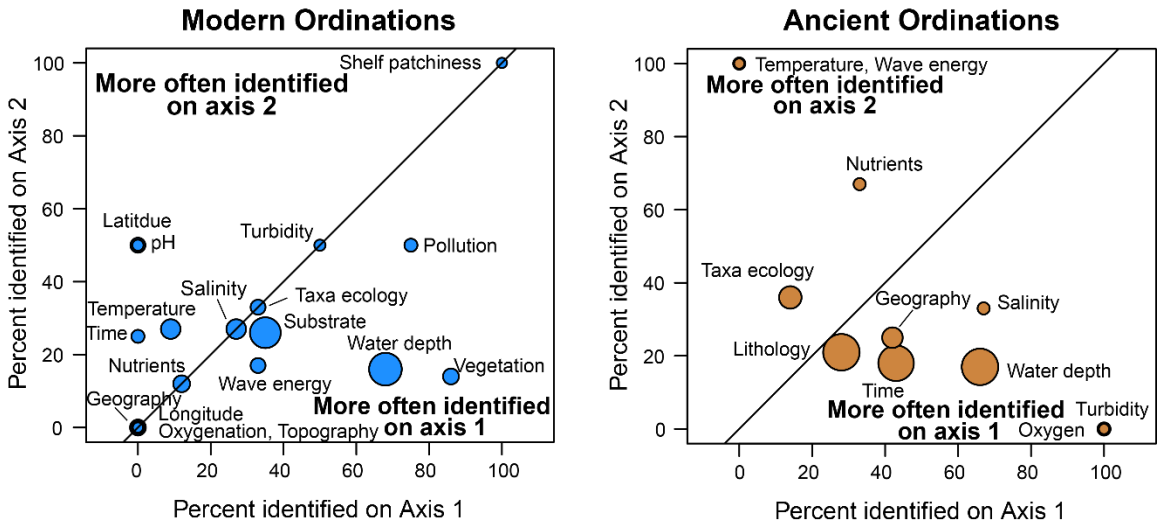

Figure 2.7: Weighted comparison of gradient distributions along Axis 1 and Axis 2 in modern and ancient studies. Percent identification represents the frequency a gradient was identified using only the ordinations in which it was included. The sizes of the circles are proportional to the number of ordinations in which a gradient was included.

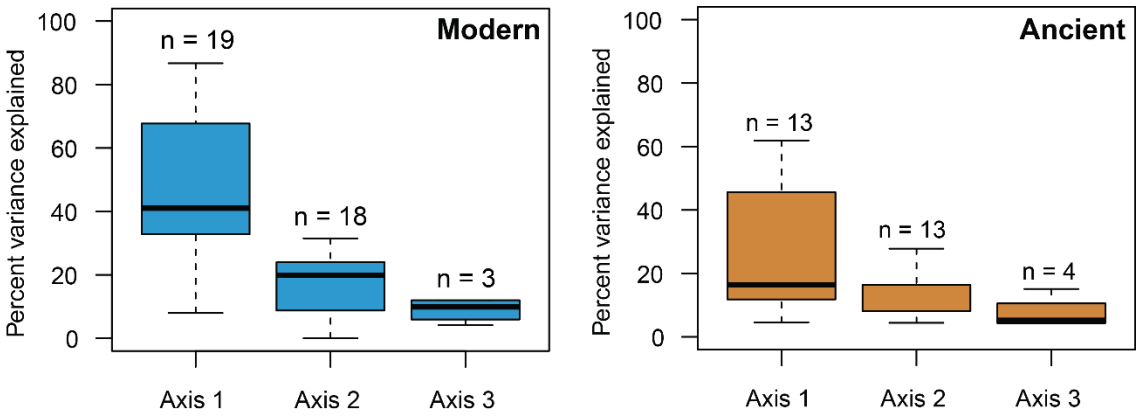

Figure 2.8: Percent variance explained for the first three axes of ordination as reported by the authors for modern and fossil ordinations of marine benthic invertebrates. n represents the number of ordinations that reported percent variance for each axis.

CHAPTER 3

ENVIRONMENTAL CONTROLS ON SHALLOW SUBTIDAL MOLLUSCAN DEATH ASSEMBLAGES ON SAN SALVADOR ISLAND, THE BAHAMAS[2]

[2] Brown, G.M. and E. Larina. 2019. Palaeogeography, Palaeoclimatology, Palaeoecology v. 527, p. 14–24. Reprinted here with permission from the publisher

ABSTRACT

Ecological studies that span multiple marine depositional environments frequently find that benthic invertebrate assemblages are correlated primarily with an onshore-offshore gradient. Variability within the same depositional environment is inferred to not result from water depth differences, but other parameters such as substrate consistency and shear stress. Modern studies focusing on assemblage variations within the same depositional environment can identify which variables affecting assemblage compositions are independent of water depth. This study examines the environmental controls on the composition of molluscan death assemblages from the shallow subtidal environments of San Salvador Island. Molluscan assemblages were tabulated from twenty-nine bulk samples collected from four locations around San Salvador Island representing seagrass meadows, open sandflats, and patch reef systems common in the shallow subtidal. In addition, quantitative environmental data for each sample was characterized, including seagrass density, water depth, temperature, pH, dissolved oxygen, and grain-size, as well as qualitative observations of wave energy and bioturbation. Cluster analysis and canonical correspondence analysis (CCA) were performed to identify environmental gradients associated with molluscan assemblage composition. Cluster analysis and CCA Axis 1 identify seagrass coverage and substrate consistency as the primary environmental variables describing molluscan death assemblage compositions. CCA Axis 2 identifies wave energy, bioturbation, and dissolved oxygen as the secondary environmental variables, though the small range of dissolved oxygen values (17–21 mg/L) collected using single, instantaneous measurements make it unclear whether the oxygen gradient is ecologically significant for our time-averaged assemblages. Our analysis demonstrates

the variability of assemblages within a single depositional environment, as well as the utility of fine-resolution studies for identifying secondary environmental variables that control the composition of marine invertebrate assemblages.

INTRODUCTION

Numerous large-scale modern and ancient ecological studies identify water depth as the major variable associated with differences in marine invertebrate assemblage compositions (see Patzkowsky and Holland, 2012 for review). Water depth is a complex gradient that encompasses several correlated variables such as substrate type, salinity, oxygen and nutrient levels, sunlight penetration, and temperature. The variation of assemblages across multiple depositional environments results from a combination of water depth and these correlated variables. Several paleoecological studies examining fossil assemblages within a single depositional environment (e.g. shoreface, shallow subtidal, offshore, etc.) identify considerable within-environment faunal variation (Holland et al., 2001; Webber, 2002; Redman et al., 2007; Perera and Stigall, 2018). Since depositional environments are interpreted to be of approximately similar depths within a given basin, variation in assemblage composition within a depositional environment should result from factors uncorrelated with water depth.

Modern ecological studies of life and death assemblages of marine benthic invertebrates demonstrate that benthic communities vary within the same depositional environment and that this variation results from environmental parameters such as substrate type (i.e., hard substrates versus soft sediments; Llewellyn and Messing, 1993; Ivany et al.,1994), variations in seagrass diversity and density (Miller, 1988; Ferguson and Miller, 2007; Ferguson, 2008; Reich, 2014), wave energy (Casebolt and Kowalewski,

2018), and pollution (Moore, 1974; Smith et al., 2001). These variables, while commonly correlated with changes in water depth, were determined to be depth-independent because these studies examined assemblages within a limited geographic area and within the same depositional environment. Except for substrate type, these variables can be difficult to measure in the fossil record and must be inferred from a few proxies derived from lithologic and skeletal material, and these proxies can be impacted by preservation. Given the heterogenic nature of modern and fossil marine benthic communities from the same depositional environment (e.g., shoreface, offshore transition, etc.), fine-resolution, replicate sampling is needed to identify differences in assemblage compositions within such limited spatial scales (Bennington, 2003; Webber, 2005). Studies in modern settings using fine-resolution sampling of benthic communities, coupled with measurements of environmental factors that are potentially preservable may reveal which parameters correlate to within-environment variation in the fossil record.

Here we examine the environmental controls on variation of modern molluscan death assemblages from a limited bathymetric range (1–5.2 m) within the shallow subtidal of San Salvador Island, The Bahamas to identify depth-independent sources of community variation. This carbonate platform has a high diversity of mollusks (Redfern, 2013) within seagrass meadows, patch reefs, sandflats, restricted lagoons, and tidal inlets (Hinman, 1994). Previous work on San Salvador Island identify distinct molluscan assemblages based on seagrass density and wave energy in the shallow subtidal (Reich, 2014; Casebolt and Kowalewski, 2018). This study builds off that approach by including additional environmental parameters likely to be preserved in the fossil record, specifically, grain size, and bioturbation intensity as well as less common variables such

as temperature and oxygenation, which can be inferred in the lithologic record using geochemical and sedimentological proxies. By restricting our sampling to shallow subtidal areas, the effects of water depth should be minimized such that water depth should not be the primary environmental variable explaining the differences in death assemblage compositions. Rather, based on previous works on shallow subtidal assemblages in the Caribbean Sea (Miller, 1988; Deehr et al., 2001; Zimmerman et al., 2001; Ferguson and Miller, 2007; Reich, 2014; Casebolt and Kowalewski, 2018), we predict that vegetation density and substrate type will be the primary controls on death assemblage compositions.

STUDY AREA

San Salvador Island is located on the eastern edge of the Grand Bahama Bank (24.1° N, 74.5° W; Figure 3.1A). This subtropical isolated carbonate platform contains a wide variety of coastal environments that include seagrass meadows, patch reefs, sandflats, rocky substrates, restricted lagoons, and tidal inlets (Hinman, 1994). Within the shallow subtidal zone, seagrass meadows, patch reefs, and open sandflats are the most common environments. Each exhibit different substrate types (i.e. vegetated, hard, and soft respectively) and can all be found under different wave-energy conditions.

Four locations were chosen to capture the environmental variability of open marine, shallow subtidal environments around San Salvador Island (Figure 3.1B). Graham's Harbour (24.121° N, 74.466° W) is a moderate energy, protected lagoon on the northern side of the island (Colby and Boardman, 1989; Reich, 2014). While Graham's Harbour contains seagrass meadows, sandflats, and patch reefs within its 6 km^2 area (Colby and Boardman, 1989; Deehr et al., 2001; Zimmerman et al., 2001), we sampled

only within the seagrass meadows located just north of the entrance to the Gerace Research Center because the sandflats and patch reefs are located far from shore. French Bay (23.951° N, 74.544° W) is the second vegetated site and is a high-energy (Troy Dexter personal communication, 2017) seagrass meadow on the southwestern side of the island. Sampling at French Bay was limited to approximately 50 m from shore owing to intense waves, whereas sampling at other sites ranged from 100 m to 250 m from shore. Fernandez Bay (24.021° N, 74.526° W) is a low-energy embayment (Casebolt and Kowalewski, 2018) on the western side of the island. We sampled within the unvegetated sandflats located between the rocky subtidal environments and the reefs farther offshore at the rim of the platform. Sand Dollar Beach (24.106° N, 74.520° W) is the second unvegetated site and is a moderate- to high-energy sandflat (Hinman, 1994) on the northwestern side of the island. Two areas were sampled at Sand Dollar Beach (Figure 3.1C). The first are sandflats protected by the Rocky Point promontory, and the second are exposed sandflats windward of several patch reefs (24.107° N, 74.522° W). These reef-proximal sandflats were sampled as proxies for the patch reef environment as direct sampling from the patch reef was not authorized, and these reef-proximal sandflats were expected to include sediment and shell material washed in from adjacent patch reefs.

The possibility of vertical and lateral mixing of assemblages must be considered with any death assemblage study. Shallow-subtidal sediments on San Salvador Island are rich in shell and skeletal material (Randazzo and Baisley, 1995) and contain an abundant molluscan assemblage. Radiocarbon dating of thirty *Tucetonia pectinata* collected from the shallow subtidal of Fernandez Bay indicate the molluscan death assemblage is time-averaged over the last 4000 years, with an average age of 1830 years before present

(Kowalewski et al., 2018). Fine-scale patchiness of death assemblages is still evident on San Salvador Island (Casebolt and Kowalewski, 2018), even though it is frequently hit by hurricanes and storms. This indicates the impact of transport and reworking by storm events is not sufficient to homogenize the assemblage, which is consistent with other death assemblage studies (Miller and Cummins, 1990; Kidwell and Bosence, 1991; Miller et al., 1992; Albano and Sabelli, 2011; Casebolt and Kowalewski, 2018).

METHODS

Sample Collection and Processing

Twenty-nine death assemblage samples were collected from shallow subtidal environments at the four locations around San Salvador Island (Figure 3.1B). Death assemblages were collected as 1-gallon (3.78 L) surficial, bulk samples using SCUBA along 30 m transects perpendicular to the shoreline. Each sample was collected at lateral intervals of 15 m along each transect using a measuring tape. Three transects were conducted at Graham's Harbour, two at French Bay, two at Fernandez Bay, and three from Sand Dollar Beach. Each transect contains three samples, except for one French Bay transect containing two samples. Nine samples were collected from Graham's Harbour, five from French Bay, six from Fernandez Bay, and nine from Sand Dollar Beach. Water depths for all samples ranged from 1 to 5.2 m, with an average depth of 3 m.

Bulk samples were wet-sieved at the Gerace Research Centre using a 1-mm mesh. Mollusks from the death assemblage were collected from a random subsample of the sieved material, identified to species using Redfern (2013), and counted until approximately fifty individuals were reached. A sample size of fifty individuals was

chosen as analyses of both modern and ancient studies demonstrate that datasets with a median sample size of fifty individuals produce the same multivariate results and preserve the same ecological signals as datasets with much larger sample sizes (Forcino, 2012; Forcino et al., 2015). The number of bivalve individuals for a given species is the sum of the number of articulated specimens and the number of left or right valves that had complete umbos, whichever is greater. Gastropod individuals are those with complete apices.

Environmental data was also collected at each site to determine potential environmental variables controlling assemblage compositions. For each sample, water depth, temperature, and observations on the amount of bioturbation (i.e., density of callianassid burrows, feeding traces, resting traces) and qualitative wave energy were recorded. Bioturbation and wave energy were given a numeric score from 1 to 4 based on intensity at time of recording, with a score of 1 indicating rare bioturbation (1–2 surficial burrows or traces adjacent to sampling area) or relatively low wave energy, and a score of 4 indicating abundant bioturbation (7+ surficial burrows or traces adjacent to sampling area) or extremely high wave energy. A 20 mL water sample was collected from the sediment-water interface, and pH and dissolved oxygen levels (mg/L) were measured on this sample at the Gerace Research Center.

Seagrass and algae were collected from within a 25 cm by 25 cm grid to standardize collection size, identified to species level, and counted. Algae accounted for a small proportion of vegetation, so analyses only considered seagrass. Seagrass density was calculated using the seagrass coefficient of Zimmerman et al. (2001) (modified from Miller 1988):

$$S.C. = 0.0025T + 0.0007S + 0.0002H \quad (1)$$

where T, S, and H are the blade counts per m^2 of *Thalassia testudinum, Syringodium filiforme,* and *Halodule wrightii*, the three most abundant species of seagrass on San Salvador Island (Smith et al., 1990; Deehr et al., 2001; Zimmerman et al., 2001; Reich, 2014). The coefficients represent the m^2 surface area per m^2 area of seafloor for each seagrass genus (Deehr et al., 2001; Zimmerman et al., 2001).

A small amount of sediment (< 250 g) was collected at each site for grain-size analysis. Sediment samples were gathered after vegetation collection but prior to faunal collection to minimize loss of fine-grained material. Sediment samples were dried under a fume hood for several weeks at the University of Georgia. Approximately 180 g of dried sediment was dry-sieved through a series of meshes ranging from -1 to 4 ϕ. Mean grain size for each sample was calculated using the first-moment method (see Lewis and McConchie, 1994)

$$\phi = \frac{\Sigma fd}{N} \quad (2)$$

where *f* is the weight (in g) of sediment in the sieve, *d* is the sieve size (in ϕ), and N is the total weight (in g) of the sieved material, and ϕ is the mean grain size of the sample (reported on the phi-scale).

Statistical Analyses

Spearman's rank correlation tests were performed among the environmental variables to identify monotonic relationships between them. Spearman's rho values were considered statistically significant (i.e., non-zero) when p-values are less than 0.05.

Q-mode cluster analysis was performed on a culled species-abundance matrix using the cluster package of the statistical software R (R Development Core Team, 2015) to identify relationships in faunal similarity among samples. The culled species-abundance matrix was created by removing species with proportional abundances less than 1% of the original species-abundance matrix. Before cluster analysis, the culled abundance matrix was transformed into a proportional abundance of a species relative to the total number of individuals to account for variation in sample size. Q-mode cluster analysis was performed on a Bray-Curtis dissimilarity matrix among samples. Ward's Method was used as the linkage method as it minimizes the increase of error in the sum of squares of distances between samples and produces well-defined, compact clusters (McCune and Grace, 2002).

R-mode cluster analysis was also performed on the culled species-abundance matrix using the cluster package of R (R Development Core Team, 2015) to determine which taxa co-occur. Prior to cluster analysis, the data were transformed first by the proportional abundance of species to correct for differences in sample size, followed by a percent transformation of each species relative to its maximum abundance to correct for variations in species abundance. The R-mode cluster analysis used the Bray-Curtis distance matrix and the Ward's Method for linkage. The R-mode cluster analysis was combined with the Q-mode cluster analysis using the pheatmap package for R (R Development Core Team, 2015) to produce a two-way cluster analysis that was used to define the biofacies of each sample.

The faunal data and the environmental data were jointly analyzed using canonical correspondence analysis (CCA) to identify environmental gradients driving variations in

the faunal composition of samples. CCA ordinates the species-abundance matrix using correspondence analysis, in which samples are ordinated based on taxonomic similarities such that samples with similar taxonomic compositions plot closer to one another (ter Braak, 1986; McCune and Grace, 2002). The ordination is then constrained by a multiple linear regression using a second data set composed of the environmental variables (ter Braak, 1986; McCune and Grace, 2002). By constraining the faunal data with environmental data, CCA is a direct gradient analysis where the distribution of samples along the axes of ordination relates directly to the measured environmental variables (ter Braak, 1986; McCune and Grace, 2002). This is graphically represented in the ordination diagram where samples and taxa are plotted within the ordination space and the environmental variables are overlain as a series of vectors. The direction of these vectors identifies how well correlated each variable is with each ordination axis. As a result, interpretations of environmental gradients controlling sample distributions are more apparent than in indirect gradient analyses such as nonmetric multidimensional scaling or detrended correspondence analysis. CCA was performed using the vegan package for R (R Development Core Team, 2015). The species-abundance matrix was transformed first by proportional abundance then by percent maximum transformation. No data transformations were applied to the environmental matrix. Default settings were used in the CCA, with the exception that samples with missing values for environmental variables were removed from the analysis (2 samples).

RESULTS

Environmental Variable Correlations

Sixteen of the sixty-six environmental variable correlations are statistically significant ($p < 0.05$; Table 3.1). The strongest correlations are between water depth and distance from shore ($\rho = 0.792$, $n = 29$, $p < 0.001$), seagrass density and percent fine-grained sediments ($\rho = 0.813$, $n = 27$, $p < 0.001$), percent fine-grained sediments and percent sands ($\rho = -0.703$, $n = 29$, $p < 0.001$), and percent sands and percent gravel ($\rho = -0.915$, $n = 29$, $p < 0.001$). Seagrass density is moderately, negatively correlated with pH ($\rho = -0.517$, $n = 27$, $p < 0.001$), water depth ($\rho = -0.454$, $n = 27$, $p < 0.05$), dissolved oxygen ($\rho = -0.392$, $n = 27$, $p < 0.05$), and percent sands ($\rho = -0.491$, $n = 27$, $p < 0.01$). Bioturbation is moderately, positively correlated with water depth ($\rho = 0.390$, $n = 29$, $p < 0.05$), temperature ($\rho = 0.450$, $n = 29$, $p < 0.05$), and moderately, negatively correlated with wave energy ($\rho = -0.429$, $n = 29$, $p < 0.05$) and percent fine-grained sediments ($\rho = -0.362$, $n = 29$, $p < 0.05$). Wave energy is moderately, negatively correlated with percent sands ($\rho = -0.620$, $n = 29$, $p < 0.001$) and percent gravel ($\rho = -0.674$, $n = 29$, $p < 0.001$). Percent fine-grained sediments are moderately, positively correlated with percent gravel ($\rho = 0.448$, $n = 29$, $p < 0.01$), and moderately, negatively correlated with water depth ($\rho = -0.441$, $n = 29$, $p < 0.05$).

Taxonomic Composition of Samples

In this study, 1444 individuals from 109 molluscan species were counted among twenty-nine samples. Bivalves (42 species, 48% of individuals) and gastropods (64 species, 51% of individuals) dominate, with rarer scaphopods (3 species, 1% of individuals). Common bivalves include *Transennella conradina* (n=224), *Crenella*

divaricata (n=97), and *Ctenocardia guppyi* (n=62). Common gastropods include *Finella adamsi* (n=149), *Eulithidium thalassicola* (n=86), *Cerithium eburneum* (n=53), *Acteocina sp*. (n=53), and *Zebina browniana* (n=50).

Cluster Analysis

Cluster analysis identified two major groups of molluscan associations that represent assemblages from either vegetated or unvegetated substrates (Figure 3.2). Samples in Cluster 1 are all from seagrass meadows in Graham's Harbour and French Bay. Cluster 1A contain samples predominately from French Bay that are highly diverse with high abundances of the chemosymbiotic bivalve *Lucina pensylvanica*, the epiphytic gastropods *Eulithidium thalassicola* and *Smaragdia viridis*, and the epifaunal grazing gastropods *Cerithium litteratum*, *Cerithium atratum*, and *Cerithium eburneum*. Cluster 1B contains samples predominately from Graham's Harbour that are less diverse than Cluster 1A with high abundances of the gastropods *Eulithidium thalassicola* and *Cerithium eburneum* and the bivalves *Lucina pensylvanica* and *Transennella conradina*.

Seagrass densities between Cluster 1A and Cluster 1B are similar overall, with overlapping seagrass coefficient values (Figure 3.3). Seagrass coefficients for Cluster 1A (predominantly French Bay samples) range from 3.23 to 8.19, with a median value of 5.36. Seagrass coefficients for Cluster 1B (predominantly Graham's Harbour samples) have a greater range from 0 to 8.67 and a smaller median value of 4.72.

Samples in Cluster 2 are from the unvegetated open sandflats of Sand Dollar Beach and Fernandez Bay and the reef-proximal sandflats from Sand Dollar Beach (Figure 3.2). Cluster 2 is defined by high abundances of the gastropod *Finella adamsi* and the bivalves *Transennella conradina* and *Ctenocardia guppyi*. Specifically, Cluster 2A is

a mixture of reef proximal and open sandflat samples from Sand Dollar Beach that are dominated by the gastropod *Finella adamsi*. Cluster 2B is a mixture of reef-proximal samples from Sand Dollar Beach and open sandflat samples from Fernandez Bay that are dominated by the bivalve *Transennella conradina*.

Canonical Correspondence Analysis

Constraining the species-abundance ordination by the environmental data explains a total of 46% of the variation in assemblages (Table 3.2). The first three axes of ordination were examined based on diminishing returns in the change of inertia and the percent variance explained after the third axis (Table 3.3). These first three axes explain 7.14%, 6.33%, and 5.12% of the variation respectively for a cumulative 18.59% variance explained. These values are common for CCA as the method frequently produces percent variance explained measurements of less than 10% for strong gradients within ecological datasets (ter Braak and Verdonschot, 1995).

Biplot scores for the environmental variables along the first three axes of ordination were also calculated to determine their loadings on a given axis (Table 3.4). A higher magnitude score (positive or negative) indicates an environmental variable has a higher correlation with that axis. Axis 1 contrasts seagrass density (-0.867) and percent fine-grained sediments (-0.817) versus distance offshore (0.438), water depth (0.489), and percent sand (0.538). Axis 2 contrasts wave energy (-0.699) and dissolved oxygen (-0.498) against bioturbation (0.652). Axis 3 contrasts mean grain size (-0.379) and water depth (-0.328) versus bioturbation (0.451) and temperature (0.604). Percent gravel was removed by the *cca* function as it was found to be collinear with percent sand.

Species scores along the first three axes of ordination were also calculated to determine their loadings on a given axis (Table 3.5, Supplementary Table 3.1). A higher magnitude score (positive or negative) indicates a species has a higher correlation with that axis. Abundant species with large negative values for CCA Axis 1 scores includes the chemosymbiotic bivalves *Lucina pensylvanica* (-0.865) and *Parvilucina costata* (-0.904) and epifaunal gastropods *Cerithium atratum* (-1.153), *Cerithium litteratum* (-0.577), *Eulithidium thalassicola* (-0.872), *Patelloida pustulata* (-1.174), and *Smaragdia viridis* (-1.225) (see Table 3.5). Taxa with negative CCA Axis 1 scores are associated with samples that are shallower, vegetated, and contain a greater percentage of fine-grained sediments (Figure 3.4C). Abundant species with large positive values for CCA Axis 1 scores includes the bivalves *Ctenocardia guppyi* (0.478), *Ervilia concentrica* (0.447), *Fugleria tenera* (0.696), *Scissula similis* (0.446), *Transennella conradina*. (0.479), and the gastropods *Eulithidium affine* (0.682), *Finella adamsi* (0.589), and *Rissoina krebsii* (0.702) (Table 3.5). Taxa with strong positive CCA Axis 1 scores are associated with samples that are deeper, unvegetated, and contain a greater percentage of coarser grained sediments (Figure 3.4C). Abundant species with large negative CCA Axis 2 scores include the chemosymbiotic bivalve *Lucina pensylvanica* (-0.647) and the gastropods *Cerithium atratum* (-0.895), *Patelloida pustulata* (-1.237), and *Smaragdia viridis* (-1.225) (Table 3.5), and are associated with higher wave energy and dissolved oxygen values, and less bioturbation (Figure 3.4C and D). Abundant species with large positive CCA Axis 2 scores include the bivalves *Angulus sybariticus* (0.453) and *Chione elevata* (0.354) and the gastropod *Zebina browniana* (0.882) (Table 3.5), and are associated with lower wave energy and dissolved oxygen values, and more bioturbation

(Figure 3.4C and D). Abundant species with large negative CCA Axis 3 scores include the bivalves *Ervilia concentrica* (-0.483) and *Fugleria tenera* (-0.506) (Table 3.5), and are associated with cooler, less bioturbated samples (Figure 3.4D). Species with strong positive CCA Axis 3 scores include the bivalve *Crenella divaricata* (0.455) and the gastropods *Eulithidium affine* (0.425) and *Finella adamsi* (0.353) (Table 3.5), and are associated with warmer, more bioturbated samples (Figure 3.4D). Although many single occurrence and low abundance species (i.e., those with proportional abundances less than 1% of the overall dataset) also have strong species scores (Supplementary Table 3.1), their low abundances are not likely to drive the patterns within the CCA.

DISCUSSION

Seagrass Density in Graham's Harbour and French Bay

Seagrass densities of samples collected at Graham's Harbour and French Bay are overall similar, with median seagrass coefficient values of 4.72 and 5.36 and overlapping ranges (Figure 3.3). Graham's Harbour samples has greater variability in seagrass density (Cluster 1B; Figure 3.3), and a lower density of seagrass than French Bay (Cluster 1A). Seagrass coefficients in our study for Graham's Harbour are generally lower than those found in previous studies for seagrass meadows in Graham's Harbour (Deehr et al., 2001; Zimmerman et al., 2001). In our study, seagrass coefficients in Graham's Harbour ranges from 0 to 8.67. Zimmerman et al. (2001) calculated seagrass coefficients from approximately 8 to 10 for seagrass meadows in Graham's Harbour. Only two Graham's Harbour samples from our study have coefficient values comparable to those from seagrass meadows in Zimmerman et al (2001). Most Graham's Harbour samples in our study have values comparable to the less dense seagrass-sand "transitional zone" of

Zimmerman et al. (2001). Additionally, lower vegetation densities have been reported in Graham's Harbour directly north of the Gerace Research Centre, where our study was located, compared with other seagrass meadows around San Salvador Island (Smith et al., 1990; Reich, 2014). In our study, seagrass coefficients at French Bay correspond to the low end of Zimmerman et al.'s (2001) seagrass meadows and transitional zone in Graham's Harbour, but no previous studies are available of seagrass coefficients in French Bay for comparison.

Correlation of Environmental Variables

Relatively few variables correlate with water depth (Table 3.1). Samples farther from shore were frequently deeper, as expected. Although San Salvador Island is a relatively flat-topped carbonate platform, the shallow subtidal still has a shallow bathymetric gradient. In Graham's Harbour, for example, water depth a kilometer from shore is approximately six meters (Colby and Boardman, 1989). Bioturbation also increases with water depth. This may reflect a change in substrate with depth, as seagrass density decreases with increasing water depth.

Although bioturbation and seagrass density are both correlated with water depth, there is no statistically significant relationship between seagrass density and bioturbation. The vegetated French Bay samples (Cluster 1A, Figure 3.3) were given a bioturbation score of 1 (i.e., rare surficial traces), indicating we observed only 1–2 traces, typically callianassid burrows, at each sample location. The more variable Graham's Harbour samples (Cluster 1B) were given a bioturbation score of 3 (i.e., common surficial traces), indicating we observed approximately 5 traces, typically callianassid burrows, at each sample location. Unvegetated samples (Clusters 2A and 2B, Figure 3.3) were given

scores ranging from 2–4 with an average bioturbation score of 3, similar to the vegetated Graham's Harbour samples. While there is no statistical relationship in abundance of surficial traces and seagrass density, there is a qualitative observation of increasing trace diversity among the unvegetated samples. In addition to callianassid burrows, starfish resting traces and dugouts formed by fish and sting rays were also identified on the sandflats. It is likely that these types of traces are also present in the seagrass meadows but may have been obscured by the vegetation and thus were not observed.

Seagrass density is negatively correlated with water depth, with seagrass meadows present in shallower samples, and completely unvegetated sandflats typically deeper. While our pattern is consistent with previous work in Graham's Harbour (Colby and Boardman, 1989; Randazzo and Baisley, 1995; Deehr et al., 2001; Zimmerman et al., 2001), this relationship may reflect our sampling methods as we specifically targeted different locations to represent our vegetated and unvegetated sites. The deeper, less vegetated areas of Graham's Harbour and French Bay were not accessible, owing to their greater distance from shore and strong waves respectively. The historically unvegetated Fernandez Bay and Sand Dollar Beach were easier to access as the sandflats were approximately the same distance from shore as the seagrass meadow in Graham's Harbour, and the waves were much calmer relative to French Bay. Even though the sandflats at Fernandez Bay and Sand Dollar Beach are slightly deeper than the seagrass meadows of Graham's Harbour and French Bay, all of our samples were collected in less than five meters water depth and are well within the depth range for seagrass growth in Graham's Harbour (Deehr et al., 2001; Zimmerman et al., 2001). *T. testudinum, S. filiforme,* and *H. wrightii* have been observed to grow within five meters of water depth

at other open marine sites around the eastern Gulf of Mexico and Caribbean (Vicente and Rivera, 1982; Iverson and Bittaker, 1986; Williams, 1988). Additionally, waters around San Salvador Island are historically clear, with the seafloor visible up to 20 m (Gerace et al., 1998), so light attenuation from either depth or turbidity should not be a factor given our shallow depth range.

Seagrass is positively correlated with percent fine-grained sediments, and negatively correlated with percent sand. This pattern is consistent with the hydrodynamics and morphology of seagrasses. Seagrass blades produce drag, which lowers the current velocity and causes deposition of fine-grain sediments (Fonesca et al., 1983; Scoffin, 1970). For example, dense *Thalassia* meadows can reduce current velocity from 40 cm/sec to almost 0 cm/sec at the sediment-water interface and allow for deposition of fine-grained sediments where adjacent sparsely vegetated and barren sandflats experience erosion (Scoffin, 1970). Additionally, the intricate root network of *Thalassia,* other seagrasses, and algal holdfasts trap fine-grained sediments and inhibit reactivation (Scoffin, 1970). This baffle-and-trap dynamic of seagrass explains the strong positive correlation between seagrass density and percent fine-grained sediments, and the negative correlation between seagrass density and percent sand.

Seagrass density is negatively correlated with pH at the sediment-water interface. Although the correlation is strong and statistically significant, we argue that this relationship may not be ecologically significant. Unvegetated samples have pH values that range from 7.96 to 8.09 with a mean value of 8.04. Vegetated sites have pH values that range from 7.78 to 8.10 with a mean value of 7.96. These pH values alone should not

preclude the growth of seagrass as the range of pH values for vegetative sites largely overlap those for unvegetated sites.

Seagrass density is also negatively correlated with dissolved oxygen. This relationship is expected as seagrass adds organic material to the sediment, which creates more anoxic conditions. While this correlation is strong and statistically significant, we argue that this relationship may also not be ecologically significant. Unvegetated and vegetated samples are all similarly oxygenated. Unvegetated samples have dissolved oxygen values that range from 18.4–20.6 mg/L with a mean value of 20.0 mg/L. Vegetated sites have dissolved oxygen values that range from 17.0–20.9 mg/L with a mean value of 19.6 mg/L. The range values are almost completely overlapping and are similar enough that the difference in dissolved oxygen is negligible, likely due to vegetated samples not being densely vegetated (Figure 3.3).

Bioturbation is negatively correlated with wave energy. Callianassid burrows were present in all sites. Feeding traces, resting traces, and other types of burrows were less frequent at sites with stronger waves. The surficial feeding and resting traces are presumed to be less common as the result of sediment reworking by waves, which destroys surficial evidence of bioturbation. While the seagrass at French Bay might explain this negative relationship, the windward exposed sandflat samples at Sand Dollar Beach had less surficial bioturbation than the protected samples at Sand Dollar Beach. It is unclear whether bioturbation below the surface is the same at all sites, as our observations were limited to surficial traces.

Bioturbation is also positively correlated with temperature, but this relationship is likely not ecologically significant. Bioturbation levels can differ across broad temperature

ranges as temperature affects the metabolic rates of the bioturbators (Hymel and Plante, 2000; Ouellette et al., 2004; Przeslawski et al., 2009). However, temperature values from our sites exhibited a narrow range, from 30.0°C to 31.7°C. Given this low range, it is unlikely that temperature would substantially affect bioturbation levels.

5.3 Environmental controls on death assemblages

Seagrass presence and density are the predominant environmental variables correlated with death-assemblage compositions in these shallow-water samples. Cluster analysis and CCA both show a clear distinction between assemblages collected from vegetated sites and those collected from unvegetated sites (Figures 3.2 and 3.4). Additionally, seagrass density loads highly on CCA Axis 1 (Table 3.4; Figure 3.4A). Compositional differences in molluscan associations reflecting the presence of seagrass and variation in seagrass density was expected based on the findings of similar studies on San Salvador Island (Deehr et al., 2001; Zimmerman et al., 2001; Reich, 2014; Casebolt and Kowalewski, 2018), in the U.S. Virgin Islands (Miller, 1988; Ferguson and Miller, 2007), and in Florida Bay (Brewster-Wingard and Ishman, 1999). Sandflat samples adjacent to patch reefs plotted among those from open sandflat sites in both the cluster analysis and the CCA, reflecting their similar compositions. We expected reef-adjacent samples to be distinct from the open sandflats as they were hypothesized to incorporate a greater proportion of taxa washed in from nearby patch reefs, but the data do not indicate this. The taxonomic distinctness of unvegetated sites relative to vegetated sites indicates the importance of seagrass in determining molluscan assemblage composition.

Grain size also loads strongly on Axis 1, with percent fine-grained sediments having a strong negative loading and percent sands having a moderate positive loading

(Table 3.4; Figure 3.4). As noted earlier, this appears to relate to seagrass density. Unvegetated samples did not have any vegetation-mediated stabilization, allowing the fine-grained sediments to be winnowed away and accumulating greater concentrations of sand-sized sediments.

Seagrass meadows are rather different habitats from sandflats, and therefore have different molluscan assemblages. The three-dimensional structure of leaves and roots provide more habitat complexity than the sandflats. Seagrass blades support diverse and large populations of epifaunal grazers and infaunal chemosymbionts in addition to infaunal and semi-infaunal mollusks more commonly found in open sandflats (Hemminga and Duarte, 2000). For example, our vegetated sites contained high abundances of multiple epifaunal grazing gastropods such as *Eulithidium thalassicola*, *Cerithium atratum*, *Cerithium eburneum*, *Cerithium litteratum*, and *Smaragdia viridis* and the chemosymbiotic bivalves *Lucina pensylvanica* and *Parvilucina costata*, whereas our unvegetated sites were dominated by only one epifaunal grazing gastropod *Finella adamsi* and the infaunal suspension feeding bivalve *Transennella conradina* (Figure 3.2). As noted earlier, seagrass roots also trap and bind fine-grained sediment (Scoffin, 1970), providing sediment stability and protection from predators for infaunal mollusks (Coen and Heck, 1991; Irilandi and Peterson, 1991; Nakaoka, 2000; Peterson and Heck, 2001) that foster a more diverse infaunal assemblage (Hemminga and Duarte, 2000). Food and nutrient availability differ within seagrass meadow compared to unvegetated sites. Seagrass blades directly provide food for epifaunal grazers and detrital feeders, while food availability in the sandflats depends mainly on currents importing detritus and suspended particles.

Despite limiting the study to 1–5.2 m of water depth, a water-depth gradient was also identified along Axis 1 of the CCA (Table 3.4, Figure 3.3). As a result, water depth also explains a large portion of variation in the molluscan data. It is unclear whether or not this signal is ecologically important. A four-meter depth range does not seem sufficiently large enough to affect assemblage compositions. Temperature, pH, and dissolved oxygen commonly covary with water depth, yet the variation of these variables is very small (1.67°C, 0.38, and 4.0 mg/L respectively) and none are correlated with water depth in this study. Wave energy was also not correlated with depth change, and has a strong loading on Axis 2, which implies independence from the water-depth gradient along Axis 1. Seagrass density and percent fine-grained sediments were the only variables found to directly vary with water depth, and both load highly along CCA Axis 1 opposite to the vector for water depth. However, the percent of fine-grained sediments is also directly linked to seagrass density, and seagrass density may reflect sample location more so than a difference in water depth. Sampling assemblages and seagrass density from the deeper and more offshore areas of Graham's Harbour would be required to test if water depth is anti-correlated seagrass density and percent fine-grained sediments or if it is the result of our sampling method. As it stands, the water-depth gradient along CCA Axis 1 implies that either the taxa are constrained to a very narrow depth range, tied to the narrow depth range of the seagrass, or there are additional unmeasured correlated variables influencing molluscan assemblage compositions.

Wave energy and bioturbation have strong loadings on CCA Axis 2 (Table 3.4, Figure 3.4). Along Axis 2, samples grade from the high-energy French Bay and the exposed reef-proximal sandflats at Sand Dollar Beach at negative Axis 2 scores to the

lower energy, protected Graham's Harbour at positive Axis 2 scores. Observations of surficial bioturbation were lower in the high-energy samples clustering in the negative Axis 2 scores, and greater in the low-energy samples clustering in the positive Axis 2 scores. It is reasonable that wave energy and surficial bioturbation should be negatively correlated with one another, as increased wave energy will rework the sediment and remove evidence of surficial bioturbators. Identifying wave energy as an important environmental parameter is consistent with earlier studies assessing the suitability of molluscan death assemblages for ecological studies on San Salvador Island, which found a clear distinction between assemblages from the windward eastern side of the island and those from the leeward western side (Casebolt and Kowalewski, 2018).

Dissolved oxygen also has a moderate loading on CCA Axis 2 (Table 3.4, Figure 3.4). Higher oxygen samples (19.80–21.00 mg/L) cluster in the negative Axis 2 scores, whereas the lower oxygen samples (17.00–19.70 mg/L) generally cluster at positive Axis 2 scores. As with water depth, it is unclear whether this small range of dissolved oxygen is ecologically important. French Bay samples had both the highest wave energy and levels of dissolved oxygen, but the least amount of bioturbation. Graham's Harbour samples had both the lowest wave energy and levels of dissolved oxygen, but the greatest amount of bioturbation. It is reasonable that wave energy and oxygenation levels should be positively correlated with one another, through mixing by waves. Even so, wave energy and dissolved oxygen are not significantly correlated (Table 3.1), and the greater intensity of bioturbation at the low-energy Graham's Harbour indicates it was sufficiently oxygenated to support a diverse benthic assemblage. Regardless of their relationship,

wave energy, bioturbation, and dissolved oxygen are highly correlated with CCA Axis 2, and as a result, they explain the second greatest amount of variation in our dataset.

Comparing Measurements in the Modern to the Fossil Record

A fundamental issue underlying actualistic studies is how to apply them to the fossil record, as methods in data collection differ between modern and paleoecological studies. Actualistic studies have identified key aspects of modern death assemblages such as compositional and spatial fidelity (Kowalewski et al. 2003; Lockwood and Chastant, 2006; Kidwell, 2008, Tomašových and Kidwell, 2009a; 2009b), and temporal fidelity and time-averaging (Kidwell and Bosence, 1991; Flessa et al., 1993; Flessa and Kowalewski, 1994; Kidwell, 2001,), and these provide insight into the construction of the fossil record. Actualistic studies of environmental variables (i.e., vegetation, oxygenation, temperature, salinity, etc.) pose other challenges for application to ancient systems, and these studies should be modified to reflect how these environmental variables are preserved in the fossil record. Our study succeeds in this regard for some of the variables sampled (i.e. depth, wave energy, bioturbation, seagrass, and substrate types), but is unable for others (dissolved oxygen, temperature, and pH).

Water depth was constrained to the shallow subtidal environment prior to sampling based on characteristics that define the shallow subtidal on a wave-dominated shelf. First, sampling was conducted between mean low tide and above fair-weather wave base. Second, callianassid burrows were found at all sites. These burrows are common in shallow marine settings and are recorded as the *Ophiomorpha* trace fossils in the Pleistocene and Holocene shallow subtidal deposits on San Salvador Island (Curran and White, 1991; Curran and Seike, 2016). Third, two-dimensional vortex ripples were

present at many of our sites, and these are also preserved in ancient shallow-marine facies. No vortex ripples were observed in the seagrass meadows in Graham's Harbour and French Bay, likely due to the baffling effect of seagrass blades, but we are confident we sampled the seagrass meadows within the shallow subtidal based on the abundance of callianassid burrows and the presence of waves just above the seagrass surface. Depth measurements were also made using dive computers to ensure we sampled from similar depths at both the sandflats and the seagrass meadows. While these measurements were incorporated into our analyses, the 0.3 m resolution at which we recorded water depth is at a far higher resolution than could be expected in the fossil record. Bedforms, sedimentary structures, and trace fossils are all commonly recognizable features of depositional environments in both in the modern and the stratigraphic record. Using these features in addition to numerical depth values to discuss modern environmental gradients within and among depositional environments may facilitate comparisons between the modern and fossil records.

Bioturbation is relatively simple to quantify in the fossil record and our observations on San Salvador Island reflect what we would expect in fossil record. Surficial traces identify burrows, resting traces, feeding traces, and walking traces at all sites. Callianassid burrows are the most abundant form of bioturbation, which is consistent with previous modern studies on San Salvador Island (Curran and Seike, 2016). Box coring would provide us a complete three-dimensional view of the bioturbation at each site and allow comparisons with the ichnofabric index created by Droser and Bottjer (1986) used to quantify bioturbation intensity in the stratigraphic record, but it was not logistically feasible. Even without box core data, our observations

of the surface level bioturbation identified features comparable to trace fossils found in the Pleistocene deposits on San Salvador Island (Curran and White, 1991; Curran and Martin, 2003; Curran and Seike, 2016), indicating that surficial observations of callianassid burrows are still useful when comparing modern systems to the fossil record.

Our qualitative characterization of wave energy based on wave-induced sampling difficulty (i.e., how much we were buffeted around when sampling), while coarse, was supplemented by observations from previous literature (Colby and Boardman, 1989; Hinman, 1994; Casebolt and Kowalewski, 2018). These historic patterns of wave energy provided context for our time-averaged assemblages and including them ensured we did not record an unusually quiet or rough period at the time of sampling. Ideally, we would like to have measured wave energy directly using flow meters at each site every day over the course of the study to get an average flow velocity but doing so was not logistically feasible. From this methodology, we identified locations of relatively high and low wave energy and could test whether they were correlated with grain-size distributions. Wave energy can affect grain size distributions in carbonate environments by winnowing away fine-grained sediments, provided they can be transported away faster than produced (Tucker and Wright, 1990). Unfortunately, our high wave energy samples at French Bay had grain sizes comparable to our lower wave energy samples at Graham's Harbour. The seagrass meadows at both sites baffled the water column and trapped the fine-grained sediments, which enabled a greater percentage of fine-grained sediments to accumulate despite the difference in wave energy.

Seagrass as an environmental variable in the fossil record becomes more difficult to measure. Direct evidence of seagrass in the fossil record is rare, owing to the poor

preservation potential of seagrass. The oldest fossils of seagrass are from the Late Cretaceous (den Hartog, 1970; Brasier, 1975; Voight, 1981; Dilcher, 2016), and they are only sparsely preserved through the Cenozoic (Ivany et al., 1990; Moissette et al., 2007; Reich et al. 2015). Since the fossil record of seagrass is very poor, many studies have turned to indirect paleo-seagrass indicators as a way of identifying the presence of seagrass habitats (see Reich et al., 2015 for a full review). Associations of other fossil taxa such as epiphytic foraminifera (Brasier, 1975; Cann and Clarke, 1993; Reuter et al., 2010; O'Connell et al., 2012), encrusting bryozoans (James and Bone 2007, Reuter et al., 2010), and mollusks (Daley, 2002, James and Bone, 2007; Zuschin et al., 2007; Reuter et al., 2012; Reich, 2014; Reich et al., 2014) have been used to infer seagrass meadows in the fossil record. Many of these taxa are common outside of seagrass habitats today and are therefore weak proxies for seagrass individually but are suggestive of seagrass when many of them co-occur (Reich et al., 2015). Faunal associations coupled with sedimentological characteristics (i.e. unsorted, fine-grained sediments and micrite envelopes) and taphonomic wear on shell and skeletal material (i.e. bioerosion, root etchings) can suggest the presence of seagrass, but a positive identification in the fossil record cannot be made without the seagrass fossils themselves (Reich et al., 2015).

Our measurements of temperature, pH, and dissolved oxygen are not suitable for extrapolating to the fossil record. Each was based on a single, instantaneous measurement, used to verify that the sampling sites were within normal, open marine conditions. Single measurements will not accurately reflect the impact these variables will have on death assemblages, which are time-averaged accumulations. Long term data collection over the course of months to years would be required to develop comparably

time-averaged records of temperature, pH, and dissolved oxygen. As a result, we are not confident in the ecological significance of the statistical correlations or gradients correlated with these variables within the ordination.

CONCLUSIONS

Seagrass coverage and substrate consistency are the dominant environmental variables determining the molluscan death assemblage compositions in the shallow subtidal of San Salvador Island, which is consistent with previous work on San Salvador Island and in the Western Atlantic. Cluster analysis distinguishes assemblages between vegetated and unvegetated sites, and CCA Axis 1 is highly correlated with presence of seagrass, seagrass density, and the percentage of fine-grained sediments trapped by seagrass. Water depth is also correlated with Axis 1, but negatively correlated with seagrass density. However, it is unclear whether or not this water-depth gradient is ecologically important for either seagrass density or the molluscan assemblages. All samples were collected from a 4.2 m depth range within the shallow subtidal, and within the depth tolerances for the three species of seagrass. CCA Axis 2 is highly correlated with wave energy, bioturbation, and dissolved oxygen, indicating that the combination of these three variables explain the second greatest amount of variation in the dataset. While the correlation with wave energy is consistent with previous studies, we are not certain these variables are impacting assemblage compositions in the manner our ordination suggests. Our highest energy samples from French Bay are from within a seagrass meadow, which reduced the flow conditions at the sediment-water interface enough to accumulate fine-grained sediments at comparable levels to Graham's Harbour, our lowest energy vegetated site. This suggests that seagrass may be decreasing the effects of wave

energy on the mollusks at the sediment-water interface and possibly bioturbators in the subsurface. Additionally, dissolved oxygen was recorded as single, instantaneous measurements that do not characterize oxygen conditions for a time-averaged death assemblage as accurately as long-term data. This fine-resolution analysis highlights the variability of assemblages found within the same depositional environment and enables us to identify additional sources of variation that might otherwise be dominated by the predominant water depth signal typically found in when examining multiple depositional environments. Identifying such fine-resolution variation in the fossil record are important as they inform as to how changes in environmental variables impact not only the distributions of individual taxa, but paleocommunity compositions through both space and time.

TABLES

Table 3.1: Spearman's rank correlation between environmental variables. Significant p-values are in bold and denoted by asterisks: * = 0.01–0.05, ** = 0.001–0.01; *** = 0–0.001. Only correlation values with three asterisks would remain significant with a Bonferroni correction.

	Distance offshore	Depth	Temperature	pH	Dissolved oxygen	Seagrass density	Bioturbation	Energy	Mean grain size	% fines	% sand	% gravel
Distance offshore	—	—	—	—	—	—	—	—	—	—	—	—
Depth	**0.792*** **	—	—	—	—	—	—	—	—	—	—	—
Temperature	-0.119	-0.055	—	—	—	—	—	—	—	—	—	—
pH	-0.210	0.063	0.339	—	—	—	—	—	—	—	—	—
Dissolved. oxygen	0.043	0.004	-0.080	0.156	—	—	—	—	—	—	—	—
Seagrass density	-0.246	**-0.450***	-0.044	**-0.517****	**-0.392***	—	—	—	—	—	—	—
Bioturbation	0.310	**0.390***	**0.450***	-0.004	-0.190	-0.248	—	—	—	—	—	—
Energy	-0.063	-0.022	0.251	0.196	0.290	0.014	**-0.429***	—	—	—	—	—
Mean grain size	0.107	-0.005	-0.276	-0.219	-0.101	0.046	0.167	0.030	—	—	—	—
% fines	-0.185	**-0.441***	0.119	-0.242	-0.072	**0.813*****	**-0.362***	0.337	0.068	—	—	—
% sand	-0.141	0.044	-0.265	0.111	-0.023	**-0.491****	0.135	**-0.620*****	-0.162	**-0.703*****	—	—
% gravel	0.329	0.203	0.316	-0.053	0.058	0.284	0.007	**-0.674*****	0.159	**0.488****	**-0.915*****	—

Table 3.2: Proportion of variance in the CCA as explained by the environmental dataset.

	Inertia	Proportion
Constrained	3.44	0.46
Unconstrained	3.98	0.54
Total	7.42	1.00

Table 3.3: Eigenvalues and percent variance explained for CCA Axes 1 through 3

	CCA1	CCA2	CCA3
Eigenvalue	0.53	0.47	0.38
% variance explained	7.14%	6.33%	5.12%
Cumulative % variance explained	7.14%	13.47%	18.59%

Table 3.4: Biplot scores for environmental variables for CCA Axes 1 through 3. Strong loadings (i.e., greater than 0.40 and less than -0.40) are in bold.

	CCA 1	CCA 2	CCA 3
Distance offshore	**0.438**	0.234	-0.197
Depth	**0.489**	0.300	-0.328
Temperature	-0.368	0.050	**0.608**
pH	0.234	0.048	-0.088
Dissolved oxygen	0.270	**-0.498**	-0.210
Seagrass density	**-0.867**	-0.088	-0.067
Bioturbation	0.263	**0.652**	**0.451**
Wave energy	-0.225	**-0.699**	-0.229
Mean grain size	0.073	0.077	-0.379
Percent fine grains	**-0.817**	-0.013	-0.274
Percent sand	**0.538**	0.095	0.183

Table 3.5: Taxon scores for CCA Axis 1–3 of taxa with a proportional abundance of greater than 1% of the total assemblage are shown here. A full list of taxon scores is presented in Supplementary Table 3.1.

Taxon name	CCA Axis 1	CCA Axis 2	CCA Axis 3
Acteocina sp.	0.225	-0.112	0.353
Angulus sybariticus	0.091	0.453	-0.305
Atys sharpi	-0.146	-0.200	0.128
Cerithium atratum	-1.153	-0.895	-0.164
Cerithium eburneum	-0.048	-0.233	0.089
Cerithium litteratum	-0.577	-0.372	0.031
Chione elevata	-0.074	0.354	-0.010
Crenella divaricata	0.075	0.078	0.455
Ctenocardia guppyi	0.478	0.047	-0.058
Ervilia concentrica	0.447	-0.390	-0.483
Eulithidium affine	0.682	0.104	0.425
Eulithidium thalassicola	-0.872	-0.182	-0.092
Finella adamsi	0.589	-0.148	0.353
Fugleria tenera	0.696	-0.330	-0.506
Lucina pensylvanica	-0.865	-0.647	0.113
Parvilucina costata	-0.904	-0.233	0.123
Patelloida pustulata	-1.174	-1.237	-0.125
Rissoina krebsii	0.702	0.039	0.200
Scissula similis	0.446	-0.040	-0.075
Smaragdia viridis	-1.225	-1.220	-0.291
Transennella conradina	0.479	0.067	-0.015
Zebina browniana	-0.444	0.882	-0.268

FIGURES

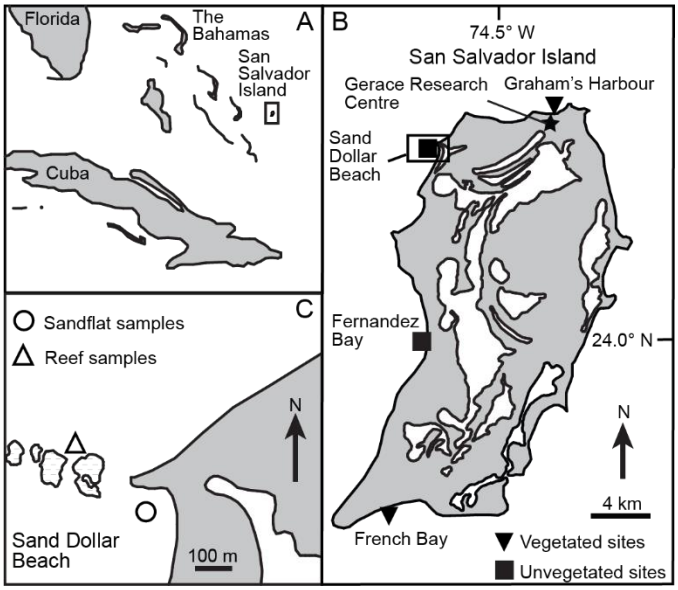

Figure 3.1: Map of study areas on San Salvador Island, The Bahamas. A) San Salvador Island is located on the eastern edge of the Bahamas Island chain. B) Molluscan death assemblages and environmental data were sampled at four sites. C) At Sand Dollar Beach, samples were collected from exposed sandflats proximal to the patch reef system and from protected sandflats closer to shore. The stippled pattern represents the location of patch reefs.

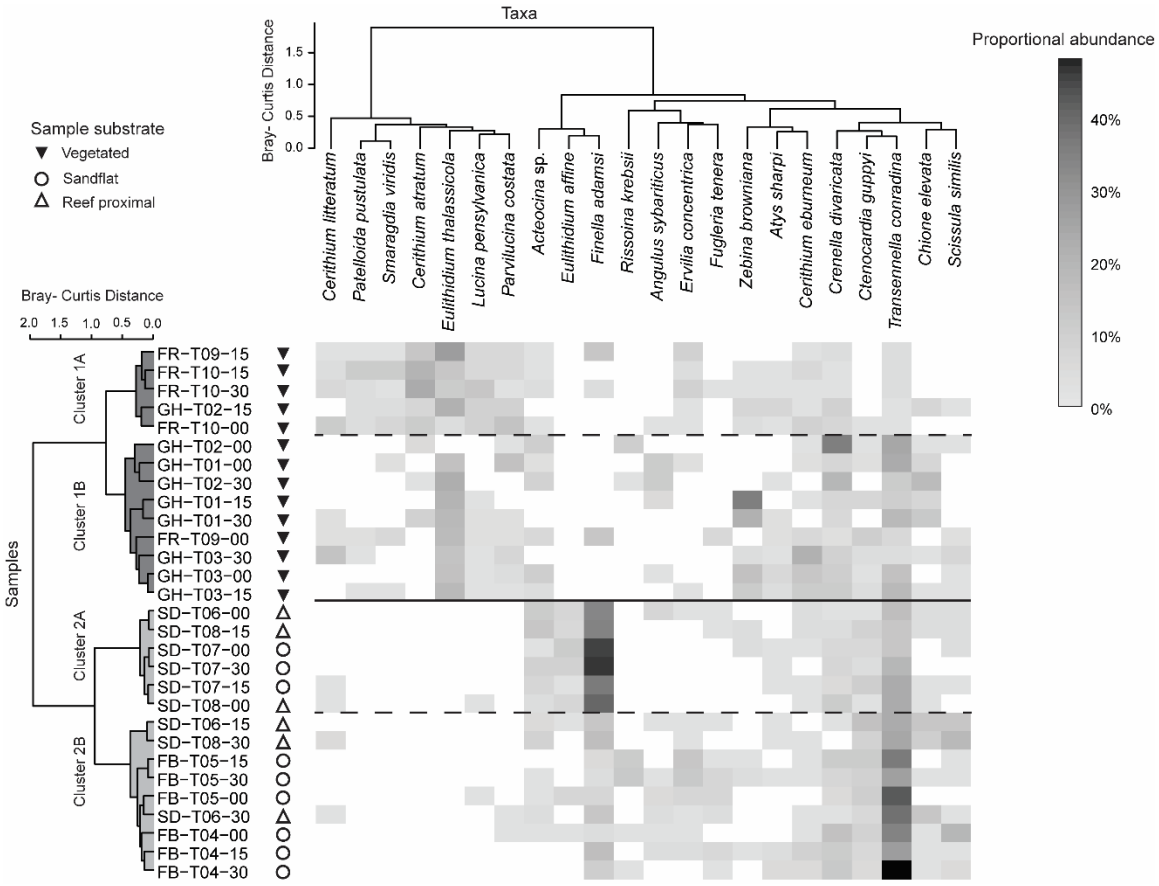

Figure 3.2: Two-way cluster analysis of death assemblages. The color of each cell represents the proportional abundance of each taxon in each sample. Samples are labeled according to their location (i.e., GH= Graham's Harbour, FR= French Bay, SD= Sand Dollar Beach, and FB= Fernandez Bay), transect number, and interval along transect (i.e., 0 m, 15 m, or 30 m). The taxa displayed are those with a proportional abundance greater than 1% of the overall assemblage.

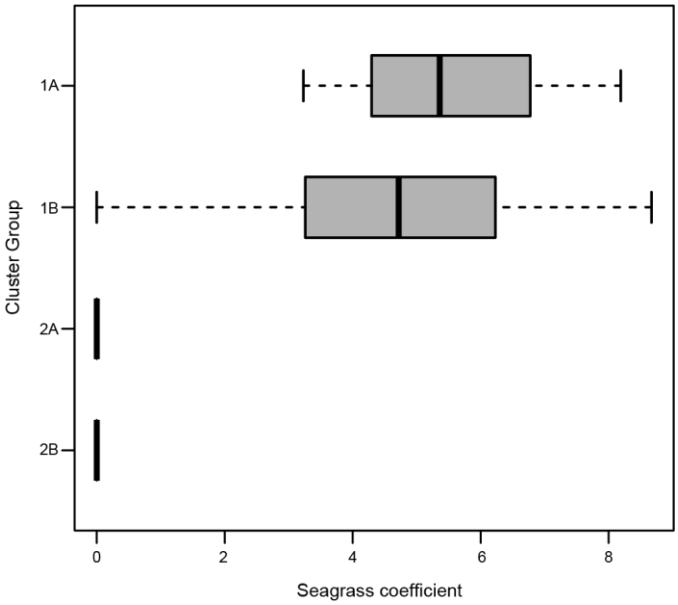

Figure 3.3: Box and whisker plot of seagrass coefficient values for sub-clusters defined in the two-way cluster analysis (Figure 3.2). Cluster 1A is predominantly French Bay samples, Cluster 1B is predominantly Graham's Harbour samples, and Clusters 2A and 2B are a mixture of reef-proximal samples from Sand Dollar Beach and open sandflat samples from Fernandez Bay and Sand Dollar Beach. Coefficient values represent the m^2 area of seagrass blades per m^2 of seafloor.

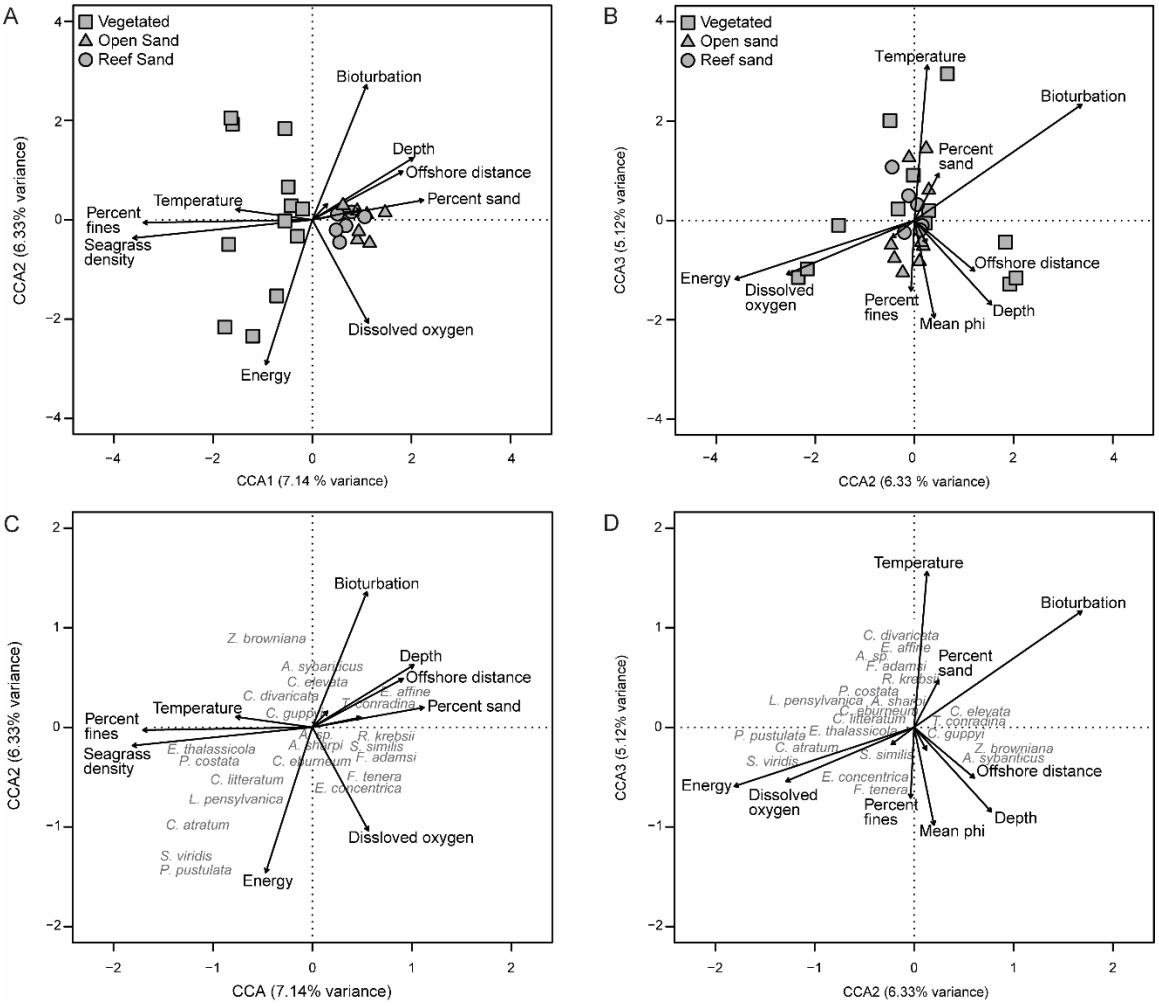

Figure 3.4: Canonical correspondence analysis (CCA), showing samples as points, species as gray text, and environmental data as vectors. Samples that plot closer to one another have similar taxonomic composition. The direction of an environmental vector indicates its correlation with the CCA axes, and the length of the vector reflects the strength of that relationship. A) Ordination of samples and environmental data along Axis 1 and Axis 2. Mean phi and pH are not shown in this ordination because they plot close to the center and are difficult to discern from the surrounding points. B) Ordination of samples and environmental data along Axis 2 and Axis 3. Seagrass density and pH are not shown in this ordination because they plot close to the center and are difficult to discern from the surrounding points. C) Ordination of taxa and environmental data along Axis 1 and Axis 2. D) Ordination of taxa and environmental data along Axis 2 and Axis 3. Ordinations of taxa are rescaled such that taxa names are more clearly visible. Only species with a proportional abundance of greater than 1% of the overall assemblage are shown for figure clarity.

CHAPTER 4

LITHOLOGICAL AND PALEOCOMMUNITY VARIATION ON A MISSISSIPPIAN (TOURNAISIAN) CARBONATE RAMP, MONTANA, USA[3]

[3] Brown, G.M. To be submitted to Palaios

ABSTRACT

Ecological analyses of ancient marine communities are impacted by the environmental gradients controlling assemblage compositions and the heterogeneous distribution of sediment types. Closely spaced, replicate sampling of fauna has been suggested to mitigate the effects of heterogeneity and improve gradient analyses, but this technique has rarely been combined with similar sampling of lithologic data. This study analyses lithological and faunal data to determine the environmental gradients controlling the composition of Mississippian fossil assemblages of the lower Madison Group in Montana. Eighty-one lithological and faunal samples were collected from four stratigraphic columns in Montana, which represent the deep-subtidal, foreshoal, and ooid-shoal depositional environments within one 3rd-order depositional sequence. Cluster analysis identifies three distinct lithological associations across all depositional environments— crinoid-dominated carbonates, peloidal-crinoidal carbonates, and micritic-crinoidal carbonates. Cluster analysis and nonmetric multidimensional scaling identifies a highly diverse brachiopod biofacies and a solitary coral-dominated biofacies along an onshore–offshore gradient. Lithological data and ecologic characteristics indicate that substrate and wave energy are two potential variables that covary with the onshore–offshore gradient. Overlaying lithological information on the NMS indicates a secondary gradient reflecting oxygen that is expressed by increasing bioturbation and gradation from a brown to dark gray carbonates to medium-light gray carbonates. This study demonstrates how combining closely spaced, replicate sampling of faunal assemblages with lithologic samples enhances multivariate analyses and allows for a greater understanding of environmental gradients.

INTRODUCTION

For ancient benthic marine communities, assemblage compositions are commonly associated primarily with an onshore–offshore gradient, also known as a water-depth gradient (Patzkowsky and Holland, 2012). Water depth is a complex gradient that comprises other direct or resource environmental gradients (Whittaker, 1956; Austin et al., 1984), such as temperature, substrate, sunlight penetration, oxygenation, nutrients, shear stress, and salinity (Tait and Dipper, 1998). Species respond to these covarying environmental gradients, giving rise to community changes along onshore–offshore or water-depth gradients. Examination of the lithological data (i.e., grain size, grain composition, bioturbation levels, and biogenic structures) as well as the ecological characteristics of assemblages (i.e., life mode and feeding ecology) indicate that substrate and wave-energy gradients can commonly be identified in the fossil record (Cisne and Rabe, 1978; Lafferty et al., 1994; Patzkowsky, 1995; Holland et al., 2001; Webber, 2002; Novack-Gotshall and Miller, 2003; Scarponi and Kowalewski, 2004; McMullen et al., 2014; Scarponi et al., 2014; Zuschin et al., 2014). Evaluating these same lithological and faunal characteristics has also identified primary and secondary gradients that are uncorrelated with water depth (Holland et al., 2001; Olszewski and Patzkowsky, 2001; Scarponi and Kowalewski, 2004; Tomašových, 2006; Redman et al., 2007; Bush and Brame, 2010; Perera and Stigall, 2018).

Interpreting ancient environmental gradients is also impacted by the spatial distribution of fossils along bedding surfaces and within depositional environments (Bennington, 2003; Webber, 2005; Perera and Stigall, 2018). Fossils distributions are usually heterogeneous, such that a count for a single bed may not sufficiently characterize

the communities within the depositional environment (Kidwell and Bosence, 1991; Bennington, 2003; Webber, 2005). Additionally, the lithological record is heterogeneous at small spatial scales, especially within carbonate systems, where varying percentages of sediment grains, matrix, and bioturbation intensity indicate multiple microfacies within a depositional environment (Flügel, 2010). To account for the heterogeneous nature of the fossil and lithological records when examining environmental gradients, closely spaced, replicate sampling of faunal and lithological samples is needed from the same depositional environment at each sampling locality (Bennington, 2003; Webber, 2005; Patzkowsky and Holland, 2012; Perera and Stigall, 2018).

The Mississippian lower Madison Group in Montana is an excellent location to examine the effect of heterogeneity in faunal distributions and lithological characteristics on the interpretations of environmental gradients. The lower Madison Group contains diverse assemblages of crinoids (Laudon and Severson, 1953), brachiopods (Shaw, 1962; Rodriguez and Gutschick, 1968, 1969; Christensen, 1999), rugose corals (Sando, 1960; Waters and Sando, 1987) and other benthic invertebrates across multiple depositional environments (Elrick and Read, 1991; Sonnenfeld, 1996; Smith et al., 2004). This study will test the efficacy of high-resolution, replicate sampling of lithological data and faunal counts in answering two main questions. First, can replicate sampling distinguish environmental gradients that covary with and therefore create the water-depth gradient? Second, can additional gradients unrelated to water depth be identified? The collection of replicate lithological data in conjunction with faunal data will allow lithological information to be directly linked to each assemblage, potentially expanding the number of environmental gradients that can be identified in the fossil record.

GEOLOGIC SETTING

The study area encompasses the fossiliferous members of the lower Madison Group in the Central Montana Trough and northwestern Montana (Figure 4.1). Conodont biostratigraphy places the lower Madison Group within the lower to middle Tournaisian (approximately 357–353 Ma; Gutschick et al., 1980; Sando, 1985; Cohen et al., 2013; Figure 4.2).The lower Madison Group is exposed in Wyoming, Idaho, Montana, and North Dakota in the United States (Andrichuk, 1955; Mudge et al., 1962; Moore, 1973; Sando, 1976; Poole and Sandberg, 1977; Gutschick et al., 1980) and Alberta and Saskatchewan in Canada (Johnston et al., 2010).

The Mississippian Madison Group is part of a carbonate ramp system that extended from New Mexico to western Canada (Gutschick et al., 1980; Maughan, 1983; Smith et al., 2004). In the Mississippian, this area was bounded by the Transcontinental Arch to the east and the Antler Highlands to the west (Figure 4.1; Gutschick et al., 1980; Gutschick and Sandberg, 1983; Maughan, 1983; Smith et al., 2004), and it was located approximately 0–10° north of the equator (McKerrow and Scotese, 1990). Although it has been studied mostly along the shallow portions of the ramp, the Madison Group also includes deeper-water facies of the Antler Foreland Basin, the Williston Basin, and Central Montana Trough (Figure 4.1; Gutschick et al., 1980, Elrick and Read, 1991; Sonnenfeld, 1996; Smith et al., 2004).

In Montana, Idaho, and western Wyoming, the lower Madison Group unconformably overlies Devonian carbonate and siliciclastic rocks of the Beirdneau, Darby, and Three Forks formations (Gutschick et al., 1980), but in central Wyoming, the Madison Group overlies the Ordovician Bighorn Dolomite (Gutschick et al., 1980). In the

study area, the lower Madison Group is represented by the Lodgepole Formation in central and southwestern Montana and by the Allan Mountain Limestone in northwestern Montana. These formations unconformably overlie the Upper Devonian Sappington Formation, a yellow–tan siliciclastic member of the Three Forks Group (Figure 4.2; Mudge et al., 1962; Gutschick et al., 1980). The lower Madison Group is overlain by members of the upper Madison Group. In central and southwestern Montana, the Lodgepole Formation is conformably overlain by the Mission Canyon Formation, and in northwestern Montana the Allan Mountain Limestone is overlain by the Castle Reef Dolomite (Figure 4.2). In central and southern Montana and Wyoming, the upper Madison Group is unconformably overlain by the Pennsylvanian Amsden Formation (Gutschick et al., 1980; Sonnenfeld, 1996), whereas in northwestern Montana and southern Alberta, the Madison group is unconformably overlain by the Middle Jurassic Sawtooth Formation (Cobban, 1945; Gutschick et al., 1980).

The Lodgepole Formation and Allan Mountain Limestone are ramp and slope carbonates that include peritidal, shoal, foreshoal, deep subtidal, and offshore environments (Figure 4.3; Elrick and Read, 1991; Chen and Webster, 1994; Sonnenfeld, 1996; Smith et al., 2004). The Mission Canyon Formation and the Castle Reef Dolomite of the overlying upper Madison Groupe are dolomitized, crinoidal grainstones deposited in inner ramp and peritidal carbonate environments (Mudge et al., 1962; Reid and Dorobek, 1993).

Previous sequence-stratigraphic interpretations of the lower Madison Group have focused primarily on the Lodgepole Formation in Wyoming and southwestern Montana (Elrick and Read, 1991; Sonnenfeld, 1996; Smith et al., 2004). Two (Sonnenfeld, 1996)

to three (Elrick and Read, 1991) 3rd-order sequences are recognized in the Lodgepole Formation within the Madison Shelf of Wyoming and southern Montana (Elrick and Read, 1991; Sonnenfeld, 1996). Down depositional dip into the Central Montana Trough, the distinction between these sequences becomes less clear and sequence boundaries pass into correlative conformities (Elrick and Read, 1991). This study will apply the sequence-stratigraphic frameworks established along the Madison Shelf (Elrick and Read, 1991; Sonnenfeld, 1996; Smith et al., 2004) to contextualize lithofacies and biofacies changes within the lower Madison Group in the Central Montana Trough and northwestern Montana.

METHODS

Data Collection

Four stratigraphic columns of the lower Madison Group (the Lodgepole Formation and Allan Mountain Limestone) were measured in central and western Montana (Figure 4.1). Localities were chosen based on site accessibility and to maximize paleogeographic coverage. Each column was measured with a Jacob staff demarcated in 0.1 m intervals and a Brunton transit. At each column, beds were described according to lithology, carbonate grain type (i.e., skeletal, ooid, peloid, etc.), bed thickness, bioturbation index, sedimentary structures, trace-fossil diversity, and fossil fragmentation. Carbonate lithology was classified following Dunham (1962), bed thickness following Ingram (1954), and bioturbation index following Droser and Bottjer (1986). Lithological descriptions were used to classify beds and bedsets by lithofacies along the carbonate ramp using the facies model of Elrick and Read (1991).

Eighty-one field counts of fossils were conducted among the four columns. For each field count, lithology, stratigraphic position, and taphonomic features of fossils was recorded. Most (52) field counts were conducted along bedding surfaces wherever possible to reduce the amount of time-averaging. *In situ* bedding surfaces were preferentially targeted as to preserve the stratigraphic context of the field count. Multiple field counts were conducted along some bedding surfaces to examine the lateral heterogeneity of assemblages; such replicate counts were a minimum 15 m apart. Some (25) field counts were conducted along vertical rock faces, where fossiliferous horizons could be constrained to less than 10 cm vertically. A few (5) field counts were conducted on float samples that could be constrained to a specific interval within the stratigraphic column.

For each field count, fossils were counted for thirty minutes or until at least two species and twenty-four individuals were reached, which ever took the greater amount of time. Fossil specimens were identified to species where possible, although preservation of some brachiopods and solitary corals required identification at the genus or family level. Most bryozoans and crinoids were identified to order or morphological form (i.e., trepostome or fenestrate, round or elliptical crinoid ossicle), except where calices were well preserved.

The minimum number of individuals (MNI) was calculated in several ways based on taxonomic group. For brachiopods and bivalves, the MNI was calculated as the sum of the number of articulated specimens, the greater amount of brachial or pedicle and left or right valves respectively, and one-half of the number of indeterminate valves. Colonial corals were counted as individuals based on the cohesiveness of corallites. Every 3-cm

length of bryozoan was treated as an individual to provide a rough standardization by biovolume (see Holland and Patzkowsky, 2004). For trilobites, the MNI was counted as the maximum number of either cranidia or pygidia. For gastropods and solitary corals individuals, the MNI is the number of complete apices or calices. The MNI of crinoids was not calculated because individuals disarticulate into ossicles that became the dominant skeletal grain of most field counts. For crinoids, presence-absence data was used instead for the various morphospecies of crinoid ossicles, except where calices could be identified.

Eighty-one lithological samples were collected from the same beds as the faunal counts to confirm field identification of lithology and to quantify lithological properties. Thin sections were prepared from these samples and counted to 300 points. These counts include the components of grain type, micrite, cement, quartz, authigenic minerals and pore space. The hue, value, and chroma of each hand sample was estimated on a freshly cut surface using the Munsell Color System (Munsell Color, 1976) to assess potential variations in oxygenation and redox state.

Data Analysis

Before statistical analysis, the point-count and the species-abundance matrices were culled to remove rare petrographic components and species. Components with proportional abundances less than 5% of the overall petrographic assemblage were removed from the point-count matrix. Species with proportional abundances and less than 1% of the overall species assemblage were removed from the species-abundance matrix. This reduced the petrographic components from 23 to 14, and the number of species from 84 to 20 species. All analyses were also conducted using the original datasets, and the

patterns were similar to analyses using the culled dataset. This culling improved figure clarity and their interpretation by reducing the number of data points without altering any of the results.

Data standardizations were applied to the culled components and species-abundance matrices. The culled components matrix underwent the percent maximum standardization as sample sizes were already standardized to 300 counts, and analyses needed to account only for variations in component abundances. The culled species-abundance matrix received percent sample standardization followed by percent maximum standardization of each species to account for variations in both sample size and species abundance.

Q-mode cluster analysis was performed separately on the culled components and species-abundance matrices to identify the compositional and taxonomic similarities between samples. Q-mode clusters were identified using the *cluster* package of the statistical software R (Maechler et al., 2019). Q-mode cluster analysis used Bray-Curtis dissimilarity for the distance matrices and Ward's Method for linkage method. Ward's Method minimizes the increase of error in the sum of squares distances between samples, and it produces compact, well-defined clusters (McCune and Grace, 2002).

The R-mode cluster was performed separately on the culled components and species-abundance matrices to identify co-occurring components and species. R-mode clusters were identified using the *cluster* package of the statistical software R (Maechler et al., 2019). R-mode cluster analysis also used Bray-Curtis dissimilarity for the distance matrices and Ward's Method for linkage method.

Two-way cluster analysis was performed separately on the culled components and species-abundance matrices to define petrographic clusters and biofacies. Two-way clusters were calculated by using the *pheatmap* package of the statistical software R (Kolde, 2019) This package combines the Q-mode and R-mode analyses, and it displays the proportional abundances of the components or species within each sample, which assists in identifying the different petrographic clusters and biofacies.

Nonmetric Multidimensional Scaling (NMS) of the culled species-abundance matrix was performed to identify environmental gradients correlated with assemblage variations. NMS was performed using the *metaMDS* function in *vegan* package of the statistical software R (Oksanen et al., 2019). It used a percent sample standardization on the culled species-abundance matrix, Bray-Curtis dissimilarity matrix, three dimensions, and fifty restarts to avoid local optima. The number of dimensions used in NMS is typically selected based on stress values, which represents the goodness of fit between the original distance matrix and the reduced distance matrix of the ordination (McCune and Grace, 2002). The NMS in three dimensions calculated stress to be 0.146, which is within the acceptable range for interpreting NMS results (Kruskal, 1964a; Clarke, 1993), and additional dimensions provided subsequently smaller reductions in stress values. The *metaMDS* function rotates the NMS solution using a principal components analysis (PCA) such that NMS axis 1 reflects the most source of variation and higher axes reflect progressively less variation. Environmental variables were overlain on the NMS ordination using the *envfit* function in the *vegan* package of the statistical software R (Oksanen et al., 2019). Variables used in *envfit* include component percentages, bioturbation index, hue, and color value. The *envfit* function correlates variables in a

secondary matrix with sample scores from the NMS, allowing environmental variables to be displayed as vectors within the ordination space. The direction and length of a vector identifies how well that variable is correlated to each NMS axis.

RESULTS

Carbonate Facies Association Descriptions

The lower Madison Group carbonate ramp preserves carbonate facies associations from six depositional environments— the offshore, deep subtidal, the foreshoal, ooid shoal, crinoid shoal, and peritidal (Figure 3, Table 4.1). These facies associations were interpreted using only lithological data, and they do not consider faunal associations as to avoid circularity when interpreting environmental gradients.

Offshore.— Thinly-bedded, planar laminated, un-fossiliferous dark gray carbonate mudstone interbedded with very thin shale beds (Figure 4.4A, B, and C) indicate a dysoxic offshore environment with a poorly developed infauna (Elrick and Read, 1991; Sonnenfeld, 1996; Boyer and Droser, 2011). The presence of planar lamination within these carbonate mudstones and lack of wave or current structures suggests deposition below storm-wave base (Elrick and Read, 1991; Burchette and Wright, 1992; Sonnenfeld, 1996). The alternations between carbonate and siliciclastic lithologies reflects either variation in storm intensity along the ramp (Elrick et al., 1991) or sediment input via gravity flows and suspension (Sonnenfeld, 1996). The ratio of carbonate mudstone to shale increases up-section, indicating an increase in shear stress that is consistent with a transition from the distal offshore (Figure 4.4A) to the proximal offshore environments (Figure 4.4B).

Deep Subtidal.— Thin-bedded, moderately bioturbated (ii2–ii4), dark gray skeletal packstone interbedded with yellow–tan shale to argillaceous partings (Figure 4.4D) with diverse fossil assemblages suggest deposition in the subtidal. Ichnofossils identified include *Taenidium*?, *Zoophycus* (Figure 4.4E and F), *Thalassinoides*, and other horizontal burrows. Fossils include crinoid ossicles and calices, fenestrate and trepostome bryozoans, brachiopods, and solitary corals (Figure 4.4G). The increase in ichnofabric index, presence of burrows, and diversity of skeletal material in this facies association suggests more oxic conditions than in the offshore facies association (Droser and Bottjer, 1986; Boyer and Droser, 2011), although the variation in ichnofabric index and planar lamination may indicate variable oxygen levels (Boyer and Droser, 2011). Bedforms and sedimentary structures such as vortex ripples, wave-ripple lamination (Figure 4.4H) and planar lamination are present but rare. Vortex ripples and wave-ripple lamination indicates reworking by storm waves (Elrick and Read, 1991; Burchette and Wright, 1992; Sonnenfeld, 1996) and the argillaceous drapes represent settlement of terrigenous material during fair-weather conditions (Elrick and Read, 1991). Dense fossil concentrations along thin argillaceous bedding surfaces indicate sedimentation rates from settlement were slow within the deep-subtidal (Elrick and Read, 1991; Kidwell and Bosence, 1991).

Foreshoal.— Two lithofacies are identified in this association representing two depositional environments. The most common lithofacies is the medium-bedded, bioturbated (ii3–ii5), fossiliferous, medium gray skeletal-peloidal grainstone (Figure 4.5A and D) with planar lamination and silicified vertical and horizontal burrows. The presence of burrows and greater ichnofabric indices indicate oxic conditions, although

variation in ichnofabric index may suggest fluctuations in oxygen levels (Droser and Bottjer, 1986; Boyer and Droser, 2011). Fossils include crinoid ossicles, solitary corals (Figure 4.5F), colonial corals, brachiopods, and mollusks. The increase in abundance of coarse skeletal grains indicates that this lithofacies was deposited within fair-weather wave base (Elrick and Read, 1991; Burchette and Wright, 1992; Sonnenfeld, 1996). Sedimentary structures typical of the foreshoal on carbonate ramps such as hummocky, tabular, or trough cross-stratification (Elrick and Read, 1991, Sonnenfeld, 1996) were not observed, possibly as the result of bioturbation. The skeletal grainstone lithofacies likely represents a skeletal shoal or bank sub-environment within the foreshoal facies association that was deposited in somewhat deeper water than the ooid-shoal facies association (Elrick and Read, 1991; Smith and Read, 2001).

The second lithofacies within the foreshoal facies association is a medium-bedded, bioturbated (ii3–ii5), fossiliferous dark-gray carbonate mudstone (Figure 4.5B and E). Silicified vertical and horizontal burrows such as *Thalassinoides* are common (Figure 4.5C). Fossils include crinoid ossicles and calices, solitary corals, colonial corals, and brachiopods. Ichnofabric indices, heavy burrowing, and fossil diversity indicate that this lithofacies was deposited in an oxygenated environment similar to the skeletal grainstone lithofacies (Droser and Bottjer, 1986; Boyer and Droser, 2011). Sedimentary structures are rare, with rare planar lamination, indicating less influence of waves. The carbonate mudstone lithofacies likely represents a muddy intershoal deposit in a topographic low protected from waves between the skeletal bank deposits within the foreshoal facies association (Elrick and Read, 1991).

Ooid Shoal.— This facies association is characterized by medium-bedded, medium to light gray oolitic grainstone (Figure 4.5G). Bioturbation levels vary, with ichnofabric index ranging from ii1–ii4. Small scale cross stratification can be observed in beds that have little bioturbation (Figure 4.5H), indicating deposition in a high shear stress setting above fair-weather wave base. Color and ichnofabric index indicate that the ooid-shoal facies association was well-oxygenated (Berner, 1981; Maynard, 1982; Droser and Bottjer, 1986; Boyer and Droser, 2011). Fossils are rare, but include crinoid ossicles, solitary corals, and brachiopods.

Crinoid Shoal.— Overlying the ooid-shoal facies association is a thin to medium-bedded, tan crinoidal grainstone (Figure 4.5G). No sedimentary or biogenic structures are observed, and coarse crinoid ossicles are the only fossils identified. Its position above the ooid-shoal facies association, and the low faunal diversity and abundance indicates the that this association was deposited in a restricted lagoon (Sonnenfeld, 1996). The tan color is caused by intense dolomitization (Flügel, 2010). In near shore environments, dolomitization is commonly caused by mixing of meteoric water (Badiozamani, 1973; Choquette and Steinen 1980; Tucker and Wright, 1990; Flügel, 2010) but may have also been caused by evaporation, seawater pumping, or subsurface burial (see Tucker and Wright, 1990; Flügel, 2010 for review). It is impossible to determine the exact dolomitization mechanism without geochemical data or the presence of evaporites (Tucker and Wright, 1990; Flügel, 2010).

Peritidal.— This facies association is characterized by non-fossiliferous, non-bioturbated (ii1),thin to medium-bedded, light gray carbonate mudstone (Figure 4.5I). The lack of fossils and low bioturbation intensity indicates this facies was also deposited

within restricted conditions, and its position above the crinoid-shoal facies association suggests this facies was deposited in the peritidal environment (Elrick and Read, 1991; Sonnenfeld, 1996; Smith et al., 2004). Laminated beds are interbedded with non-laminated beds. Lamination are interpreted as algal in origin as they are slightly irregular and not completely planar (Elrick and Read, 1991; Sonnenfeld, 1996; Smith et al., 2004).

Sequence-stratigraphic Architecture

One 3rd-order depositional sequence is identified in the lower Madison Group at all four localities (Figure 4.6). The lower sequence boundary (SB1) is placed at the contact between the lower Madison Group and the underlying Sappington Formation (Elrick and Read, 1991; Sonnenfeld, 1996; Smith et al., 2004). This contact is present at Sappington Canyon, but was not observed at the other localities. A talus-covered interval beneath the measured section at Gibson Reservoir covers the contact and obscures the relationship between the Allan Mountain Limestone and the underlying Sappington Formation. The Sappington Formation is not exposed at Milligan Canyon as a poorly-lithified conglomerate covers the Lodgepole Formation down section. While the Sappington Formation is not exposed along the roadcut at Crystal Lake, although it is present in less accessible places nearby.

The lowstand systems tract (LST) is observed only at Crystal Lake, where it is characterized by shallowing-upward offshore through foreshoal deposits to foreshoal deposits no net trend in water depth. Here, the LST is capped by a transgressive lag of iron-stained chert, mudstone pebble, and skeletal grains overlain by deepening-upward deep-subtidal deposits. At Sappington Canyon, the contact between the lower Madison Group and the underlying Sappington Formation is interpreted as both the sequence

boundary and the transgressive surface, as deepening-upward parasequences are identified immediately above this contact indicating the TST. At Milligan Canyon, the measured section begins above a thrust fault, and the base of the Lodgepole Formation is not exposed. At Gibson Reservoir, talus obscures the base of the lower Allan Mountain Limestone, preventing assessment of stacking patterns to determine if the LST was present.

The transgressive surface is present at Sappington Canyon and Crystal Lake. At Sappington Canyon, it is combined with SB1, and the overlying parasequences are deepening upwards, indicating the TST. At Crystal Lake, the transgressive surface is identified as the lag of iron-stained carbonate rock, mudstone pebble, and skeletal grains.

The transgressive systems tract (TST) is present at all localities, and it is defined by the upsection loss of shallower facies associations and the presence of deepening-upward parasequences. At Milligan Canyon and Crystal Lake, the foreshoal facies association is lost upsection, the deep-subtidal facies association decreases in thickness, and the offshore facies association appears and increases in its percentage of shale. At Sappington Canyon, the foreshoal and deep-subtidal facies associations are lost upsection, and the TST is mostly represented by the offshore facies association, although it is largely covered by vegetation. At Gibson Reservoir, no facies are lost upsection, and the TST is represented by a thick package of carbonate mudstone of the foreshoal facies association at the base of the section. The thickness of the TST is similar at all localities, approximately 20 m at Sappington Canyon and Milligan Canyon, approximately 25 m at Gibson Reservoir, and approximately 30 m at Crystal Lake.

The maximum flooding zone (mfz) is present at all localities (Figure 4.6). At Milligan Canyon and Crystal Lake Road, the maximum flooding zone is represented by a shale interval interbedded with thin-bedded skeletal packstone. At Sappington Canyon, the maximum flooding zone is represented by a covered interval with a few exposed very thin beds of carbonate mudstone interbedded with shale. At Gibson Reservoir, the maximum flooding zone is represented by a thick interval of medium-bedded carbonate mudstone overlain by a single bed of skeletal grainstone near the base of the measured section (Figure 4.6).

The highstand systems tract (HST) is present at all localities, and it is recognized by aggradationally-stacked to shallowing-upward parasequences. At Gibson Reservoir, the HST is approximately 280 m thick and parasequences shallow upwards from carbonate mudstone lithofacies to the skeletal grainstone lithofacies of the foreshoal facies association. Parasequences shallow upwards into the peritidal facies association at 315 m in the section. At Sappington Canyon, the HST is approximately 225 m thick and begins as the offshore facies association with parasequences showing no net trend in water depth. Parasequences then shallow upwards from offshore to deep-subtidal, then offshore to foreshoal, carbonate mudstone lithofacies to skeletal grainstone lithofacies within the foreshoal, foreshoal to ooid-shoal, and finally ooid-shoal into peritidal facies. At Milligan Canyon, the HST is approximately 50 m thick and includes one parasequence that shallows upward from offshore to foreshoal facies associations and a second one that shallows upward from offshore to crinoid-shoal facies associations. Four to five additional parasequences that shallow upward from ooid shoal through peritidal are present at the top of the Milligan Canyon column but placing them into stratigraphic

context was impossible, owing to changing bed geometries and dense vegetation. At Crystal Lake, the HST is approximately 85 m thick and includes parasequences of deep-subtidal facies association that show no net trend in water depth for approximately 30 m, followed by shallowing-upward parasequences of deep-subtidal facies to foreshoal capped by ooid-shoal facies associations.

The upper sequence boundary (SB2) is present only at Gibson Reservoir and Sappington Canyon, where it is placed at as the contact between the peritidal facies association of the lower Madison Group and the poorly bedded, crystalline grainstone of the upper Madison Group. At Gibson Reservoir, SB2 separates the well-bedded foreshoal and peritidal of the Allan Mountain Limestone from the poorly bedded, recrystallized grainstone of the Castle Reef Dolomite. At Sappington Canyon, SB2 separates the peritidal facies association of the Lodgepole Formation with well-bedded carbonate mudstone and silicified grikes from the poorly bedded, recrystallized grainstone of the Mission Canyon Formation. These silicified grikes are vertical kart fissures (Monroe, 1970) and are direct evidence of subaerial unconformity. Grikes, while common in the peritidal facies association, are present in the ooid-shoal facies association at Sappington Canyon away laterally from the stratigraphic column, indicating these beds were also subaerially exposed. SB2 is present at Milligan Canyon and Crystal Lake. However, changes in bed geometries of the peritidal facies association at Milligan Canyon and discontinuous exposure at Crystal Lake made it difficult to place SB2 and overlying recrystallized grainstones into stratigraphic perspective.

Carbonate Point-count Data

Fourteen different petrographic components have abundances greater than 5% of the aggregate (Figure 4.7). Crinoidal grains are the most common component and are present in all eighty-one samples. Micrite is the next most common component (72 samples), followed by smooth (56 samples) and ribbed brachiopods (52 samples). While not as ubiquitous, other common components include spar (46 samples), indeterminant brachiopod fragments (43 samples), peloids (43 samples), and chert (31 samples). Less common components include pore space (17 samples), solitary corals (12 samples), algae (11 samples), fenestrate (8 samples) and trepostome (9 samples) bryozoans, and ooids (5 samples).

Two-way cluster analysis of thin-section components identifies three distinct petrographic clusters (Figure 4.7). The first cluster is crinoid-dominated, with crinoid abundances of 50% or greater, and micrite and ribbed, smooth and indeterminate brachiopod fragments making up the next abundant common components. The crinoid-dominated cluster (45 samples) includes samples from the foreshoal (31 samples), deep-subtidal 13 samples), and ooid-shoal facies associations (1).

The second cluster includes samples that contain abundant peloids and crinoid grains, with smooth, ribbed, and indeterminate brachiopod fragments making up the next most common grains. This peloidal-crinoidal cluster (12 samples) includes samples from the foreshoal (8 samples) and deep-subtidal facies associations (4 samples).

The third cluster includes samples that have abundant micrite and crinoid grains, with brachiopod fragments making up the next most common grains. This micritic-crinoidal cluster (24 samples) includes samples from the foreshoal (14 samples), deep-subtidal (9 samples), and ooid-shoal facies associations (1 sample).

Petrographic clusters are weakly uncorrelated with depositional facies associations in the two-way cluster analysis. Samples from the foreshoal facies association are dominant in the crinoid-dominated facies (69% of samples in facies), the peloidal-crinoidal (67% of samples in facies), and the micritic-crinoidal facies (58% of samples in facies). Samples from the deep-subtidal facies association are distributed at similar frequencies among the crinoid-dominated facies (29% of samples in facies), the peloidal-crinoidal cluster (33% of samples in facies), and the micritic-crinoidal facies (38% of samples in facies).

Faunal Data

Among the eighty-one samples, 2537 individuals from eighty-four species were counted. Solitary corals (10 species, 60% of individuals) and brachiopods (46 species, 28% of individuals) dominate the assemblages. Bryozoans (4 species, 3% of individuals), colonial corals (4 species, 1.5% of individuals), and gastropods (4 species, 1.5% of individuals) are less common. Bivalves (4 species), cephalopods (1 species), and proetid trilobites (1 species) are rare. Crinoids are present in all samples and include seven ossicle morphotaxa. Two crinoid species are identified with well-preserved calices and one calyx morphospecies from poorly preserved calices.

The culled species-abundance matrix reduced the original matrix to 2119 individuals and twenty species. Solitary corals dominate the culled dataset (7 species, 70% of culled individuals). Brachiopods from Rhynchonellata (7 species, 15% of culled individuals) and Strophomenata (2 species, 7% of culled individuals) are the next most common groups, followed by the round crinoid ossicle morphotaxon (3% of culled individuals), fenestrate bryozoans (2% of culled individuals), elliptical crinoid ossicle

morphotaxon (1.5% of culled individuals), and the trepostome bryozoan *Rhombopora* (1.5% of culled individuals).

Two-way cluster analysis of the culled species-abundance matrix indicates two clusters (Figure 4.8). The first cluster is the diverse brachiopod biofacies, dominated by the brachiopods *Schuchertella chemungensis* and *Spirifer centronatus*. Other common brachiopods include *Rhipidomella* sp. (15 samples), *Composita humilis* (11 samples), and *Camarotoechia* sp. (10 samples), but they are not ubiquitous across samples. Also common within this assemblage are round crinoid ossicles (26 samples) and the solitary corals *Cyathaxonia arcuata* (17 samples), *Zaphrentites* sp. (14 samples), and *Rylstonia* sp. (11 samples) . The diverse brachiopod biofacies is present in eighteen deep-subtidal samples, ten foreshoal samples, and no ooid-shoal samples.

The second cluster is the solitary coral-dominated biofacies, with *Cyathaxonia arcuata* (50 samples) and *Rylstonia* sp. (48 samples) being the most abundant solitary corals. Other common solitary corals include *Homalophyllites* sp. (35 samples), *Vesiculophyllum* sp. (25 samples), *Menophyllum* sp. (22 samples), and *Zaphrentites* sp. (21 samples). Round crinoid ossicles are also common within this biofacies (38 samples). Brachiopods are rarely identifiable to genus but include productids and spiriferids. The solitary coral-dominated biofacies comprises of samples predominantly from the foreshoal facies association (41 samples), but also includes some deep-subtidal (9 samples) and ooid-shoal (2) samples.

Nonmetric Multidimensional Scaling

The NMS/PCA ordination plots samples and species such that samples close to one another are similar in composition, and species that plot close to one another tend to

co-occur (Figure 4.9A and B). The amount of explained variation decreases from axis 1 to axis 2, and so on. Coding the samples by depositional environment indicates an onshore–offshore gradient along NMS axis 1 (Figure 4.9A). Samples grade from the deep-subtidal association in negative values of NMS axis 1 to the foreshoal association in positive values of NMS axis 1. Ooid-shoal samples plot with the foreshoal samples, indicating that their assemblage compositions are similar. Species also show a gradation along NMS axis 1, with brachiopods at negative values of NMS axis 1 and solitary corals at positive values (Figure 4.9B). Samples from the deep-subtidal facies association are dominated by brachiopods, whereas the samples from the foreshoal facies association are dominated by solitary corals. The clustering of species and samples within the NMS ordination space is similar to biofacies clustering within the two-way cluster analysis, which also indicates the diverse brachiopod biofacies is predominantly samples from the deep-subtidal facies association and the solitary coral-dominated biofacies is predominantly samples from the foreshoal facies association (Figure 4.8).

NMS axis 2 indicates greater variation in samples from the foreshoal facies association than the deep-subtidal facies association (Figure 4.9A). Samples from the ooid-shoal facies association occur only at negative values of NMS axis 2 (Figure 4.9A). Taxa indicate a gradation along NMS axis 2 when coded by class (Figure 4.9B). Brachiopod taxa mostly cluster close together and centrally along NMS axis 2, although, the rhynchonellids *Nucleospira obesa* and *Atrypa* sp. are common at high positive NMS axis 2 values, and indeterminate productids plot at negative NMS axis 2 scores. Solitary corals clustering centrally along NMS axis 2 include *Amplexoccarina* sp., *Rylstonia* sp., *Cyathaxonia arcuata*, and *Vesiculophyllum* sp., whereas *Menophylum* sp.,

Homalophyllites sp., and *Zaphtentites* sp. are at negative values along NMS axis 2. Fenestrate bryozoans also are at negative NMS axis 2 scores.

The *envfit* correlation between ordination scores and lithological variables plots vectors in the ordination space where the length of the vector signifies the strength of relationship along a given axis (Figure 4.9C). Ordination scores of the lithological variables are calculated for each axis of ordination (Table 4.2). Variables with large axis scores have a strong correlation with that axis. Positive scores on NMS axis 1 indicate samples rich in solitary coral (axis 1 score of 0.97) and peloid (axis 1 score of 0.89) constituents. Negative scores on NMS axis 1 indicate samples rich in micrite (axis 1 sore of –0.99) and trepostome bryozoan (axis 1 score of –0.90) constituents and grayer hue (axis 1 score of –0.88). Positive scores on NMS axis 2 indicate samples rich in smooth brachiopod (axis 2 score of 1.00) constituents. Negative scores on NMS axis 2 indicate samples with high bioturbation (axis 2 score of –1.00), rich in crinoid (axis 2 score of –0.96), spar (axis 2 score of –0.95), ooid constituents (axis 2 score of –0.94) and indeterminant brachiopod constituents (axis 2 score of –0.80), and have a lower value (axis 2 score of –0.88), indicating a lighter rock color.

DISCUSSION

Carbonate Facies Associations

The carbonate facies associations identified in the lower Madison Group are mostly congruent with those of Elrick and Read (1991), as well as Sonnenfeld (1996) and Smith et al. (2004). One major difference is that fewer lithofacies are recognized here than in previous studies. Elrick and Read (1991) identified eleven lithofacies across six facies associations and Sonnenfeld (1996) identified sixteen lithofacies across five

depositional environments, compared with the seven lithofacies across six depositional environments recognized here. Sonnenfeld (1996) also included the upper Madison Group, which may record his greater number of lithofacies from the lagoonal and peritidal environments that dominate the upper Madison Group. The number of facies and environments identified are most comparable to Smith et al. (2004), who identified seven lithofacies and depositional environments.

The offshore facies association in central Montana is comparable to the ramp-slope of Elrick and Read (1991) and outer ramp facies of Sonnenfeld (1996). All studies characterized this facies association as a carbonate mudstone interbedded with shale or argillite couplets deposited in a dysoxic to oxic environment below storm-wave base (Elrick and Read, 1991; Sonnenfeld, 1996). Elrick and Read (1991) also identified bryozoan-crinoidal bioherms, interpreted as offshore carbonate mud mounds. These were identified only at one of their localities and may represent a more localized feature.

The deep-subtidal facies association is comparable to the deep ramp of Elrick and Read (1991) and middle ramp facies of Sonnenfeld (1996) and Smith et al. (2004). The bioturbated, skeletal packstone with argillaceous partings is interpreted as being deposited above storm-wave base, and is common in all studies of the lower Madison Group with only subtle variations. Elrick and Read (1991), and Sonnenfeld (1996) all noticed graded bedding within their facies associations. Skeletal grains were denser along argillaceous partings, but actual grading within beds was not noticed in this study. Elrick and Read (1991) also included skeletal-ooid grainstone caps within their deep ramp facies association, based on the presence of hummocky cross-stratification, which commonly form from storm activity (Aigner, 1982; Dott and Bourgeois, 1982; Duke, 1985; Tucker

and Wright, 1990; Flügel, 2010). Hummocky cross-stratification was not identified within any skeletal grainstone lithofacies of this study, and as a result, all skeletal-grainstones were interpreted as above fair-weather wave base.

The skeletal grainstone and carbonate mudstone lithofacies of the foreshoal facies association corresponds to the shallow subtidal of Elrick and Read (1991) and foreshoal-intershoal and bank of Smith et al. (2004) depositional environments. The skeletal grainstone represent localized reworking of skeletal grains to form the shoal and bank deposits (Elrick and Read, 1991; Smith et al., 2004) with cross-stratification identified in previous studies suggesting high shear stress environment. No cross-stratification was identified within the skeletal grainstone lithofacies, but was presumably destroyed by bioturbation. The carbonate mudstones are interpreted as more protected intershoal deposits where fossils and skeletal grains are inferred to be a mixture of autochthonous material and those transported from adjacent shoal and bank deposits (Elrick and Read, 1991; Smith et al., 2004). Foreshoal bank-intershoal complexes are found in other Mississippian carbonate ramps (Carr, 1973, Smith and Read, 1999, 2001; Burrowes, 2006; Bonelli and Patzkowsky, 2008) as well as in modern carbonate environments (Hine, 1977; Read, 1985; Tucker and Wright, 1990; Burchette and Wright, 1992; Flügel, 2010).

Ooid-shoal facies are identified in all previous studies of the lower Madison Group (Elrick and Read, 1991; Sonnenfeld, 1996; Smith et al., 2004), as are thick cycles of ooid-shoal facies, which were also observed in the HST of this study. Ooid-shoals in modern settings such as the Bahamas and the Persian Gulf form within warm, shallow water that experience strong tidal currents and waves (Ball, 1967; Hine, 1977; Harris,

1979; Halley et al., 1983; Wanless and Tedesco, 1993), supporting the tropical setting of the lower Madison Group during the Mississippian (McKerrow and Scotese, 1990). Ooid shoals are typically poorly fossiliferous, sediment-mobile environments (Feldman et al., 1993), which matches the low diversity and abundance of fossils observed in this study.

The crinoid-shoal facies association is interpreted as lagoonal by Elrick and Read (1991) and Smith et al. (2004) or as another sub-environment of the foreshoal by Elrick and Read (1991) depending on its stratigraphic context. If it appears stratigraphically below the ooid shoals, crinoidal grainstones can be interpreted as foreshoal facies, and if it appears above the ooid shoal it is lagoonal (Elrick and Read, 1991). In this study, the crinoid-shoal facies association appears above the ooid-shoal facies association in shallowing-upward parasequences, indicating it represents a lagoonal depositional environment. Further evidence supporting a lagoonal interpretation is lack of cross-stratification that would be expected in the foreshoal (Elrick and Read, 1991; Smith et al., 2004). The low diversity and abundance of fossils also support more restricted conditions. The light tan color of this facies association is also evident in the Madison Shelf (Elrick and Read, 1991; Smith et al., 2004), suggesting that this facies was commonly dolomitized from exposure to meteoric water (Badiozamani, 1973; Choquette and Steinen 1980; Tucker and Wright, 1990; Flügel, 2010) across the entire shelf.

The peritidal facies association is similar to that of previous studies (Elrick and Read, 1991; Sonnenfeld, 1996; Smith et al., 2004). Planar-laminated carbonate mudstones interbedded with structureless carbonate mudstones indicate a quiet water, restricted lagoonal to supratidal environment (Elrick and Read, 1991, Tucker and Wright, 1990; Sonnenfeld, 1996; Smith et al., 2004). Lamination are likely caused by algal mats

living on the sediment surface (Elrick and Read, 1991; Smith et al., 2004) that trap and bind the sediment (Tucker and Wright, 1990; Flügel, 2010). In addition to the grikes observed in this study, this facies association commonly contains brecciation and other karst features where exposed beneath sequence boundaries on the Madison Shelf (Elrick and Read, 1991; Sonnenfeld, 1996; Smith et al, 2004), indicating the presence of a subaerial unconformity.

Sequence-stratigraphic Architecture

One 3rd-order depositional sequence (*sensu* Van Wagoner et al., 1988) for the lower Madison Group is identified at the four localities in central Montana. The interval between the lower sequence boundary (SB1) at the unconformity with the Sappington Formation and the upper sequence boundary (SB2) at the contact with the upper Madison Group spans approximately 4 million years. Previous studies of the lower Madison group identified two (Sonnenfeld, 1996; Smith et al., 2004) or three (Elrick and Read, 1991) 3rd-order depositional sequences during the same interval.

One possibility for the difference in the number of sequences is that three of the columns in this study represent the more distal Central Montana Trough (Figure 4.1) where the sequence boundaries of the more proximal Madison Shelf are not easily distinguishable (Elrick and Read, 1991; Sonnenfeld, 1996; Smith et al., 2004). In fact, Elrick and Read (1991) could not confidently extend the sequence boundary overlying their second sequence up-dip into central Wyoming, owing to lack of change in stacking patterns, and they combined the sequence boundary with a flooding surface down-depositional dip into central Montana. Additional measured sections within the Central Montana and along the northwestern shelf near the Gibson Reservoir locality would

provide the necessary information to identify changes in stacking patterns that can be correlated to sequence boundaries on Madison Shelf.

The second possibility for this difference is the different approaches in defining sequence boundaries. This study and Elrick and Read (1991) apply the Van Wagoner et al. (1988) model of placing sequence boundaries at unconformities separating the HST and from the overlying LST where stacking patterns transition from progradational stacking patterns to aggradational stacking patterns and are typically associated with subaerial exposure. Sonnenfeld (1996) and Smith et al., (2004) use transitions from decreasing accommodation cycles (i.e., regressive) to increasing accommodation cycles (i.e., transgressive) to demarcate sequence boundaries and not changes in progradational stacking or subaerial unconformities (cf. Embry and Johannessen, 1992). This may account for discrepancies between this study and Sonnenfeld (1996). It does not explain the differing number of depositional sequences between this study and Elrick and Read (1991), which is better explained by the lack of identifying the correlative conformities of Elrick and Read (1991).

The position of SB1 at the basal contact with the Sappington Formation corresponds with the lowest sequence boundary of the first depositional sequence of Elrick and Read (1991), Sonnenfeld (1996), and Smith et al. (2004). The position of SB2 at the upper contact with the Mission Canyon Formation and Castle Reef Dolomite of the upper Madison Group corresponds to the upper sequence boundaries of the second depositional sequence of Sonnenfeld (1996) and Smith et al. (2004) and with the upper sequence boundary of the third depositional sequence of Elrick and Read (1991). Thus, although all studies agree that there is a sequence boundary at the base and top of the

Lodgepole Formation, they disagree on whether the Lodgepole Formation contains any unconformities.

While carbonate facies associations differ between the more distal Central Montana Trough (i.e., this study) and the more proximal Madison Shelf (Elrick and Read, 1991; Sonnenfeld, 1996; Smith et al., 2004), stacking patterns of parasequences allow for comparison of systems tract architecture. The LST in this study is defined similarly to Elrick and Read (1991), with parasequences grading from progradationally stacked to aggradationally stacked. Neither Sonnenfeld (1996) nor Smith et al. (2004) recognize an LST in their sequences as they place progradationally stacked packages into their HST and aggradationally stacked packages into their TST.

The TST in this study is defined identically with Elrick and Read (1991) and similar to Sonnenfeld (1996) and Smith et al. (2004), where all retrogradationally stacked parasequences are placed within the TST. Sonnenfeld (1996) and Smith et al. (2004) include all aggradationally stacked parasequences within the TST.

The HST in this study is defined similarly to Elrick and Read (1991) with parasequences grading from aggradationally stacked to progradationally stacked. The HST in this study differs from Sonnenfeld (1996) and Smith et al. (2004) as those studies considered only progradationally stacked parasequences that also binned portions of the LST within their HST.

As this study identified only one 3rd-order depositional sequence, the systems tracts in this study do not match those identified by Elrick and Read (1991), Sonnenfeld (1996), and Smith et al. (2004). The position of the TST and HST of this study may correlate however with the TST and HST of the 3rd-order composite sequence of

Sonnenfeld (1996) that examines more long-term trends in accommodation history within the lower Madison Group.

The boundary between the TST and HST at the four central Montana localities in this study is marked by the furthest landward progression of the deepest carbonate facies association. While an individual maximum flooding surface could not be identified, a several meter interval signifying the presence of the deepest water faces known as a maximum flooding zone is present at all localities. Sonnenfeld (1996) also used maximum flooding zones to distinguish the boundary between their TST and HST along the Madison Shelf. Elrick and Read (1991) discuss the difficulty of correlating a single maximum flooding surface across along the Madison Shelf, and apply the maximum flooding zone approach for their second and third depositional sequences. Assuming the TST and HST of this study correlates to the TST and HST of the 3rd-order composite sequence of Sonnenfeld (1996), the maximum flooding zone correlated among Sappington Canyon, Milligan Canyon, Crystal Lake, and Gibson Reservoir is equivalent to the maximum flooding zone of the lowermost 3rd-order depositional sequence along the Madison Shelf (Elrick and Read, 1991; Sonnenfeld, 1996; Smith et al., 2004). This implies that the HST of this study incorporates not only the HST of the lowermost 3rd-order sequence but also the remaining 3rd-order sequences of the lower Madison Group. Future studies should examine these beds in the HST to identify additional sequence boundaries or correlative conformities for better correlations with the sequence-architecture established on the Madison Shelf (Mudge et al., 1962; Reid and Dorobek, 1993).

Lithologic Variations

Crinoid ossicles are the predominant skeletal grain in these samples, they and are abundant in all depositional environments, which is common in the Mississippian carbonate rocks (Ausich, 1997; Kammer and Ausich, 2006). Crinoids reached their peak abundance and diversity during the Tournaisian and Visean (Kammer and Ausich, 2006), and dispersed themselves through a wide range of water depths, substrates, and wave energies (Kammer and Ausich, 1987; Kammer et al., 1997, 1998; Kammer and Ausich, 2006). Camerate crinoids are especially common in carbonate facies and are one the most diverse group during the Mississippian (Kammer and Ausich, 2006). Camerates are particularly diverse and abundant within the lower Madison Group (Laudon and Severson, 1953; Laudon, 1967), but the syntaxial cement surrounding most crinoid grains made taxonomic identification impossible in thin section.

The foreshoal and deep-subtidal samples of the crinoidal-dominated association (Figure 4.7) are encrinites, carbonate rocks with compositions at least fifty-percent crinoid grains (Ausich, 1997; Kammer and Ausich, 2006). Encrinites from the Mississippian form thick, regional deposits and are found in North America, Europe, the Middle East, and Asia (Waters and Sevastopulo, 1984; Chen and Yao, 1993; Ausich, 1999ab; Webster et al., 2003; Debout and Denayer, 2018). While not true encrinites, the peloidal and micritic point-count clusters (Figure 4.7) are also rich in crinoid grains, pointing to the dominance of crinoids during the Mississippian. The presence of thick, crinoidal deposits in the lower Madison Group indicates that open-marine stenohaline

conditions were prevalent in Montana during the Mississippian, similar to other coeval carbonate ramps in North America and Europe (Kammer and Ausich, 2006).

The presence of a micrite-rich petrographic clusters within deep-subtidal and foreshoal samples is consistent with the facies model of Elrick and Read (1991) and Sonnenfeld (1996), who both reported carbonate wackestone with these facies associations. Micrite is produced in high-energy and low-energy environments of the carbonate factory, but its accumulation is determined by production rate, proximity to micrite source, and how quickly the micrite can be deposited and bound before it can be transported (Tucker and Wright, 1990; Flügel, 2010). Packstones in the deep subtidal generally have a high percentage of micritic matrix, as the deep subtidal is a location of micrite production as well as a recipient of micrite from shallower environments. Additionally, the deep subtidal experiences less frequent wave action to transport the micrite away as it is below fair-weather wave base (Tucker and Wright, 1990; Flügel, 2010). The foreshoal samples in this micritic-crinoidal association are sampled primarily from the carbonate mudstone lithofacies of intershoal environment (Table 4.1), which is also a location of micrite production, a recipient of micrite from adjacent shoals and banks, and protected from waves by the shoals and skeletal banks of the foreshoal facies association, similar to lagoons behind barrier islands and reefs (Tucker and Ward, 1990; Flügel, 2010).

Peloids are common in many samples from the deep subtidal and foreshoal, and they are a defining attribute of the third petrographic cluster (Figure 4.7). Peloids are identified in these facies by Sonnenfeld (1996) and Smith et al. (2004). Peloids are also common in the lithofacies model established by Elrick and Read (1991), although they

called them as pellets. The term “pellets” indicates the fecal matter of a macrophagous detrital feeder (Flügel, 2010), but pellets and non-fecal peloids in this study could not be distinguished, as is generally true (Tucker and Wright, 1990; Flügel, 2010). The large abundance of peloids likely indicates the presence of macrophagous detrital feeders such as gastropods or polychaete worms (Shinn, 1968; Garrett, 1977; Wanless et al., 1981; Tucker and Wright, 1990; Flügel, 2010), which are common detrital feeders in tropical, highly bioturbated carbonates (Flügel, 2010) such as the lower Madison Group. Peloids can also be created from small fragments of micritized bioclasts (Bathurst, 1975; Reid et al., 1992; Reid and MacIntyre, 1998). This is equally plausible as whole and coarse skeletal grains are observed to have partially or completely micritized when viewed in thin section.

Faunal Variations and Environmental Gradients

Faunal variation in the lower Madison Group is primarily correlated with water depth (Figures 4.8 and 4.9A). The two-way faunal cluster analysis indicates that the high-diversity brachiopod biofacies includes samples predominantly from the deep-subtidal facies association, whereas the solitary coral biofacies is predominantly found in the foreshoal facies association (Figure 4.8). NMS axis 1 mirrors these results with samples grading from the deep subtidal to the foreshoal (Figure 4.9A), and with taxa grading from brachiopod to solitary coral dominated (Figure 4.9B). The lithological data is also consistent with a water-depth gradient. Samples grade along NMS axis 1 from an increased amount of micrite and bryozoan fragments to samples rich in peloids and coral fragments. While micrite is produced through a variety of mechanisms within most environments of a carbonate ramp, micrite-rich samples are typically interpreted as lower

energy environments, such as lagoons, the deep subtidal, and offshore (Tucker and Wright, 1990; Flügel, 2010). Additionally, bryozoans are mostly identified in assemblages from the deep subtidal and are only identified in thin sections of skeletal packstone samples.

As water depth is a complex gradient (*sensu* Whittaker, 1956; Austin et al., 1984), it is far more likely that taxa responded to one of many covarying variables (i.e., substrate, wave energy, temperature, oxygenation, nutrients) that contribute to the water-depth gradient than they did to water depth itself (Tait and Dipper, 1998; Patzkowsky and Holland, 2012). Taxa morphology, life habits, and ecology can provide clues to which of the covarying environmental variables are correlated with assemblage variation (see Lafferty et al., 1994; Patzkowsky, 1995; Holland et al., 2001; Olszewski and Patzkowsky, 2001; Webber, 2002; Scarponi and Kowalewski, 2004; Tomašových, 2006; Redman et al., 2007; Perera and Stigall, 2018).

Examining the distribution of brachiopod life mode within the NMS shows no relationship to the water-depth gradient. Brachiopods in the deep-subtidal facies association are predominantly rhynchonellids, which are pedunculate epifauna inferred to attach on the substrate surface (Rudwick, 1970; Fürsich and Hurst, 1974). Brachiopods in the foreshoal facies association are predominantly spiriferids, which are also pedunculate epifauna, and productids, which are sessile taxa with ornamentation adapted for resting on or semi-infaunally within soft substrates (Rudwick, 1970; Fürsich and Hurst, 1974). Typically, soft substrate environments commonly contain infaunal, semi-infaunal or resting epifaunal taxa, whereas firm or hard substrate have common attaching epifaunal taxa (Rudwick, 1970; Fürsich and Hurst, 1974; Holland et al., 2001; Tomašových, 2006;

Perera and Stigall, 2018). The ubiquitous distribution of pedunculate brachiopods indicates firm substrates may have been common in all facies associations within the lower Madison Group.

The occurrence of rugose corals may indicate a substrate gradient that covaries with water depth. Paleozoic rugose corals are found in a wide range of water depths but are more abundant and diverse in shallow waters (Sando, 1980; Scrutton, 1998). Most solitary corals live a liberosessile lifestyle in which they rest epifaunally or semi infaunally in the substrate (Elias et al., 1988; Bolton and Driese, 1990; Scrutton, 1998). Substrate composition and firmness, however, affect the hydrodynamic stability of rugose corals (Bolton and Driese, 1990). Rugose corals resting on muddy substrates are often found in hydrodynamically unstable positions, whereas those resting on less muddy or firmer substrates are in more stable positions (Bolton and Driese, 1990). The distribution of rugose corals in these assemblages is consistent with Mississippian and Paleozoic rugose coral ecology. Rugose corals in the lower Madison Group are present in the muddy skeletal packstone of the deep-subtidal facies association and carbonate mudstone lithofacies of the foreshoal facies associations. However, their increased diversity and dominance in the skeletal grainstone lithofacies of the foreshoal facies association coincides with a decrease in micrite (Figure 4.9B and C). This decrease in micrite and muddy substrate may have led to more hydrodynamically stable rugose corals and increased survival (Bolton and Driese, 1990).

Brachiopod ornamentation and rugose coral orientation also suggest wave energy may have covaried with water depth, as is expected on carbonate ramps (Read, 1985; Burchette and Wright, 1992). Brachiopods in the deep subtidal are predominantly smooth

or fine-ribbed, suggesting quiet-water environments (Rudwick, 1970; Fürsich and Hurst, 1974). The presence of the coarse-ribbed *Camarotoechia sp*. as well as pedunculate rhynchonellids within the deep-subtidal facies associations may indicate the occurrence strong waves produced by storms (Rudwick, 1970; Fürsich and Hurst, 1974). Rugose corals in the deep-subtidal facies association are commonly preserved in a vertical orientation with calices opening upwards and apices pointed downwards with respect to bedding surfaces. Rugose corals in the skeletal grainstone lithofacies of the foreshoal association are preserved oblique and on their sides with respect to the bedding surface, a position implying frequent wave action (Elias et al., 1988). Such differences in orientation suggests an increase in wave energy from the deep subtidal to the foreshoal (Elias et al., 1988).

Lithological data suggests that NMS axis 2 represents an oxygen gradient. Bioturbation, Munsell hue, and Munsell value are all highly correlated along NMS axis 2 (Table 4.2, Figure 4.9C). As NMS axis 2 scores become more negative, Munsell hues and values indicate that rock color grades from brownish-dark gray to medium-light gray carbonate rocks. Color is commonly used as a qualitative assessment of redox state and oxygenation, with darker colors representing relatively carbon-rich, reduced conditions and lighter colors representing more carbon-poor and oxic conditions (Berner, 1981; Maynard, 1982; Svarda et al., 1984; Algeo and Maynard, 2004; Piper and Calvert, 2009). Incorporating Munsell hues and values into the multivariate analysis allows a qualitative variable to be transformed into a quantitative one to track gradational changes in color and oxidation. In addition to a lightening in color, ichnofabric indices increases as NMS axis 2 becomes more negative, indicating greater vertical burrowing in the sediment

surface (Droser and Bottjer, 1986), suggesting more aerobic pore-water conditions (Boyer and Droser, 2011). If NMS axis 2 represents oxygen, it implies that the brachiopods *Nucleospira obesa* and *Atrypa* sp. prefer settings with more reduced pore-water conditions, whereas solitary corals in the lower Madison Group prefer settings with well-oxygenated pore waters (Figure 4.9B).

Biogenic structures indicate that oxygenation levels for all samples range from slightly dysaerobic to fully aerobic (*sensu* Boyer and Droser, 2011) and that the oxygen gradient is independent and uncorrelated with the water-depth gradient. *Zoophycus*, *Taenadium?*, and other horizontal traces are identified only in the deep-subtidal facies association and variations in abundances may indicate occasional dysaerobic conditions (Boyer and Droser, 2011). Similar ichnofabric indices and multiple, large vertical burrows such as *Thalassinoides* in the deep-subtidal and the foreshoal associations indicate aerobic bottom was common across all depths (Boyer and Droser, 2011). Although glauconite is a rare constituent in two samples from Sappington Canyon, the absence of authigenic minerals overall provides additional support for aerobic pore waters within the lower Madison Group.

CONCLUSIONS

1. Six carbonate facies associations and seven depositional environments are identified in the lower Madison Group at the four localities in this study. While fewer lithofacies are identified in this study compared with previous studies of the Madison Group, patterns between carbonate facies associations and depositional environment are consistent between studies.

2. One 3rd-order depositional sequence is identified for the lower Madison Group within the Central Montana Trough and on the northwestern shelf, which differs from the two or three 3rd-order depositional cycles identified to the southwest along the Madison Shelf. The 3rd-order depositional sequence identified here is likely a composite sequence that incorporates the same timeframe of the previously identified sequences on the Madison Shelf.
3. Two-way cluster analysis of petrographic components identifies three petrographic clusters within the lower Madison Group in central Montana: crinoid dominated, peloid-crinoid, and micrite-crinoid. These groupings are do not correlate with lithological facies associations nor do they correlate with an onshore–offshore gradient. Lithological variations are consistent with lithologic patterns along the Madison Shelf to the south as well as other carbonate ramp systems in the Mississippian.
4. Two-way cluster analysis of faunal data identifies two biofacies. The diverse brachiopod biofacies is dominated by *Schuchertella chemungensis* and *Spirifer centronatus*, and it includes samples predominantly from the deep-subtidal facies association as well as samples from the carbonate mudstone lithofacies of the foreshoal facies association. The solitary coral-dominated biofacies is dominated by *Cyathaxonia arcuata* and *Rylstonia sp*., and it includes samples predominantly from the foreshoal facies association.
5. Water depth is the gradient associated with variation in faunal assemblages along NMS axis 1. Deep-subtidal assemblages are defined by the diverse brachiopod biofacies and foreshoal assemblages are defined by a rugose coral-dominated

assemblage. The carbonate facies associations, biofacies and lithological data grade along the first axis of ordination in relation to the onshore–offshore gradient, indicating a transition to less muddy and higher energy conditions more proximal to shore.

6. Lithological data ordinated within the NMS identifies a secondary oxygen gradient potentially associated with faunal variation reflected by increase in bioturbation and a lightening of rock color. Samples from the foreshoal association display greater variation along NMS axis 2. Distribution of species along NMS axis 2 indicate the brachiopods *Nucleospira obesa* and *Atrypa* sp. are more abundant in settings with reduced, pore-water conditions whereas solitary corals prefer settings with more oxygenated pore waters.
7. This study demonstrates the efficacy of directly linking lithological data to faunal data when conducting ecological analyses. Combining closely spaced, replicate sampling of lithological data in conjunction with faunal data unlocks additional sources of environmental variation driving fossil assemblage compositions, providing more detailed environmental reconstructions and understanding of community compositions in the fossil record.

TABLES

Table 4.1: Carbonate facies associations of the lower Madison Group

Facies associations	Lithology	Sedimentary and biogenic structures	Fossils	Geometry and contact relationships
Offshore	Very thin- to thin-bedded dark gray carbonate mudstone . Commonly interbedded with dark gray to black shales. Commonly expresses as vegetated covered interval.	Planar lamination abundant. Ichnofabric index ii1	None observed	Tabular. Sharp basal contact. Grades upwards into deep-subtidal facies association.
Deep subtidal	Thin bedded, medium to dark gray skeletal packstone with tan argillaceous partings	Vortex ripples, wave-ripple lamination, and planar lamination rare. Ichnofabric index ii2–ii4; *Zoophycus*, *Thalassinoides* and *Taenidium*?	Whole fossils and coarse fragments of crinoids, fenestrate and trepostome bryozoans, brachiopods, solitary corals and proetid trilobites	Tabular. Gradationally overlies offshore association and is gradationally overlain by the foreshoal association.
Foreshoal	Medium-bedded medium to light gray skeletal, peloidal, oolitic grainstone	Planar lamination rare Ichnofabric index ii3–ii5; silicified vertical and horizontal burrows	Whole fossils and coarse fragments of crinoids, solitary corals, colonial corals, brachiopods, and mollusks	Tabular. Gradationally interbedded with carbonate mudstone lithofacies. Gradationally overlies deep-subtidal association and gradationally overlain by ooid-shoal association
	Medium-bedded dark gray carbonate mudstone	Planar lamination rare; Ichnofabric index ii3–ii5; Silicified *Thalassinoides* and other burrows	Whole fossils and coarse fragments of crinoids, solitary corals, colonial corals, brachiopods	Tabular. Gradationally interbedded with skeletal-oolitic grainstone lithofacies

Table 4.1 (continued): Carbonate facies associations of the lower Madison Group

Facies associations	Lithology	Sedimentary and biogenic structures	Fossils	Geometry and contact relationships
Ooid shoal	Medium-bedded, medium to light gray oolitic grainstone	Small-scale cross-stratification common Ichnofabric index ii1–ii4	Whole and coarse fossil fragments of crinoids, solitary corals, brachiopods occasionally observed.	Tabular. Gradationally overlies skeletal-ooid grainstone of the foreshoal association. Gradationally overlain by crinoid-shoal and peritidal associations
Crinoid shoal	Thin to medium-bedded tan crinoidal grainstone	None observed Ichnofabric index ii4	Only coarse crinoid ossicles	Tabular. Gradationally overlies ooid-shoal association. Gradationally overlain by peritidal association
Peritidal	Thin to medium-bedded light gray carbonate mudstone where exposed. Commonly expresses as vegetated covered intervals up section of the foreshoal and ooid-shoal facies.	Well-laminated; Brecciation and silicified grikes common. Ichnofabric index ii1	None observed.	Tabular. Gradationally overlies ooid-shoal and crinoid-shoal associations. Upper contact is sharp.

Table 4.2: Ordination scores for lithological variables. Strong loadings (i.e., greater than 0.80 and less than –0.80) are in bold.

	NMS Axis 1	NMS Axis 2
Brachiopod indet.	0.60	**–0.80**
Ribbed brachiopod	–0.75	0.66
Smooth brachiopod	–0.04	**1.00**
Crinoid	0.29	**–0.96**
Fenestrate bryozoan	–0.66	–0.75
Trepostome bryozoan	**–0.90**	0.44
Solitary coral	**0.97**	0.26
Peloid	**0.89**	0.46
Ooid	–0.35	**–0.94**
Algae	0.62	–0.78
Micrite	**–0.99**	0.13
Pore space	0.64	0.77
Spar	–0.33	**–0.95**
Chert	0.74	–0.67
Bioturbation	0.07	**–1.00**
Munsell hue	**–0.88**	–0.47
Munsell value	–0.47	**–0.88**

Table 4.3: Taxonomic codes for the NMS ordination (Figure 4.9)

Species	Code
Amplexocarina sp.	Amc
Atrypa sp.	Atr
Camarotoechia sp.	Cam
Composita humilis	Com
Cyathaxonia arcuata	Cya
Elliptical crinoid ossicle	Ecr
Fenestrate bryozoan	Fen
Homalophyllites sp.	Hom
Menophyllum sp.	Men
Nucleospira obesa	Nuc
Productid indeterminate	Pro
Rhipidomella sp.	Rhi
Rylstonia sp.	Ryl
Schuchertella chemungensis	Sch
Spiriferid indeterminate	Sp
Spirifer centronatus	Spc
Vesiculophyllum sp.	Ves
Zaphrentites sp.	Zap

FIGURES

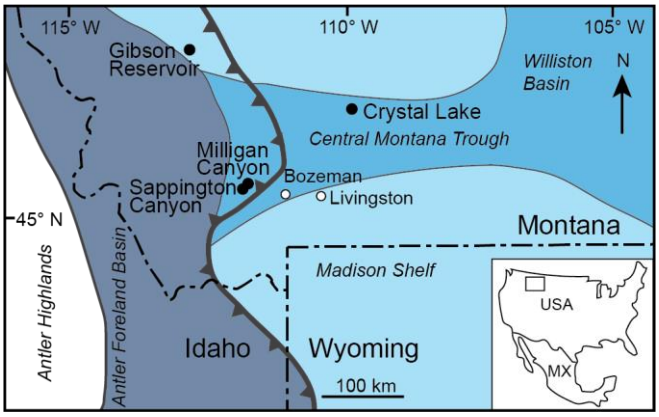

Figure 4.1.— Study sites and paleogeography of the lower Madison Group. Study sites are noted by black circles and cities by white circles. Light blue indicates shallow carbonate shelves and darker blues indicate deeper–water carbonate basins. Modified from Smith et al. (2004).

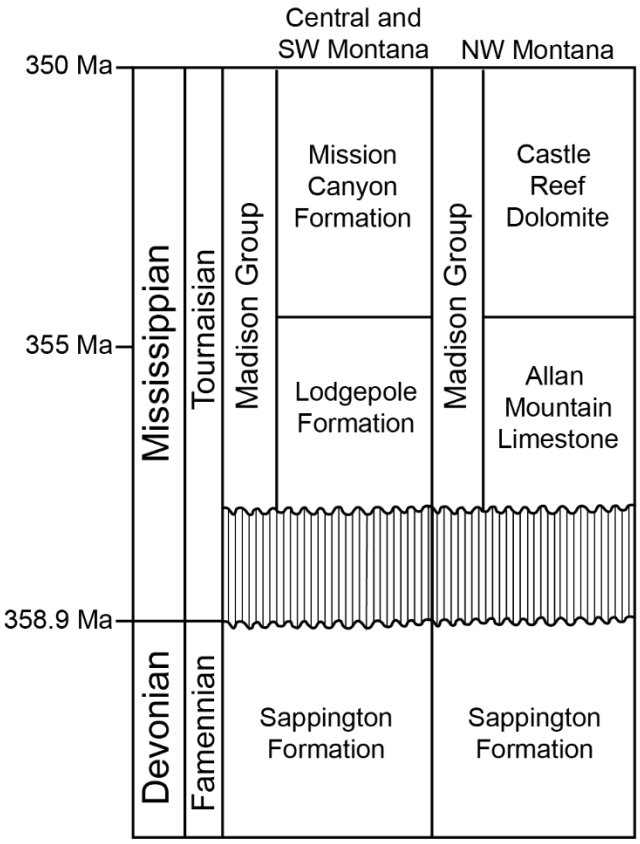

Figure 4.2.— Chronostratigraphic and lithostratigraphic framework of the Madison Group carbonates and underlying Upper Devonian Sappington Formation in southwestern, central, and northwestern Montana. Modified from Elrick and Read (1991), Sonnenfeld (1996), and Johnston et al. (2010). Correlations based on Gutschick et al. (1980) and Sando (1985). Time scale is from Cohen et al. (2013)

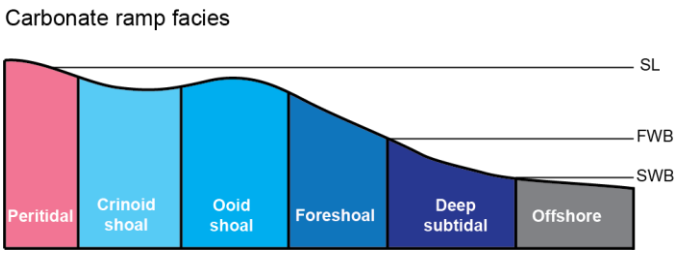

Figure 4.3.— Onshore–offshore distribution of carbonate facies on the Madison shelf. Based on Elrick and Read (1991)

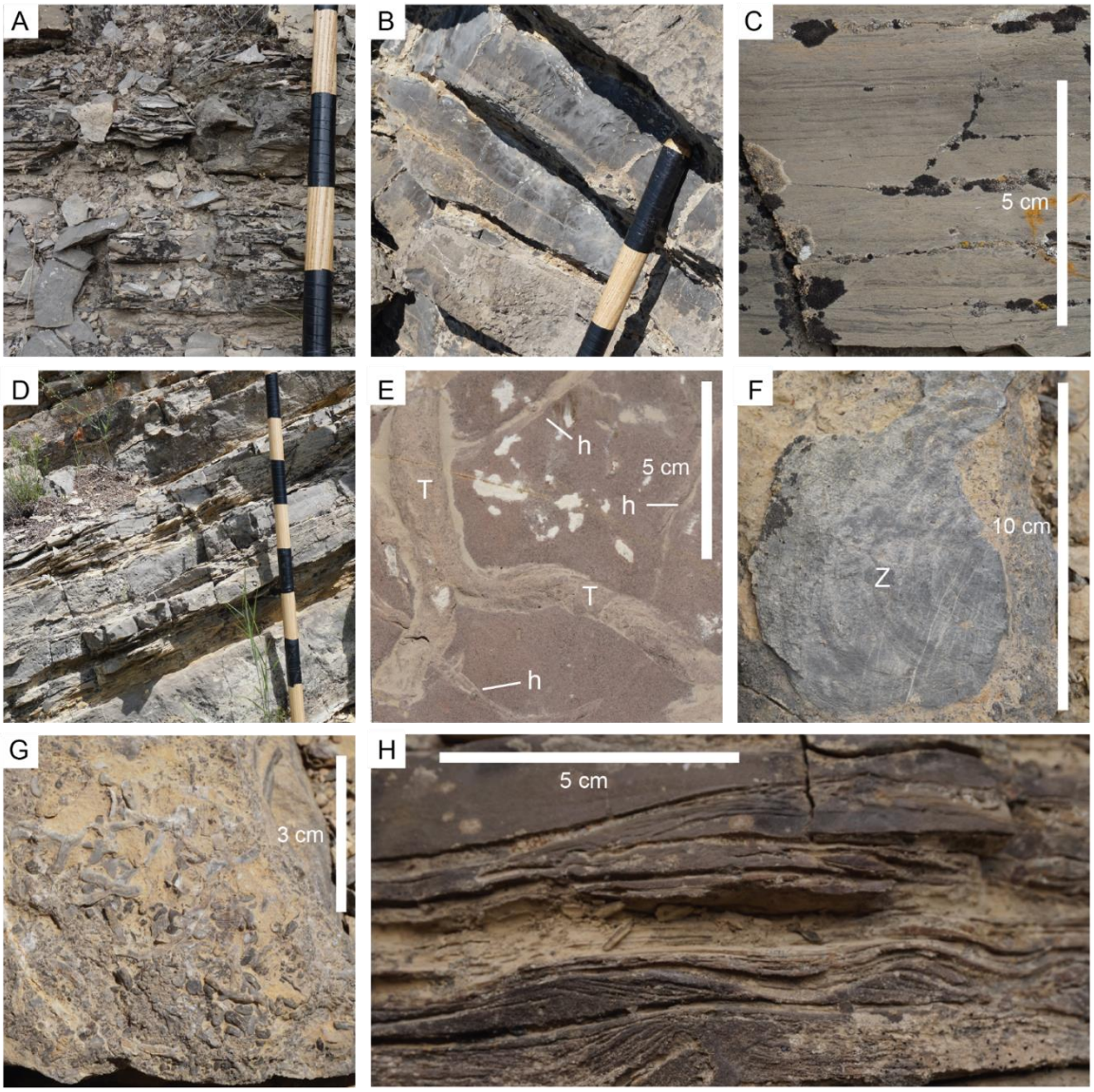

Figure 4.4.— Offshore and deep-subtidal facies. A) Interbedded shale and thin-bedded carbonate mudstone of the distal offshore facies association, Sappington Canyon, 30 m. B) Thin-bedded carbonate mudstone of the proximal offshore facies association, Sappington Canyon, 30 m. C) Well-preserved planar lamination within the offshore carbonate mudstone of the offshore facies association facies association, Sappington Canyon, 30 m. D) Thin-bedded skeletal packstone with argillaceous to shale partings of the deep-subtidal facies association, Milligan Canyon, 21 m. E) *Taenidium*? (T) and other horizontal burrows (h) on bedding surface within the deep-subtidal facies association, Crystal Lake, 108 m. F) *Zoophycus* (Z) ichnofossil on along bedding surfaces in the deep-subtidal facies association, Milligan Canyon, 2 m. G) Shell hash within the deep-subtidal facies association with bryozoans, crinoid ossicles, and brachiopod fragments, Milligan Canyon, 2.5 m. H) Wave-ripple lamination in the deep-subtidal facies association, Crystal Lake, 58 m.

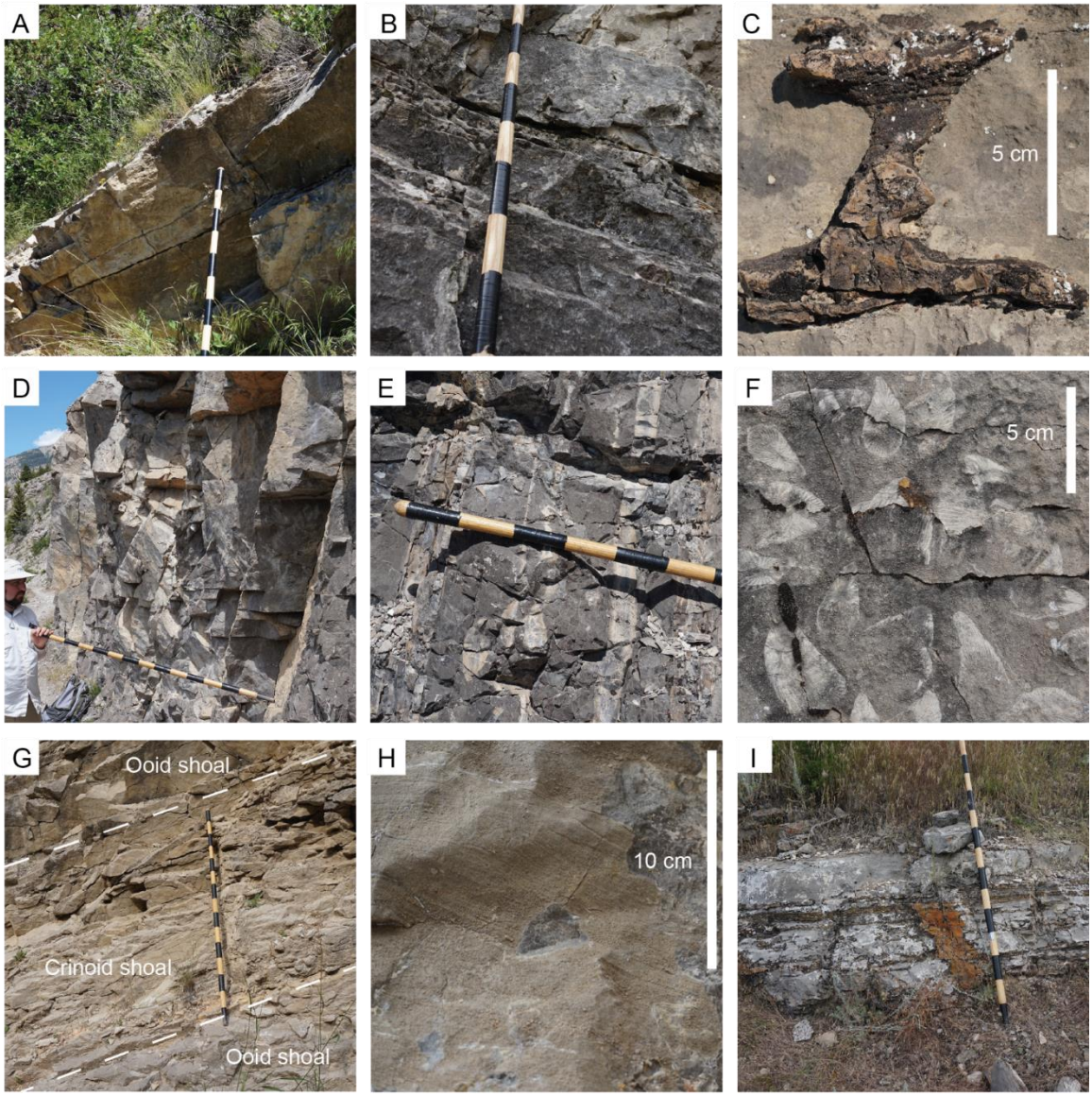

Figure 4.5.— Foreshoal through peritidal facies. A) Medium-bedded skeletal grainstone of the foreshoal facies association cap most parasequences, Milligan Canyon, 3 m. B) Medium-bedded carbonate mudstone interbedded with bedsets of the skeletal grainstone of the foreshoal facies association, Milligan Canyon, 46 m. C) Silicified burrow within the foreshoal facies association, Sappington Canyon, 93 m. D) Medium-bedded skeletal grainstone of the foreshoal facies association, Gibson Reservoir, 234 m. E) Medium-bedded carbonate mudstone interbedded with bedsets of the skeletal grainstone of the foreshoal facies association, Gibson Reservoir, 4 m. F) Solitary corals of the foreshoal facies association, Gibson Reservoir, 238 m. G) Medium bedded oolitic grainstone and tan, dolomitized crinoidal grainstone of the ooid-shoal and crinoid-shoal facies associations, Milligan Canyon, 64 m. H) Ooid grainstone with small scale cross-stratification, Milligan Canyon, 54 m. I) Peritidal facies association consist of planar laminated carbonate mudstone cut by silicified grikes, Sappington Canyon, 224 m.

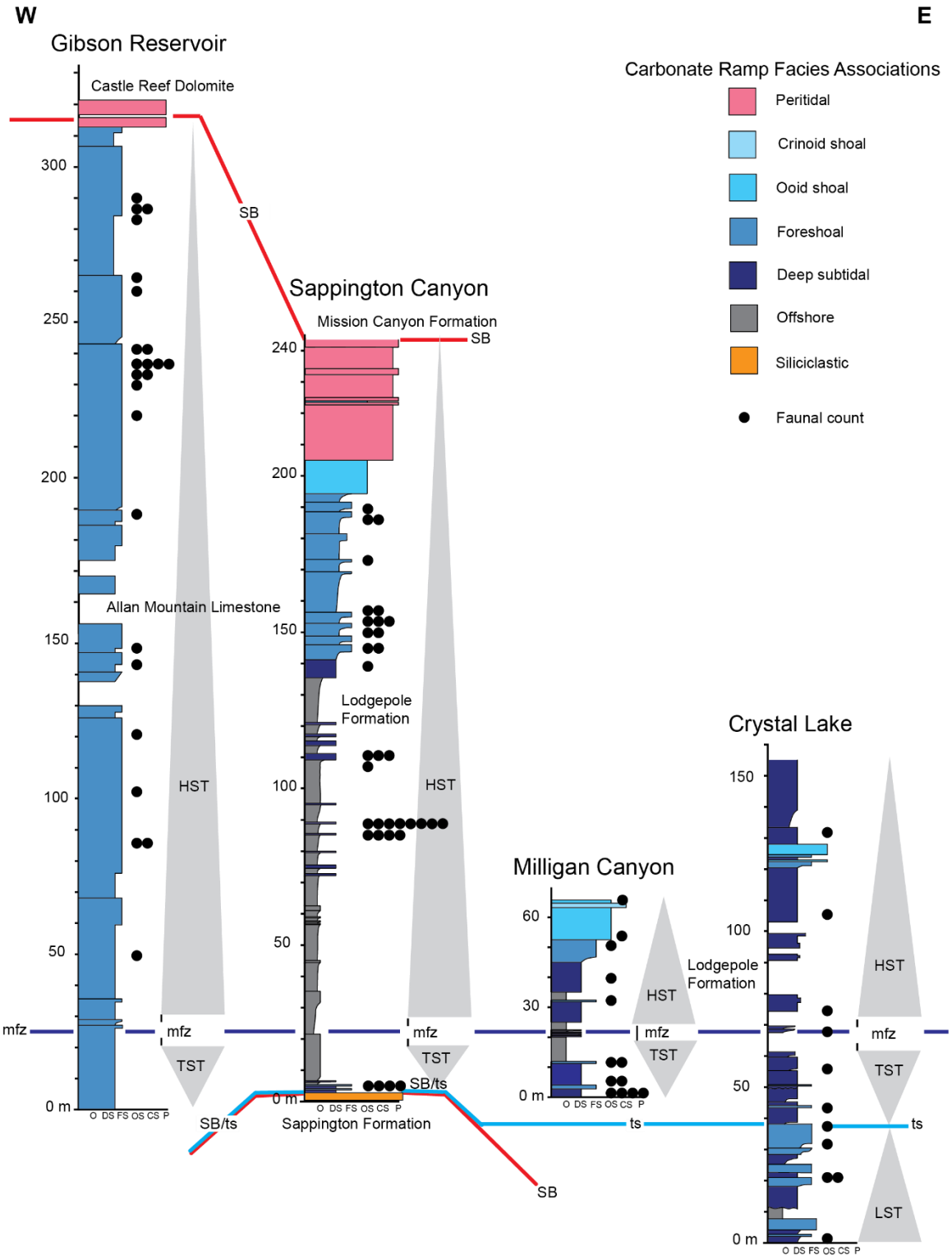
W
E
Gibson Reservoir
Castle Reef Dolomite
300
250
200
150
100
50
0 m
O DS FS OS CS P
SB
Allan Mountain Limestone
HST
mfz
TST
SB/ts
Sappington Canyon
Mission Canyon Formation
SB
240
200
150
100
50
0 m
Lodgepole Formation
HST
mfz
TST
SB/ts
Sappington Formation
SB
Milligan Canyon
60
30
0 m
HST
mfz
TST
ts
Crystal Lake
150
100
50
0 m
Lodgepole Formation
HST
mfz
TST
ts
LST
Carbonate Ramp Facies Associations
Peritidal
Crinoid shoal
Ooid shoal
Foreshoal
Deep subtidal
Offshore
Siliciclastic
Faunal count

Figure 4.6.— Stratigraphic cross section of the Lodgepole Formation and Allan Mountain Limestone. Black circles represent the stratigraphic position of field counts. Facies associations are abbreviated as follows: O–offshore; DS–deep subtidal; FS–foreshoal; OS–ooid shoal; CS–crinoid shoal; P–peritidal. Sequence-stratigraphic terminology is abbreviated as follows: SB–sequence boundary; ts–transgressive surface; mfz–maximum flooding zone; LST–lowstand systems tract; TST–transgressive systems tract; HST–highstand systems tract.

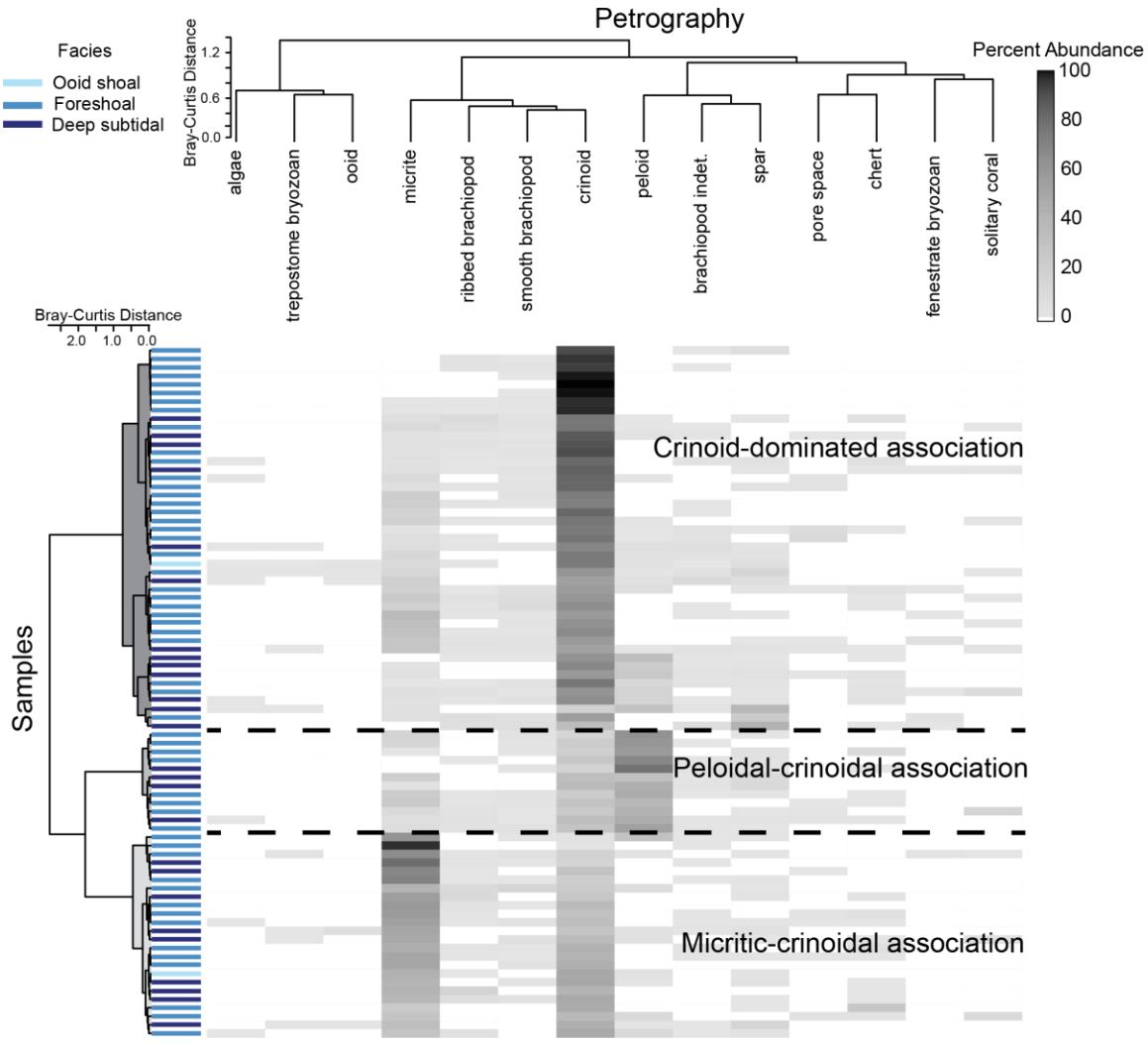

Figure 4.7.— Two-way cluster analysis of thin-section point counts. The color of each cell represents the proportional abundance of a petrographic component within a sample. Samples are color-coded by depositional environment. Values < 5% of the total petrographic assemblage are not shown.

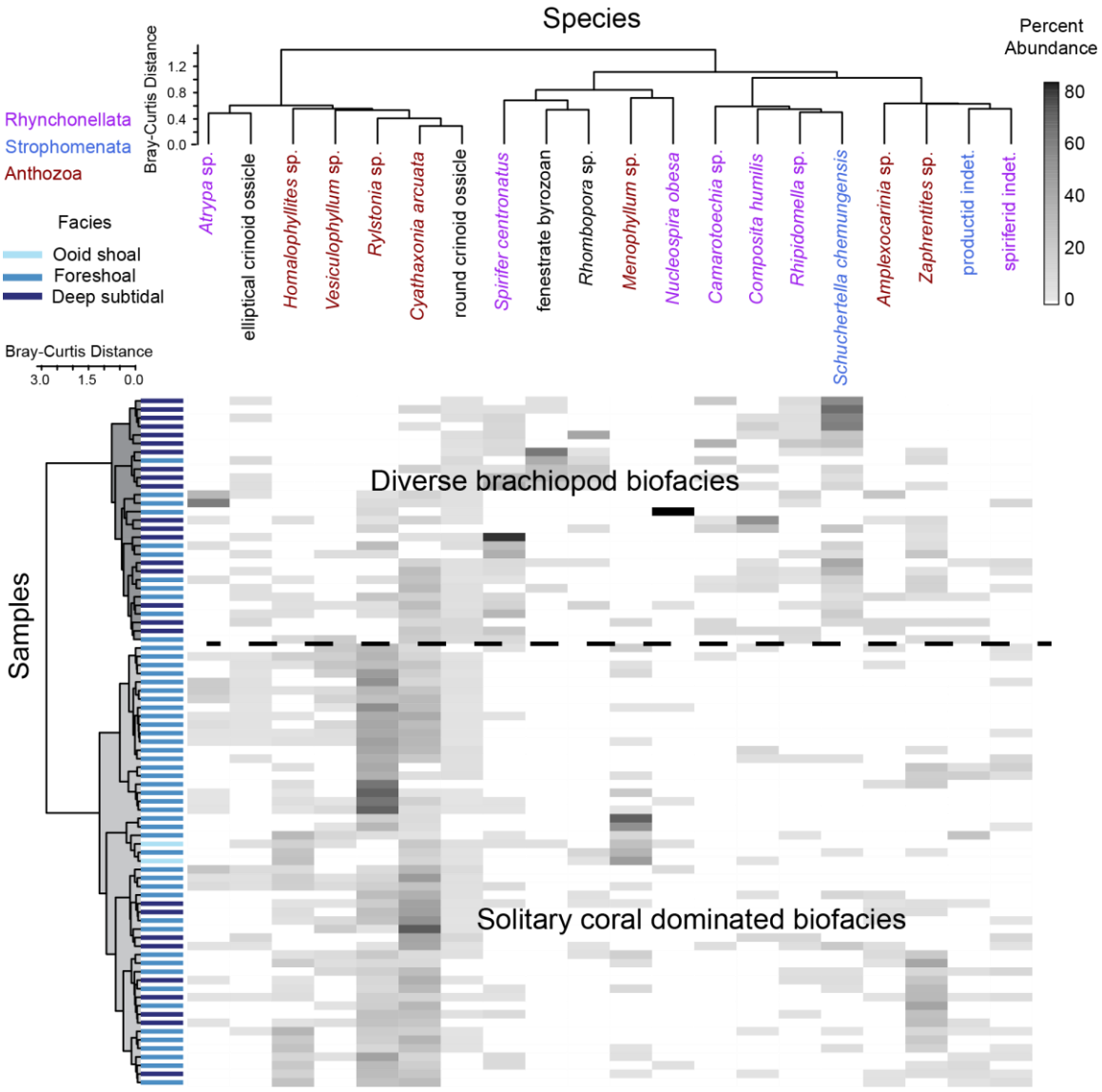

Figure 4.8.— Two-way cluster analysis of faunal counts. The color of each cell represents the proportional abundance of a taxon in a sample. Samples are color-coded by depositional environment and taxa are color-coded by taxonomic class. Values < 1% the total faunal assemblage are not shown.

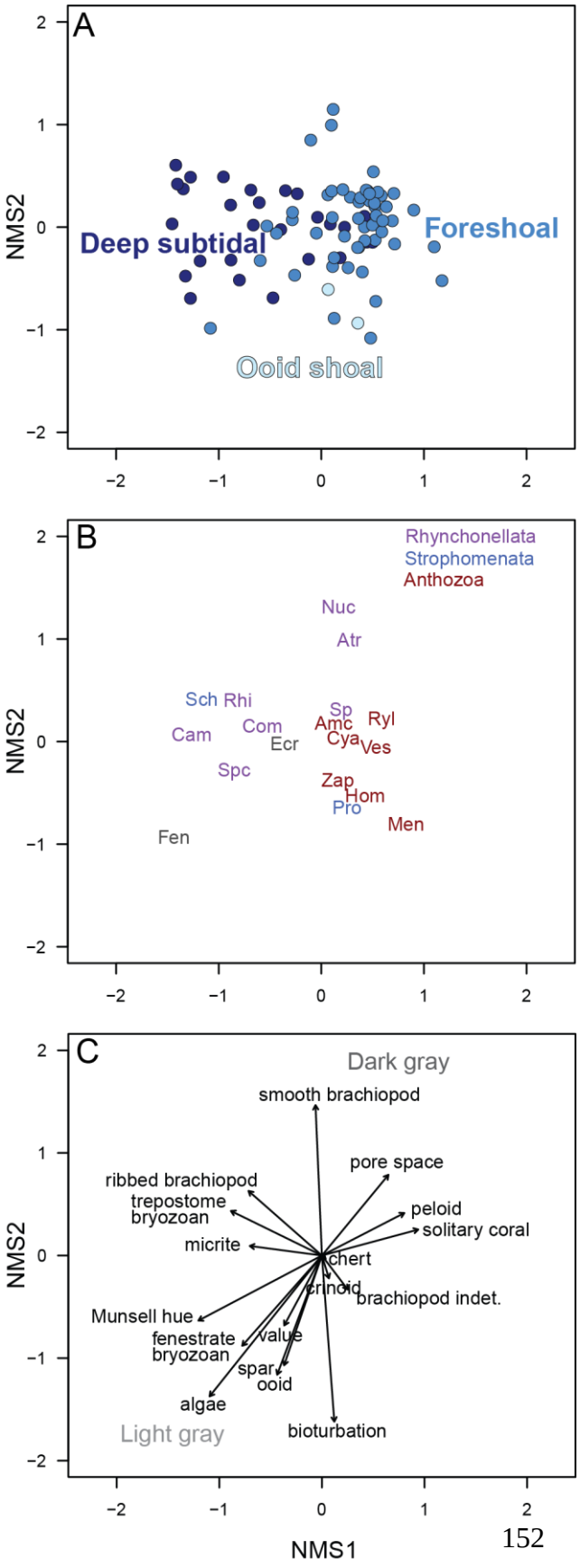
A
Deep subtidal
Foreshoal
Ooid shoal
B
Rhynchonellata
Strophomenata
Anthozoa
Nuc
Atr
Sch Rhi
Sp
Amc
Ryl
Cam
Com
Ecr
Cya
Ves
Spc
Zap
Hom
Pro
Men
Fen
C
Dark gray
smooth brachiopod
pore space
ribbed brachiopod
trepostome bryozoan
peloid
solitary coral
micrite
chert
crinoid
brachiopod indet.
Munsell hue
fenestrate bryozoan
value
spar
ooid
algae
Light gray
bioturbation
NMS1
NMS2

Figure 4.9.— NMS ordination of sample-by-taxon matrix along axes 1 and 2. A) Samples coded by depositional environment. B) Taxa coded by taxonomic class. Only taxa with a proportional abundance greater than 1% are shown for clarity. See Table 4.3 for taxon codes. C) Ordination of environmental variables within the sample by taxon ordination space. The direction of the vector indicates its correlation with the NMS axis, and the length of the vector reflects the strength of the relationship.

CHAPTER 5

CONCLUSIONS

This dissertation identifies water depth as the most common environmental variable correlated with the greatest amount of variation in the assemblage composition of marine benthic communities. Many gradient analyses of modern and fossil record identified water depth along the first axis of ordination, as well as the second axis in many ancient studies. Direct sampling methods in the modern enabled substrate variation (i.e., grain size, composition, firmness) to be identified as the most common gradient that covaries with water depth, followed by nutrients, temperature, and oxygenation levels. Sampling methods in the ancient are more indirect, but the lithological data used to interpret depositional environments also suggests that substrate and wave energy commonly covary with water depth. Examining gradients not correlated with water depth shows that substrate variations are the most next most common gradient for modern and ancient benthic assemblages. This frequent identification of substrate variations suggests that lithological characteristics should be examined in detail for future gradient analyses of ancient benthic assemblages.

Molluscan death assemblages from the shallow subtidal of San Salvador Island are strongly controlled by seagrass density and substrate variation. Seagrass-meadow assemblages are distinct from sand-flat assemblages. Additionally, assemblage composition within the seagrass meadow varies with the level of seagrass density. Heavily vegetated samples are distinct from less vegetated samples. Although limiting

the range of water depth of sampling on San Salvador Island was hypothesized to minimize the impact of water depth, correlations are still found between seagrass density, death assemblage compositions and water depth. This indicates either seagrass density and death assemblages are also controlled by water depth or there are other covarying variables not measured in this study. Wave energy, bioturbation, and oxygenation are interpreted as the gradients explaining the second most amount of variation in the shallow-subtidal assemblages of San Salvador Island. While wave energy is consistent with previous work on San Salvador Island (Casebolt and Kowalewski, 2018), counts of burrows and oxygen as single, instantaneous measurements do not accurately characterize their impact on time-averaged assemblages. This study highlights the variability of assemblages within the same depositional environment as well as the utility of closely spaced, replicate sampling in identifying sources of environmentally driven variation that might otherwise be dominated by the predominant water-depth signal.

Applying closely spaced, replicate sampling of faunal and lithological data to the faunal assemblages of the lower Madison Group of Montana identified detailed environmental gradients. Water depth is the primary gradient associated with assemblage variation as NMS and cluster analysis identify a diverse brachiopod biofacies in the deep-subtidal facies association and a solitary coral-dominated biofacies in the foreshoal facies association. The lithological data indicates that petrographic components are not correlated with facies associations along an onshore–offshore gradient, but the NMS indicates that samples from the deep subtidal are more micritic than foreshoal samples. Ecological characteristics of brachiopods and rugose corals suggest that substrate and shear stress are the covarying variables along this complex water-depth gradient. The

lithological data also suggests that bioturbation and pore-water oxygenation explain the second greatest amount of variation in the lower Madison Group assemblages, and that solitary corals prefer well-oxygenated pore-water conditions compared to the brachiopods *Nucleospira obesa* and *Atrypa* sp. This study demonstrates the efficacy of directly linking lithological data to faunal data to identify additional sources of environmental variation, providing more detailed environmental reconstructions and their impacts on community compositions in the fossil record.

There are several future directions that this research can be taken. First, additional sampling of the lower Madison Group would greatly build upon work done in Chapter 4. Including additional fossiliferous assemblages representing the offshore facies association from the Central Montana Trough and Antler Foreland Basin in Montana and Idaho would encompass more environmental variability of the carbonate ramp. Additionally, including more localities from the shallow shelves in Wyoming and northwestern Montana may identify paleogeographic trends in assemblages, as well as strengthening the sequence-stratigraphic correlation to previously established frameworks.

Second, additional studies beyond the Madison Group would improve and test the combined replicate sampling methodology used here. The first step would be to broaden sampling to other environments (e.g., carbonate platforms, wave-dominated siliciclastic shelves, tidal dominated systems) and varying the spatial and temporal duration represented by the assemblages. Some of gradients (e.g., substrate, wave energy, ecological characteristics) may be commonly examined for most settings, and others may be included depending on faunal and lithological preservation. For example, the Middle

Mississippian carbonate and siliciclastic units of Illinois, Indiana, and Kentucky may highlight sources of environmental variation at larger spatial scales than the study conducted in Montana. Ramp geometries, carbonate production, siliciclastic input, and oceanographic conditions vary along the shelf of the Midcontinent during the Mississippian. Such variation would be beneficial for identifying any gradients that covary with water depth, for examining community response to spatial and temporal environmental changes across the basin, and for examining community variation within each depositional environment. Comparing the gradients controlling these communities in Illinois, Indiana, and Kentucky to the lower Madison Group of Montana would broaden this work to a continental scale and potentially highlight environmental differences between the Mississippian of the western United States and the Midcontinent.

Third, other environmental proxies such as geochemical and stable isotope data should be included in future studies. Many of the lower Madison Group facies associations underwent dolomitization, and many specimens were micritized or silicified. Any geochemical or stable isotope data collected may not have reflected the environmental conditions at the time of deposition, but possibly the diagenetic history. Sampling other, less altered localities may allow for bulk rock or fossil geochemical data to be included in gradient analyses.

Finally, this project can be expanded by examining the impact potential gradients may have on species through time and test for clines (i.e., morphological variation with respect to an environmental gradient) in the fossil record. Water-depth clines have already been identified in the fossil record for several groups (Raup, 1956; Alexander, 1975; Cisne et al., 1980; Cisne et al., 1982; Bayer and McGhee, 1985; Titus, 1989;

Pachut and Cuffey, 1991; Hageman, 1994; Daley, 1999; Webber and Hunda, 2007; Kim et al., 2009). However, when morphological change is not associated with water depth, it has traditionally been interpreted as evolutionary change (see Patzkowsky and Holland 2012 for review). One application is to examine which gradients are covarying with the water-depth cline to determine which environmental parameters the organisms are responding to. The second is to test the null hypothesis of evolutionary change in the absence of a water-depth gradient and examine if morphology is instead changing with respect to any gradients not correlated with water depth. Overall, closely spaced replicate sampling of lithological data in conjunction with faunal data can explain detailed sources of environmentally driven variation in fossil communities, and potentially within the taxa themselves.

REFERENCES

AIGNER, T., 1982, Calcareous tempestites: storm-dominated stratification, Upper Muschelkalk limestones (Middle Triassic, SW-Germany), *in* Einsele, G. and Seilacher, A. (eds.), Cyclic and Event Stratigraphy: Springer, Berlin, p. 180–198.

ALBANO, P.G. and SABELLI, B., 2011, Comparison between death and living molluscs assemblages in a Mediterranean infralittoral off-shore reef: Palaeogeography, Palaeoclimatology, Palaeoecology, v. 310, p. 206–215.

ALDEA, C., OLABARRIA, C. and TRONCOSO, J.S., 2008, Bathymetric zonation and diversity gradient of gastropods and bivalves in West Antarctica from the South Shetland Island to the Bellingshausen Sea: Deep-Sea Research I, v. 55, p. 350–368.

ALEXANDER, R.R., 1975, Phenotypic lability of the brachiopod *Rafinesquina alternata* (Ordovician) and its correlation with the sedimentologic regime: Journal of Paleontology, v. 49, p. 607–618.

ALGEO, T.J. and MAYNARD, J.B., 2004, Trace-element behavior and redox facies in core shales of Upper Pennsylvanian Kansas-type cyclothems: Chemical Geology, v. 206, p. 289–318.

ALLISON, P.A., WIGNALL, P.B. and BRETT, C.E., 1995, Palaeo-oxygenation: effects and recognition, *in* Bosence, D.W.J., Allison, P.A. (eds.), Marine Palaeoenvironmental Analysis from Fossils: Geological Society of London Special Publications, v. 83, p. 97–112.

AMOROSI, A., ROSSI, V., SCARPONI, D., VAIANI, S.C. and GHOSH, A., 2014, Biosedimentary record of postglacial coastal dynamics: high-resolution sequence stratigraphy from the northern Tuscan coast (Italy): Boreas, v. 43, p. 939-954.

ANDERSON, M.J., ELLINGSEN, K.E. and MCARDLE, B.H., 2006, Multivariate dispersion as a measure of beta diversity: Ecology Letters, v. 9, p. 683–693.

ANDERSON, T.F. and ARTHUR, M.A., 1983, Stable isotopes of oxygen and carbon and their application to sedimentologic and paleoenvironmental problems, *in* Arthur, M.A., Anderson, T.F., Kaplan, I.R., Vezier, J., and Land, L.S. (eds.), Stable isotopes in sedimentary geology, v. 10, p. 1–151.

ANDRICHUK, J.M., 1955, Mississippian Madison Group stratigraphy and sedimentation in Wyoming and Southern Montana: American Association of Petroleum Geologists Bulletin, v. 39, p. 2170–2210.

AUSICH, W.I., 1997, Regional encrinites: a vanished lithofacies, *in* Brett, C.E. and Baird, G.C (eds.), Paleontological Events: Stratigraphic, Ecologic and Evolutionary Implications, Colombia University Press, New York, p. 509–519.

AUSICH, W.I., 1999a, Lower Mississippian Hampton Formation at LeGrand, Iowa, USA, *in* Ausich, W.I., Brett, C.E., Hess, H., and Simms, M.J. (eds.), Fossil Crinoids, Cambridge University Press, Cambridge, p. 135–138.

AUSICH, W.I., 1999b, Lower Mississippian Burlington Limestone along the Mississippi River Valley in Iowa, Illinois, and Missouri, USA; *in* Ausich, W.I., Brett, C.E., Hess, H., and Simms, M.J. (eds.), Fossil Crinoids, Cambridge University Press, Cambridge, p. 139–144.

AUSTIN, M.P., 1980, Searching for a model for use in vegetation analysis: Vegetatio, v, 42, p. 11–21.

AUSTIN, M.P., CUNNINGHAM, R.B and FLEMING, P.M., 1984, New approaches to direct gradient analysis using environmental scalars and statistical curve-fitting procedures: Vegetatio, v. 55, p. 11–27.

BADIOZAMANI, K., 1973, The dorag dolomitization model—application to the Middle Ordovician of Wisconsin: Journal of Sedimentary Petrology, v. 43, p. 965–984.

BALL, M.M., 1967, Carbonate sand bodies of Florida and The Bahamas: Journal of Sedimentary Petrology, v. 37, p. 556–591.

BALSEIRO, D. 2016, Compositional turnover and ecological changes related to the waxing and waning of glaciers during the late Paleozoic ice age in ice-proximal regions (Pennsylvanian, western Argentina): Paleobiology, v. 42, p. 335–357.

BARROS, F., HATJE, V., FIGUEIREDI, M.B., MAGALHÃES, W.F., DÓREA, H.S. and EMÍDIO, E.S., 2008, The structure of the benthic macrofaunal assemblages and sediments characteristics of the Paraguaçu estuarine system, NE, Brazil: Estuarine, Coastal and Shelf Science, v. 78, p. 753–762.

BARROS, F, DE CARVALHO, G.C., COSTA, Y. and HATJE, V., 2012, Subtidal benthic macroinfaunal assemblages in tropical estuaries: Generality amongst highly variable gradients: Marine Environmental Research, v. 81, p. 43–52.

BATHURST, R.G.C., 1975, Carbonate Sediments and Their Diagenesis: Elsevier, Amsterdam, p. 658.

BAYER, U., and MCGHEE, G.R., 1985, Evolution in marginal marine epicontinental basins: the role of phylogenetic and ecologic factors (Ammonite replacements in

the German Lower and Middle Jurassic) i*n* Bayer, U. and Seilacher, A. (eds.), Sedimentary and Evolutionary Cycles: Springer-Verlag, New York, p. 164–220.

BELANGER, C.L. and GARCIA, M.V., 2014, Differential drivers of benthic foraminiferal and molluscan community composition from a multivariate record of early Miocene environmental change: Paleobiology, v. 40, p. 398–416.

BENNINGTON, J.B., 2003, Transcending patchiness in the comparative analysis of paleocommunities: a test case from the Upper Cretaceous of New Jersey: Palaios, v. 18, p. 22–33.

BERNER, R.A., 1981, A new geochemical classification of sedimentary environments: Journal of Sedimentary Petrology, v. 51, p. 359–365.

BLANCHARD, A.L., PARRIS, C.L., KNOWLTON, A.L. and WADE, N.R., 2013, Benthic ecology of the northeastern Chukchi Sea. Part I. Environmental characteristics and macrofaunal community structure, 2008-2010: Continental Shelf Research, v. 67, p. 52–66.

BOLAM, S.G., EGGLETON, J., SMITH, R., MASON, C., VANSTAEN, K. and REES, H., 2008, Spatial distribution of macrofaunal assemblages along the English Channel: Journal of Marine Biological Association of the United Kingdom, v. 88, p. 675–687.

BOLTON J.C. and DRIESE, S.G., 1990, The determination of substrate conditions from the orientations of solitary rugose corals: Palaios, v. 5, p. 479–483.

BONELLI, J.R., and PATZKOWSKY, M.E., 2008, How are global patterns of faunal turnover expressed at regional scales? Evidence from the Upper Mississippian (Chesterian Series), Illinois Basin, USA: Palaios, v. 23, p.760–772.

BOYER, D.L., and DROSER, M.L, 2011, A combined trace- and body-fossil approach reveals high-resolution record of oxygen fluctuations in Devonian seas: Palaios, v. 26, p. 500–508.

BRASIER, M.D., 1975, An outline history of seagrass communities: Paleontology, v. 18, p. 681–702.

BREMNER, J., ROGERS, S.I. and FRID, C.L.J., 2006, Matching biological traits to environmental conditions in marine benthic ecosystems: Journal of Marine Systems, v. 60, p. 302–316.

BREWSTER-WINGARD, G.L, ISHMAN, S.E., 1999. Historical trends in salinity and substrate in central Florida Bay: a paleoecological reconstruction using modern analogue data: Estuaries, v. 22, p. 369–383.

BROMLEY, R.G., 1996, Trace Fossils: Biology, Taphonomy and Applications (2nd edition): Chapman & Hall, London, 361 p.

BURCHETTE, T.P. and WRIGHT, V.P., 1992, Carbonate ramp depositional systems: Sedimentary Geology, v. 79, p. 3–57.

BURROWES, G., 2006, Genesis of Mississippian shoal topography, Weyburn Field, Saskatchewan, *in* Nickel, E.H. (ed.), Saskatchewan and Northern Plains Oil and Gas Symposium Core Workshop Volume: Saskatchewan Geological Society Special Publication, v. 20, p. 22–31.

BUSH, A.M. and BRAME, R.I., 2010, Multiple paleoecological controls on the composition of marine fossil assemblages from the Frasnian (Late Devonian) of Virginia, with a comparison of ordination methods: Paleobiology, v. 36, p. 573–91.

CANN, J.H. and CLARKE, J.D., 1993, The significance of *Marginopora vertebralis* (Foraminifera) in surficial sediments at Esperance, Western Australia, and in last interglacial sediments in northern Spencer Gulf, Australia: Marine Geology, v. 111, p. 171–187.

CARR, D.E., 1973, Geometry and origin of oolite bodies in the Ste. Genevieve Limestone (Mississippian) in the Illinois Basin: Indiana Geological Survey Bulletin, v. 48, p. 1–81.

CASEBOLT, S. and KOWALEWSKI, M., 2018, Mollusk shell assemblages as archives of spatial structuring of benthic communities around subtropical islands: Estuarine, Coastal and Shelf Science, v. 215, p. 132–143.

CHEN, X., and WEBSTER, G.D., 1994 Sedimentology, tectonic control and evolution of a Lower Mississippian carbonate ramp with offshore bank, central Wyoming to eastern Idaho and northeastern Utah, U.S.A., *in* Embry, A.F., Beauchamp, B, and Glass, D.J. (eds.), Pangea: Global Environments and Resources: Canadian Society of Petroleum Geologists Memoir, v. 17, p. 557–587.

CHEN, Z.T. and YAO, J.H., 1993, Paleozoic Echinoderm Fossils of Western Yunnan, China: Geological Publishing House, Beijing, 102 p.

CHOQUETTE, P.W. and STEINEN, R.P., 1980, Mississippian non-supratidal dolomite, Ste. Genevieve Limestone, Illinois Basin: evidence for mixed-water dolomitization, *in* Zeneger, D.H., Dunham, J.B., and Ethington, R.H. (eds.), Concepts and Models of Dolomitization: SEPM Special Publications, v. 28, p. 168–196.

CHRISTENSEN, A.M., 1999, Brachiopod paleontology and paleoecology of the Lower Mississippian Lodgepole Limestone in southeastern Idaho, *in* Hughes, S.S., and

Thackray, G.D. (eds.), Guidebook to the Geology of Eastern Idaho: Pocatello, Idaho Museum of Natural History, p. 57–67.

CISNE, J.L. and RABE, B.D., 1978, Coenocorrelation: gradient analysis of fossil communities and its applications in stratigraphy: Lethaia, v. 11, p. 341–364.

CISNE, J.L., MOLENOCK, J. and RABE, B.D., 1980, Evolution in a cline: The trilobite *Triarthrus* along an Ordovician depth gradient: Lethaia , v. 11, p. 47–59.

CISNE, J.L., CHANDLEE, G.O., RABE, B.D. and COHEN, J.A., 1982, Clinal variation, episodic evolution, and possible parapatric speciation: The trilobite *Flexacalymene senaria* along an Ordovician depth gradient: Lethaia, v. 15, p. 325–341.

CLARKE, K.R., 1993, Non-parametric multivariate analyses of changes in community structure: Australian Journal of Ecology, v. 18, p. 117-143.

CLARKE, K.R. and GORLEY, R.N., 2015, PRIMER v7: user manual/tutorial. PRIMER-E, Plymouth.

CLAPHAM, M.E., 2011, Ordination methods and the evaluation of Ediacaran communities, *in* Laflamme, M., Schiffbaouer, J.D., and Dornbos, S.Q. (ds.), Quantifying the Evolution of Early Life: Springer, Dordrecht, p. 3–21.

CLAPHAM, M.E. and JAMES, N.P., 2008, Paleoecology of Early-Middle Permian marine communities in Eastern Australia: response to global climate change in the aftermath of the Late Paleozoic Ice Age: Palaios, v. 23, p. 738–750.

COBBAN, W.A., 1945, Marine Jurassic formations of Sweetgrass Arch, Montana: American Association of Petroleum Geologists Bulletin, v. 29, p. 1262–1303.

COEN, L.D., and HECK, K.L. Jr., 1991, The interacting effects of siphon nipping and habitat on bivalve [*Mercenaria mercenaria* (L)] growth in a subtropical seagrass (*Halodule wrightii* Uschers) meadow: Journal of Experimental Marine Biology and Ecology, v. 145, p. 1–13.

COHEN, K.M., FINNEY, S.C., GIVVARD, P.L. and FAN, J.X., 2013, The ICS International Chronostratigraphic Chart: Episodes, v. 36, p. 199–204.

COLBY, N.D. and BOARDMAN, M.R., 1989, Depositional evolution of a windward, high-energy lagoon, Graham's Harbor, San Salvador, Bahamas: Journal of Sedimentary Petrology, v. 59, p. 819–834.

COMPTON, T.J., BOWDEN, C., PITCHER, C.R., HEWITT, J.E. and ELLIS, N., 2013, Biophysical patterns in benthic assemblages across contrasting continental margins of New Zealand, Journal of Biogeography, v. 40, p. 75–89.

CURRAN, H.A. and WHITE, B., 1991, Trace fossils of shallow subtidal to dunal ichnofacies in Bahamian carbonates: Palaios, v. 6, p. 498–510.

CURRAN, H.A. and MARTIN, A.J., 2003, Complex decapod burrows and ecological relationships in modern and Pleistocene intertidal carbonate environments, San Salvador Island, Bahamas: Palaeogeography, Palaeoclimatology, Palaeoecology, v. 192, p. 229–245.

CURRAN, H.A. and SEIKE, K., 2016, Modern and fossil callianassid burrows of the Bahamas: comparisons and implications for paleoenvironmental analysis, *in* Glumac, B. and Savarese, M. (eds.), Proceedings of the 16th symposium on the geology of the Bahamas and other carbonate regions: Gerace Research Centre, San Salvador, p. 153–167.

DALEY, G.M., 1999, Environmentally controlled variation in shell size of *Ambonychia* Hall (Mollusca: Bivalvia) in the type Cincinnatian (Upper Ordovician): Palaios, v. 14, p. 520–529.

DALEY, G.M., 2002, Creating a paleoecological framework for evolutionary and paleoecological studies: an example from the Fort Thompson Formation (Pleistocene) of Florida: Palaios, v. 17, p. 419–434.

DANISE, S. and HOLLAND, S.M., 2017, Faunal response to sea-level and climate change in a short-lived seaway: Jurassic of the Western Interior, USA: Palaeontology, v. 60, p. 213–232.

DEBOUT, J. and DENAYER, J., 2018, Palaeoecology of the upper Tournaisian (Mississippian) crinoidal limestones from South Belgium: Geologica Belgica, v. 24, p. 111–127.

DEEHR, R.A., CUMMINS, H., BOARDMAN, M.R. and ZIMMERMAN, R.A., 2001, Paleocommunity reconstruction of a tropical carbonate lagoon, Graham's Harbor, San Salvador, Bahamas, *in* Greenstein, B.J. and Carney, C.K. (eds.), Proceedings of the 10th symposium on the geology of the Bahamas and other carbonate regions: Gerace Research Centre, San Salvador, p. 187–200.

DEN HARTOG, C., 1970, The Seagrasses of the World: North Holland Publishing, Amsterdam, 275 p.

DICKSON, A.J., COHEN, A.S. and COE, A.L., 2012, Seawater oxygenation during the Paleocene-Eocene Thermal Maximum: Geology, v. 40, p. 639–642.

DILCHER, D., 2016, Fossil plants from the Coon Creek Formation of Tennessee: Bulletin of the Alabama Museum of Natural History, v. 33, p. 118–121.

DINEEN, A.A., FRAISER, M.L. and ISBELL, J.L., 2013, Palaeoecology and sedimentology of Carboniferous glacial and post-glacial successions in the Paganzo and Río Blanco basins of northwestern Argentina: Geological Society of London Special Publications, v. 376, p. 109–140.

DOTT, R.H. and BOURGEOIS, J., 1982, Hummocky stratification: significance of its variable bedding sequences: Geological Society of America Bulletin, v. 93, p. 663–680.

DROSER, M.L. and BOTTJER, D.J., 1986, A semiquantitative field classification of ichnofabric: Journal of Sedimentary Research, v., 56, p. 558–559.

DUKE, W.L., 1985, Hummocky cross-stratification, tropical hurricanes, and intense winter storms: Sedimentology, v. 32, p. 167–194.

DUNHAM, R.J., 1962, Classification of carbonate rocks according to depositional texture, *in* Ham, W.E. (ed.) Classification of Carbonate Rocks: American Association of Petroleum Geologists Memoir, v. 1, p. 108–121.

ELIAS, R.J., ZEILSTRA, R.G. and BAYER, T.N., 1988, Paleoenvironmental reconstruction based on horn corals, with an example from the Late Ordovician of North America: Palaios, v. 3, p. 22–34.

ELRICK, M. and READ, J.F., 1991, Cyclic ramp-to-basin carbonate deposits, Lower Mississippian, Wyoming and Montana: a combined field and computer modeling study: Journal of Sedimentary Petrology, v. 61, p. 1194–1224.

ELRICK, M., READ, J.F. and CORUH, C., 1991, Short-term paleoclimactic fluctuations expressed in Lower Mississippian ramp-slope deposits, southwestern Montana: Geology, v. 19, p. 799–802.

EMBRY, A.F. and JOHANNESSEN, E.P., 1992, T–R sequence stratigraphy, facies analysis and reservoir distribution in the uppermost Triassic—Lower Jurassic succession, western Sverdrup Basin, Arctic Canada, *in* Vorren, T.O., Bergsager, E., Dahl-Stamnes, O.A., Holter, E., Johansen, B., Lie, E., and Lund, T.B. (eds.), Arctic Geology and Petroleum Potential: Norwegian Petroleum Society Special Publication, v. 2, p. 121–146.

EPSTEIN. S., BUCHSBAUM, R., LOWENSTAM, H.A. and UREY, H.C., 1953, Revised carbonate-water isotopic temperature scale: Geological Society of America Bulletin, v. 64, p. 1315–1326.

EPSTEIN, S. and MAYEDA, T.K., 1953, Variation of ^{18}O content of waters from natural sources: Geochimica et Cosmochimica Acta, v. 4, p. 213–224.

ERWIN, D.H., 1989, Regional paleoecology of Permian gastropod genera, Southwestern United States and the End-Permian mass extinction: Palaios, v. 4, p. 424–438.

FALL, L.M. and OLSZEWSKI, T.D., 2010, Environmental disruptions influence taxonomic composition of brachiopod paleocommunities in the Middle Permian Bell Canyon Formation (Delaware Basin, West Texas): Palaios, v. 25, p. 247–259.

FELDMAN, H.R., BROWN, M.A. and ARCHER, A.W., 1993, Benthic assemblages as indicators of sediment stability: evidence from grainstones of the Harrodsburg and Salem Limestones (Mississippian, Indiana) , *in* Kieth, B.D. and Zuppmann, C.W. (eds.), Mississippian Oolites and Modern Analogs: American Association of Petroleum Geologists Studies in Geology, v. 35, p.115–128.

FERGUSON, C.A., 2008, Nutrient pollution and the molluscan death record: use of mollusc shells to diagnose environmental change: Journal of Coastal Research, v. 24, p. 250–259.

FERGUSON, C.A. and MILLER, A.I., 2007, A sea change in Smuggler's Cove? Detection of decadal scale compositional transitions in the subfossil record: Palaeogeography, Palaeoclimatology, Palaeoecology, v. 254, p. 418–429.

FERGUSON, J.E., HENDERSON, G.M., KUCERA, M. and RICKABY, R.E.M., 2008, Systematic change of foraminiferal Mg/Ca ratios across a strong salinity gradient: Earth and Planetary Science Letters, v. 265, p. 153–166.

FERNÁNDEZ, M., HERNÁNDEZ, D. and ROUX, A., 2007, Distribución espacial del langostino patagónico (Peloticus muelleri, (Bate, 1888)) y su relación con las variables ambientales, Golfo San Jorge, Argentina: Revista de Biología Marina y Oceanografia, v. 42, p. 335–344.

FLESSA, K.W. and KOWALEWSKI, M., 1994, Shell survival and time-averaging in nearshore and shelf environments: estimates from the radiocarbon literature: Lethaia, v. 27, p. 153–165.

FLESSA, K.W., CUTLER, A.H. and MELDAHL, K.H., 1993, Time and taphonomy: quantitative estimates of time-averaging and stratigraphic disorder in a shallow marine habitat: Paleobiology, v. 19, p. 266–286.

FLÜGEL, E., 2010, Microfacies of Carbonate Rocks: Analysis, Interpretation and Application: Springer, London, 984 p.

FONESCA, M.S., ZIEMAN, J.C., THAYER, G.W. and FISHER, J.S., 1983, The role of current velocity in structuring eelgrass (*Zostera marina* L.) meadows: Estuarine and Coastal Shelf Science, v. 17, p. 367–380.

FORCINO, F.L., 2012, Multivariate assessment of the required sample size for community paleoecological research: Palaeogeography, Palaeoclimatology, Palaeoecology, v. 315–316, p. 134–141.

FORCINO, F.L., LEIGHTON, L.R., TWERDY, P. and CAHILL, J.F., 2015, Reexamining sample size requirements for multivariate, abundance-based community research: when resources are limited, the research does not have to be: PLoS ONE, v. 10, doi: https://doi.org/10.1371/journal.pone.0128379

FOSTER, W.J., DANISE, S., SEDLACEK, A., PRICE, G.D., HIPS, K. and TWITCHETT, R.J., 2015, Environmental controls on post-Permian recovery of benthic, tropical marine ecosystems in western Palaeotethys (Aggtelek Karst, Hungary): Palaeogeography, Palaeoclimatology, Palaeoecology, v. 440, p. 374–394.

FÜRSICH, F.T. and HURST, J.M., 1974, Environmental factors determining the distribution of brachiopods: Palaeontology, v. 17, p. 879–900.

GARRETT, P., 1977, Biological communities and their sedimentary record, *in* Hardie, L.A. (ed.), Sedimentation on the Modern Carbonate Flats of Northwest Andros Island: Johns Hopkins University Studies in Geology, Baltimore, v. 22, p. 124–158.

GERACE, D.T., OSTRANDER, G.K. and SMITH, G.W., 1998, San Salvador, Bahamas, *in* Kjerfve, B (ed.), CARICOMP– Caribbean coral reef, seagrass and mangrove sites: UNESCO, Paris, p. 229–245.

GLEASON, H.A., 1926, The individualistic concept of the plant association: Bulletin of the Torrey Botanical Club, v. 53, p. 7–26.

GOODALL, D.W., 1954, Objective methods for the classification of vegetation. III. an essay in the use of factor analysis: Australian Journal of Botany, v. 2, p. 304–324.

GOWER, J.C., 1991, Statistical methods for comparing different multivariate analyses of the same data, *in* Hudson, J.R., Kendall, D.G., and Tautu, P. (eds.), Mathematics in the Archaeological and Historical Sciences: Edinburgh University Press, Edinburgh, p. 138—149.

GUTSCHICK, R.C. and SANDBERG, C.A., 1983, Mississippian continental margins of the conterminous United States: SEPM Special Publication, v. 33, p. 79–96.

GUTSCHICK, R.C., SANDBERG, C.A. and SANDO, W.J., 1980, Mississippian shelf margin and carbonate platforms from Montana to Nevada, *in* Fouch, T.D., and Magathan, E.R., (eds.), Paleozoic Paleogeography of the West-Central United States: Rocky Mountain Paleogeography Symposium v. 1, p. 111–128.

HAGEMAN, S.J., 1994, Microevolutionary implications of clinal variation in the Paleozoic bryozoan Streblotrypa: Lethaia, v. 24, p. 209–222.

HALLEY, R.B., HARRIS, P.M., and HINE, A.C., 1983, Bank margin environments, *in* Schoole, P.A., Bebout, D.G., and Moore, C.H. (eds.), Carbonate Depositional Environments: American Association of Petroleum Geologists Memoir, v. 33, p. 463–506.

HARRIS, P.M., 1979, Facies Anatomy and Diagenesis of a Bahamian Ooid Shoal: Sedimenta VII: Comparative Sedimentology Lab, Miami, p. 163.

HEARD, T.G. and PICKERING, K.T. 2008. Trace fossils as diagnostic indicators of deep-marine environments, Middle Eocene Ainsa-Jaca basin, Spanis Pyrenees: Sedimentology, v. 55, p. 809–844.

HEMMINGA, M.A. and DUERTE, C.M., 2000, Seagrass Ecology: Cambridge University Press, Cambridge, U.K. 298 p.

HENDY, A.J.W., 2013, Spatial and stratigraphic variation of marine paleoenvironments in the Middle-Upper Miocene Gatun Formation, Isthmus of Panama: Palaios, v. 28, p. 210–227.

HILL, M.O., 1973, Reciprocal averaging: an eigenvector method of ordination: Journal of Ecology, v. 61, p. 237–249.

HILL, M.O. and GAUCH, H.G., 1980, Detrended correspondence analysis: An improved ordination technique. Vegetatio, v. 42, p. 47–58.

HINE, A.C., 1977, Lily Bank, Bahamas: history of an active ooid sand shoal: Journal of Sedimentary Petrology, v. 47, p. 1554–1581.

HINMAN, G., 1994, A Teacher's Guide to the Depositional Environments on San Salvador Island, Bahamas: Bahamian Field Station, San Salvador, Bahamas. 62 p.

HOLLAND, S.M. and PATZKOWSKY, M.E., 2004, Ecosystem structure and stability: middle Upper Ordovician of Central Kentucky, USA: Palaios, v. 19, p. 316–331.

HOLLAND, S.M., MILLER, A.I., MEYER, D.L. and DATTILO, B.F., 2001, The detection and importance of subtle biofacies within a single lithofacies: the Upper Ordovician Kope Formation of the Cincinnati, Ohio Region: Palaios, v. 16, p. 205–217.

HÖNISCH, B., ALLEN, K.A., LEA, D.W., SPERO, H.J., EGGINS, S.M., ARBUSZEWSKI, J., DEMENOCAL, P., ROSENTHAL, Y., RUSSEL, A.D. and ELDERFIELD, H. 2013. The

influence of salinity on Mg/Ca in planktic foraminifers—Evidence from cultures, core-top sediments and complementary $\delta^{18}O$: Geochimica et Cosmochimica Acta, v. 121, p. 196–213.

HYMEL, S.N. and PLANTE, C.J., 2000, Feeding and bacteriolytic responses of the deposit-feeder *Abarenicola pacifica* (Polychaeta: Arenicolidae) to chances in temperature and sediment food concentration: Marine Biology, v. 136, p. 1019–1027.

INGRAM, R.L., 1954, Terminology for thickness of stratification and parting units in sedimentary rocks: Geological Society of America Bulletin, v. 65, p. 937–938.

IRILANDI, E.A. and PETERSON, C.H., 1991, Modification of animal habitat by large plants: mechanisms by which seagrasses influence clam growth: Oecologia, v. 87, p. 307–318.

IVANY, L.C., PORTELL, R.W. and JONES, D.S., 1990, Animal-plant relationships and paleobiogeography of an Eocene seagrass community from Florida: Palaios, v. 5, p. 244–258.

IVANY, L.C., NEWTON, C.R. and MULLINS, H.T., 1994, Benthic invertebrates of a modern carbonate ramp: a preliminary survey: Journal of Paleontology, v. 68, p. 316–331.

JAMES, N.P. and BONE., Y. 2007, A late Pliocene–early Pleistocene, inner shelf, subtropical seagrass-dominated carbonate: Roe Calcarenite, Great Australian Bight, Western Australia: Palaios, v. 22, p. 343–359.

JOHNSTON, D.I., HENDERSON, C.M. and SCHMIDT, M.J., 2010, Upper Devonian to Lower Mississippian conodont biostratigraphy of uppermost Wabamun Group and Palliser Formation to lowermost Banff and Lodgepole formations, southern Alberta and southeastern British Columbia, Canada: implications for correlations

and sequence stratigraphy: Bulletin of Canadian Petroleum Geology, v. 58, p. 295–341.

KAMMER, T.W. and AUSICH, W.I., 1987, Aerosol suspension feeding and current velocities: distributional controls for late Osagean crinoids: Paleobiology, v. 13, p. 379–395.

KAMMER, T.W. and AUSICH, W.I., 2006, The "Age of Crinoids": a Mississippian biodiversity spike coincident with widespread carbonate ramps: Palaios, v. 21, p. 238–248.

KAMMER, T.W., BAUMILLER, T.K. and AUSICH, W.I., 1997, Species longevity as a function of niche breadth: evidence from fossil crinoids: Geology, v. 25, p. 219–222.

KAMMER, T.W., BAUMILLER, T.K. and AUSICH, W.I., 1998, Evolutionary significance of differential species longevity in Osagean–Meramecian (Mississippian) crinoid clades: Paleobiology, v. 24, p. 155–176.

KATZ, M.E., CRAMER, B.S., FRANZESE, A., HÖNISCH, B., MILLER, K.G., ROSENTHAL, Y. and WRIGHT. J.D., 2010, Traditional and emerging geochemical proxies in foraminifera: Journal of Foraminiferal Research, v. 40, p. 165–192.

KENKEL, N.C. and ORLÓCI, L., 1986, Applying metric and nonmetric multidimensional scaling to ecological studies: some new results: Ecology, v. 67, p. 919–928.

KENKEL, N.C. and BURCHILL, C.E., 1990, Rigid rotation of nonmetric multidimensional scaling axes to environmental congruence: Abstracta Botanica, v. 14, p. 109–119.

KESSELL, S.R. and WHITTAKER, R.H., 1976, Comparison of three ordination techniques: Vegetatio, v. 32, p. 21–29.

KIDWELL, S.M., 2001, Time-averaging and fidelity of modern death assemblages: building a taphonomic foundation for conservation palaeobiology: Palaeontology v. 56, p. 487–522.

KIDWELL, S.M., 2008, Ecological fidelity of open marine molluscan death assemblages: effects of post-mortem transport, shelf health, and taphonomic inertia: Lethaia, v. 41, p. 199–217.

KIDWELL, S.M. and BOSENCE, D.W.J., 1991, Taphonomy and time-averaging of marine shelly faunas, *in* Allison, P.A. and Briggs, D.E.G. (eds.), Taphonomy: Releasing the Data Locked in the Fossil Record: Plenum Press, New York, p. 115–209.

KIM, K., SHEETS, H.K, and MITCHELL, C.E., 2009, Geographic and stratigraphic change in the morphology of *Triarthrus beckii* (Green) (Trilobita): A test of the Plus ça change model of evolution: Lethaia, v. 42, p. 108–125.

KOLDE, R., 2019, pheatmap: pretty heatmap. R package version 1.0.12. https://CRAN.R-project.org/package=pheatmap.

KONAR, B., IKEN, K. and EDWARDS, M., 2009, Depth-stratified community zonation patterns on Gulf of Alaska rocky shores: Marine Ecology, v. 30, p. 63–73.

KOWALEWSKI, M., CARROLL, M, CASAZZA, L., GUPTA, N.S., HANNISDAL, B., HENDY, A., KRAUSE, R.A., LABARBERA, M., LAGO, D.G., MESSINA, C., PUCHALSKI, S., ROTHFUS, T.A., SÄLGEBACK, J., STEMPEIN, J., TERRY, R.C. and TOMAŠOVÝCH, A., 2003, Quantitative fidelity of brachiopod-mollusk assemblages from modern subtidal environments of San Juan Islands, USA: Journal of Taphonomy, v. 1, p. 44–66.

KOWALEWSKI, M., CASEBOLT, S., HUA, Q., K.E., KAUFMAN, D.S. and KOSNIK, M.A., 2018, One fossil record, multiple time resolutions: disparate time-averaging of echinoids and mollusk on a Holocene carbonate platform: Geology, v. 45, p. 51–54.

KOWALEWSKI, M., GÜRS, K., NEBELSICK, J.H., OSCHMANN, W., PILLER, W.E. and HOFFMEISTER, A.P., 2002, Multivariate hierarchical analyses of Miocene mollusk assemblages of Europe: paleogeographic, paleoecological, and biostratigraphic implications: Geological Society of America Bulletin, v. 114, p. 239–256.

KRUSKAL, J.B., 1964a, Multidimensional scaling by optimizing goodness of fit to a nonmetric hypothesis: Psychometrika, v. 29, p. 1–27.

KRUSKAL, J.B., 1964b, Nonmetric multidimensional scaling: a numerical method: Psychometrika, v. 29, p. 115–129.

KUKLINSKI, P., BARNES, D.K.A. and TAYLOR, P.D., 2006, Latitudinal patterns of diversity and abundance in North Atlantic intertidal boulder-fields: Marine Biology, v. 149, p. 1577–1583.

LAFFERTY, A.G., MILLER, A.I. and BRETT, C.E., 1994, Comparative spatial variability in faunal composition along two Middle Devonian paleoenvironmental gradients: Palaios, v. 9, p. 224–236.

LAUDON, L.R., 1967, Ontogeny of the Mississippian crinoid *Platycrinites bozemanensis* (Miller & Gurley), 1897: Journal of Paleontology, v. 41, p. 1492–1497.

LAUDON, L.R. and SEVERSON, J.L., 1953, New crinoid fauna, Mississippian, Lodgepole Formation, Montana: Journal of Paleontology, v. 27, p. 505–536.

LAYOU, K.M., 2009, Ecological restructuring after extinction: the Late Ordovician (Mohawkian) of the Eastern United States: Palaios, v. 24, p. 118–130.

LEBOLD, J.G. and KAMMER, T.W., 2006, Gradient analysis of faunal distributions associated with rapid transgression and low accommodation space in Late Pennsylvanian marine embayment: biofacies of the Ames Member (Glenshaw Formation, Conemaugh Group) in the northern Appalachian Basin, USA: Palaeogeography, Palaeoclimatology, Palaeoecology, v. 231, p. 291–314.

LEGENDRE, P. and BIRKS, H.J.B., 2012, From classical to canonical ordination, *in* Birks, H.J.B, Lotter, A.F., Juggins, S, and Smol, J.P. (eds.), Tracking Environmental Change Using Lake Sediments: Springer, Dordrecht, p. 201–248.

LEGENDRE, P. and LEGENDRE, L., 1998, Numerical Ecology: Elsevier, Amsterdam. 853 p.

LEWIS, D.W. and MCCONCHIE, D., 1994, Analytical Sedimentology: Chapman and Hall, New York.

LLEWELLYN, G. and MESSING, C.G., 1993, Compositional and taphonomic variations in modern crinoid-rich sediments from the deep-water margins of a carbonate bank: Palaios, v. 8, p. 554–573.

LOCKWOOD, R. and CHASTANT, L.R., 2006, Quantifying taphonomic bias of compositional fidelity, species richness, and rank abundance in molluscan death assemblages from the Upper Chesapeake Bay: Palaios, v. 21, p. 376–383.

LONG, B.G. and POINER, I.R., 1994, Infaunal benthic community structure and function in the Gulf of Carpentaria, Northern Australia: Australian Journal of Marine and Freshwater Research, v. 45, p. 293–316.

MAECHLER, M., ROUSSEEUW, W, P., STRUYF, A., HUBERT, M. and HORNIK, K., 2019, cluster: cluster analysis basics and extensions. R package version 2.1.0.

MARENCO, K.N. and BOTTJER, D.J., 2010, The intersection grid technique for quantifying the extent of bioturbation on bedding planes: Palaios, v. 25, p. 457–462.

MARIANO, D.L.S. and BARROS, F., 2015, Intertidal benthic macrofaunal assemblages: changes in structure along entire tropical estuarine salinity gradients: Journal of Marine Biological Association of the United Kingdom, v. 95, p. 5–15.

MAUGHAN, E.K., 1983, Tectonic setting of the Rocky Mountain region during the late Paleozoic and the early Mesozoic, *in* Babcock, J.W. (ed.), Proceedings of Symposium on the Genesis of Rocky Mountain Ore Deposits: Changes with Time and Tectonics: Denver Regional Exploration Geologists Society, p. 39–50.

MAYNARD, J.B., 1982, Extension of Berner's "New geochemical classification of sedimentary environments" to ancient sediments: Journal of Sedimentary Petrology, v. 52, p. 1325–1331.

MCCLAIN, C.R., LUNDSTEN, L., BARRY, J. and DEVOGELAERE, A., 2010, Assemblage structure, but not diversity or density, change with depth on a northeast Pacific seamount: Marine Ecology, v. 31, 14–25.

MCCUNE, B. and GRACE, J.B., 2002., Analysis of Ecological Communities: MjM Software Design, Gleneden Beach, Oregon.

MCKERROW, W.S. and SCOTESE, C.R., 1990, Revised world maps and introduction, *in* McKerrow, W.S. and Scotese, C.R. (eds.), Paleozoic Paleogeography and Biogeography: Geological Society Memoir, v. 12, p. 1–24.

MCKINNEY, F.K. and HAGEMAN, S.J., 2006, Paleozoic to modern marine ecological shift displayed in the northern Adriatic Sea: Geology, v. 34, p. 881–884.

MCMULLEN, S.K., HOLLAND, S.M. and O'KEEFE, F.R., 2014, The occurrence of vertebrate and invertebrate fossils in a sequence stratigraphic context: the Jurassic Sundance Formation, Bighorn Basin, Wyoming, USA: Palaios, v. 29, p. 227–294.

MILLER, A.I., 1988, Spatial resolution in subfossil molluscan remains: implications for paleobiological analyses: Paleobiology, v. 14, p. 91–103.

MILLER, A.I. and CUMMINS, H., 1990, A numerical model for the formation of fossil assemblages: estimating the amount of post-mortem transport along environmental gradients: Palaios, v. 5, p. 303–316.

MILLER, A.I., LLEWELLYN, G., PARSONS, K.M., CUMMINS, H., BOARDMAN, M.R., GREENSTEIN, B.J. and JACOBS, D.K., 1992,. Effect of Hurricane Hugo on molluscan skeletal distributions, Salt River Bay, St. Croix, US Virgin Islands: Geology, v. 20, p. 23–26.

MILLER, M.F. and SMAIL, S.E., 1997, A semiquantitative field method for evaluating bioturbation on bedding planes: Palaios, v. 12, p. 391–396.

MINCHIN, P.R., 1987, An evaluation of the relative robustness of techniques for ecological ordination: Vegetatio, v. 69, p. 89–107.

MOISSETTE, P., KOSKERIDOU, E., CORNÉE, J., GUILLOCHEAU, F. and LÉCUYER, C., 2007, Spectacular preservation of seagrasses and seagrass-associated communities from the Pliocene of Rhodes, Greece: Palaios, v. 22, p. 200–211.

MONROE, W.H., 1970, A glossary of karst terminology: Geological Survey Water-Supply Paper, v. K, p. 1–26.

MOORE, G.T., 1973, Lodgepole Limestone facies in southwestern Montana: American Association of Petroleum Geologists Bulletin, v. 57, p. 1703–1713.

MOORE, P.G., 1974, The kelp fauna of northeast Britain. III. Qualitative and quantitative ordinations and the utility of a multivariate approach: Journal of Experimental Marine Biology and Ecology, v. 16, p. 252–300.

MUDGE, M.R., SANDO, W.J., and DUTRO, J.T., 1962, Mississippian rocks of Sun River Canyon area, Sawtooth Range, Montana: American Association of Petroleum Geologists Bulletin, v. 46, p. 2003–2018.

MUNSELL COLOR, 1976, Munsell Book of Color: Matte Finish Collection: Kollmorgen Corporation, Baltimore, Maryland.

NAKAOKA, M., 2000, Nonlethal effects of predators on prey populations: predator-mediated change in bivalve growth: Ecology, v. 81, p. 1031–1045.

NETTO, S.A., WARWICK, R.M. and ATTRILL, M.J., 1999, Meiobenthic and macrobenthic community structure in carbonate sediments of Rocas Atoll (North-east, Brazil): Estuarine, Coastal and Shelf Science, v. 48, p. 39–50.

NOVACK-GOTTSHALL, P.M. and MILLER, A.I., 2003, Comparative taxonomic richness and abundance of Late Ordovician gastropods and bivalves in mollusc-rich strata of the Cincinnati Arch: Palaios, v. 18, p. 559–571.

O'CONNELL, L.G., JAMES, N.P. and BONE, Y., 2012, The Miocene Nullarbor Limestone, southern Australia: deposition on a vast subtropical epeiric platform: Sedimentary Geology, v. 253, p. 1–16.

O'NEIL, J.R., CLAYTON, R.N. and MAYEDA, T.K., 1969, Oxygen isotope fractionation in divalent metal carbonates: Journal of Chemical Physics, v. 51, p. 5547–5558.

OKSANEN. J. 2019. *metaMDS, in* Oksanen, J., Blanchet, F.G., Friendly, M., Kindt, R., Legendre, P., McGlinn, D., Minchin, P.R., O'Hara, R.B., Simpson, G.L., Solymos, P., Stevens, M.H.H., Szoecs, E., and Wagner, H. (eds.). vegan: Community Ecology Package. R package version 2.5-5. https://CRAN.R-project.org/package=vegan

OKSANEN, J., BLANCHET, F.G., FRIENDLY, M., KINDT, R., LEGENDRE, P., MCGLINN, D., MINCHIN, P.R., O'HARA, R.B., SIMPSON, G.L., SOLYMOS, P., STEVENS, M.H.H., SZOECS, E., and WAGNER, H., 2019, vegan: Community ecology package. R package version 2.5-6. https://CRAN.R-project.org/package=vegan.

ØKLAND, R.H., 1999, On the variation explained by ordination and constrained ordination axes: Journal of Vegetation Science, v. 10, p. 131–136.

OLABARRIA, C., 2006, Faunal change and bathymetric diversity gradient in deep-sea prosobranchs from northeastern Atlantic: Biodiversity and Conservation, v. 15, p. 3685–3702.

OLSZEWSKI, T.D. and ERWIN, D.H., 2009, Change and stability in Permian brachiopod communities from western Texas: Palaios, v. 24, p. 27–40.

OLSZEWSKI, T.D. and PATZKOWSKY, M.E., 2001, Measuring recurrence of marine biotic gradients: a case study from the Pennsylvanian-Permian Midcontinent: Palaios, v. 16, p. 444–460.

OUELLETTE, D., DESROSIERS, G., GAGNE, J.P., GILBERT, F., POGGIALE, J.C., BLIER, P.U. and STORA, G., 2004, Effects of temperature on in vitro sediment reworking processes by a gallery biodiffuser, the polychaete *Neanthes virens*: Marine Ecology Progress Series, v. 266, p. 185–193.

PACHUT, J.F., and CUFFEY, R.J., 1991, Clinal variation, intraspecific heterochrony, and microevolution in the Permian bryozoan *Tabulipora carbonaria*: Lethaia, v. 24, p. 165–185.

PATZKOWSKY, M.E., 1995, Gradient analysis of Middle Ordovician brachiopod biofacies: biostratigraphic, biogeographic, and macroevolutionary implications: Palaios, v. 10, p. 154–179.

PATZKOWSKY, M.E. and HOLLAND, S.M., 2012, Stratigraphic Paleobiology: Understanding the Distribution of Fossil Taxa in Time and Space: The University of Chicago Press, Chicago. 255 p.

PEMBERTON, S.G. and FREY, R.W., 1984, Quantitative methods in ichnology: spatial distribution among populations: Lethaia, v. 17, p. 33–49.

PEMBERTON, S.G., MACEACHERN, J.A. and FREY, R.W., 1992, Trace fossil facies models: environmental and allostratigraphic significance, *in* VanWagoner, J.C., and Bertram, G.T. (eds.), Sequence Stratigraphy of Foreland Basin Deposits, p. 429–475.

PERERA, S.N. and STIGALL, A.L., 2018, Identifying hierarchical spatial patterns within paleocommunities: An example from the Upper Pennsylvanian Ames Limestone of the Appalachian Basin: Palaeogeography, Palaeoclimatology, Palaeoecology, v. 506, p. 1–11.

PETERSON, B.J. and HECK, K.L., 2001, Positive interactions between suspension-feeding bivalves and seagrass– a facultative mutualism: Marine Ecology Progress Series, v. 213, p. 143–155.

PIELOU, E.C., 1984, The Interpretation of Ecological Data: a Primer on Classification and Ordination: Wiley, New York, 263 p.

PIPER, D.Z. and CALVERT, S.E., 2009, A marine biogeochemical perspective on black shale deposition: Earth-Science Reviews, v. 95, p. 63–96.

PODANI, J., 1991, On the standardization of Procrustes statistics for the comparison of ordinations: Abstracta Botanica, v. 15, p. 43–46.

POOLE, F.G. and SANDBERG, C.A., 1977, Mississippian paleogeography and tectonics of the western United States, *in* Stewart, J.H., Stevens, C.H., and Fritsche, A.E. (eds.), Paleozoic Paleogeography of the Western United States: SEPM Pacific Coast Paleogeography Symposium 1, p. 67–86.

PRZESLAWSKI, R, ZHU, Q. and Aller, R., 2009. Effects of abiotic stressors on infaunal burrowing and associated sediment characteristics: Marine Ecology Progress Series, v. 392, p. 33–42.

R DEVELOPMENT CORE TEAM, 2015, R: A language and environment for statistical comp uting: R Foundation for Statistical Computing, Vienna, Austria. https://www.R-project.org/.

RAILSBACK, L.B., ANDERSON, T.F., ACKERLY, S.C. and CISNE, J.L., 1989, Paleoceanographic modeling of temperature-salinity profiles from stable isotopic data: Paleoceanography, v. 4, p. 585–591.

RANDAZZO, A.F. and BAISLEY, K.J., 1995, Controls on carbonate facies distribution in a high-energy lagoon, San Salvador Island, Bahamas, *in* Curran, H.A and White, B. (eds.) Terrestrial and Shallow Marine Geology of the Bahamas and Bermuda: Geological Society of America Special Paper, v. 300, p. 157–176.

RAUP, D. 1956. *Dendraster*: A problem in echinoid taxonomy: Journal of Paleontology, v. 30, p. 685–694.

READ, J.F., 1985, Carbonate platform facies models: American Association of Petroleum Geologists Bulletin, v. 69, p. 1–21.

REDFERN, C., 2013, Bahamian Seashells: 1161 Species from Abaco, Bahamas: Bahamianseashells.com, Inc, Boca Raton, Florida.

REDMAN, C.M., LEIGHTON, L.R., SCHELLENBERG, S.A., GALE, C.N., NIELSEN, J.L., DRESSLER, D.L. and KLINGER, M.K., 2007, Influence of spatiotemporal scale on the interpretation of paleocommunity structure: lateral variation in the Imperial Formation of California: Palaios, v. 22, p. 630–641.

REID, R.P. and MACINTYRE, I.G., 1998, Carbonate recrystallization in shallow marine environments: a widespread diagenetic process forming micritized grains: Journal of Sedimentary Research, v. 68, p. 928–946.

REID, R.P., MACINTYRE, I.G., and POST, J.E., 1992, Micritized skeletal grains in northern Belize lagoon: a major source of Mg-calcite mud: Journal of Sedimentary Petrology, v. 62, p. 145–156.

REID, S.K. and DOROBEK, S.L., 1993, Sequence stratigraphy and evolution of a progradational, foreland carbonate ramp, Lower Mississippian Mission Canyon Formation and stratigraphic equivalents, Montana and Idaho, *in* Loucks, R.G., and Sarg, J.F. (eds.), Carbonate Sequence Stratigraphy: Recent Developments and Applications: American Association of Petroleum Geologists Memoir, v. 57, p. 327–352.

REICH, S., 2014, Gastropod associations as a proxy for seagrass vegetation in a tropical, carbonate setting (San Salvador, Bahamas): Palaios, v. 29, p. 467–482.

REICH, S., WESSLINGH, F.P. and RENEMA, W., 2014, A highly diverse molluscan seagrass fauna from the early Burdigalian (early Miocene) of Banyunganti (south-central Java, Indonesia): Annalen des Naturhistorischen Museums in Wien, Series A, p. 1–129.

REICH, S., DI MARTINO, E., TODD, J.A., WESSLINGH, F.P. and RENEMA, W., 2015, Indirect paleo-seagrass indicators (ISPIs): a review: Earth Science Review, v. 143, p. 161–186.

REUTER, M., PILLER, W.E., HARZHAUSER, M., KROH, A., ROEGL, F. and CORIC, S., 2010, The Quilon Limestone, Kerala Basin, India: an archive for Miocene Indo-Pacific seagrass beds: Lethaia, v. 44, p. 76–86.

REUTER, M., PILLER, W.E. and ERHART, C., 2012, A middle Miocene carbonate platform under silici-volcanoclastic sedimentation stress (Leitha Limestone, Styrian Basin, Austria)—depositional environments, sedimentary evolution and paleoecology: Palaeogeography, Palaeoclimatology, Paleoecology, v. 350–352, p. 198–211.

RODRIGUEZ, J. and GUTSCHICK, R.C., 1968, *Productina*, *Cyrtina*, and *Dielasma* (Brachiopoda) from the Lodgepole Limestone (Mississippian) of southwestern Montana: Journal of Paleontology, v. 42, p. 1027–1032.

RODRIGUEZ, J. and GUTSCHICK, R.C., 1969, Silicified brachiopods from the lower Lodgepole Limestone (Kinderhookian), southwestern Montana: Journal of Paleontology, v. 43, p. 952–960.

ROSALES, I., ROBLES, S. and QUESADA, S., 2004, Elemental and oxygen isotope composition of Early Jurassic belemnites: salinity vs. temperature signals: Journal of Sedimentary Research, v. 74, p. 342–354.

RUDWICK, M.J.S., 1970, Living and Fossil Brachiopods: Hutchinson and Company, London, 199 p.

SANDO, W.J., 1960, Corals from well cores of Madison Group, Williston Basin: United States Geological Survey Bulletin, v. 1071-F, p. 157–190.

SANDO, W.J., 1976, Mississippian history of the northern Rocky Mountains region: Journal of Research, U.S. Geological Survey, v. 4, p. 317–338.

SANDO, W.J., 1980, The paleoecology of Mississippian corals in the western conterminous United States: Acta Palaeontologica Polonica, v. 25, p. 619–637.

SANDO, W.J., 1985, Revised Mississippian time scale, western interior region, conterminous United States: U.S. Geological Survey Bulletin 1605A, p. A15–A26.

SCARPONI, D. and KOWALEWSKI, M., 2004, Stratigraphic paleoecology: bathymetric signatures and sequence overprint of mollusk associations from upper Quaternary sequences of the Po Plain, Italy: Geology, v. 32, p. 989–992.

SCARPONI, D., HUNTLEY, J.W., CAPRARO, L. and RAFFI, S., 2014, Stratigraphic paleoecology of the Valle di Manche section (Crotone Basin, Italy): A candidate GSSP of the Middle Pleistocene: Palaeogeography, Palaeoclimatology, Palaeoecology, v. 402, p. 30–43.

SCHNEIDER, J.W. and BORLUND, P., 2006, Matrix comparison, part 2: measuring the resemblance between proximity measures or ordination results by use of the

Mantel and Procrustes statistics: Journal of the American Society for Information Science and Technology, v. 58, p. 1596–1609.

SCOFFIN, T.P., 1970, The trapping and binding of subtidal carbonate sediments by marine vegetation in Bimini Lagoon, Bahamas: Journal of Sedimentary Petrology, v. 40, p. 249–273.

SCRUTTON, C.T., 1998, The Palaeozoic corals, II: structure, variation and palaeoecology: Proceeding of the Yorkshire Geological Society, v. 52, p. 1–57.

SEIDERER, L.J. and NEWELL, R.C., 1999, Analysis of the relationship between sediment composition and benthic community structure in coastal deposits: implications for marine aggregate dredging: ICES Journal of Marine Science, v. 65, p. 757–765.

SHAW, A.B., 1962, Rhynchonellid brachiopods and a *Torynifer* from the Madison Group (Mississippian): Journal of Paleontology, v. 36, p. 630–637.

SHI, G.R., 1993, Multivariate data analysis in palaeoecology and palaeobiogeography—a review: Palaeogeography, Palaeoclimatology, Palaeoecology, v. 105, p. 199–234.

SHINN, E.A., 1968, Burrowing in recent lime sediments of Florida and the Bahamas: Journal of Paleontology, v. 42, p. 879–894.

SMALE, D.A., 2008, Continuous benthic community change along a depth gradient in Antarctic shallows: evidence of patchiness but not zonation: Polar Biology, v. 31, p. 189–198.

SMITH, L.B., and READ, J.F., 1999, Application of high-resolution sequence stratigraphy to tidally influenced Upper Mississippian carbonates, Illinois Basin, *in* Harris, P.M., Saller, A.H., and Simo, J.A. (eds.), Advances in Carbonate Sequence

Stratigraphy: Application to Reservoirs, Outcrops, and Models: SEPM Special Publication, v. 63, p. 107–126.

SMITH, L.B., and READ, J.F., 2001, Discrimination of local and global effects on Upper Mississippian stratigraphy, Illinois Basin, U.S.A.: Journal of Sedimentary Research, v. 71, p. 985–1002.

SMITH, G.W., SHORT, F.T. and KAPLAN, D.I., 1990, Distribution and biomass of Seagrasses in San Salvador, Bahamas, *in* Smith, R.R. (eds.), Proceedings of the 3rd symposium on the botany of the Bahamas: Gerace Research Centre, p. 67–77.

SMITH, R.W., BERGEN, M., WEISBERG, S.B., CADIEN, D., DALKEY, A., MONTAGNE, D., STULL, J.K. and VELARDE, R.G., 2001, Benthic response index for assessing infaunal communities on the southern California mainland shelf: Ecological Applications, v. 11, p. 1073–1087.

SPRINGER, D.A. and FLESSA, K.W., 1996, Faunal gradients in surface and subsurface shelly accumulations from a recent clastic tidal flat, Bahia la Choya, northern Gulf of California, Mexico: Palaeogeography, Palaeoclimatology, Palaeoecology, v. 126, p. 261–279.

SONNENFELD, M.D., 1996, Sequence evolution and hierarchy within the lower Mississippian Madison Limestone of Wyoming, *in* Longman, M.W. and Sonnenfeld, M.D. (eds), Paleozoic Systems of the Rocky Mountain Region: Rocky Mountain Section SEPM, p. 165–192.

SUMIDA, P.Y.G. and PIRES-VANIN, A.M.S., 1997, Benthic associations of the shelfbreak and upper slope off Ubatuba-SP, south-eastern Brazil: Estuarine, Coastal and Shelf Science, v. 44, p. 779–784.

SVARDA, C.E., BOTTJER, D.J. and GORSLINE, D.S., 1984, Development of a comprehensive oxygen-deficient marine biofacies model: evidence from Santa Monica, San Pedro, and Santa Barbara Basins, California Continental Borderland: American Association of Petroleum Geologists Bulletin, v. 68, p. 1179–1192.

TAIT, R.V. and DIPPER, F.A., 1998, Elements of Marine Ecology: Butterwork-Heinemann, Oxford, 462 p.

TAYLOR, A.M. and GOLDRING, R., 1993, Description and analysis of bioturbation and ichnofabric: Journal of the Geological Society, London, v. 150, p. 141–148.

TER BRAAK, C.J.F., 1986, Canonical correspondence analysis: a new eigenvector technique for multivariate direct gradient analysis: Ecology, v. 67, p. 1167–1179.

TER BRAAK, C.J.F. and VERDONSCHOT, P.F.M., 1995, Canonical correspondence analysis and related multivariate methods in aquatic ecology: Aquatic Sciences, v. 57, p. 255–289.

TITUS, R., 1989, Clinal variation in the evolution of *Ectenocrinus simplex*: Journal of Paleontology, v. 63, p. 81–91.

TOMAŠOVÝCH, A., 2006, Brachiopod and bivalve ecology in the Late Triassic (Alps, Austria): onshore-offshore replacements caused by variations in sediment and nutrient supply: Palaios, v. 24, p. 344–368.

TOMAŠOVÝCH, A., and KIDWELL, S.M., 2009a, Fidelity of variation in species composition and diversity partitioning by death assemblages: time-averaging transfers diversity from beta to alpha levels: Paleobiology, v. 35, p. 94–118.

TOMAŠOVÝCH, A., and KIDWELL, S.M., 2009b, Preservation of spatial and environmental gradients by death assemblages: Paleobiology, v. 35, p. 119–145.

TUCKER, M.E. and WRIGHT, P., 1990, Carbonate Sedimentology: Blackwell Scientific Publications, Oxford 482 p.

TUCKEY, M.E. and ANSTEY, R.L., 1989, Gradient analysis: a quantitative technique for biostratigraphic correlation: Palaios, v. 4, p. 475–479.

TYLER, C.L. and KOWALEWSKI, M., 2014, Utility of marine benthic associations as multivariate proxy of paleobathymetry: a direct test from recent coastal ecosystems of North Carolina: PLOS One, v. 9, p. 1–15.

VAN HOEY, G., DEGRAER, S. and VINCX, M., 2004, Macrobenthic community structure of soft-bottom sediments at the Belgian continental shelf: Estuarine, Coastal and Shelf Science, v. 59, p. 599–613.

VAN WAGONER, J.C., POSAMENTIER, H.W., MITCHUM, R.M., VAIL, P.R., SARG, J.F., LOUTIT, T.S. and HARDENBOL, J., 1988, An overview of sequence stratigraphy and key definitions, *in* Wilgus, C.K., Hastings, B.S., Kendall, C.G. St. C., Posamentier, H.W., Ross, C.A., Van Wagoner, J.C. (eds.), Sea Level Changes—An Integrated Approach: SEPM Special Publications, v. 42, p. 39–45.

VICENTE, V.P. and RIVERA, J.A., 1982, Depth limits of the seagrass *Thalassia testudinum* (König) in Jobos and Guayanilla Bays, Puerto Rico: Caribbean Journal of Science, v. 17, p. 73–76.

VOEGELIN, A.R., NÄGLER, T.F., BEUKES, N.J. and LACASSIE, J.P., 2010, Molybdenum isotopes in late Archean carbonate rocks: implications for early Earth oxygenation: Precambrian Research, v. 182, p. 70–82.

Voight. E., 1981. Upper Cretaceous bryozoan-seagrass association in the Maastrichtian of the Netherlands, in: Larwood, G.P., Nielsen, C. (Eds.), Recent and fossil Bryozoa, pp. 281–298.

WANLESS, H.R., BURTON, E.A. and DRAVIS, J., 1981, Hydrodynamics of carbonate fecal pellets: Journal of Sedimentary Petrology, v. 51, p. 27–36.

WANLESS, H.R. and TEDESCO, L.P., 1993, Comparison of oolitic sand bocies generated by tidal vs. wind-wave agitation, *in* Kieth, B.D. and Zuppmann, C.W. (eds.), Mississippian Oolites and Modern Analogs: American Association of Petroleum Geologists Studies in Geology, v. 35, p. 199–225.

WATERS, D.L. and SANDO, W.J., 1987, Corals from the Madison Group, Williston Basin, North Dakota: Fifth International Williston Basin Symposium, p. 83–97.

WATERS, J.A. and SEVASTOPULO, G.D., 1984, The stratigraphical distribution and palaeoecology of Irish Lower Carboniferous blastoids: Irish Journal of Earth Sciences, v. 6, p. 137–154.

WEBBER, A.J., 2002, High-resolution faunal gradient analysis and an assessment of the causes of meter-scale cyclicity in the type Cincinnatian Series (Upper Ordovician): Palaios, v. 17, p. 545–555.

WEBBER, A.J., 2005, The effects of spatial patchiness on the stratigraphic signal of biotic composition (type Cincinnatian Series; Upper Ordovician): Palaios, v. 20, p. 37–50.

WEBBER, A.J. and HUNDA, B.R., 2007. Quantitatively comparing morphological trends to environment in the fossil record (Cincinnatian Series; Upper Ordovician): Evolution v., 61, p. 1455–1465.

WEBBER, K. and ZUSCHIN, M., 2013, Delta-associated molluscan life and death assemblages in the northern Adriatic Sea: implications for paleoecology, regional diversity and conservation: Palaeogeography, Palaeoclimatology, Palaeoecology, v. 370, p. 77–91.

WEBSTER, G.D., MAPLES, C.G., MAWSON, R. and DASTANPOUR, M., 2003, A cladid-dominated early Mississippian crinoid and conodont fauna from Kerman province, Iran and revision of the glossocrinids and rhenocrinids: Journal of Paleontology, v. 77, p. 1–36.

WEFER, G. and BERGER, W.H., 1991, Isotope paleontology: growth and composition of extant calcareous species: Marine Geology, v. 100, p. 207–248.

WESTERMANN, S., VANCE, D., CAMERON, V., ARCHER, C. and ROBINSON, S.A., 2014, Heterogenous oxygenation states in the Atlantic and Tethys oceans during Oceanic Anoxic Event 2: Earth and Planetary Science Letters, v. 404, p. 178–189.

WHITTAKER, R.H., 1956, Vegetation of the Great Smoky Mountains: Ecological Monographs, v. 26, p. 1–80.

WHITTAKER, R.H., 1960, Vegetation of the Siskiyou Mountains, Oregon and California: Ecological Monographs, v. 30, p. 279–338.

WHITTAKER, R.H., 1967, Gradient analysis of vegetation: Biological Reviews, v. 42, p. 207–264.

WHITTAKER, R.H., 1973, Direct gradient analysis: techniques: Handbook of Vegetation Science, v. 5, p. 9–31.

WILLIAMS, A., FRANZISKA, A., DUNSTAN, P.K., POORE, G.C.B., BAX, N.J., KLOSER, R.J. and MCENNULTY, F.R., 2010, Scales of habitat heterogeneity and megabenthos

biodiversity on an extensive Australian continental margin (100 – 1100 m depths): Marine Ecology, v. 31, p. 222–236.

WILLIAMS, S.L., 1988, *Thalassia testudinum* productivity and grazing by green turtles in a highly disturbed seagrass bed: Marine Biology, v. 98, p. 447–455.

ZIMMERMAN, R.A., CUMMINS, H., BOARDMAN, M.R. and DEEHR, R.A., 2001, Living molluscan community distribution and species composition as it relates to seagrass density in a tropical carbonate lagoon, Graham's Harbour, San Salvador, Bahamas, *in* Greenstien, B.J. and Carney, C.K. (eds.), Proceedings of the 10th symposium on the geology of the Bahamas and other carbonate regions: Gerace Research Centre, San Salvador, p. 175–186.

ZUSCHIN, M., HARZHAUSER, M. and MANDIC, O., 2007, The stratigraphic and sedimentologic framework of fine-scale faunal replacements in the middle Miocene of the Vienna Basin (Austria): Palaios, v. 22, p. 285–295

ZUSCHIN, M., HARZHAUSER, M., HENGST, B., MANDIC, O. and ROETZEL, R., 2014, Long-term ecosystem stability in an Early Miocene estuary: Geology, v. 42, p. 7–10.

APPENDIX A

DATA, R CODE, AND SUPPLEMENTARY MATERIAL FOR CHAPTER 2

Part 1: Data

Ordination frequency in the modern studies examined.

Ordination	Frequency
NMS	22
PCA	12
CCA	4
DCA	2
PCO	2
Parital PCA	1
Partial Redundancy	1
Polar	1
RA	1

Ordination frequency in the ancient studies examined.

Ordination	Frequency
DCA	21
NMS	10
CA	10
Polar	3
MDS	3
PCA	1

Frequency of taxonomic groups in modern ordinations examined.

Taxonomic Group	Ordinations
Gastropods	22
Bivalves	19
Echinoderms	13
Crustacean	12
Polychaetes	11
Bryozoans	5
Corals	5
Other “worms”	5
Did not list	5
Sponges	4
Arthropods	4
Ostracodes	3

Frequency of taxonomic groups in ancient ordinations examined.

Taxonomic Group	Ordinations
Bivalves	25
Gastropods	22
Brachiopods	19
Bryozoans	9
Trilobite	7
Crinoids	7
Ostracodes	4
Echinoderms	4
Rugose Coral	2
Cephalopod	2
Sponges	1
Did not list	1

Modern gradient results depicting the number of studies that examined each gradient and the amount of times it was identified along each axis. “Water depth” includes any covarying gradients that were also identified.

Gradient	Studies examined	Axis 1	Axis 2	Axis 3
Water depth	25	17	4	1
Substrate	23	8	6	1
Vegetation	7	6	1	0
Salinity	11	3	3	0
Pollution	4	3	2	0
Taxa ecology	6	2	2	1
Wave energy	6	2	1	0
Temperature	11	1	3	0
Nutrients	8	1	1	0
Shelf patchiness	1	1	1	0
Turbidity	2	1	1	0
Latitude	6	0	3	0
pH	2	0	1	0
Time	4	0	1	0
Geography	7	0	0	0
Longitude	3	0	0	0
Oxygenation	3	0	0	0
Topography	1	0	0	0

Ancient gradient results depicting the number of studies that examined each gradient and the amount of times it was identified along each axis. “Water depth” includes any covarying gradients that were also identified.

Gradients	Studies examined	Axis 1	Axis 2	Axis 3
Water Depth	29	19	5	0
Time	28	12	5	1
Lithology	29	8	6	1
Oxygen	2	4	0	0
Taxa ecology	14	2	5	0
Salinity	3	2	1	1
Geography	12	5	3	0
Turbidity	1	1	0	0
Nutrients/Productivity	1	1	2	0
Wave energy	2	0	3	0
Temperature	1	0	1	0

Modern studies that reported the percent variance explained or relative inertia along axes of ordination. Ordination types are abbreviated as follows: ra—redundancy analysis; cca—canonical correspondence analysis; pca—principal components analysis; dca—detrended correspondence analysis.

Study	Ordination Type	Axis 1	Axis 2	Axis 3	Total variation explained
Barros et al., 2008	pca	37.90%	19.90%	—	57.80%
Barros et al., 2008	pca	40.80%	20.30%	—	61.10%
Barros et al., 2012	ra	8.00%	5.60%	—	13.60%
Barros et al., 2012	pca	29.50%	21.40%	—	50.90%
Blanchard et al., 2013	cca	9.40%	4.10%	—	13.50%
Blanchard et al., 2013	cca	15.30%	6.40%	—	21.70%
Ferguson and Miller, 2007	dca	62.00%	27.00%	—	89.00%
Fernandez et al., 2007	cca	86.70%	9.20%	4.10%	100.00%
Llewellyn and Messing, 1993	pca	75.00%	20.00%	—	95.00%
Llewellyn and Messing, 1993	pca	77.00%	12.00%	—	89.00%
Mariano and Barros, 2015	pca	49.70%	28.90%	—	78.60%
Mariano and Barros, 2015	pca	50.70%	31.50%	—	82.20%
Mariano and Barros, 2015	pca	67.50%	18.30%	—	85.80%
McKinney and Hageman, 2006	pca	36.00%	23.00%	12.00%	71.00%
McKinney and Hageman, 2006	pca	41.00%	19.00%	12.00%	72.00%
Moore, 1974	pca	13.49%	8.31%	7.77%	29.57%
Netto et al., 1999	pca	40.00%	29.00%	—	69.00%
Sumida and Pires-Vanin, 1997	cca	67.90%	—	—	67.90%
Van Houey et al., 2004	dca	75.00%	25.00%	—	100.00%

Ancient studies that reported the percent variance explained or relative inertia along axes of ordination. Ordination types are abbreviated as follows: ca—correspondence analysis; pca—principal components analysis; dca—detrended correspondence analysis

	Ordination type	Axis 1	Axis 2	Axis 3	Total variation explained
Belanger and Garcia, 2014	dca foraminifera	45.60%	14.00%	—	59.60
Belanger and Garcia, 2014	dca mollusk	61.90%	23.80%	—	85.70
Belanger and Garcia, 2014	pca	48.60%	17.80%	15.10%	81.50
Fall and Olszewski, 2010	ca	30.80%	16.40%	—	47.20
Olszewski and Erwin, 2009	ca	4.60%	4.40%	4.30%	13.30
Olszewski and Erwin, 2009	ca	9.30%	8.10%	6.00%	23.40
Olszewski and Erwin, 2009	ca	11.80%	5.90%	4.40%	22.10
Olszewski and Erwin, 2009	ca	13.80%	9.60%	—	23.40
Olszewski and Erwin, 2009	ca	16.90%	10.40%	—	27.30
Olszewski and Patzkowsky, 2001	ca all	12.70%	5.70%	—	18.40
Olszewski and Patzkowsky, 2001	ca bivalve	16.40%	13.90%	—	30.30
Olszewski and Patzkowsky, 2001	ca brachiopods	9.50%	8.10%	—	17.60
Patzkowsky, 1995	dca	48.20%	27.80%	—	76.00

Part 2: R Code to Analyze Data and Produce Figures

Adding the necessary libraries

```
install.packages("viridis")#Viridis package for colorblind scales
library(viridis)
library(vegan)

#Taxonomic frequencies
#Modern
ModernTaxa<-read.csv("Modern taxa freq.csv", row.names= 1, header=TRUE)
ModernTaxa<-as.matrix(ModernTaxa)

#Ancient
AncientTaxa<-read.csv("Fossil tax freq.csv", row.names=1, header=TRUE)
AncientTaxa<-as.matrix(AncientTaxa)


dev.new()
par(mfrow= c(1,2))
barplot(ModernTaxa, beside=TRUE, names.arg=rownames(ModernTaxa),
main="Taxa in modern studies", ylab= "Number of studies",  ylim= c(0,
25), las= 1, cex.names= 0.2, col="dodgerblue")
barplot(AncientTaxa, beside=TRUE, names.arg=rownames(AncientTaxa),
main="Taxa in ancient studies", ylab= "Number of studies", las= 1,
cex.names= 0.2, col="tan3")


#Ordination Frequencies
#Modern
ModernOrds<-read.csv("Modern ord freq.csv", row.names=1, header=TRUE)
ModernOrds<- as.matrix(ModernOrds)

#Ancient
AncientOrds<- read.csv("Ancient ord freq.csv", row.names=1,
header=TRUE)
AncientOrds<- as.matrix(AncientOrds)

dev.new()
par(mfrow= c(1,2))
barplot(ModernOrds, beside=TRUE, names.arg=rownames(ModernOrds),
main="Ordinations in modern studies", ylab= "Number of ordinations",
ylim= c(0, 25), las= 1, cex.names= 0.2, col="dodgerblue")
barplot(AncientOrds, beside=TRUE, names.arg=rownames(AncientOrds),
main="Ordinations in ancient studies", ylab= "Number of ordinations",
ylim= c(0,25), las= 1, cex.names= 0.2, col="tan3")
```

Analysis of all modern gradient results

```
#Modern Gradients
mgr<-read.csv("Modern Gradient results.csv", row.names=1, header=TRUE)

#All modern gradients considered by authors
allMod<-mgr[ , 1]
allMod<-as.data.frame(allMod)
```

```
allMod$gradients<-rownames(mgr)
colnames(allMod)<-c("studies", "gradients")
allMod<- allMod[order(-allMod$studies), ]

barplot(allMod$studies, beside=TRUE, names.arg=allMod$gradients,
main="Gradients considered by Modern studies", ylab= "Number of
studies",  las= 1, cex.names= 0.2, col="gray")

# Determining the percentage of each modern gradient along an axis
percentMGR<-(decostand(mgr [ , 2:3], method="total", MARGIN= 2)*100)

attach(percentMGR)
sortedPercentMGR<- percentMGR[order(-Axis.1, Axis.2), ]
sortedPercentMGR<- as.matrix(sortedPercentMGR)
dev.new()
barplot(sortedPercentMGR, ylab= "Percent of ordinations", main= "Modern
Ordinations", las=1, legend.text=TRUE,
col=plasma(length(rownames(sortedPercentMGR))))

detach(percentMGR)
#Adding plasma colors as a variable within matrix. This makes labeling
by color easier.
sortedPercentMGR<-as.data.frame(sortedPercentMGR) #need to return to
data frame to add the vector of colors
percentMGRcol<- plasma(length(rownames(sortedPercentMGR)))
sortedPercentMGR$colors<-percentMGRcol
percentMGRaxis1<-sortedPercentMGR[ , c(1,3)]

attach(percentMGRaxis1)
SortpercentMGRaxis1<- percentMGRaxis1[order(-Axis.1), ]
detach(percentMGRaxis1)

Axis1cols<- SortpercentMGRaxis1$colors #Pulls out plasma colors as a
vector

freqMGRaxis1<-SortpercentMGRaxis1[ , 1]
freqMGRaxis1<- as.matrix(freqMGRaxis1)
rownames(freqMGRaxis1)<- rownames(SortpercentMGRaxis1)


dev.new()
barplot(freqMGRaxis1, xlab="Axis 1", ylab= "Percent of ordinations",
main= "Modern Ordinations", las=1, legend.text=TRUE, col=Axis1cols)

percentMGRaxis2<- sortedPercentMGR[ , c(2,3)]
attach(percentMGRaxis2)
SortpercentMGRaxis2<- percentMGRaxis2[order(-Axis.2), ]
detach(percentMGRaxis2)
Axis2cols<- SortpercentMGRaxis2$colors#Pulls out colors as a vector

freqMGRaxis2<-SortpercentMGRaxis2[ , 1]
freqMGRaxis2<- as.matrix(freqMGRaxis2)
rownames(freqMGRaxis2)<- rownames(SortpercentMGRaxis2)
```

```
dev.new()
barplot(freqMGRaxis2, xlab="Axis 2", ylab= "Percent of ordinations",
main= "Modern Ordinations", las=1, legend.text=TRUE, col=Axis2cols)

#Side-by-side plot of modern gradation frequencies on Axis 1 and 2
dev.new()
par(mfrow= c(1 ,2))
barplot(freqMGRaxis1, xlab="Axis 1", ylab= "Percent of ordinations",
main= "Modern Ordinations", las=1, legend.text=TRUE, col=Axis1cols)
barplot(freqMGRaxis2, xlab="Axis 2", ylab= "Percent of ordinations",
main= "Modern Ordinations", las=1, legend.text=TRUE, col=Axis2cols)

#Percentages of modern gradients as a scater plot
rownames(percentMGR)<- c("Water depth", "Substrate", "Vegetation",
"Temperature", "Trace Minerals", "Salinity", "Nutrients", "Pollution",
"Latitude", "Life habit", "Turbidity", "Wave Energy", "Shelf
patchiness", "pH", "Time")#clean up rownames form those imported via
csv file

dev.new()
plot(percentMGR$Axis.1, percentMGR$Axis.2, xlab="Percent identified on
Axis 1", ylab= "Percent identified on Axis 2", main="Modern
Ordinations", las=1, asp= 1, pch= 16, cex= 1.3)
text(percentMGR$Axis.1, percentMGR$Axis.2,
labels=rownames(percentMGR),pos=3)
text(8, 17, labels= "More often Identified on Axis 2", cex= 1.2)
text(17, 8, labels= "More often Identified on Axis 1", cex= 1.2)
abline(a=0, b=1)

#Examining gradients weighted by studies
weightedMGR<-format(round((mgr/mgr$Studies.examined), 2), nsmall=2)

#add back the total studies
weightedMGR$Studies.examined<-mgr$Studies.examined
weightedMGR


dev.new()
plot(weightedMGR$Axis.1, weightedMGR$Axis.2, xlab="Percent identified
on Axis 1", ylab= "Percent identified on Axis 2", main="Modern
Ordinations", las=1, asp= 1, pch= 16, col= "dodgerblue", cex=
(weightedMGR$Studies.examined * .1) +1)
text(x=weightedMGR$Axis.1, y=weightedMGR$Axis.2 ,
labels=rownames(weightedMGR))
abline(a=0, b=1)
```

Analysis of ancient gradients

```
#ancient Gradients
fgr<-read.csv("Fossil Gradients.csv", header=TRUE, row.names=1)

#All fossil gradients considered by authors
allFossil<-fgr[ , 1]
allFossil<-as.data.frame(allFossil)
allFossil$gradients<-rownames(fgr)
colnames(allFossil)<-c("studies", "gradients")
```

```
allFossil<- allFossil[order(-allFossil$studies), ]

barplot(allFossil$studies, beside=TRUE, names.arg=allFossil$gradients,
main="Gradients considered by ancient studies", ylab= "Number of
studies", ylim= c(0,30), las= 1, cex.names= 0.2, col="gray")

#combination plot comparing all gradients examined
dev.new()
par(mfrow= c(1,2))
barplot(allMod$studies, beside=TRUE, names.arg=allMod$gradients,
main="Gradients considered by Modern studies", ylab= "Number of
studies",  las= 1, cex.names= 0.1, col="gray")
barplot(allFossil$studies, beside=TRUE, names.arg=allFossil$gradients,
main="Gradients considered by ancient studies", ylab= "Number of
studies", ylim= c(0,30), las= 1, cex.names= 0.1, col="gray")
dev.off()

#Determining the percentage of each ancient gradient along an axis
percentFGR<-(decostand(fgr [ , 2:3], method="total", MARGIN= 2)*100)
percentFGR<- as.matrix(percentFGR)

percentFGR<- as.data.frame(percentFGR)
attach(percentFGR)
sortedPercentFGR<- percentFGR[order(-Axis.1, Axis.2), ]

sortedPercentFGR<- as.matrix(sortedPercentFGR)

dev.new()
barplot(sortedPercentFGR, ylab= "Percent of ordinations", main=
"Ancient Ordinations", las=1, legend.text=TRUE,
col=plasma(length(rownames(sortedPercentFGR))))

detach(percentFGR)

dev.new()
barplot(percentFGR, ylab= "Percent of ordinations", main= "Ancient
Ordinations", las=1, legend.text=TRUE,
col=plasma(length(rownames(percentFGR))))

#Adding plasma colors as a variable within matrix. This makes labeling
by color easier
sortedPercentFGR<- as.data.frame(sortedPercentFGR)
percentFGRcol<- plasma(length(rownames(sortedPercentFGR)))
sortedPercentFGR$colors<-percentFGRcol

percentFGRaxis1<-sortedPercentFGR[ , c(1,3)]

attach(percentFGRaxis1)
SortpercentFGRaxis1<- percentFGRaxis1[order(-Axis.1), ]
detach(percentFGRaxis1)

Axis1cols<- SortpercentFGRaxis1$colors

freqFGRaxis1<-SortpercentFGRaxis1[ , 1]
freqFGRaxis1<- as.matrix(freqFGRaxis1)
```

```
rownames(freqFGRaxis1)<- rownames(SortpercentFGRaxis1)

dev.new()
barplot(freqFGRaxis1, xlab="Axis 1", ylab= "Percent of ordinations",
main= "Ancient Ordinations", las=1, legend.text=TRUE, col=Axis1cols)

percentFGRaxis2<-sortedPercentFGR[ , c(2,3)]

attach(percentFGRaxis2)
SortpercentFGRaxis2<- percentFGRaxis2[order(-Axis.2), ]
detach(percentFGRaxis2)

Axis2cols<- SortpercentFGRaxis2$colors

freqFGRaxis2<-SortpercentFGRaxis1[ , 1]
freqFGRaxis2<- as.matrix(freqFGRaxis2)
rownames(freqFGRaxis2)<- rownames(SortpercentFGRaxis2)

dev.new()
barplot(freqFGRaxis2, xlab="Axis 1", ylab= "Percent of ordinations",
main= "Ancient Ordinations", las=1, legend.text=TRUE, col=Axis2cols)

# Side-by-side plot of ancient gradation frequencies on Axis 1 and 2
dev.new()
par(mfrow= c(1 ,2))
barplot(freqFGRaxis1, xlab="Axis 1", ylab= "Percent of ordinations",
main= "Ancient Ordinations", las=1, legend.text=TRUE, col=Axis1cols)
barplot(freqFGRaxis2, xlab="Axis 1", ylab= "Percent of ordinations",
main= "Ancient Ordinations", las=1, legend.text=TRUE, col=Axis2cols)
dev.off()

#Percentages of gradients as a scater plot
rownames(percentFGR)<- c("Water depth", "Time", "Substrate", "Oxygen",
"Taxa ecology", "Salinity", "Geography", "Turbidity", "Nutrients",
"Wave Energy", "Temperature")

dev.new()
plot(percentFGR$Axis.1, percentFGR$Axis.2, xlab="Percent identified on
Axis 1", ylab= "Percent identified on Axis 2", main="Ancient
Ordinations", ylim= c(0, 25), las=1, asp= 1, pch= 16, cex= 1.3)
text(percentFGR$Axis.1, percentFGR$Axis.2,
labels=rownames(percentFGR),pos=3)
text(9, 22, labels= "More often Identified on Axis 2", cex= 1.2)
text(22, 5, labels= "More often Identified on Axis 1", cex= 1.2)
abline(a=0, b=1)

#Examining fossil gradients weighted by studies
weightedFGR<-format(round((fgr/fgr$Ordinations.examined), 2), nsmall=2)

#add back the total studies
weightedFGR$Ordinations.examined<-fgr$Ordinations.examined
weightedFGR

#Combo plot comparing modern and ancient axes
```

```
dev.new()
par(mfrow= c(1,2))
plot(percentMGR$Axis.1, percentMGR$Axis.2, xlab="Percent identified on
Axis 1", ylab= "Percent identified on Axis 2", main="Modern
Ordinations", ylim= c(0, 25), asp= 1, las=1, pch= 16, cex= 1.3)
text(percentMGR$Axis.1, percentMGR$Axis.2,
labels=rownames(percentMGR),pos=3)
text(8, 17, labels= "More often Identified on Axis 2", cex= 1.2)
text(17, 8, labels= "More often Identified on Axis 1", cex= 1.2)
abline(a=0, b=1)
plot(percentFGR$Axis.1, percentFGR$Axis.2, xlab="Percent identified on
Axis 1", ylab= "Percent identified on Axis 2", main="Ancient
Ordinations", ylim= c(0, 25), las=1, asp= 1, pch= 16, cex= 1.3)
text(percentFGR$Axis.1, percentFGR$Axis.2,
labels=rownames(percentFGR),pos=3)
text(9, 22, labels= "More often Identified on Axis 2", cex= 1.2)
text(22, 5, labels= "More often Identified on Axis 1", cex= 1.2)
abline(a=0, b=1)

#Combo plot of weighted modern and ancient axes
dev.new()
par(mfrow=c(1,2))
plot(weightedMGR$Axis.1, weightedMGR$Axis.2, xlab="Percent identified
on Axis 1", ylab= "Percent identified on Axis 2", main="Modern
Ordinations", xlim= c(0,1), ylim= c(0, 1), las=1, asp= 1, pch= 21, col=
"black", bg= "dodgerblue", cex= (weightedMGR$Studies.examined * .1) +1)
abline(a=0, b=1)
plot(weightedFGR$Axis.1, weightedFGR$Axis.2, xlab="Percent identified
on Axis 1", ylab= "Percent identified on Axis 2", main="Ancient
Ordinations", xlim= c(0,1), ylim= c(0,1), las=1, asp= 1, pch= 21, col=
"black", bg= "tan3", cex= (weightedFGR$Ordinations.examined * .1) +1)
abline(a=0, b=1)
```

Explained variation along axes of ordination

```
#Modern gradients
mav<-read.csv("Modern axis variation.csv", header=TRUE)
cmav<-mav[ , c(3:5, 7)]
colnames(cmav)<-c("Axis 1", "Axis 2", "Axis 3", "Total")

dev.new()
boxplot(cmav[ , 1:3],ylim=c(0,100), las=1, col="gray80",
main="Modern Axis Variation", ylab="Percent variance explained")

length(cmav$"Axis 1")
length(cmav$"Axis 2")
length(cmav$"Axis 3", na.rm=TRUE)

quantile(cmav$"Axis 1")
quantile(cmav$"Axis 2", na.rm=TRUE)
quantile(cmav$"Axis 3", na.rm=TRUE)

#Fossil gradients
fav<-read.csv("Fossil axis variation.csv", header=TRUE)
cfav<-fav[ , c(3:5,7)]
```

```
colnames(cfav)<-c("Axis 1", "Axis 2", "Axis 3", "Total")

quantile(cfav$"Axis 1")
quantile(cfav$"Axis 2", na.rm=TRUE)
quantile(cfav$"Axis 3", na.rm=TRUE)

dev.new()
boxplot(cfav[ , 1:3],ylim=c(0,100), las=1, col="gray80",
main="Ancient Axis Variation", ylab="Percent variance explained")
dev.off()
```

Part 3: Supplementary Tables

Supplementary tables contain the complete list of modern and ancient studies examined in Chapter 2. Species studies, location, study duration, marine environment/ depositional environment, ordination type used, all environmental variables considered, and the environmental gradients authors interpreted along each axis of ordination.

Supplementary Table 2.1: Complete list of modern studies examined and the taxa studied, locations, environments, ordination types and gradients as identified by the authors.

Paper	Taxa	Study location	Study duration	Environment	All variables considered	Ordination type	Axis 1	Axis 2	Axis 3
Aldea et al. 2008	Bivalves and gastropods	South Shetland Islands, West Antarctica	January–February 1995, 2003, 2006	Shelf to basin (0–4000 m), high latitude	Water depth; taxa ecology; geographic location	NMDS	Water depth	Not explained	Not explored
Anderson et al. 2006	Invertebrates in kelp holdfasts	New Zealand	1 year	Subtidal kelp forest stands.	Water depth; substrate; nutrients; vegetation; taxa ecology	NMDS	Kelp holdfast volume	Not explained	Not explored
	Invertebrates in soft sediment	Norway	3 years	Continental shelf		NMDS	Norwegian shelf heterogeneity	Norwegian shelf heterogeneity	Not explored
Barros et al. 2008	Crustaceans, polychaetes, molluscs, echinoderms, sponges, bryozoans, cnidarians	Paraguacu estuarine system, Brazil	2005	Estuary, siliciclastic	Water depth; time; oxygenation; pollution; nutrients; salinity; geographic location	NMDS	Salinity and sediment coarseness	Salinity and sediment coarseness	Not explored
						PCA	Winter: Zn levels 40.8%; Summer: depth and substrate 37.9 %	Winter: Cr levels 20.3%; Summer: Zn and pH 19.9%	Not explored

Paper	Taxa	Study location	Study duration	Environment	All variables considered	Ordination type	Axis 1	Axis 2	Axis 3
Barros et al. 2012	Various benthic marine invertebrates	Paraguacu estuarine system, Brazil	1 month in rainy season; 1 month in dry season	Estuary, siliciclastic	Water depth; substrate; time; pollution; geographic location; salinity	partial PCA	Trace metals: Arsenic and Cr; Zn and Pb; 29.5%	Sediment, salinity, and distance from mouth; 21.4%	Not explored
)						partial Redundancy Analysis	Salinity, Arsenic, Chromium, copper; 8%	Undefined 5.6%	Not explored
Blanchard et al. 2013	Various benthic marine invertebrates	Chukchi Sea, Alaska	late August 2008, early September 2009, early to mid-August 2010	Shallow marine shelf (35–45 m), polar latitudes	Water depth; substrate; nutrients; temperature	CCA; 28.8% total var	Depth and percent mud; 15.3%	Organic carbon, mud, depth; 6.4%	Not explored
						CCA no mammals; 19.9% total var	Depth, mud, organic carbon; 9.4%	Latitude; 4.1%	Not explored
Bolam et al. 2008	Various benthic marine invertebrates	English Channel	June and July 2005	Shallow marine (less than 50 m), siliciclastic	Water depth; substrate; salinity temperature; wave energy	PCA	Stratification of water, percent gravel, tidal stress	depth, grain size sorting and kurtosis, wave stress	Not explored
Bremner et al. 2006	Various benthic marine invertebrates	English Channel and Irish Sea	August–September 1998	Nearshore siliciclastic	Water depth; substrate; temperature; salinity; wave energy; latitude; taxa ecology	PCA; 41.6% total variance	Sea surface temperature, salinity, and fish species richness; 25.5% variance	Depth, algae biomass and weight of rocks in catch; 16.1% variance	Not explored

Paper	Taxa	Study location	Study duration	Environment	All variables considered	Ordination type	Axis 1	Axis 2	Axis 3
Casebolt and Kowalewski 2018	Benthic mollusks	San Salvador, Bahamas	death assemblages less than 1800 years old	Carbonate shallow subtidal within a 5 m depth range	Water depth; substrate; vegetation; wave energy	NMDS	Wave energy	Seagrass	Not explored
Compton et al. 2012	Various benthic marine invertebrates	Challenger Plateau, New Zealand		Topographically complex, marine shelf, siliciclastic.	Water depth; temperature; nutrients; wave energy; topography	NMDS	Water depth and temperature at depth	Not explained	Not explored
		Chatum Rise, New Zealand		Topographically complex, marine shelfs, siliciclastic.		NMDS	Depth	Temperature	Not explored
Ferguson 2008	Benthic mollusks	Cross Bank, Florida Bay, Florida		Shallow water (~30 cm water depth); protected bay; carbonate sediment and seagrass beds	Vegetation; substrate	NMDS	Vegetation blade size	Not explained	Not explored
Ferguson and Miller 2007	Benthic mollusks	Smuggler's Cove, St. Croix, U.S. Virgin Island		Nearshore shallow marine lagoon behind barrier reef, vegetated and non-vegetated	Water depth; vegetation; time	DCA	Seagrass density: Inertia = 62%	Sample collection date: 1980 samples vs 2002 samples; Inertia = 27%	Not explored
Fernandez et al. 2007	Shrimp	San Jorge Gulf, Argentina	June 2003	shallow marine, siliciclastic, temperate gulf	Water depth; substrate; taxa ecology; nutrients; salinity; temperature; oxygenation	CCA	Water depth, age of shrimp, percent clay, and total organic carbon; Inertia = 86.7%	Temperature; Inertia = 9.2%	Not explained; Inertia = 4.1%

Paper	Taxa	Study location	Study duration	Environment	All variables considered	Ordination type	Axis 1	Axis 2	Axis 3
Konar et al. 2009	Mollusks, polychaetes, echinoderms	Prince William Sound, Kachemak Bay, Kodiak Island, Gulf of Alaska, USA	Summer 2003	Intertidal and shallow subtidal rocky coasts	Water depth; temperature; nutrients; substrate	NMDS	Water depth	Intertidal zonation	Not explored
Kuklinski et al. 2006	Encrusting polychaetes and bryozoans	North Atlantic, Europe Coast from 50°–80° latitude	Spring and summer 2002–2005	Marine siliciclastic coastlines	Temperature; salinity; latitude; wave energy	NMDS	Not explained	Latitude	Not explored
Llewellyn and Messing 1993	Crinoids	Little Bahama Bank, The Bahamas	February 1991	Carbonate bank	Water depth; substrate; wave energy	PCA of sediments	Percent lithic grains; 75% variance	Percent planktic material; 20% variance	Not explored
						PCA of skeletal fragments	Percent echinoid grains; 77% variance	Percent gastropod, benthic foraminifera, and alcyonarian coral fragments; 12% variance	Not explored
Long and Ponier 1994	Infaunal benthic marine invertebrates	Gulf of Carpentinari, Australia	November and December 1990	Tropical marine, soft substrate	Water depth; substrate; temperature; salinity; turbidity	Principle Coordinates	Sediment type	Not explored	Not explored

Paper	Taxa	Study location	Study duration	Environment	All variables considered	Ordination type	Axis 1	Axis 2	Axis 3
Mariano and Barros 2015	Various benthic marine invertebrates	Paraguacu, River Estuary, Brazil	March, June and October 2011	Estuary, siliciclastic	Substrate; geographic location; salinity; nutrients	PCA	Grain size and organic material; 67.5% variance	Grain size and salinity 18.3% variance	Not explored
Mariano and Barros 2015 (continued)		Subae River Estuary, Brazil				PCA	Grain size; 50.7% variance	Grain size; 31.5% variance	Not explored
		Jaguaripe River Estuary, Brazil				PCA	Grain size and percent calcium carbonate; 49.7% variance	Grain size, 28.9% variance	Not explored
McClain et al. 2010	Various benthic marine invertebrates	Seamount SW of Monterey Bay, California, USA	2006	Deep sea: 1000–3500 m depth	Water depth; substrate	NMDS	Water depth	Not explained	not explored
McKinney and Hageman 2006	Various benthic marine invertebrates	North Adriatic Sea, Italian coast to Balkan Coast	1920s–1930s	Sediment starved shelf: mostly Pleistocene sands and Holocene muds	Taxa ecology; substrate; geographic location	PCA	Sedentary, epibenthic, suspension feeders; 41% variance	Bioturbating endobenthic, detrital feeders; 19% variance	Mobile, non-bioturbating omnivores; 12% variance
	Skeletal benthic marine invertebrates					PCA	Mobile, non-bioturbating, epibenthic omnivores; 36% variance	Bioturbating, endobenthic, detrital feeders; 13% variance	Sedentary, epibenthic, suspension feeders; 12% variance

Paper	Taxa	Study location	Study duration	Environment	All variables considered	Ordination type	Axis 1	Axis 2	Axis 3
Miller 1988	Benthic mollusks	Smuggler's Cove, St. Croix, U.S. Virgin Island	December 1979–July 1980	Nearshore shallow marine lagoon behind barrier reef, vegetated and non-vegetated	Water depth; substrate; vegetation	Polar Ordination	Seagrass density	Not explored	Not explored
Moore 1974	Bryozoans, mollusks, amphipods, nematodes	North Sea, NE coast of UK	Not given	Kelp forests, British North Sea	Vegetation; pollution; turbidity	PCA	Kelp holdfast volume	Turbidity	Unclear
						Reciprocal Averaging	Turbidity	Unclear	Unclear
Netto et al. 1999	Various benthic marine invertebrates	Rocas Atoll, Brazil, South Atlantic	May 1996	Equatorial reef complex, tidal to sublittoral carbonate environments	Water depth; substrate; temperature; salinity	PCA	Depth, amount organic material, and sediment sorting; 40% variance	Temperature, salinity, grain size; 29% variance	Not explored
Olabarria 2006	Prosobranchia gastropods	Procupine Abyssal Plain, Northeast Atlantic (200 km SW of Ireland)	23 years	Deep offshore marine: 500 – 4500+ m depth	Water depth; geographic location	NMDS	Water depth	Not explored	Not explored
Reich 2014	Gastropods	San Salvador, The Bahamas	Summer 2012	Sea grass beds and sand flats in open marine shallow subtidal and lagoons	Vegetation; substrate; geographic location	NMDS	Occurrence of sea grass and the presence of gastropods typically associated with sea grass beds	Restricted lagoon vs. open marine and abundance of *Zebina browniana*	Not explained
							Presence of seagrass	Not explained	Presence of seagrass

Paper	Taxa	Study location	Study duration	Environment	All variables considered	Ordination type	Axis 1	Axis 2	Axis 3
Seiderer and Newell 1999	Crustaceans and polychaetes	SE coast, UK	August 1996	Nearshore siliciclastic (~ 30 m water depth)	Substrate; geographic location	NMDS	Sediment sorting	Not explained	Not explored
Smale 2008	Various benthic marine invertebrates	Adelaide Island, West Antarctic Peninsula	October 2005; January 2006	Shallow, nearshore marine	Water depth; taxa ecology; latitude; geographic location	NMDS	Water depth	Latitudinal gradient and geographic location	Not explored
Smith et al. 2001	Various benthic marine invertebrates	Pacific Coast, SW California	July–September; 1973–1994; 21 years	California coast and shelf; 0–200 m water depth	Water depth; substrate; time; pollution; nutrients; geographic location	Principle Coordinates Analysis	Pollution	Pollution	Depth and sediment
Springer and Flessa 1996	Mollusks	Bahia la Choya, Mexico, Gulf of California	March 1991	Rocky and sandy tidal flats, tidal channels, and marsh	Water depth; substrate	NMDS	Water depth	Substrate	Not explained
Sumida and Pires-Vanin 1997	Mollusks and arthropods	Ubatuba region, SE Brazil (Sao Paulo)	July 1986, July 1987, December 1988	Shelf break and upper slope	Water depth; latitude; longitude; temperature; salinity; oxygenation	CCA	Water depth, Inertia = 67.9%	Not explained	Not explored
Tyler and Kowalewski 2014	Mollusks, echinoderms, annelids	Beaufort, North Carolina, USA	2011–2013	Nearshore marine, lagoon and open ocean	Water depth; latitude; longitude	PCoA, CA, DCA, NMDS	Water depth for all ordinations	Not explained	Not explored

Paper	Taxa	Study location	Study duration	Environment	All variables considered	Ordination type	Axis 1	Axis 2	Axis 3
Van Hoey et al. 2004	Polychaetes, crustaceans, mollusks, echinoderms	Belgian continental shelf	1994 through 2000	Sand bars, intertidal and subtidal	Water depth; substrate	DCA	Water depth and percent mud content; Eigenvalue: 0.645; Relative Inertia=75%	Substrate Eigenvalue: 0.215; Relative Inertia= 25%	Not explored
Webber and Zuschin 2013	Mollusks	Isonzo River, northern Adriatic Sea, Italy	June and July 2010	Tidal flats, delta, and shallow subtidal; siliciclastic	Water depth; substrate; pH; oxygenation; temperature; salinity	NMDS	Water depth	Not explored	Not explored
Williams et al. 2010	Various benthic marine taxa	West coast of Australia	2005	shelf and slope	Water depth; substrate; temperature; longitude; topography	NMDS	Water depth, temperature and oxygen	Not explained	Not explored

Supplementary Table 2.2: Complete list of ancient studies examined and the taxa studied, locations, environments, ordination types and gradients as identified by the authors.

Paper	Taxa	Age and duration	Study location	Environments	All variables considered	Ordination type	Axis 1	Axis 2	Axis 3
Amorosi et al. 2014	Ostracods, foraminifera, and mollusks	Pleistocene–Holocene, ~12 kyr	Single core, Tuscany, Italy	Coastal plain, estuarine valley, deltaic system	Water depth; substrate; salinity	DCA of mollusks	Salinity	Not explained	Not explored
Balsiero 2016	Brachiopods and bivalves	late Carboniferous (Pennsylvanian); ~ 20 m.y.	western Argentina	shallow subtidal through offshore	Water depth; sequence stratigraphic position	NMDS	Age of samples and water depth	Water depth	Not explored
Belanger and Garcia 2014	Benthic foraminifera and molluscs	early Miocene; ~ 2 m.y.	western Oregon, U.S.A.	Siliciclastic middle to outer shelf near storm wave base	Water depth; geologic age; temperature; nutrients; substrate	DCA of foraminifera	Age of samples and oxygenation; Inertia = 45.6%;	Productivity; Inertia = 14%;	Not explored
						DCA of mollusks	Water depth; Inertia = 61.9%	Productivity; Inertia = 23.8%	Not explored
						PCA of proxy variables	Organics, productivity, and oxygenation; 48.6% variance	Organics and temperature; 17.8% variance	Percent mud; 15.1% variance
Bush and Brame 2010	Brachiopods	Late Devonian (Frasnian)	southwest Virginia, U.S.A.	siliciclastic offshore to basinal	Water depth; geologic age; substrate	DCA	Substrate type as proxy for depth gradient	Not explained	Not explored

Paper	Taxa	Age and duration	Study location	Environments	All variables considered	Ordination type	Axis 1	Axis 2	Axis 3
Bush and Brame 2010 continued						NMDS	Substrate type	Paleoenvironmental energy and taxa morphology	Not explored
Cisne and Rabe 1978	Brachiopods, graptolites and other marine invertebrates	Middle Ordovician; ~2 m.y.	New York, U.S.A.	Carbonate bank and slope; siliciclastic slope and basin	Water depth; geologic age; substrate	Polar, PCA and Reciprocal Averaging	Water depth	Not explored	Not explored
Clapham and James 2008	Brachiopods, bivalves, gastropods, rugose corals	early–middle Permian; ~35 m.y..	Australia	Carbonate and siliciclastic shoreface to offshore	Water depth; geologic age; geographic location; substrate	DCA	Age of samples and sedimentary basin	Sedimentary basin	Not explored
						NMDS	Age of samples	Water depth	Not explored
Danise and Holland 2017	Bivalves, gastropods, echinoderms, brachiopods, bryozoans	Middle to Late Jurassic; ~13 m.y.	Wyoming, U.S.A.	Carbonate and siliciclastic foreland basin	Water depth; substrate; geologic age	NMDS	Age of samples and lithology	Age of samples and water depth	Not explored
						NMDS of lithologies	Water depth	Age of samples	Not explored
Dineen et al. 2013	Brachiopods, bivalves, gastropods, crinoids	late Carboniferous; ~25 m.y.	Paganzo Basin and Rio Blanco Basin, Argentina	Fluvial, estuarine, siliciclastic shoreface to foreshore	Water depth; substrate; geologic age; taxa ecology	DCA	Age of samples	Taxa ecology	Not explored

Paper	Taxa	Age and duration	Study location	Environments	All variables considered	Ordination type	Axis 1	Axis 2	Axis 3
Erwin 1989	Gastropods	Permian (Wolfcampian); ~ 20 m.y.	southwest U.S.A.	Carbonate and siliciclastic shelf to basin environments	Water depth; substrate; geographic location; geologic age	DCA	Water depth	Taxa diversity	Not explored
		middle Permian (Leonardian through middle Guadalupian); ~ 15 m.y.				DCA	Lithology	Taxa diversity	Not explored
	Gastropods	Permian (Wolfcampian through middle Guadalupian); ~ 35 m.y.	southwest U.S.A.	Carbonate and siliciclastic shelf to basin environments		DCA	Age of samples	Not explained	not explored
Fall and Olszewski 2010	Brachiopods	Capitanian (Guadalupian, Middle Permian); ~ 5.4 m.y.	west Texas, U.S.A.	Siliciclastic slope and basin with interbedded carbonate reef deposits	Water depth; geologic age	CA	Age of samples between stratigraphic sequences; Relative Inertia = 30.8%	Age of samples within stratigraphic sequences; Relative Inertia = 16.4%	Not explored
Foster et al. 2015	Bivalves, brachiopods, echinoderms, ostracods, gastropods	Early Triassic; ~4 m.y.	northern Hungary	Carbonate and siliciclastic tidal flat through outer ramp	Water depth; substrate; geologic age	NMDS	Lithology	Not explained	Not explored

Paper	Taxa	Age and duration	Study location	Environments	All variables considered	Ordination type	Axis 1	Axis 2	Axis 3
Hendy 2013	Mollusks	middle-late Miocene; ~4 m.y.	Panama	Siliciclastic nearshore to offshore	Water depth; substrate; geologic age; taxa ecology	DCA	Water depth, lithology and taxa ecology	Taxa ecology	Not explored
Holland and Patzkowsky, 2004	Brachiopods, bivalves, gastropods, bryozoans, trilobites	Late Ordovician; ~2 m.y.	Kentucky, U.S.A.	Mixed carbonate-siliciclastic ramp	Water depth; substrate; geologic age; taxa ecology	DCA	Water depth	Age of samples	Not explored
Holland et al. 2001	Brachiopods, crinoids, mollusks, trilobites, bryozoans	Late Ordovician	Ohio, Kentucky, Indiana, U.S.A.	Storm-dominated siliciclastic and carbonate ramp	Water depth substrate; geologic age; taxa ecology	DCA	Water depth	Substrate consistency and taxa ecology	Not explored
Kowalewski et al. 2002	Molluscs	early to middle Miocene; ~4 m.y.	Europe	Carbonate and siliciclastic passive margin	Geographic location; substrate; geologic age; taxa ecology	CA	Biogeographic province	Taxa ecology	Not explored
Lafferty et al. 1994	Brachiopods, crinoids, trilobites, molluscs	Middle Devonian (Givetian); ~ 5 m.y.	northwest New York, U.S.A.	Carbonate and siliciclastic foreland basin	Water depth; substrate; geographic location; taxa ecology	Polar ordination of Hills Gulch Bed	Water depth, lithology and geographic location	Not explained	Not explored
						Polar ordination of Browns Creek Bed	Abundance of atrypids	Water depth, lithology and geographic location	Not explored
Layou 2009	Brachiopods, mollusks, ostracods, bryozoans, crinoids	Late Ordovician (Mohawkian); ~4 m.y.	Virginia, Kentucky, and Tennessee, U.S.A.	Carbonate and siliciclastic foreland basin	Water depth; substrate; geologic age; geographic location	MDS	Water depth	Age of samples	Not explored

Paper	Taxa	Age and duration	Study location	Environments	All variables considered	Ordination type	Axis 1	Axis 2	Axis 3
Layou 2009 continued						MDS of individual sequences	Geography	Not explained	Not explored
Lebold and Kammer 2006	Brachiopods, bivalves, crinoids, bryozoans	late Carboniferous (Late Pennsylvanian); ~400 kyr	Pennsylvania, Ohio, Kentucky, Maryland and Virginia, U.S.A.	Carbonate and siliciclastic foreland basin	Water depth; substrate; geographic location; taxa ecology	MDS	Turbidity, salinity and oxygenation	Lithology and geography	Not explored
McMullen et. al 2014	Mollusks, crinoids, marine reptiles, fish, and shark	Middle to Late Jurassic; ~9 m.y.	Wyoming, U.S.A.	Tidal estuary, shallow carbonate ramp, siliciclastic wave dominated shelf	Water depth; substrate; geographic location; geologic age	NMDS	Water depth	Not explained	Not explored
Novack-Gottshall and Miller 2003	Gastropods and bivalves	Late Ordovician	Ohio, Indiana, Kentucky, U.S.A.	Peritidal to deep subtidal carbonates and offshore siliciclastics	Water depth; substrate; geologic age; turbidity; salinity	NMDS	Age of samples	Water depth and lithology	Salinity
Olszewski and Erwin 2009	Brachiopods	middle Permian; ~15 m.y.	west Texas, U.S.A.	Carbonate and siliciclastic shelf, slope and basin	Geologic age; geographic location	CA	Age of samples; Inertia = 4.6%	Not explained; Inertia = 4.4%	Not explained; Inertia = 4.3%
						CA of cluster 1	Geography; Inertia = 9.3%	Geography; Inertia = 8.1%	Age of samples; Inertia = 6.0%
						CA of cluster 2	Geography; Inertia = 11.8%	Geography; Inertia = 5.9%	Not explained; Inertia = 4.4%

Paper	Taxa	Age and duration	Study location	Environments	All variables considered	Ordination type	Axis 1	Axis 2	Axis 3
Olszewski and Erwin 2009 continued						CA of cluster 3	Geography; Inertia = 16.9%	Age of samples; Inertia = 10.4%	Not explored
						CA of cluster 4	Age of samples; Inertia = 13.8%	Unclear; Inertia = 9.6%	Not explored
Olszewski and Patzkowsky 2001	Brachiopods and bivalves	late Carboniferous (Late Pennsylvanian) to early Permian; ~25 m.y.	Kansas, U.S.A.	Carbonates and siliciclastics; open-marine, tidal flats, deltas	Water depth; substrate; geologic age; geographic location; oxygen; taxa ecology	CA	Water depth; Inertia = 12.7%	Not explained; Inertia = 5.7%	Not explored
						CA of brachiopods	Oxygen gradient; Inertia = 9.5%	Not explained; Inertia = 8.1%	Not explored
						CA of bivalves	Restricted to open marine; Inertia = 16.4%	Not explained; Inertia = 13.9%	Not explored
Patzkowsky 1995	Brachiopods	Middle Ordovician (Darriwilian); ~5 m.y.	Tennessee and Virginia, U.S.A.	Carbonate peritidal, shelf, and ramp through siliciclastic slope and basin	Water depth; substrate; geographic location; geologic age	DCA	Water depth; Relative Inertia = 48.2%	Not explained; Relative Inertia = 27.8%	Not explored

Paper	Taxa	Age and duration	Study location	Environments	All variables considered	Ordination type	Axis 1	Axis 2	Axis 3
Perera and Stigall 2018	Brachiopods, mollusks, corals, crinoids, bryozoans, sponges, echinoids, trilobites	Late Permian; ~10 kyr	Ohio, U.S.A.	Carbonate subtidal to offshore shale	Water depth; substrate; geographic location; taxa ecology	DCA	Substrate type and taxa ecology	Not explained	Not explored
Redman et al. 2007	Mollusks	early Pliocene	southern California (~0.32 km^2)	Lagoon, backreef, shoreface	Water depth; substrate; geologic age; taxa ecology	DCA	Substrate and taxa ecology	Not explained	Not explored
Scarponi and Kowalewski 2004	Mollusks	Pleistocene-Holocene; ~ 150 kyr	northeast Italy	Shallow marine, delta	Water depth; substrate; geologic age; taxa ecology; salinity; wave energy	DCA	Water depth	Wave energy and salinity	Not explored
							Systems tract	Not explained	Not explored
Scarponi et al. 2014	Mollusks	early to middle Pleistocene; ~ 300 kyr	southern Italy	Siliciclastic nearshore shelf and slope	Water depth; substrate; geologic age; taxa ecology; oxygen	DCA	Water depth	Not explored	Not explored
Tomašových 2006	Brachiopods and bivalves	Late Triassic (Rhaetian)	Austria	Restricted siliciclastic-carbonate basin, subtidal to offshore environments	Water depth; substrate; geologic age; taxa ecology	NMDS	Substrate and taxa ecology	Not explained	Not explored

Paper	Taxa	Age and duration	Study location	Environments	All variables considered	Ordination type	Axis 1	Axis 2	Axis 3
Tuckey and Anstey 1989	Bryozoans	Late Ordovician to middle Silurian; ~ 20 m.y.	Estonia, North America, and Baltics	Carbonate and siliciclastic marine	Substrate; geologic age; geographic location	DCA	Age of samples	Lithology	Not explored
Webber 2002	Brachiopods, crinoids, mollusks, trilobites, bryozoans	Late Ordovician	Ohio, Kentucky, Indiana, U.S.A.	Storm dominated siliciclastic and carbonate ramp	Water depth; substrate; geologic age	DCA	Water depth and storm activity	Not explored	Not explored
Webber 2005	Brachiopods, crinoids, mollusks, trilobites, bryozoans	Late Ordovician	Ohio, Kentucky, Indiana, U.S.A.	Storm dominated siliciclastic and carbonate ramp	Water depth; substrate; geologic age	DCA	Water depth and storm activity at the bedset level	Not explored	Not explored
Zuschin et al. 2014	Mollusks	early Miocene; ~700 kyr	Austria	Estuary and siliciclastic tidal flat to carbonate subtidal	Water depth; substrate; geologic age; wave energy; taxa ecology	DCA	Water depth	Wave energy and taxa ecology	Not explored

APPENDIX B

DATA, R CODE, AND SUPPLEMENTARY TABLE FOR CHAPTER 3

Part 1: Data

Data matrix for the Bahamas study on shallow subtidal death assemblages. Matrix includes environmental variables and species abundances for each sample.

Sample	Location	Transect No	Distance from shore (m)	Depth (m)	Temperature (C)	pH	Dissolved O_2 (mg/L)	Substrate	Seagrass coefficient	Bioturbation
GH-T1-0	Graham's Harbour	1	150	3.4	31.1	8.02	19.26	V	4.72	3
GH-T1-15	Graham's Harbour	1	135	3.7	30.6	7.98	17	V	6.23	3
GH-T1-30	Graham's Harbour	1	120	3.1	30.6	8.02	19.7	V	5.54	3
GH-T2-0	Graham's Harbour	2	10	1.0	31.7	8.09	18.4	V	0	3
GH-T2-15	Graham's Harbour	2	25	1.5	31.7	7.98	19.2	V	8.19	3
GH-T2-30	Graham's Harbour	2	40	2.1	31.1	8.06	20.1	V	3.68	3
GH-T3-0	Graham's Harbour	3	200	2.4	30.6	7.85	19.8	V	2.59	2
GH-T3-15	Graham's Harbour	3	215	2.7	30.6	7.78	20.1	V	3.26	3
GH-T3-30	Graham's Harbour	3	230	2.7	30.6	7.79	20.1	V	6.86	3
FB-T4-0	Fernandez Bay	4	120	3.1	30.0	8.02	20.1	SO	0	2
FB-T4-15	Fernandez Bay	4	135	3.1	30.0	8.04	20.6	SO	0	2
FB-T4-30	Fernandez Bay	4	150	3.1	30.0	8.03	20.2	SO	0	2
FB-T5-0	Fernandez Bay	5	120	3.1	30.6	8.06	20.2	SO	0	3
FB-T5-15	Fernandez Bay	5	135	3.1	30.0	8.05	19.6	SO	0	3
FB-T5-30	Fernandez Bay	5	150	3.1	30.0	8.05	19.8	SO	0	2
SD-T6-0	Sand Dollar Beach	6	200	4.6	31.1	7.96	20.3	SR	0	3
SD-T6-15	Sand Dollar Beach	6	215	4.9	31.7	8.05	20.0	SR	0	3
SD-T6-30	Sand Dollar Beach	6	230	5.2	31.1	8.05	20.1	SR	0	4
SD-T7-0	Sand Dollar Beach	7	100	2.4	31.1	7.96	20.1	SO	0	4
SD-T7-15	Sand Dollar Beach	7	115	2.4	31.1	8.04	20.2	SO	0	4
SD-T7-30	Sand Dollar Beach	7	130	2.7	31.1	8.06	19.9	SO	0	3
SD-T8-0	Sand Dollar Beach	8	175	4	31.1	8.06	20.0	SR	0	3
SD-T8-15	Sand Dollar Beach	8	190	4.6	31.1	8.06	19.9	SR	0	3
SD-T8-30	Sand Dollar Beach	8	205	4.6	31.1	8.05	19.9	SR	0	3
FR-T9-0	French Bay	9	50	1.8	30.6	7.94	19.8	V	8.67	1
FR-T9-15	French Bay	9	65	1.8	30.6	8.0	19.7	V	5.36	1
FR-T10-0	French Bay	10	50	1.8	30.6	8.02	21	V	—	1
FR-T10-15	French Bay	10	65	2.1	31.1	8.1	20.9	V	3.23	1
FR-T10-30	French Bay	10	80	1.8	31.1	8.08	21	V	—	1

Sample	Energy	Weight Before (g)	2.00 mm Weight (g)	1.00 mm Weight (g)	0.50 mm Weight (g)	0.25 mm Weight (g)	0.125 mm Weight (g)	Less than 0.125 mm Weight (g)	Summed Weight (g)	Weight After(g)	*Acetabularia crenulata*	*Cymopolia barbata*
GH-T1-0	1	177.332	8.734	17.931	32.329	50.935	53.953	12.487	176.369	176.295	3	0
GH-T1-15	1	178.451	6.087	24.236	39.593	52.723	44.597	10.392	177.628	177.61	0	0
GH-T1-30	1	190.255	8.347	27.823	37.139	46.89	52.154	16.456	188.809	188.799	0	0
GH-T2-0	1	188.628	0.056	3.558	98.795	63.476	20.74	1.248	187.873	187.877	0	43
GH-T2-15	1	199.105	3.381	4.529	10.926	44.32	128.388	4.558	196.102	196.713	35	0
GH-T2-30	1	184.183	4.246	14.736	35.095	62.942	63.908	2.478	183.405	183.398	5	0
GH-T3-0	1	187.998	5.868	24.136	51.272	58.825	34.809	12.013	186.923	186.894	0	0
GH-T3-15	1	184.375	9.213	17.267	48.443	70.295	31.91	6.355	183.483	183.472	2	0
GH-T3-30	1	193.988	13.098	23.415	49.829	53.739	34.031	18.906	193.018	192.926	1	0
FB-T4-0	1	186.915	0.19	1.702	19.695	143.645	20.351	0.431	186.014	186.012	0	0
FB-T4-15	1	186.408	0.05	0.895	12.688	110.7	60.97	0.348	185.651	185.68	0	0
FB-T4-30	1	189.757	0.051	0.823	16.44	112.478	59.351	0.462	189.605	189.597	0	0
FB-T5-0	1	174.935	0.04	1.415	10.464	141.744	19.868	0.342	173.873	173.867	0	0
FB-T5-15	1	194.342	0.064	1.316	14.583	124.336	52.656	0.445	193.4	193.407	0	0
FB-T5-30	1	198.252	0.093	1.69	15.275	109.402	70.643	0.566	197.669	197.671	0	0
SD-T6-0	2	171.566	5.024	36.034	61.849	57.698	9.299	0.821	170.725	170.73	0	0
SD-T6-15	2	171.422	11.469	28.039	60.465	49.786	18.086	2.688	170.533	170.575	0	0
SD-T6-30	2	185.511	36.077	30.191	58.318	47.089	12.747	1.14	185.562	185.566	0	0
SD-T7-0	1	185.815	3.507	25.907	107.121	44.513	3.44	0.282	184.77	184.765	0	0
SD-T7-15	1	195.66	5.754	25.271	96.959	49.033	15.431	1.864	194.312	194.328	0	0
SD-T7-30	1	184.954	4.774	27.513	80.039	41.944	25.743	3.504	183.517	183.518	0	0
SD-T8-0	2	186.152	25.314	52.608	64.599	37.978	4.584	0.367	185.45	185.456	0	0
SD-T8-15	2	194.72	13.264	47.177	73.65	49.389	10.44	0.763	194.683	194.676	0	0
SD-T8-30	2	171.397	32.649	41.478	59.601	31.801	5.092	0.535	171.156	171.161	0	0
FR-T9-0	3	179.196	12.571	16.427	34.492	48.741	52.842	13.864	178.937	178.822	0	0
FR-T9-15	3	187.258	6.263	7.074	25.082	71.84	62.486	14.488	187.233	187.192	0	0
FR-T10-0	3	77.514	6.185	2.218	3.909	12.562	38.875	14.646	78.395	77.933	—	—
FR-T10-15	3	184.286	10.797	14.82	24.501	49.731	68.388	15.709	183.946	183.921	0	0
FR-T10-30	3	167.272	9.347	2.71	11.582	51.52	76.433	15.544	167.136	167.111	—	—

Samples	*Dasycladus vermicularis*	*Halimeda incrassata*	*Halimeda* sp.	*Penicillus capitatus*	*Penicillus dumetosus*	*Penicillus pyriformis*	*Penicillus* sp.	*Rhipocephalus phoenix*	*Udotea cyathiformis*	*Udotea flabellum*
GH-T1-0	0	8	0	2	0	0	0	0	0	0
GH-T1-15	0	1	0	1	3	0	0	0	0	0
GH-T1-30	0	0	0	2	1	0	0	0	3	0
GH-T2-0	0	0	0	0	0	0	0	0	0	0
GH-T2-15	0	5	0	27	0	0	0	0	0	2
GH-T2-30	65	4	0	0	0	0	0	3	0	1
GH-T3-0	0	2	0	1	0	0	1	0	0	1
GH-T3-15	0	1	0	0	0	0	3	0	0	0
GH-T3-30	0	3	0	0	0	2	0	0	4	0
FB-T4-0	0	0	0	0	0	0	0	0	0	0
FB-T4-15	0	0	0	0	0	0	0	0	0	0
FB-T4-30	0	0	0	0	0	0	0	0	0	0
FB-T5-0	0	0	0	0	0	0	0	0	0	0
FB-T5-15	0	0	0	0	0	0	0	0	0	0
FB-T5-30	0	0	0	0	0	0	0	0	0	0
SD-T6-0	0	0	0	0	0	0	0	0	0	0
SD-T6-15	0	0	0	0	0	0	0	0	0	0
SD-T6-30	0	0	0	0	0	0	0	0	0	0
SD-T7-0	0	0	0	0	0	0	0	0	0	0
SD-T7-15	0	0	0	0	0	0	0	0	0	0
SD-T7-30	0	0	0	0	0	0	0	0	0	0
SD-T8-0	0	0	0	0	0	0	0	0	0	0
SD-T8-15	0	0	0	0	0	0	0	0	0	0
SD-T8-30	0	0	0	0	0	0	0	0	0	0
FR-T9-0	0	1	0	0	0	0	0	0	0	0
FR-T9-15	0	0	0	0	0	0	0	0	0	0
FR-T10-0	—	—	—	—	—	—	—	–	—	
FR-T10-15	0	0	0	0	0	0	0	0	0	0
FR-T10-30	—	—	—	—	—	—	—	—	—	—

Samples	*Udotea* sp.	*Padina sanctae-crucis*	Blade area *Halodule*/m2	Blade area *Syringodium*/m2	Blade area *Thalassia*/m2	Sum Alga	*Acteocina lepta*	*Acteocina* sp B (Redfern 2013)	*Angulus merus*	*Angulus sybariticus*	*Anodontia alba*
GH-T1-0	0	0	528	2880	1040	10	0	1	0	3	0
GH-T1-15	0	0	624	1920	1904	5	0	0	0	2	1
GH-T1-30	0	0	304	4288	992	6	0	0	0	0	0
GH-T2-0	0	15	0	0	0	58	0	4	0	0	0
GH-T2-15	0	0	224	4784	1920	34	2	0	0	0	0
GH-T2-30	0	0	192	400	1344	73	0	3	0	4	0
GH-T3-0	0	0	768	112	944	5	0	5	0	1	1
GH-T3-15	0	0	160	208	1232	4	0	2	0	0	0
GH-T3-30	0	0	64	2128	2144	9	0	0	0	0	0
FB-T4-0	0	0	0	0	0	0	0	1	0	1	0
FB-T4-15	0	0	0	0	0	0	0	0	1	2	0
FB-T4-30	0	0	0	0	0	0	1	0	0	0	0
FB-T5-0	0	0	0	0	0	0	0	1	0	2	0
FB-T5-15	0	0	0	0	0	0	1	0	0	0	0
FB-T5-30	0	0	0	0	0	0	0	1	0	1	1
SD-T6-0	0	0	0	0	0	0	0	5	0	3	0
SD-T6-15	0	0	0	0	0	0	0	2	0	1	0
SD-T6-30	0	0	0	0	0	0	0	2	0	2	0
SD-T7-0	0	0	0	0	0	0	0	1	0	0	0
SD-T7-15	0	0	0	0	0	0	0	3	0	0	0
SD-T7-30	0	0	0	0	0	0	0	4	0	0	0
SD-T8-0	0	0	0	0	0	0	0	2	0	0	0
SD-T8-15	0	0	0	0	0	0	0	6	0	0	0
SD-T8-30	0	0	0	0	0	0	0	3	0	0	0
FR-T9-0	0	0	0	672	3280	1	0	2	0	0	0
FR-T9-15	1	0	0	112	2112	1	0	1	0	0	0
FR-T10-0	—	—	—	—	—	—	0	1	0	1	0
FR-T10-15	0	0	848	480	1088	0	0	1	0	0	0
FR-T10-30	—	—	—	—	—	—	0	2	0	0	0

Samples	*Antalis antillarum*	*Antalis cerata*	*Arene venustula*	*Astralium phoebium*	*Atys sharpi*	*Barbatia cancellaria*	*Berthella stellata*	*Brachidontes exustus*	*Bulla occidentalis*	*Calliostoma javanicum*	*Calliostoma pulchrum*	*Callucina keenae*
GH-T1-0	2	2	0	0	0	0	0	0	0	0	0	0
GH-T1-15	0	1	0	1	0	0	0	0	0	0	0	0
GH-T1-30	1	0	0	0	1	0	0	0	0	0	0	0
GH-T2-0	0	0	0	0	0	0	0	1	0	0	0	0
GH-T2-15	0	0	1	0	3	0	1	1	0	0	0	0
GH-T2-30	0	1	0	0	1	0	0	0	0	0	0	0
GH-T3-0	1	0	0	0	3	0	0	0	0	0	0	0
GH-T3-15	1	0	0	0	2	0	0	0	0	0	0	0
GH-T3-30	1	0	0	0	1	0	0	1	1	0	0	0
FB-T4-0	0	0	0	0	0	0	0	0	0	0	0	0
FB-T4-15	0	0	0	0	2	0	0	0	0	0	0	0
FB-T4-30	0	0	0	0	2	0	0	0	0	1	0	0
FB-T5-0	0	0	0	0	0	0	0	0	0	0	0	0
FB-T5-15	0	0	0	0	0	0	0	0	0	0	0	0
FB-T5-30	0	0	0	0	1	0	0	0	0	0	1	0
SD-T6-0	0	0	0	0	0	0	0	0	1	0	0	0
SD-T6-15	0	0	0	0	1	0	0	0	0	0	0	0
SD-T6-30	0	0	0	0	0	0	0	0	2	0	0	0
SD-T7-0	0	0	0	0	1	0	0	0	0	0	0	0
SD-T7-15	0	0	0	0	1	0	0	0	0	0	0	0
SD-T7-30	0	0	0	0	1	0	0	0	0	0	0	0
SD-T8-0	0	0	0	0	0	0	0	0	0	0	0	0
SD-T8-15	0	0	0	0	0	0	0	0	0	0	0	0
SD-T8-30	0	0	0	0	1	0	0	0	3	0	0	0
FR-T9-0	0	0	0	0	1	3	0	0	1	0	0	0
FR-T9-15	0	0	0	0	0	0	0	0	0	0	0	0
FR-T10-0	0	0	0	0	1	0	0	0	0	0	0	0
FR-T10-15	0	0	0	0	1	0	0	0	0	0	0	2
FR-T10-30	0	0	0	0	1	0	0	0	0	0	0	0

Samples	*Cerithium atratum*	*Cerithium eburneum*	*Cerithium litteratum*	*Cerithium* sp.	*Chama florida*	*Chione elevata*	*Cochliolepis parasitica*	*Columbella mercatoria*	*Conus flavescens*	*Conus patae*	*Crenella divaricata*	*Ctena orbiculata*
GH-T1-0	0	1	0	0	0	2	0	0	0	0	2	0
GH-T1-15	0	1	0	0	0	3	0	0	1	0	3	0
GH-T1-30	3	0	1	0	0	4	0	0	0	0	2	1
GH-T2-0	2	1	0	0	0	1	0	0	0	0	13	0
GH-T2-15	3	1	0	0	0	3	0	0	0	0	4	0
GH-T2-30	1	0	0	0	0	6	0	0	0	0	7	0
GH-T3-0	0	6	0	0	0	0	0	0	0	0	5	0
GH-T3-15	0	5	0	0	0	1	0	0	0	1	5	0
GH-T3-30	0	9	6	0	0	1	0	0	0	0	4	0
FB-T4-0	0	1	0	0	0	1	0	0	0	0	7	0
FB-T4-15	0	4	0	0	0	1	0	0	0	0	5	0
FB-T4-30	0	2	0	0	0	1	1	0	0	0	5	0
FB-T5-0	0	0	0	0	1	0	0	0	0	0	2	0
FB-T5-15	0	1	0	0	0	0	0	0	0	0	4	0
FB-T5-30	0	1	0	0	0	1	0	0	0	0	3	0
SD-T6-0	0	2	0	0	0	2	0	0	0	0	1	0
SD-T6-15	0	0	0	0	0	5	0	0	0	0	1	0
SD-T6-30	0	1	1	0	0	6	0	0	0	0	1	0
SD-T7-0	0	1	0	0	0	0	0	0	0	0	3	0
SD-T7-15	0	1	1	0	0	1	0	0	1	0	2	0
SD-T7-30	0	0	0	0	0	0	0	0	0	1	3	0
SD-T8-0	0	1	1	0	0	1	0	0	0	0	5	0
SD-T8-15	0	2	0	0	0	2	0	0	0	0	2	0
SD-T8-30	0	1	2	0	0	4	0	0	0	0	0	0
FR-T9-0	0	2	1	1	1	0	0	1	0	0	1	0
FR-T9-15	6	1	1	0	0	0	0	0	0	0	2	0
FR-T10-0	5	4	5	2	0	0	0	0	0	0	3	0
FR-T10-15	9	3	2	2	0	0	0	0	0	0	1	0
FR-T10-30	10	1	3	2	0	0	0	0	0	0	1	0

Samples	*Ctenocardia guppyi*	*Ctenoides scabra*	*Diodora minuta*	*Diplodonta nucleiformis*	*Divalinga quadrisulcata*	*Divaricella dentata*	*Dentimargo reductus*	*Ervilia concentrica*	*Ervilia nitens*	*Eulithidium thalassicola*	*Eulithidium affine*
GH-T1-0	1	0	0	0	0	0	0	1	0	4	0
GH-T1-15	3	0	0	0	0	0	1	0	0	8	0
GH-T1-30	0	0	0	0	0	3	0	0	0	6	0
GH-T2-0	1	0	0	0	0	0	1	0	0	0	0
GH-T2-15	0	0	0	0	0	0	0	1	0	9	0
GH-T2-30	0	0	0	0	0	0	1	0	0	8	0
GH-T3-0	1	0	0	1	1	0	0	0	0	7	0
GH-T3-15	2	0	0	0	0	0	0	1	0	8	0
GH-T3-30	2	0	0	0	3	0	1	0	0	6	0
FB-T4-0	4	0	0	0	0	0	0	1	0	0	1
FB-T4-15	3	0	0	0	0	0	0	2	0	0	0
FB-T4-30	2	0	0	0	0	0	0	0	0	0	0
FB-T5-0	4	2	0	0	0	0	0	3	0	0	3
FB-T5-15	4	0	0	1	1	0	0	5	2	0	0
FB-T5-30	4	0	0	0	0	0	0	5	1	0	0
SD-T6-0	1	0	0	0	0	0	2	1	0	0	3
SD-T6-15	6	0	0	0	0	0	0	1	0	0	1
SD-T6-30	3	0	0	0	0	0	0	1	0	0	0
SD-T7-0	3	0	0	0	0	0	2	0	0	0	5
SD-T7-15	4	0	0	0	0	0	1	0	0	0	1
SD-T7-30	2	0	0	0	0	0	2	0	0	0	4
SD-T8-0	1	0	2	0	0	1	2	0	0	0	3
SD-T8-15	4	0	0	0	0	0	1	0	0	0	3
SD-T8-30	3	0	0	0	1	0	0	1	0	0	0
FR-T9-0	3	0	0	0	0	0	0	0	0	5	0
FR-T9-15	0	0	1	0	0	0	0	4	0	12	0
FR-T10-0	1	0	0	0	0	0	0	1	0	2	0
FR-T10-15	0	0	0	0	0	0	0	2	0	6	0
FR-T10-30	0	0	0	0	0	0	0	4	0	5	0

Samples	*Eurytellina angulosa*	*Finella adamsi*	*Fugleria tenera*	*Gari circe*	*Gemma gemma*	*Glycymeris decussata*	*Gouldia cerina*	*Graptacme eborea*	*Haminoea succiena*	*Heliacus cylindricus*	*Hemimarginula dentigera*	*Iniforis gudeliae*
GH-T1-0	0	0	0	0	0	0	0	0	6	0	0	0
GH-T1-15	0	0	0	0	0	0	0	0	0	0	0	0
GH-T1-30	0	0	0	0	0	1	2	0	0	0	1	0
GH-T2-0	0	0	0	0	6	0	0	0	0	0	0	0
GH-T2-15	2	0	0	0	0	1	0	0	0	1	0	0
GH-T2-30	0	0	0	0	1	0	1	0	0	0	0	0
GH-T3-0	1	0	0	0	0	0	0	0	0	0	0	0
GH-T3-15	0	0	0	0	0	0	0	0	0	0	0	0
GH-T3-30	1	0	0	0	0	0	1	0	0	0	0	0
FB-T4-0	0	2	0	0	0	0	0	0	0	0	1	0
FB-T4-15	0	7	3	0	0	0	0	0	0	0	0	0
FB-T4-30	0	4	1	2	0	0	1	0	0	0	0	0
FB-T5-0	0	3	3	0	0	0	0	0	0	0	1	0
FB-T5-15	0	2	1	0	0	0	0	1	0	0	1	0
FB-T5-30	0	2	3	0	0	0	0	0	0	0	0	0
SD-T6-0	0	14	1	0	0	0	0	0	0	0	0	0
SD-T6-15	0	5	1	0	0	0	0	2	0	0	1	0
SD-T6-30	0	6	2	0	0	0	0	0	0	0	0	0
SD-T7-0	0	20	0	0	0	0	0	0	0	0	0	0
SD-T7-15	0	14	0	0	0	0	0	0	0	0	0	0
SD-T7-30	0	19	0	0	0	0	0	0	0	0	0	0
SD-T8-0	0	17	0	0	0	0	0	0	0	0	0	0
SD-T8-15	0	16	1	0	0	0	0	0	0	0	0	0
SD-T8-30	0	6	0	0	0	0	0	0	0	0	0	0
FR-T9-0	0	4	2	0	0	0	0	0	1	0	0	1
FR-T9-15	0	6	0	0	0	0	0	0	0	0	0	0
FR-T10-0	0	0	0	0	0	0	0	0	0	0	0	0
FR-T10-15	0	0	0	0	0	0	0	0	0	0	0	0
FR-T10-30	0	2	1	0	0	0	0	0	0	0	0	1

Sample	*Laciolina magna*	*Laevicardium serratum*	*Lindapecten exasperatus*	*Lottia albicosta*	*Lucina pensylvanica*	*Marevalvata tricarinata*	*Melanella eulimoides*	*Mitra barbadensis*	*Myrtea pristiphora*	*Nannodiella melanitica*
GH-T1-0	0	2	0	0	0	0	0	0	0	0
GH-T1-15	0	0	0	0	1	0	0	0	0	0
GH-T1-30	0	0	0	0	1	0	0	0	0	0
GH-T2-0	0	0	0	0	0	0	0	0	0	0
GH-T2-15	0	0	0	0	4	0	0	0	0	0
GH-T2-30	0	0	0	0	0	0	0	0	0	1
GH-T3-0	0	0	0	0	1	0	0	0	0	0
GH-T3-15	0	0	0	0	1	0	0	0	0	0
GH-T3-30	0	0	0	0	1	0	0	0	0	0
FB-T4-0	0	0	0	0	0	0	0	0	1	0
FB-T4-15	0	0	0	0	0	0	0	0	0	0
FB-T4-30	0	0	1	0	0	0	1	0	0	0
FB-T5-0	0	0	0	1	1	0	0	0	0	0
FB-T5-15	0	0	0	0	0	0	0	0	0	0
FB-T5-30	0	0	0	0	0	0	0	0	0	0
SD-T6-0	0	0	0	0	0	0	0	0	0	0
SD-T6-15	1	0	0	0	0	0	0	0	0	0
SD-T6-30	0	1	0	0	0	0	0	0	0	0
SD-T7-0	0	0	0	0	0	0	0	0	0	0
SD-T7-15	0	0	0	0	0	0	1	0	0	0
SD-T7-30	0	0	0	0	0	0	3	0	0	0
SD-T8-0	0	0	0	0	1	0	0	0	0	0
SD-T8-15	0	0	0	0	0	0	1	0	0	0
SD-T8-30	0	0	0	0	0	0	0	0	0	0
FR-T9-0	0	0	0	0	1	0	1	0	0	0
FR-T9-15	0	0	0	0	3	4	2	0	0	0
FR-T10-0	0	0	0	0	4	0	1	0	0	0
FR-T10-15	0	0	0	0	3	0	0	1	0	0
FR-T10-30	0	0	0	0	6	0	0	0	0	0

Sample	*Nassarius paucicostatus*	*Natica livida*	*Nucinella adamsii*	*Nuculana acuta*	*Oliva reticularis*	*Olivella exilis*	*Olivella nivea*	*Opalia pumilio*	*Parvilucina costata*	*Patelloida pustulata*	*Planktomya henseni*	*Polinices lacteus*
GH-T1-0	0	0	0	0	0	0	0	0	4	0	0	0
GH-T1-15	0	0	0	0	2	0	0	0	0	0	0	0
GH-T1-30	0	0	1	0	2	0	0	0	1	0	0	0
GH-T2-0	0	0	0	0	1	0	0	0	1	0	0	0
GH-T2-15	0	0	0	0	0	0	0	0	4	2	0	0
GH-T2-30	1	0	0	0	0	0	0	0	0	0	0	0
GH-T3-0	0	1	0	0	0	0	0	0	2	0	0	0
GH-T3-15	1	0	0	0	0	0	0	0	1	1	0	0
GH-T3-30	1	0	0	0	0	0	0	0	3	1	0	0
FB-T4-0	0	0	0	0	0	0	0	0	1	0	0	0
FB-T4-15	0	1	0	0	0	0	0	0	0	0	0	0
FB-T4-30	0	2	0	0	0	0	0	0	0	0	0	0
FB-T5-0	0	0	0	0	0	0	0	0	0	0	0	0
FB-T5-15	0	0	0	1	0	1	0	0	0	0	1	0
FB-T5-30	0	0	0	0	0	0	0	0	0	0	0	0
SD-T6-0	0	0	0	0	0	0	2	0	0	0	0	0
SD-T6-15	1	2	0	0	0	0	1	0	0	0	0	0
SD-T6-30	1	0	0	0	0	1	0	0	1	0	0	0
SD-T7-0	0	0	0	0	1	0	0	0	0	0	0	0
SD-T7-15	1	0	0	0	0	0	1	2	0	0	0	0
SD-T7-30	0	0	0	0	0	0	0	0	0	0	0	0
SD-T8-0	0	0	0	0	0	0	0	0	0	0	0	0
SD-T8-15	0	0	0	0	0	0	0	0	0	0	0	0
SD-T8-30	0	1	0	0	0	0	0	0	0	0	0	1
FR-T9-0	1	0	0	0	0	0	0	0	1	1	0	0
FR-T9-15	0	0	0	0	0	0	0	0	3	1	0	0
FR-T10-0	0	0	0	0	0	0	0	0	6	2	0	0
FR-T10-15	0	0	0	0	0	0	0	0	3	5	0	0
FR-T10-30	0	0	0	0	0	0	0	0	1	2	0	0

Sample	*Prunum* sp.	*Pseudostomatella erythrocoma*	*Psilaxis krebsi*	*Pryamidella dolabrata*	*Risomurex roseus*	*Rissoella* sp.	*Rissoina decussata*	*Rissoina krebsii*	*Scissula similis*	*Seila* sp.	*Semele bellastriata*	*Semele proficua*
GH-T1-0	1	0	1	0	0	0	5	0	0	0	0	0
GH-T1-15	0	0	0	0	0	0	0	0	0	0	0	0
GH-T1-30	1	0	1	0	0	0	0	0	0	0	0	0
GH-T2-0	0	0	0	0	0	0	0	4	1	0	0	0
GH-T2-15	0	0	0	0	0	0	0	0	1	0	0	0
GH-T2-30	0	0	0	0	0	0	0	1	0	0	0	0
GH-T3-0	0	0	0	0	0	0	0	0	1	0	1	0
GH-T3-15	0	0	0	0	0	0	0	0	1	0	0	0
GH-T3-30	0	0	0	0	0	0	0	0	3	0	0	0
FB-T4-0	0	0	0	0	0	0	0	1	9	0	0	1
FB-T4-15	0	2	0	0	0	0	0	0	1	0	0	1
FB-T4-30	0	1	0	0	0	0	0	1	2	0	0	0
FB-T5-0	0	0	0	0	0	1	0	0	0	1	0	0
FB-T5-15	0	0	0	0	0	0	0	4	1	0	0	0
FB-T5-30	0	2	0	0	0	0	0	5	1	0	0	0
SD-T6-0	0	0	0	0	1	1	0	0	2	0	0	0
SD-T6-15	0	0	0	0	0	0	0	0	5	0	0	0
SD-T6-30	0	0	0	0	0	0	0	0	1	0	0	0
SD-T7-0	0	0	0	0	0	0	0	0	2	0	0	0
SD-T7-15	0	0	0	0	0	0	0	0	1	0	0	0
SD-T7-30	0	0	0	0	0	0	0	0	0	0	0	0
SD-T8-0	0	0	0	0	0	0	0	0	0	0	0	0
SD-T8-15	0	0	0	0	0	0	0	0	2	0	0	0
SD-T8-30	0	0	0	0	0	0	0	0	7	0	0	0
FR-T9-0	0	1	0	0	0	0	1	0	1	0	0	0
FR-T9-15	0	0	0	0	0	0	0	0	0	0	0	0
FR-T10-0	0	0	0	0	0	0	1	0	0	1	0	0
FR-T10-15	0	0	0	0	0	0	0	0	0	0	0	0
FR-T10-30	0	0	0	1	0	0	0	0	0	0	0	0

Sample	Semelina nuculoides	Siphonaria alternata	Smaragdia viridis	Strigilla mirabilis	Tegula fasciata	Teinostoma cocolitoris	Tellina radiata	Timoclea pygmaea	Trabecula krumpermani	*Transennella conradina*	*Triphora abacoensis*
GH-T1-0	0	4	1	0	0	0	0	0	0	*6*	0
GH-T1-15	0	2	0	0	0	0	0	0	0	*4*	0
GH-T1-30	1	1	0	0	0	0	0	0	0	*6*	0
GH-T2-0	1	0	0	0	0	0	0	0	0	*9*	0
GH-T2-15	0	0	2	0	0	0	0	0	0	*1*	0
GH-T2-30	0	0	0	0	0	0	0	0	1	*4*	0
GH-T3-0	0	0	0	0	0	0	0	0	0	*7*	0
GH-T3-15	0	0	1	0	1	0	0	0	1	*8*	0
GH-T3-30	0	0	0	0	0	1	0	0	1	*2*	0
FB-T4-0	0	0	0	0	0	1	0	0	0	*16*	0
FB-T4-15	0	0	0	0	0	0	0	0	0	*12*	0
FB-T4-30	0	0	0	0	0	0	0	1	0	*19*	0
FB-T5-0	0	0	0	0	0	0	1	1	0	*16*	0
FB-T5-15	0	0	0	0	0	0	1	0	1	*13*	0
FB-T5-30	0	0	0	0	0	1	0	0	0	*11*	0
SD-T6-0	0	0	0	0	0	0	0	0	0	*7*	0
SD-T6-15	0	0	0	0	0	0	0	0	0	*9*	0
SD-T6-30	0	0	0	0	0	0	0	0	0	*17*	0
SD-T7-0	0	0	0	0	0	1	0	1	0	*6*	0
SD-T7-15	0	0	0	0	0	0	0	2	0	*9*	1
SD-T7-30	0	0	0	0	0	0	0	1	0	*8*	1
SD-T8-0	0	0	0	0	0	1	0	0	0	*10*	0
SD-T8-15	0	0	0	0	0	1	0	0	0	*6*	0
SD-T8-30	0	0	0	1	0	0	0	3	0	*9*	0
FR-T9-0	0	0	2	0	0	0	0	0	0	*2*	0
FR-T9-15	0	0	1	0	0	1	0	0	0	*2*	0
FR-T10-0	0	0	3	0	0	0	0	0	0	*1*	0
FR-T10-15	0	0	5	0	1	0	0	0	0	*2*	0
FR-T10-30	0	0	1	0	0	2	0	0	0	*2*	0

Sample	*Truncadaphne chrysoleuca*	*Truncatella caribaeensis*	*Tucetona pectinata*	*Turbo* sp.	*Turbonilla compsa*	*Turbonilla puncta*	*Turbonilla riisei*	*Turbonilla* sp.	*Varicorbula* sp.	*Vexillum exiguum*	*Zafrona idalina*	*Zebina browniana*
GH-T1-0	0	0	0	0	0	0	0	0	0	0	0	0
GH-T1-15	0	0	1	0	0	0	0	0	0	0	0	14
GH-T1-30	0	0	0	0	0	0	0	0	0	0	0	7
GH-T2-0	0	0	0	0	1	0	0	0	0	1	0	0
GH-T2-15	0	0	0	0	0	0	0	0	0	0	0	3
GH-T2-30	0	0	0	0	0	0	0	0	0	0	1	0
GH-T3-0	0	0	1	0	0	0	0	0	0	0	0	7
GH-T3-15	0	0	1	0	0	0	0	0	0	0	0	5
GH-T3-30	0	0	2	0	0	0	0	0	0	2	0	2
FB-T4-0	0	0	2	0	0	0	0	0	0	0	0	0
FB-T4-15	0	0	1	0	0	0	0	0	0	0	1	1
FB-T4-30	0	0	0	0	0	0	0	0	0	0	0	0
FB-T5-0	0	2	0	0	0	0	0	0	0	0	0	0
FB-T5-15	0	0	1	1	0	0	0	0	0	0	0	1
FB-T5-30	0	0	1	0	0	0	0	0	0	0	1	2
SD-T6-0	0	0	1	0	0	0	0	0	0	0	0	0
SD-T6-15	0	0	1	0	0	2	0	0	0	0	0	0
SD-T6-30	0	0	1	0	0	0	0	0	0	0	0	0
SD-T7-0	0	0	1	0	0	0	0	0	0	0	0	2
SD-T7-15	0	0	0	0	0	0	2	0	0	0	0	0
SD-T7-30	0	0	0	0	0	0	0	1	0	0	0	0
SD-T8-0	0	0	0	0	0	0	0	0	1	0	0	0
SD-T8-15	0	0	0	0	0	0	0	0	0	0	0	2
SD-T8-30	0	0	0	0	0	0	0	2	0	0	0	0
FR-T9-0	2	0	0	0	0	0	0	0	0	0	4	0
FR-T9-15	0	0	0	0	0	0	0	0	0	0	0	0
FR-T10-0	0	0	0	1	0	0	0	0	0	0	0	2
FR-T10-15	0	0	0	0	0	0	0	0	0	0	1	1
FR-T10-30	0	0	0	0	0	1	0	0	0	0	0	1

Part 2: R Code to Analyze Data and Produce Figures

```
install.packages('vegan')
library(vegan)

faunalData<-data[,40:148]
vegetationData<-data[, 21:37]

sed<-data[, 13:18]
colnames(sed)<-c("-2 to -1", "-1 to 0", "0 to 1", "1 to 2", "2 to 3",
"3 to 4")

#Mean phi of sediment
meanSed<-function(x){
  y<-decostand(x,"total")
  z<-c(-1.5, -0.5, 0.5, 1.5, 2.5, 3.5) #mean value of phi bins
  s<-rowSums(y*z) #calculates the first moment (mean) of grain sizes by
summing the products of the percent grain size weight by the phi bin
value.
  s<-as.matrix(s)
  s
}
phi<-meanSed(sed)
fines<-function(x){
y<-decostand(x,"total")
s<- y[ , 6] * 100
s<-as.data.frame(s)
rownames(s)<-row.names(sed)
s
}
percentFines<-fines(sed)


coarse<-function(x){
y<-decostand(x,"total")
s<- y[ , 1] * 100
s<-as.data.frame(s)
rownames(s)<-row.names(sed)
s
}

percentGravel<-coarse(sed)

sand<-function(x){
y<-decostand(x,"total")
z<- y[ , 2:5] * 100
s<- rowSums(z)
s<-as.data.frame(s)
rownames(s)<-row.names(sed)
s
}

percentSand<-sand(sed)
```

```
#Vegetation Exploration
cleanVegData<-vegetationData[c(1:10, 25, 26, 28), -5]
#removed all but one unvegetated sample and removed the halimeda column
of zeros.

#NMDS Ordination
vegProp<- decostand(cleanVegData, "total")
vegMax<- decostand(cleanVegData, "max")
vegDCA<- decorana(vegProp) #does not like since i have sites with a row
sum of zero

NMDSk1<-metaMDS(vegProp, distance="bray",k=1, trymax=20,
autotransform=FALSE)
NMDSk2<-metaMDS(vegProp, distance="bray",k=2, trymax=20,
autotransform=FALSE)
NMDSk3<-metaMDS(vegProp, distance="bray",k=3, trymax=20,
autotransform=FALSE)
NMDSk4<-metaMDS(vegProp, distance="bray",k=4, trymax=20,
autotransform=FALSE)

plot(NMDSk2, display= "sites", type= "t")

#NMDS without seagrass
algaData<- cleanVegData[1:12, 1:13]
#removed French Bay Sample FR-T10-15 as it had no alga, but tons of
seagrass

plot(metaMDS(algaData), display = "sites", type= "t")

algaProp<- decostand(algaData, "total")
algaMax<- decostand(algaProp, "max")

aNMDS1<-metaMDS(algaProp, distance= "bray", k= 1, trymax=20,
autotransform = FALSE )
aNMDS2<- metaMDS(algaProp, distance= "bray", k= 2, trymax=20,
autotransform = FALSE )
aNMDS3<- metaMDS(algaProp, distance= "bray", k= 3, trymax=20,
autotransform = FALSE )

plot(aNMDS2, display= "sites", type="t")

algaDist<- vegdist(algaProp, "bray", diag= TRUE)
algaClust<- agnes(algaDist, method= "ward")
plot(algaClust, which.plots = 2)

#all the alga sites still plot ontop of one another. May not be
terribly usefull.
#Environmental Data matrix
env<-data[,c(1, 3:7, 9:11)]
env<-merge(env, phi, by="row.names", sort=FALSE)
rownames(env)<-env$Row.names
env<-env[,-1]
colnames(env)<- c("Location", "Offshore Distance", "Depth",
"Temperature", "pH", "O2", "Seagrass Density", "Bioturbation",
"Energy", "Mean phi")
```

```
head(env)

env<-merge(env, percentFines, by="row.names", sort=FALSE)
rownames(env)<-env$Row.names
env<-env[,-1]
colnames(env)<- c("Location", "Offshore Distance", "Depth",
"Temperature", "pH", "O2", "Seagrass Density", "Bioturbation",
"Energy", "Mean phi", "Percent Fines")
head(env)

env<-merge(env, percentSand, by="row.names", sort=FALSE)
rownames(env)<-env$Row.names
env<-env[,-1]
colnames(env)<- c("Location", "Offshore Distance", "Depth",
"Temperature", "pH", "O2", "Seagrass Density", "Bioturbation",
"Energy", "Mean phi", "Percent Fines", "Percent Sand")
head(env)

env<-merge(env, percentGravel, by="row.names", sort=FALSE)
rownames(env)<-env$Row.names
env<-env[,-1]
colnames(env)<- c("Location", "Offshore Distance", "Depth",
"Temperature", "pH", "O2", "Seagrass Density", "Bioturbation",
"Energy", "Mean phi", "Percent Fines", "Percent Sand", "Percent
Gravel")
head(env)


#env correlations
attach(env)

#offshore distance
cor.test(`Offshore Distance`, Depth, use= "pairwise.complete.obs",
method="spearman")
#rho = 0.787, p= 4.135e-7
cor.test(`Offshore Distance`, Temperature, use=
"pairwise.complete.obs", method="spearman")
#rho= -0.119, p= 0.54
cor.test(`Offshore Distance`, pH, use= "pairwise.complete.obs",
method="spearman")
#rho= -0.210, p= 0.28
cor.test(`Offshore Distance`, O2, use= "pairwise.complete.obs",
method="spearman")
#rho= 0.043, p= 0.83
cor.test(`Offshore Distance`, `Seagrass Density`, use=
"pairwise.complete.obs", method="spearman")
#rho- -0.246, p= 0.22
cor.test(`Offshore Distance`, Bioturbation, use=
"pairwise.complete.obs", method="spearman")
#rho= 0.310, p= 0.10
cor.test(`Offshore Distance`, Energy, use= "pairwise.complete.obs",
method="spearman")
#rho= -0.063, p= 0.75
cor.test(`Offshore Distance`, `Mean phi`, use= "pairwise.complete.obs",
method="spearman")
```

```
#rho= 0.107, p= 0.58
cor.test(`Offshore Distance`, `Percent Fines`, use=
"pairwise.complete.obs", method="spearman")
#rho= -0.185, p= 0.34
cor.test(`Offshore Distance`, `Percent Sand`, use=
"pairwise.complete.obs", method="spearman")
#rho= -0.141, p= 0.46
cor.test(`Offshore Distance`, `Percent Gravel`, use=
"pairwise.complete.obs", method="spearman")
#rho= 0.329, p= 0.08

#Depth
cor.test(Depth, Temperature, use= "pairwise.complete.obs",
method="spearman")
#rho= -0.047, p= 0.81
cor.test(Depth, pH, use= "pairwise.complete.obs", method="spearman")
#rho= 0.072, p= 0.71
cor.test(Depth, O2, use= "pairwise.complete.obs", method="spearman")
#rho= -0.017, p= 0.93
cor.test(Depth, `Seagrass Density`, use= "pairwise.complete.obs",
method="spearman")
#rho= -0.45, p= 0.020
cor.test(Depth, Bioturbation, use= "pairwise.complete.obs",
method="spearman")
#rho= 0.40, p= 0.031
cor.test(Depth, Energy, use= "pairwise.complete.obs",
method="spearman")
#rho= -0.022, p= 0.91
cor.test(Depth, `Mean phi`, use= "pairwise.complete.obs",
method="spearman")
#rho= 0.007, p= 0.97
cor.test(Depth, `Percent Fines`, use= "pairwise.complete.obs",
method="spearman")
#rho= -0.44, p= 0.018
cor.test(Depth, `Percent Sand`, use= "pairwise.complete.obs",
method="spearman")
#rho=0.039, p= 0.84
cor.test(Depth, `Percent Gravel`, use= "pairwise.complete.obs",
method="spearman")
#rho= 0.26, p= 0.22

#Temperature
cor.test(Temperature, pH, use= "pairwise.complete.obs",
method="spearman")
#rho= 0.34, p= 0.07
cor.test(Temperature, O2, use= "pairwise.complete.obs",
method="spearman")
#rho= -0.080, p= 0.68
cor.test(Temperature, `Seagrass Density`, use= "pairwise.complete.obs",
method="spearman")
#rho= -0.044, p= 0.83
cor.test(Temperature, Bioturbation, use= "pairwise.complete.obs",
method="spearman")
#rho= 0.45, p= 0.015
```

```
cor.test(Temperature, Energy, use= "pairwise.complete.obs",
method="spearman")
#rho= 0.25, p= 0.19
cor.test(Temperature, `Mean phi`, use= "pairwise.complete.obs",
method="spearman")
#rho= -0.28, p= 0.15
cor.test(Temperature, `Percent Fines`, use= "pairwise.complete.obs",
method="spearman")
#rho= 0.12, p= 0.54
cor.test(Temperature, `Percent Sand`, use= "pairwise.complete.obs",
method="spearman")
#rho= -0.27, p= 0.16
cor.test(Temperature, `Percent Gravel`, use= "pairwise.complete.obs",
method="spearman")
#rho= 0.32, p= 0.09

#ph
cor.test(pH, O2, use= "pairwise.complete.obs", method="spearman")
#rho= 0.156, p= 0.42
cor.test(pH, `Seagrass Density`, use= "pairwise.complete.obs",
method="spearman")
#rho= -0.517, p= 0.0057
cor.test(pH, Bioturbation, use= "pairwise.complete.obs",
method="spearman")
#rho= -0.004, p= 0.98
cor.test(pH, Energy, use= "pairwise.complete.obs", method="spearman")
#rho= 0.196, p= 0.31
cor.test(pH, `Mean phi`, use= "pairwise.complete.obs",
method="spearman")
#rho= -0.219, p= 0.25
cor.test(pH, `Percent Fines`, use= "pairwise.complete.obs",
method="spearman")
#rho= -0.242, p= 0.21
cor.test(pH, `Percent Sand`, use= "pairwise.complete.obs",
method="spearman")
#rho= 0.111, p= 0.56
cor.test(pH, `Percent Gravel`, use= "pairwise.complete.obs",
method="spearman")
#rho= -0.053, p= 0.79

#Dissolved oxygen
cor.test(O2, `Seagrass Density`, use= "pairwise.complete.obs",
method="spearman")
#rho= -0.392, p= 0.043
cor.test(O2, Bioturbation, use= "pairwise.complete.obs",
method="spearman")
#rho= -0.190, p= 0.32
cor.test(O2, Energy, use= "pairwise.complete.obs", method="spearman")
#rho= 0.290, p= 0.13
cor.test(O2, `Mean phi`, use= "pairwise.complete.obs",
method="spearman")
#rho= -0.101, p= 0.60
cor.test(O2, `Percent Fines`, use= "pairwise.complete.obs",
method="spearman")
#rho= -0.072, p= 0.71
```

```
cor.test(O2, `Percent Sand`, use= "pairwise.complete.obs",
method="spearman")
#rho= -0.023, p= 0.91
cor.test(O2, `Percent Gravel`, use= "pairwise.complete.obs",
method="spearman")
#rho= 0.058, p= 0.76

#Seagrass Density
cor.test(`Seagrass Density`, Bioturbation,use= "pairwise.complete.obs",
method="spearman")
#rho= -0.248, p= 0.21
cor.test(`Seagrass Density`, Energy,use= "pairwise.complete.obs",
method="spearman")
#rho= 0.014, p= 0.95
cor.test(`Seagrass Density`, `Mean phi`,use= "pairwise.complete.obs",
method="spearman")
#rho= 0.046, p= 0.82
cor.test(`Seagrass Density`, `Percent Fines`, use=
"pairwise.complete.obs", method="spearman")
#rho= 0.813, p= 2.5 e-0.7
cor.test(`Seagrass Density`, `Percent Sand`, use=
"pairwise.complete.obs", method="spearman")
#rho= -0.491, p= 0.009
cor.test(`Seagrass Density`, `Percent Gravel`, use=
"pairwise.complete.obs", method="spearman")
#rho= 0.284, p= 0.15

#Bioturbation
cor.test(Bioturbation, Energy, use= "pairwise.complete.obs",
method="spearman")
#rho= -0.429, p= 0.020
cor.test(Bioturbation, `Mean phi`, use= "pairwise.complete.obs",
method="spearman")
#rho= 0.167, p= 0.39
cor.test(Bioturbation, `Percent Fines`, use= "pairwise.complete.obs",
method="spearman")
#rho= -0.362, p= 0.05
cor.test(Bioturbation, `Percent Sand`, use= "pairwise.complete.obs",
method="spearman")
#rho= 0.135, p= 0.49
cor.test(Bioturbation, `Percent Gravel`, use= "pairwise.complete.obs",
method="spearman")
#rho= 0.007, p= 0.97

#Wave energy
cor.test(Energy, `Mean phi`, use= "pairwise.complete.obs",
method="spearman")
#rho= 0.030, p= 0.88
cor.test(Energy, `Percent Fines`, use= "pairwise.complete.obs",
method="spearman")
#rho= 0.337, p= 0.07
cor.test(Energy, `Percent Sand`, use= "pairwise.complete.obs",
method="spearman")
#rho= -0.620, p= 0.0003
```

```
cor.test(Energy, `Percent Gravel`, use= "pairwise.complete.obs",
method="spearman")
#rho= -0.674, p= 6.012 e-05

#Grain sizes
cor.test(`Mean phi`, `Percent Fines`, use= "pairwise.complete.obs",
method="spearman")
#rho= 0.068, p= 0.73
cor.test(`Mean phi`, `Percent Sand`, use= "pairwise.complete.obs",
method="spearman")
#rho= -0.162, p= 0.40
cor.test(`Mean phi`, `Percent Gravel`, use= "pairwise.complete.obs",
method="spearman")
#rho= 0.159, p= 0.41

cor.test(`Percent Fines`, `Percent Sand`, use= "pairwise.complete.obs",
method="spearman")
#rho= -0.703, p= 3.4 e-05
cor.test(`Percent Fines`, `Percent Gravel`, use=
"pairwise.complete.obs", method="spearman")
#rho= 0.488, p= 0.007
cor.test(`Percent Sand`, `Percent Gravel`, use=
"pairwise.complete.obs", method="spearman")
#rho= -0.915, p= 3.0 e-07
detach(env)


#Data Transformations
propsamp<-decostand(faunalData,"total")
propsampmax<-decostand(propsamp,"max")

#Distances
Braypropsamp<-vegdist(propsamp,method="bray",diag=TRUE)
Braypropsampmax<-vegdist(propsampmax, method= "bray", diag=TRUE)

#Culled Faunal data to remove rare taxa
culledFaunalData<-faunalData[ ,
which(colSums(faunalData)/sum(faunalData) >0.01)] #removes taxa that
are less than 1% of aggregate count

#Culled Data Transformations
cpropsamp<-decostand(culledFaunalData,"total")
cpropsampmax<-decostand(cpropsamp,"max")

#Culled Distances
cBraypropsamp<-vegdist(cpropsamp,method="bray",diag=TRUE)
cBraypropsampmax<-vegdist(cpropsampmax, method= "bray", diag=TRUE)

#Culled Cluster Analysis
install.packages("sparcl")
library(sparcl)
install.packages("cluster")
library(cluster)

cCluster<-agnes(cBraypropsamp, method="ward")
```

```
dev.new()
par(las = 1, lwd= 2)
plot(cCluster,which.plots=2,cex=1,hang=-0.1, main= "", sub="")


cTaxaData <- t(culledFaunalData)
cTaxaStand <- decostand(cTaxaData, method = "total")
cTaxaStand<- decostand(cTaxaStand, method = "max")
cTaxaDist <- vegdist(cTaxaStand, "bray", diag = TRUE)
cTaxacluster<-agnes(cTaxaDist,method="ward")

dev.new()
plot(cTaxacluster,which.plots=2,cex=0.8,hang=-0.1)


#Culled pheatmap for two-way Clustering
library(vegan)
library(cluster)
install.packages('pheatmap')
library(pheatmap)
install.packages("colorRamps")
library(colorRamps)

myBreaks <- seq(0.01, max(cpropsamp), by = .01) # you can set your
breaks to any sequence you want, and they don't have to be the same
length.  You can do this manually too.

myBreaks <- c(0, 0.000001, myBreaks) # here we added a 0 to .000001 bin
to the heatmap, making this bin essentially 0.

myColors <- gray.colors(length(myBreaks) - 1, start= 0.9, end= 0.0) #
here grayscale function to create a vector of colors. 0 equals black
and 1 equals white.  It is important that this vector is one element
less than the myBreaks vector

myColors <- c("white", myColors) # now we can add "white" onto the
vector, this will be the first color bin, which we're going to set to
be (essentially) 0.

pheatmap(cpropsamp) # general function, with no custom colors. Note
that values of '0' get a color on the color bar. This makes it
difficult to distinguish a 0 from a non-zero, but small relative
abundance value

pheatmap(cpropsamp, color = myColors, breaks = myBreaks) # general
function using our breaks. This allows us to set the '0' cells to be
white

pheatmap(cpropsamp, color = myColors, breaks = myBreaks,
clustering_method = "ward") #here we use ward's method using the
argument clustering_method = "ward" and a bray-curstis distance by
specifying the Q and R mode distance matricies

pheatmap(cpropsamp, color = myColors, breaks = myBreaks,
clustering_method = "ward", clustering_distance_rows = cBraypropsamp,
```

```
clustering_distance_cols = cTaxaDist, border_color = NA) # here we fed
the function a distance matrix we wanted to use.  myDist and myTaxaDist
both are distance matricies that were made by vegdist (bray-curtis
distances).
pheatmap(cpropsamp, color = myColors, breaks = myBreaks,
clustering_method = "ward", clustering_distance_rows = cBraypropsamp,
clustering_distance_cols = cTaxaDist, border_color = NA, show_rownames
= FALSE, show_colnames = FALSE) #same as above line, but removes row
and colum names for clarity

#boxplot of seagrass density vs cluster group
env$Cluster<- c( "1B", "1B", "1B", "1B", "1A", "1B", "1B", "1B", "1B",
"2B", "2B", "2B", "2B", "2B", "2B", "2A", "2B", "2B", "2A", "2A", "2A",
"2A", "2A", "2B", "1B", "1A", "1A", "1A", "1A")
ordClust<- ordered(env$Cluster, levels = c( "2B", "2A", "1B", "1A"))
#organizes levels of the clusters in the env matrix when plotting box
plots to reflect visual distribution in two-way cluster

dev.new()
boxplot(env$'Seagrass Density'~ordClust, horizontal=TRUE, col=
"gray70", xlab= "Seagrass coefficient", ylab= "Cluster Group",
boxwex=0.5)


#seagrass coefficient metrics
SCsplit<-split(env$'Seagrass Density', env$Cluster)
range(SCsplit$'1A', na.rm=TRUE)
#3.23 to 8.19
median(SCsplit$'1A', na.rm=TRUE)
#5.36
range(SCsplit$'1B', na.rm=TRUE)
#0 to 8.67
median(SCsplit$'1B', na.rm=TRUE)
#4.72


#Canonical Correspondence Analysis
ccaSed<-cca(propsampmax~ env$'Offshore Distance' + env$Depth +
env$Temperature + env$pH + env$O2 + env$'Seagrass Density' +
env$Bioturbation + env$Energy + env$'Mean phi' + env$'Percent Fines' +
env$'Percent Sand' + env$'Percent Gravel', data= env, na.action=
na.omit)

ccaSed
#aliases (removes) % Gravel because it is collinear with %fines (-1)
and %sand (-1)

#Site Scores
ccaSed1<-scores(ccaSed, display="sites", choices=1)
ccaSed2<-scores(ccaSed, display="sites", choices=2)
ccaSed3<-scores(ccaSed, display="sites", choices=3)

siteScoresSed<-merge( ccaSed1, ccaSed2, by = "row.names", sort=FALSE)
rownames(siteScoresSed)<-siteScoresSed$Row.names
siteScoresSed<-siteScoresSed[,-1]
```

```
siteScoresSed<-merge( siteScoresSed, ccaSed3, by = "row.names",
sort=FALSE)
rownames(siteScoresSed)<-siteScoresSed$Row.names
siteScoresSed<-siteScoresSed[,-1]
write.csv(siteScoresSed, file = "Site Scores Sed CCA.csv")

#Species Scores
taxaCcaSed1<- scores(ccaSed, display="species", choices=1)
taxaCcaSed2<- scores(ccaSed, display="species", choices=2)
taxaCcaSed3<- scores(ccaSed, display="species", choices=3)

taxaScoresSed<- merge(taxaCcaSed1, taxaCcaSed2, by = "row.names",
sort=FALSE)
rownames(taxaScoresSed)<- taxaScoresSed$Row.names
taxaScoresSed<- taxaScoresSed[, -1]
taxaScoresSed<- merge(taxaScoresSed, taxaCcaSed3, by = "row.names",
sort=FALSE)
rownames(taxaScoresSed)<- taxaScoresSed$Row.names
taxaScoresSed<- taxaScoresSed[, -1]

write.csv(taxaScoresSed, file= "Taxa Scores Sed CCA.csv")

#Biplot Scores
bpCcaSed1<-scores(ccaSed, display="bp", choices=1)
bpCcaSed2<-scores(ccaSed, display="bp", choices=2)
bpCcaSed3<-scores(ccaSed, display="bp", choices=3)

bpScoresSed<- merge(bpCcaSed1, bpCcaSed2, by = "row.names", sort=FALSE)
rownames(bpScoresSed)<- bpScoresSed$Row.names
bpScoresSed<- bpScoresSed[, -1]
bpScoresSed<- merge(bpScoresSed, bpCcaSed3, by = "row.names",
sort=FALSE)
rownames(bpScoresSed)<- bpScoresSed$Row.names
bpScoresSed<- bpScoresSed[, -1]
write.csv(bpScoresSed, file= "Env Biplot Scores Sed CCA.csv")
#CCA of samples
dev.new()
plot(ccaSed, choices= c(1,2), display=c("sites","bp"), type="n",
xlim=c(-4,4), ylim= c(-4,4))
points(ccaSed1[data$Substrate=="V"], ccaSed2[data$Substrate=="V"],
pch=22, col="black", bg="grey70", cex=1.7)
points(ccaSed1[data$Substrate=="SO"], ccaSed2[data$Substrate=="SO"],
pch=24, col="black", bg="grey70", cex=1.7)
points(ccaSed1[data$Substrate=="SR"], ccaSed2[data$Substrate=="SR"],
pch=21, col="black", bg="grey70",cex=1.7)
par(lwd= 1)#makes the line width of vectors bigger
text(ccaSed, display = "bp", col="black", cex=1) #adds biplot vectors
and letters. Use to change color or size
legend("topleft",
       cex=1,
       c("Vegetated","Open Sand","Reef Sand"),
       pch=c(22, 24, 21),
       col="black",
       pt.bg="grey70",
       bty="n")
```

```
dev.new()
plot(ccaSed, choices= c(2,3), display=c("sites","bp"), type="n",
xlim=c(-4,4), ylim= c(-4,4))
points(ccaSed2[data$Substrate=="V"], ccaSed3[data$Substrate=="V"],
pch=22, col="black", bg="grey70", cex=1.7)
points(ccaSed2[data$Substrate=="SO"], ccaSed3[data$Substrate=="SO"],
pch=24, col="black", bg="grey70", cex=1.7)
points(ccaSed2[data$Substrate=="SR"], ccaSed3[data$Substrate=="SR"],
pch=21, col="black", bg="grey70",cex=1.7)
par(lwd= 1)#makes the line width of vectors bigger
text(ccaSed, display = "bp", choices= c(2,3), col="black", cex=1) #adds
biplot vectors and letters. Use to change color or size
legend("topleft",
       cex=1,
       c("Vegetated","Open Sand","Reef Sand"),
       pch=c(22, 24, 21),
       col="black",
       pt.bg="grey70",
       bty="n")

#CCA of Taxa
#cleaned up Taxa plots to plot most abundant things
maxAbund<-apply(propsamp, 2, FUN= max) #grabs the maximum propsamp
values for each taxa (2=column)
maxAbund<-as.data.frame(maxAbund) #converts maxAbund from "numeric" to
"data frame"

#Plot only taxa names to match Culled Cluster and rescale the figure
culledFaunalData
taxNames<-colnames(culledFaunalData) #creates a list of taxa names from
the 1% culled data

taxaScoresSed<- taxaScoresSed[taxNames, ] #reduces the Taxa scores
matrix to the those whose row names match the list of taxa from the 1%
culled data

dev.new()
plot(ccaSed, choices= c(1,2), display=c("species","bp"), type="n",
xlim=c(-2,2), ylim= c(-2,2))
text(taxaScoresSed$CCA1, taxaScoresSed$CCA2, labels= taxNames
,col="gray60", cex=0.75) #will only plot
text(ccaSed, display = "bp", col="black", cex=1) #adds biplot vectors
and letters. Use to change color or size


dev.new()
plot(ccaSed, choices= c(2,3), display=c("species","bp"), type="n",
xlim=c(-2,2), ylim= c(-2,2))
text(taxaScoresSed$CCA2, taxaScoresSed$CCA3, labels= taxNames
,col="gray60", cex=0.75) #will only plot
text(ccaSed, display = "bp", choices= c(2,3), col="black", cex=1) #adds
biplot vectors and letters. Use to change color or size
```

Part 3: Supplementary Table 3.1

Taxon scores for CCA Axes 1 through 3.

Taxon name	CCA1	CCA2	CCA3
Acteocina lepta	-0.082	-0.293	0.762
Acteocina sp. B. (Redfern 2013)	0.225	-0.112	0.352
Angulus merus	1.019	-0.358	-0.482
Angulus sybariticus	0.091	0.453	-0.305
Anodontia alba	0.034	0.699	-0.707
Antalis antillarum	-0.837	0.838	-0.296
Antalis cerata	-0.974	1.357	-0.454
Arene venustula	-1.484	-0.426	1.875
Astralium phoebium	-0.676	2.273	-0.561
Atys sharpi	-0.146	-0.200	0.128
Barbatia cancellaria	-1.452	-2.308	-0.810
Berthella stellata	-1.484	-0.426	1.875
Brachidontes exustus	-0.910	0.069	1.959
Bulla occidentalis	0.139	-0.323	-0.197
Calliostoma javanicum	1.177	-0.434	-0.454
Calliostoma pulchrum	1.132	-0.324	-1.418
Callucina keenae	-1.438	-1.656	-1.011
Cerithium atratum	-1.153	-0.895	-0.164
Cerithium eburneum	-0.048	-0.233	0.089
Cerithium litteratum	-0.576	-0.372	0.031
Cerithium sp.	-1.443	-1.882	-0.941
Chama florida	-0.346	-1.021	-0.646
Chione elevata	-0.074	0.354	-0.010
Cochliolepis parasitica	1.177	-0.434	-0.454
Columbella mercatoria	-1.452	-2.308	-0.810
Conus flavescens	-0.031	1.211	0.363
Conus patae	0.301	-0.052	0.799
Crenella divaricata	0.075	0.078	0.455
Ctena orbiculata	-1.493	1.791	-1.401
Ctenocardia guppyi	0.478	0.047	-0.058
Ctenoides scabra	0.784	0.293	-0.479
Dentimargo reductus	0.295	0.228	0.727
Diodora minuta	0.208	-1.141	0.592
Diplodonta nucleiformis	0.584	0.103	-0.182
Divalinga quadrisulcata	-0.180	0.079	0.179
Divaricella dentata	-0.962	1.182	-0.790
Ervilia concentrica	0.448	-0.390	-0.483
Ervilia nitens	1.369	-0.034	-0.659

Eulithidium affine	0.682	0.104	0.425
Eulithidium thalassicola	-0.872	-0.182	-0.092
Eurytellina angulosa	-1.087	-0.162	1.130
Finella adamsi	0.589	-0.148	0.353
Fugleria tenera	0.696	-0.330	-0.506
Gari circe	1.177	-0.434	-0.454
Gemma gemma	-0.407	0.415	2.617
Glycymeris decussata	-1.489	0.705	0.204
Gouldia cerina	-0.706	0.711	-0.537
Graptacme eborea	0.805	0.155	-0.043
Haminoea succiena	-1.290	1.021	-0.681
Heliacus cylindricus	-1.484	-0.426	1.875
Hemimarginula dentigera	0.399	0.525	-0.561
Iniforis gudeliae	-1.452	-2.308	-0.810
Laciolina magna	0.470	0.175	0.069
Laevicardium serratum	-0.611	1.137	-0.415
Lindapecten exasperatus	1.177	-0.434	-0.454
Lottia albicosta	0.784	0.293	-0.479
Lucina pensylvanica	-0.865	-0.647	0.113
Marevalvata tricarinata	-0.740	-2.098	-0.447
Melanella eulimoides	0.064	-0.682	0.281
Mitra barbadensis	-1.438	-1.656	-1.011
Myrtea pristiphora	0.833	0.199	-0.708
Nannodiella melanitica	-0.729	0.148	-0.001
Nassarius paucicostatus	-0.136	-0.276	0.247
Natica livida	0.603	-0.142	-0.264
Nucinella adamsi	-1.493	1.791	-1.401
Nuculana acuta	1.490	0.114	-0.272
Oliva reticularis	-0.708	1.538	-0.054
Olivella exilis	1.103	0.165	-0.094
Olivella nivea	0.865	0.021	0.368
Opalia pumilio	0.628	0.128	1.305
Parvilucina costata	-0.904	-0.233	0.123
Patelloida pustulata	-1.174	-1.267	-0.125
Planktomya henseni	1.490	0.114	-0.272
Polinices lacteus	0.262	-0.211	-0.514
Prunum sp.	-1.379	1.690	-1.034
Pseudostomatella erythrocoma	0.658	-0.694	-0.849
Psilaxis krebsi	-1.379	1.690	-1.034
Risomurex roseus	1.185	-0.112	-0.0515
Rissoella sp.	0.982	0.093	-0.217
Rissoina decussata	-1.294	0.927	-0.685
Rissoina krebsii	0.702	0.039	0.200

Scissula similis	0.446	-0.040	-0.075
Semele bellastriata	-0.395	0.092	-0.084
Semele proficua	0.928	-0.085	-0.1593
Semelina nuculoides	-0.926	1.135	0.833
Siphonaria alternata	-1.129	1.812	-0.739
Smaragdia viridis	-1.225	-1.220	-0.291
Strigilla mirabilis	0.262	-0.211	-0.514
Tegula fasciata	-0.525	-1.025	-0.241
Teinostoma cocolitoris	0.387	-0.344	-0.019
Tellina radiata	1.133	0.205	-0.377
Timocle pygmaea	0.523	0.043	0.192
Trabecula krumpermani	0.052	0.008	0.214
Transennella conradina	0.479	0.067	-0.015
Triphora abacoensis	0.430	0.215	1.195
Truncadaphne chrysoleuca	-1.452	-2.308	-0.810
Truncatella caribaeensis	0.784	0.293	-0.479
Tucetona pectinata	0.429	0.219	-0.124
Turbo sp.	1.490	0.114	-0.272
Turbonilla compsa	-0.346	0.465	3.114
Turbonilla puncta	0.470	0.175	0.069
Turbonilla riisei	0.628	0.128	1.305
Turbonilla sp.	0.252	-0.043	0.012
Varicorbula sp.	0.662	-0.681	1.092
Vexillum exiguum	-0.703	0.280	1.595
Zafrona idalina	-0.736	-1.411	-0.756
Zebina browniana	-0.444	0.882	-0.268

APPENDIX C

LOCALITY COORDINATES, POINT COUNT DATA, FAUNAL DATA, R CODE AND MONOGRAPH OF SPECIES FOR CHAPTER 4

Part 1: Locality Coordinates

Locality	Latitude	Longitude
Crystal Lake	46.818°N	109.498°W
Gibson Reservoir	47.600°N	112.780°W
Milligan Canyon	45.878°N	111.681°W
Sappington Canyon	45.778°N	111.746°W

Part 2: Point Count Data of Thin Sections

Point-count data matrix records the sample percentage of each petrographic component out of 300 constituents per count.

Sample	Brachiopod indeterminate	Ribbed brachiopod	Smooth brachiopod	crinoid	bivalve	gastropod	cephalopod	trilobite	Fenestrate bryozoan	Trepostome bryozoan	Solitary coral
CLR_19_01	0	6.6	4	56.5	0	0	0	0	3.7	0	0
CLR_19_02	6.7	6.3	7.3	34.7	0.7	0	0	0	0.7	0	0
CLR_19_03	0	0.3	3.7	85	0	0	0	0	1.3	0	1.3
CLR_19_04	0	0.3	6	57.3	0	0	0	0	1.7	0	0
CLR_19_05	0	4.3	2	89	0	0	0	0	0	0	0
CLR_19_06	0	9.7	3.7	76.3	0	0	0	0	0	0	0
CLR_19_07	0	16.3	0	41.3	0	0	0	0	0	0	0
CLR_19_08	0	7.3	3.7	48.7	0	0	0	0	0	0	0
CLR_19_09	0	4.3	0.3	62	0	0	0	0	0.3	0	8.7
CLR_19_10	0	0.7	0	30	0	0	0	0	0	0	0
CLR_19_11	0	11.3	0	28	0	0	0	0	0	0	0
GR_19_01	0	3	3.3	58.3	0	0	0	0	6.3	0	0
GR_19_02	0	0	4	74.3	0	0	0	0	0	0	0
GR_19_03	1.7	1.7	0.7	41.3	0	0	0	0	0	0	0
GR_19_04	0	0	0	47.7	0	0	0	0	0	0	0
GR_19_05	0	0	0	100	0	0	0	0	0	0	0
GR_19_06	0	0	4.3	44.7	0	0	0	0	0	0	0
GR_19_07	1	2.7	1.3	43.3	0	0	0	0	0	0	0
GR_19_08	1	0	0	2	0	0	0	0	0	0	0
GR_19_09	0.3	1.7	1.7	58.3	0	0	0	0	0.3	0	0
GR_19_10	0.3	6.7	4.3	76.7	0	0	0	0	0	0	0.7
GR_19_11	0	0	0.3	99.7	0	0	0	0	0	0	0
GR_19_12	1	1.3	0	31.7	0	0	0	0	0	0	0
GR_19_13	0.3	0	0	82.3	0	0	0	0	0	0	0
GR_19_14	0	1.3	3.3	91	0	0	0	0	0	0	0
GR_19_15	0	0.3	1.3	97.3	0	0	0	0	0	0	0
GR_19_16	1.7	2.7	1.7	72.7	0	0	0	0	0	0	0
GR_19_17	0	0.3	0.3	97.7	0	0	0	0	0	0	0
GR_19_18	0	0	0.7	99.3	0	0	0	0	0	0	0
GR_19_19	0	3.7	0.3	96	0	0	0	0	0	0	0
GR_19_20	0.7	3	2	94.3	0	0	0	0	0	0	0
GR_19_21	0	0	2.7	63.7	0	0	0	0	0	0	0.3
GR_19_22	0	0.7	0.7	67	0	0	0	0	0	0	0
GR_19_23	0	3.3	0.3	37	0	0	0	0	0	0	0
GR_19_24	0	4.3	8	61	0	0	0	0	0	0	1
MGC_18_01	1.7	0	0	68.3	0	0	0	0	0	0	0

Sample	Brachiopod indeterminate	Ribbed brachiopod	Smooth brachiopod	crinoid	bivalve	gastropod	cephalopod	trilobite	Fenestrate bryozoan	Trepostome bryozoan	Solitary coral
MGC_18_02	0.3	0	0	45	0	0	0	0	0	2.3	0
MGC_18_03	3.7	0	0	19	0	0	0	0	0	0.7	0
MGC_18_04	1.3	0	0	29	0	0	0	0	0	0.3	0
MGC_18_05	4	0	0	61.3	0	0	0	0	0	1.3	0.7
MGC_18_06	1.3	0	0	34.1	0	0	0	0	0	0	0
MGC_18_07	2.7	0	0	36.3	0	0	0	0	0	0	0
MGC_18_08	1.7	0	0	91.3	0	0	0	0	0	0	0
MGC_18_09	4.3	0	0	75	0.7	0	0	0	0	0	0
MGC_18_10	11.3	0	0	55	0	0	0	0	0	0	0
MGC_18_11	0.7	5.3	0	48.7	0	0	0	0	0	0	0
MGC_18_12	0	0.3	0	49.7	0	0	0	0	0	0	0
MGC_18_13	0.3	1	0	74.7	0	0	0	0	0	0.3	0
SPC_18_01	3	0.3	0.3	81.7	0	0	0	0	0	0	0
SPC_18_02	0.7	1.7	4.7	65.7	0	0	0	0	0	0	0
SPC_18_03	1	4.3	0.3	34	0	0	0	0.7	0	0	0
SPC_18_04	2	0	0	59	0	0	0	0	0	0	0
SPC_18_05	0.3	1.7	3.3	22.7	0	0	0	0	0	0	0
SPC_18_06	0	0	5	36	0	0	0	0	0	0.7	4
SPC_18_07	0	1.3	4	18	0	0	0	0	2.7	2.3	0.7
SPC_18_08	0.7	1.3	4	34	0	0	0	0.3	0	0	0
SPC_18_09	0	0	1.3	83.3	0	0	0	0	0	0	0
SPC_18_10	7.3	1.7	2.3	69.3	0	0	0	0	0	0.7	0
SPC_18_11	4.3	2.7	3.3	54	0	0	0	0	0	0.3	2
SPC_18_12	0	0	3.3	15	0	0	0	0	0	0	0
SPC_18_13	0.3	0	1.3	4.7	0	0	0	0	0	0	0
SPC_18_14	1.7	0.3	0.3	63	0	0	0	0	0	0	0
SPC_18_15	4	0	0	75	0	0	0	0	0	0	0
SPC_18_16	1	2	1.7	87.3	0	0	0	0	0	0	0
SPC_18_17	0	0	2	50	0	0	0	0	0	0	0
SPC_18_18	0.7	2	0.7	16.3	0	0	0	0	0	0	0
SPC_18_19	1	0.3	0	26.7	0	0	0	0	0	0	0
SPC_18_20	3.3	0.3	0	77.7	0	0	0	0	0	0	0
SPC_18_21	2	0	1	16.6	0	0	0	0	0	0	0
SPC_18_22	0	2.3	2	83	0	0	0	0	0	0	0
SPC_18_23	0	1.7	2.7	30	0	0	0	0	0	0	0
SPC_18_24	0	0	2.3	20.6	0	0	0	0	0	0	0

Sample	Brachiopod indeterminate	Ribbed brachiopod	Smooth brachiopod	crinoid	bivalve	gastropod	cephalopod	trilobite	Fenestrate bryozoan	Trepostome bryozoan	Solitary coral
SPC_18_25	0.3	2.3	10	65.3	0	0	0	0	0	0	0
SPC_18_26	2.7	0.3	3.3	76.3	0	0	0	0	0	0	0
SPC_18_27	0	10.3	15.3	23.3	0	0	0	0	0	0	0
SPC_18_28	1.3	3.3	4	29.3	0	0	0	0	0	0	0
SPC_18_29	0.3	0.3	0.7	22.3	0	0	0	0	0	0	0
SPC_18_30	0	1.3	0.3	77	0	0	0	0	0	0	1.7
SPC_18_31	0	0	0	37.7	0	0	0	0	0	0	11.7
SPC_18_32	0.7	0	1	22.7	0	0	0	0	0	0	0
SPC_18_33	0	3	0.7	25	0	0	0	0	0	0	16.3

Sample	Colonial coral	peloid	ooid	algae	micrite	dolomite	conodont	Pore space	unknown	spar	chert	glauconite
CLR_19_01	0	0	0	0	5.6	0	0	0	0	23.6	0	0
CLR_19_02	0	0	0	0	0	0	0	0	0	43	0.7	0
CLR_19_03	0	0	0	0	6.3	0	0	0	0	1	1	0
CLR_19_04	0	6.7	0	0	19.3	0	0	1.7	0	2.3	4.7	0
CLR_19_05	0	0	0	0	4.7	0	0	0	0	0	0	0
CLR_19_06	0	0.3	0	0	5.3	0	0	0	0	0.3	4.3	0
CLR_19_07	0	0	0	0	42	0	0	0	0	0	0.3	0
CLR_19_08	0	0	0	0	39	0	0	0	0	0.3	0.7	0
CLR_19_09	0	15.7	0	0	5.7	0	0	0	0	1	2	0
CLR_19_10	0	0	0	0	69	0	0	0.3	0	0	0	0
CLR_19_11	0	0	0	0	56.3	0	0	0	0	2	2.3	0
GR_19_01	0	0	0	0	27.7	0	0	0.7	0	0.7	0	0
GR_19_02	0	0	0	0	21.7	0	0	0	0	0	0	0
GR_19_03	0	0	0	0	51	0	0	1	0	1.3	1.3	0
GR_19_04	0	0	0	0	24.3	0	0	0	0	0.7	27.3	0
GR_19_05	0	0	0	0	0	0	0	0	0	0	0	0
GR_19_06	0	0	0	0	51	0	0	0	0	0	0	0
GR_19_07	0	0	0	0	45.3	0	0	0	0	0	6.3	0
GR_19_08	0	0	0	0	97	0	0	0	0	0	0	0
GR_19_09	0	0	0	0	37.3	0	0	0	0	0.3	0	0
GR_19_10	0	0.3	0	0	11	0	0	0	0	0	0	0
GR_19_11	0	0	0	0	0	0	0	0	0	0	0	0
GR_19_12	0	0	0	0	57.7	0	0	2.3	0	0	6	0
GR_19_13	0	0	0	0	17.3	0	0	0	0	0	0	0
GR_19_14	0	0	0	0	4.3	0	0	0	0	0	0	0
GR_19_15	0	0	0	0	1	0	0	0	0	0	0	0
GR_19_16	0	0	0	0	21.3	0	0	0	0	0	0	0
GR_19_17	0	0	0	0	1.7	0	0	0	0	0	0	0
GR_19_18	0	0	0	0	0	0	0	0	0	0	0	0
GR_19_19	0	0	0	0	0	0	0	0	0	0	0	0
GR_19_20	0	0	0	0	0	0	0	0	0	0	0	0
GR_19_21	0	0	0	0	33.3	0	0	0	0	0	0	0
GR_19_22	0	0	0	0	31.7	0	0	0	0	0	0	0
GR_19_23	0	0	0	0	59.3	0	0	0	0	0	0	0
GR_19_24	0	0	0	0	25	0	0	0	0	0	0.7	0
MGC_18_01	0	23.7	0	0	3.7	0	0	0	0	2.7	0	0

Sample	Colonial coral	peloid	ooid	algae	micrite	dolomite	conodont	Pore space	unknown	spar	chert	glauconite
MGC_18_02	0	1.3	2	0	34	0	0	0	0	15	0	0
MGC_18_03	0	31	0	0.3	5.3	0	0	0	0	39.3	0	0
MGC_18_04	2.7	4.7	6	0	51	0	0	0	0	4.3	0	0
MGC_18_05	0	1.7	1.3	1	13.7	0	0	0	0	15	0	0
MGC_18_06	0	32.4	0	0	21.1	0	0	0	0	11	0	0
MGC_18_07	0	45	0	0	4	0	0	0	0	12	0	0
MGC_18_08	0	0	0	0	0	0	0	0	0	7	0	0
MGC_18_09	0	4	0	0	13	0	0	0	0	3	0	0
MGC_18_10	0	4	1	0.7	20.7	0	0	0	0	7.3	0	0
MGC_18_11	0	11.3	0	1	29.7	0	0	0	0	3	0	0
MGC_18_12	0	4	0	0	43.3	0	0	0	0	2.7	0	0
MGC_18_13	0	4.3	2.7	0.3	10.7	0	0	0	0	5.7	0	0
SPC_18_01	0	0	0	0.7	5.3	0	0	0	0	3.3	5.3	0
SPC_18_02	0	16.3	0	0.7	4.7	0	0	0	0	2.3	3.3	0
SPC_18_03	0	46	0	0.3	6.7	0	0	2	0	2.7	2	0
SPC_18_04	0	26	0	0	4.7	0	0	0.3	0	4	3.3	0
SPC_18_05	0	47	0	0	23	0.3	0	0	0	1.3	0.3	0
SPC_18_06	0	4	0	0	49	0	0	0	0	0.7	0.7	0
SPC_18_07	0	3.3	0	0	66.3	0	0	0	0	1.3	0	0
SPC_18_08	0	0	0	0.7	54.7	0	0	1.3	0	1	1.7	0
SPC_18_09	0	1.7	0	0.3	11	0	0	2	0	0	0	0
SPC_18_10	0	5.7	0	0.7	8	0	0	0	0	2.3	0	0
SPC_18_11	0	0.3	0	0	28.7	0	0	1.7	0	2	0.7	0
SPC_18_12	0	63.3	0	0	17	0	0	0	0	1.3	0	0
SPC_18_13	0	30.7	0	0	62	0	0	0	0	1	0	0
SPC_18_14	0	34	0	0	0	0	0	0	0	0.3	0.3	0
SPC_18_15	0	0.7	0	0	3	0	0	9	0	0.3	0.3	0
SPC_18_16	0	3.3	0	0	4	0	0	0.3	0	0	0.3	0
SPC_18_17	0	1.3	0	0	41.7	0	0	0	0	4.7	0.3	0
SPC_18_18	0	0	0	0	80	0	0	0	0	0	0	0
SPC_18_19	0	68.7	0	0	0	0	0	0	0	3.3	0	0
SPC_18_20	0	0.3	0	0	6.3	0	0	12	0	0	0	0
SPC_18_21	0	78.1	0	0	0	0	0	0	0	2	0.3	0
SPC_18_22	0	0	0	0	5.7	0	0	3.3	0	3.7	0	0
SPC_18_23	0	38.7	0	0	25.7	0	0	0.3	0	0	0.3	0
SPC_18_24	0	58.5	0	0	2.3	2	0	0	0	4	10.3	0

Sample	Colonial coral	peloid	ooid	algae	micrite	dolomite	conodont	Pore space	unknown	spar	chert	glauconite
SPC_18_25	0	0	0	0	19.7	0	0	0	0	0	1.7	0
SPC_18_26	0	13.3	0	0	0.3	0	0	0	0	2.3	1.3	0
SPC_18_27	0.3	8.3	0	0	41.7	0	0	0	0	0.3	0	0
SPC_18_28	0	54	0	0	7.7	0	0	0	0	0.3	0	0
SPC_18_29	0	0	0	0	71.3	0.3	0	0	3.7	1	0	0
SPC_18_30	0	1.3	0	0	18.3	0	0	0	0	0	0	0
SPC_18_31	0	12	0	0	29.3	1	0	4.7	0	0	3.7	0
SPC_18_32	0.3	61	0	0	14.3	0	0	0	0	0	0	0
SPC_18_33	0.3	42.7	0	0	10.3	0	0	1.3	0	0.3	0	0

Part 3: Faunal Count Data

Data matrix for the lower Madison Group faunal assemblages. Matrix includes environmental variables and species abundances for each sample. This matrix does not include the point-count data (see Part 2).

Sample	Locality	Formation	Lithology	Northing	Easting	Elevation	Area cm2	Exposure	Meters in Section	Facies
CLR_19_01	Crystal Lake	Lodgepole	Skeletal grainstone	46.8182	-109.4981	1678	4800	Slab	1.7	FS
CLR_19_02	Crystal Lake	Lodgepole	Skeletal Packstone	46.8193	-109.4988	1691	—	Slab	21	DS
CLR_19_03	Crystal Lake	Lodgepole	Skeletal Packstone	46.8190	-109.5007	—	2691	Slab	21.5	DS
CLR_19_04	Crystal Lake	Lodgepole	Skeletal Grainstone	46.8200	-109.4989	—	—	Weather	31	FS
CLR_19_05	Crystal Lake	Lodgepole	Skeletal Packstone	46.8205	-109.4993	—	3040	Slab	38.6	DS
CLR_19_06	Crystal Lake	Lodgepole	Skeletal Packstone	46.8212	-109.4997	—	3225	slab	45	DS
CLR_19_07	Crystal Lake	Lodgepole	Skeletal Packstone	46.8220	-109.5003	—	720	float	56	DS
CLR_19_08	Crystal Lake	Lodgepole	Skeletal Packstone	46.8230	-109.5007	—	2135	float	64	DS
CLR_19_09	Crystal Lake	Lodgepole	Skeletal Packstone	46.8236	-109.5011	—	1976	float	72	DS
CLR_19_10	Crystal Lake	Lodgepole	Skeletal Packstone	46.8254	-109.5016	—	972	float	106	DS
CLR_19_11	Crystal Lake	Lodgepole	Skeletal Packstone	46.8278	-109.5024	—	2400	float	132	DS
GR_19_01	Gibson Reservoir	Allan Mt	Mudstone	47.6002	-112.7810	—	9844	Slab	50.7	FS
GR_19_02	Gibson Reservoir	Allan Mt	Skeletal Grainstone	47.6002	-112.7816	—	19780	Slab	82	FS
GR_19_03	Gibson Reservoir	Allan Mt	Skeletal Grainstone	47.6003	-112.7816	—	4200	Slab	87	FS
GR_19_04	Gibson Reservoir	Allan Mt	Skeletal Grainstone	47.6004	-112.7819	1444	3600	Slab	101	FS
GR_19_05	Gibson Reservoir	Allan Mt	Skeletal Grainstone	47.6005	-112.7822	—	1890	Slab	122	FS
GR_19_06	Gibson Reservoir	Allan Mt	Skeletal Grainstone	47.6007	-112.7826	1484	1650	Slab	144	FS
GR_19_07	Gibson Reservoir	Allan Mt	Skeletal Grainstone	47.6008	-112.7827	—	2900	Slab	148.5	FS
GR_19_08	Gibson Reservoir	Allan Mt	Mudstone	47.6008	-112.7833	1441	10800	Slab	189.5	FS
GR_19_09	Gibson Reservoir	Allan Mt	Skeletal Grainstone	47.6009	-112.7839	—	3700	Slab	220.4	FS
GR_19_10	Gibson Reservoir	Allan Mt	Skeletal Grainstone	47.6011	-112.7839	1456	13500	Slab	236.6	FS
GR_19_11	Gibson Reservoir	Allan Mt	Skeletal Grainstone	47.6011	-112.7840	1458	13500	Slab	230	FS
GR_19_12	Gibson Reservoir	Allan Mt	Skeletal Grainstone	47.6012	-112.7840	1453	12800	Slab	232	FS
GR_19_13	Gibson Reservoir	Allan Mt	Skeletal Grainstone	47.6012	-112.7841	1460	15810	Slab	233.5	FS
GR_19_14	Gibson Reservoir	Allan Mt	Skeletal Grainstone	47.6011	-112.7840	1457	14250	Slab	235	FS
GR_19_15	Gibson Reservoir	Allan Mt	Skeletal Grainstone	47.6012	-112.7841	1456	9900	Slab	236.5	FS
GR_19_16	Gibson Reservoir	Allan Mt	Skeletal Grainstone	47.6013	-112.7841	1451	4750	Slab	237	FS
GR_19_17	Gibson Reservoir	Allan Mt	Skeletal Grainstone	47.6013	-112.7842	1462	16800	Slab	241	FS
GR_19_18	Gibson Reservoir	Allan Mt	Skeletal Grainstone	47.6014	-112.7842	1454	39900	Slab	242	FS
GR_19_19	Gibson Reservoir	Allan Mt	Skeletal Grainstone	47.6016	-112.7844	—	13140	Slab	260	FS
GR_19_20	Gibson Reservoir	Allan Mt	Skeletal Grainstone	47.6016	-112.7846	1453	14355	Slab	264	FS
GR_19_21	Gibson Reservoir	Allan Mt	Mudstone	47.6019	-112.7850	1449	8064	Slab	283	FS
GR_19_22	Gibson Reservoir	Allan Mt	Mudstone	47.6019	-112.7849	1452	13200	Slab	284	FS
GR_19_23	Gibson Reservoir	Allan Mt	Mudstone	47.6019	-112.7850	—	7920	Slab	285	FS
GR_19_24	Gibson Reservoir	Allan Mt	Skeletal Grainstone	47.6019	-112.7851	1453	9900	Slab	290	FS
MGC_18_01	Milligan	Lodgepole	Skeletal Packstone	45.8790	-111.6807	—	14280	Slab	0.5	DS

Sample	Locality	Formation	Lithology	45.8791	-111.6809	Elevation	Area cm2	Exposure	Meters in Section	Facies
MGC_18_02	Milligan	Lodgepole	Skeletal Packstone	45.8790	-111.6807	—	1800	Slab	1	DS
MGC_18_03	Milligan	Lodgepole	Skeletal Packstone	45.8791	-111.6809	—	162550	Slab	2	DS
MGC_18_04	Milligan	Lodgepole	Skeletal Packstone	45.8791	-111.6807	—	—	Slab	2.5	DS
MGC_18_05	Milligan	Lodgepole	Skeletal Grainstone	45.8792	-111.6807	—	16272	Slab	4	FS
MGC_18_06	Milligan	Lodgepole	Skeletal Packstone	45.8791	-111.6814	—	7220	Slab	5	DS
MGC_18_07	Milligan	Lodgepole	Skeletal Packstone	45.8793	-111.6806	—	25500	Slab	11	DS
MGC_18_08	Milligan	Lodgepole	Skeletal Grainstone	45.8795	-111.6810	—	—	Weather	12	FS
MGC_18_09	Milligan	Lodgepole	Skeletal Grainstone	45.8793	-111.6814	—	3200	Slab	32	FS
MGC_18_10	Milligan	Lodgepole	Skeletal Packstone	45.8798	-111.6891	—	3419	Vertical	—	DS
MGC_18_11	Milligan	Lodgepole	Skeletal Grainstone	45.8796	-111.6820	—	6510	Vertical	51	FS
MGC_18_12	Milligan	Lodgepole	Oolitic grainstone	45.8798	-111.6820	—	11500	Vertical	52	OS
MGC_18_13	Milligan	Lodgepole	Oolitic grainstone	45.7794	-111.7481	—	21540	Slab	65	OS
SPC_18_01	Sappington	Lodgepole	Skeletal Grainstone	45.7794	-111.7479	1409	3900	Vertical	88	FS
SPC_18_02	Sappington	Lodgepole	Skeletal Packstone	45.7793	-111.7474	1414	8800	Slab	89	DS
SPC_18_03	Sappington	Lodgepole	Skeletal Packstone	45.7793	-111.7471	1419	8750	Slab	89	DS
SPC_18_04	Sappington	Lodgepole	Skeletal Packstone	45.7793	-111.7468	1422	6450	Vertical	89	DS
SPC_18_05	Sappington	Lodgepole	Skeletal Grainstone	45.7794	-111.7466	1414	4200	Vertical	85	FS
SPC_18_06	Sappington	Lodgepole	Skeletal Packstone	45.7794	-111.7465	1413	160	Slab	85	DS
SPC_18_07	Sappington	Lodgepole	Mudstone	45.7782	-111.7488	1418	57000	Vertical	87	FS
SPC_18_08	Sappington	Lodgepole	Skeletal Grainstone	45.7781	-111.7485	1395	1105	Vertical	6	FS
SPC_18_09	Sappington	Lodgepole	Skeletal Grainstone	45.7781	-111.7466	1396	3300	Slab	6	FS
SPC_18_10	Sappington	Lodgepole	Skeletal Packstone	45.7780	-111.7449	1412	3000	Vertical	5	DS
SPC_18_11	Sappington	Lodgepole	Skeletal Packstone	45.7789	-111.7449	1426	1050	Vertical	6	DS
SPC_18_12	Sappington	Lodgepole	Mudstone	45.7789	-111.7449	1450	1200	Slab	85.8	FS
SPC_18_13	Sappington	Lodgepole	Mudstone	45.7793	-111.7461	1450	2100	Vertical	86.3	FS
SPC_18_14	Sappington	Lodgepole	Skeletal Packstone	45.7793	-111.7461	1423	3200	Slab	88.5	DS
SPC_18_15	Sappington	Lodgepole	Skeletal Grainstone	45.7789	-111.7436	1423	2500	Slab	89	FS
SPC_18_16	Sappington	Lodgepole	Skeletal Packstone	45.7792	-111.7440	1469	1750	Vertical	88.5	DS
SPC_18_17	Sappington	Lodgepole	Skeletal Packstone	45.7796	-111.7464	1480	6500	Slab	111	DS
SPC_18_18	Sappington	Lodgepole	Skeletal Packstone	45.7796	-111.7459	1428	1950	Vertical	110	DS
SPC_18_19	Sappington	Lodgepole	Mudstone	45.7800	-111.7458	1433	780	Vertical	108	FS
SPC_18_20	Sappington	Lodgepole	Skeletal Grainstone	45.7799	-111.7454	1455	6600	Weather	145	FS
SPC_18_21	Sappington	Lodgepole	Skeletal Packstone	45.7800	-111.7452	1460	1920	Vertical	138	DS
SPC_18_22	Sappington	Lodgepole	Skeletal Grainstone	45.7800	-111.7454	1460	2250	Vertical	147	FS
SPC_18_23	Sappington	Lodgepole	Mudstone	45.7800	-111.7454	1464	26400	Vertical	150	FS
SPC_18_24	Sappington	Lodgepole	Mudstone	45.7801	-111.7459	1463	3240	Vertical	153	FS

Sample	Locality	Formation	Lithology	45.7795	-111.7429	Elevation	Area cm2	Exposure	Meters in Section	Facies
SPC_18_25	Sappington	Lodgepole	Skeletal Grainstone	45.7801	-111.7459	1456	1400	Vertical	152	FS
SPC_18_26	Sappington	Lodgepole	Mudstone	45.7800	-111.7446	1456	240	Slab	152.3	FS
SPC_18_27	Sappington	Lodgepole	Skeletal Grainstone	45.7798	-111.7442	1474	16000	Slab	155.5	FS
SPC_18_28	Sappington	Lodgepole	Skeletal Grainstone	45.7798	-111.7437	1489	2728	Weather	155	FS
SPC_18_29	Sappington	Lodgepole	Skeletal Grainstone	45.7804	-111.7456	1500	3000	Slab	172.5	FS
SPC_18_30	Sappington	Lodgepole	Skeletal Grainstone	45.7803	-111.7448	1505	1540	Vertical	146	FS
SPC_18_31	Sappington	Lodgepole	Mudstone	45.7804	-111.7450	1477	9300	Weather	186.5	FS
SPC_18_32	Sappington	Lodgepole	Skeletal Grainstone	Northing	Easting	1487	8000	Slab	186.2	FS
SPC_18_33	Sappington	Lodgepole	Skeletal Grainstone	46.8182	-109.4981	1485	18600	Slab	187.3	FS

Sample	Facies	Sequence	Bioturbation	Neutral	hue	value	chroma	*Amplexocarinia* sp.	*Amplexus* sp.	*Cyathaxonia arcuata*	*Homalophyllites* sp.
CLR_19_01	FS	LST	4	4.00	5Y	4	1	0	0	6	0
CLR_19_02	DS	LST	4	4.50	5Y	5	1	0	0	0	0
CLR_19_03	DS	LST	4	4.75	2.5YR	5	2	0	0	3	0
CLR_19_04	FS	LST	4	4.50	10R	5	1	0	0	0	0
CLR_19_05	DS	LST	4	4.25	10R	5	1	0	0	0	0
CLR_19_06	DS	TST	4	4.00	10YR	4	1	0	0	0	0
CLR_19_07	DS	TST	4	3.75	10YR	4	1	0	0	3	0
CLR_19_08	DS	TST	4	3.75	10YR	4	1	0	0	0	0
CLR_19_09	DS	TST	4	4.00	5Y	4	1	0	0	0	0
CLR_19_10	DS	HST	4	3.75	5Y	4	1	0	0	1	0
CLR_19_11	DS	HST	4	4.00	2.5Y	4	1	0	0	1	0
GR_19_01	FS	HST	5	4.50	5PB	5	1	0	0	4	1
GR_19_02	FS	HST	5	4.50	5Y	4	1	0	0	11	4
GR_19_03	FS	HST	5	4.25	5Y	4	1	1	0	23	2
GR_19_04	FS	HST	5	5.25	5Y	5	1	1	0	6	1
GR_19_05	FS	HST	5	5.25	10YR	6	1	5	0	3	0
GR_19_06	FS	HST	5	4.00	10YR	4	1	0	0	10	4
GR_19_07	FS	HST	5	4.50	10YR	5	1	0	0	11	0
GR_19_08	FS	HST	5	3.75	2.5Y	4	1	0	0	19	0
GR_19_09	FS	HST	5	4.50	2.5Y	5	1	0	0	10	1
GR_19_10	FS	HST	5	4.50	5Y	4	2	0	0	6	4
GR_19_11	FS	HST	5	4.50	10YR	5	1	0	0	11	1
GR_19_12	FS	HST	5	4.25	5Y	4	2	0	0	4	5
GR_19_13	FS	HST	5	4.00	5Y	4	1	0	0	6	1
GR_19_14	FS	HST	5	4.50	2.5Y	4	2	0	0	8	0
GR_19_15	FS	HST	5	4.75	10YR	4	1	0	0	5	0
GR_19_16	FS	HST	5	4.50	10YR	4	1	0	0	13	2
GR_19_17	FS	HST	5	4.50	5Y	4	1	0	0	8	0
GR_19_18	FS	HST	5	4.25	5Y	4	1	0	0	3	0
GR_19_19	FS	HST	5	5.00	5Y	5	1	0	0	0	0
GR_19_20	FS	HST	5	4.50	2.5Y	4	2	0	0	2	0
GR_19_21	FS	HST	5	4.50	2.5Y	4	2	0	0	3	1
GR_19_22	FS	HST	5	4.00	5Y	4	1	0	0	2	1
GR_19_23	FS	HST	5	4.75	10YR	4	1	0	0	11	0
GR_19_24	FS	HST	5	4.50	2.5Y	5	2	0	0	6	0
MGC_18_01	DS	TST	4	4.25	2.5YR	4	2	0	0	0	0

Sample	Facies	Sequence	Bioturbation	Neutral	hue	value	chroma	*Amplexocarinia* sp.	*Amplexus* sp.	*Cyathaxonia arcuata*	*Homalophyllites* sp.
MGC_18_02	DS	TST	4	4.00	10YR	4	1	0	1	4	0
MGC_18_03	DS	TST	4	4.50	5Y	5	1	0	0	6	1
MGC_18_04	DS	TST	4	4.50	5Y	4	1	0	0	10	1
MGC_18_05	FS	TST	4	8.25	5Y	8.5	1	2	0	9	0
MGC_18_06	DS	TST	4	4.25	5Y	4	1	2	0	14	0
MGC_18_07	DS	TST	4	4.50	5Y	4	1	0	0	3	0
MGC_18_08	FS	TST	4	5.50	5Y	6	1	0	2	5	0
MGC_18_09	FS	HST	4	5.75	2.5PB	6	2	0	0	7	1
MGC_18_10	DS	HST	4	4.50	5Y	5	1	0	0	7	0
MGC_18_11	FS	HST	3	5.50	5Y	5	1	0	0	5	8
MGC_18_12	OS	HST	3	6.25	5PB	8	1	0	0	4	8
MGC_18_13	OS	HST	4	6.25	5PB	7	1	0	1	4	3
SPC_18_01	FS	HST	3	3.75	5Y	4	1	0	0	10	6
SPC_18_02	DS	HST	3	4.00	5Y	5	1	1	0	14	1
SPC_18_03	DS	HST	3	3.25	10YR	4	1	1	0	6	4
SPC_18_04	DS	HST	3	4.75	5PB	5	1	1	0	4	2
SPC_18_05	FS	HST	3	5.00	5PB	6	1	0	0	6	1
SPC_18_06	DS	HST	3	4.75	5PB	5	1	0	0	0	0
SPC_18_07	FS	HST	3	3.50	5Y	3	1	0	0	0	1
SPC_18_08	FS	TST	3	4.00	10YR	4	1	0	0	5	0
SPC_18_09	FS	TST	3	4.00	5Y	4	1	0	1	4	0
SPC_18_10	DS	TST	3	4.75	5Y	5	1	2	0	13	2
SPC_18_11	DS	TST	3	3.75	5PB	4	1	1	0	5	2
SPC_18_12	FS	HST	3	3.25	5Y	3	1	0	0	3	1
SPC_18_13	FS	HST	3	3.25	5Y	3	1	2	0	3	1
SPC_18_14	DS	HST	3	5.00	5Y	5	1	0	0	6	0
SPC_18_15	FS	HST	3	3.75	5Y	3	1	0	0	9	0
SPC_18_16	DS	HST	3	4.50	5Y	5	1	0	0	7	1
SPC_18_17	DS	HST	2	3.75	5Y	4	1	0	0	0	0
SPC_18_18	DS	HST	2	3.50	5Y	4	1	1	0	2	0
SPC_18_19	FS	HST	2	3.75	5Y	2.5	1	1	0	2	0
SPC_18_20	FS	HST	3	5.75	5PB	8	1	2	1	0	2
SPC_18_21	DS	HST	3	3.75	5Y	4	1	1	0	1	0
SPC_18_22	FS	HST	3	5.00	5Y	6	1	0	0	3	3
SPC_18_23	FS	HST	3	3.50	5Y	3	2	1	0	8	7
SPC_18_24	FS	HST	4	3.25	5Y	4	1	0	0	1	0

Sample	Facies	Sequence	Bioturbation	Neutral	hue	value	chroma	*Amplexocarinia* sp.	*Amplexus* sp.	*Cyathaxonia arcuata*	*Homalophyllites* sp.
SPC_18_25	FS	HST	4	4.50	10YR	5	1	0	0	1	10
SPC_18_26	FS	HST	4	3.50	10YR	3	1	0	0	2	1
SPC_18_27	FS	HST	3	3.75	10YR	4	1	0	0	0	0
SPC_18_28	FS	HST	4	3.50	10YR	4	1	0	0	4	5
SPC_18_29	FS	HST	3	3.25	5Y	3	1	0	0	0	0
SPC_18_30	FS	HST	3	4.25	10YR	5	1	2	0	2	1
SPC_18_31	FS	HST	3	4.25	10YR	5	1	1	2	3	6
SPC_18_32	FS	HST	3	3.75	10YR	4	1	0	0	7	7
SPC_18_33	FS	HST	3	4.25	5Y	4	1	0	1	6	12

Sample	*Menophyllum* sp.	*Rotiphyllum* sp.	*Rylstonia* sp.	*Vesiculophyllum* sp.	*Zaphrentites* sp.	Rugose coral indeterminate	Colonial coral indeterminate	*Aulopora* sp.	*Cleistopora placenta*	*Syringopora aculeata*
CLR_19_01	0	0	0	0	3	0	0	0	0	0
CLR_19_02	0	0	0	0	2	0	0	0	0	0
CLR_19_03	0	0	0	0	0	0	0	0	1	0
CLR_19_04	0	0	0	0	1	0	0	0	0	0
CLR_19_05	0	0	0	0	1	0	0	0	0	0
CLR_19_06	0	0	0	0	0	0	0	0	0	0
CLR_19_07	0	0	0	0	0	0	0	0	0	0
CLR_19_08	0	0	0	0	0	0	0	0	0	0
CLR_19_09	0	0	0	0	0	0	0	0	0	0
CLR_19_10	0	0	0	0	0	0	0	0	0	0
CLR_19_11	0	0	0	0	1	0	0	0	0	0
GR_19_01	0	0	1	0	0	0	0	1	0	0
GR_19_02	0	1	3	1	0	0	0	0	0	0
GR_19_03	0	0	11	4	0	0	0	0	0	0
GR_19_04	1	0	7	6	0	0	0	0	0	2
GR_19_05	0	0	1	0	0	0	0	0	0	0
GR_19_06	0	0	40	1	0	0	0	0	0	0
GR_19_07	1	0	20	1	0	0	0	0	0	0
GR_19_08	0	0	1	5	0	0	0	0	0	0
GR_19_09	0	0	12	2	0	0	0	0	1	0
GR_19_10	1	0	4	2	0	0	0	0	0	3
GR_19_11	0	0	11	0	0	0	0	0	0	0
GR_19_12	0	0	10	5	0	0	0	0	0	0
GR_19_13	0	0	8	2	0	0	0	1	0	0
GR_19_14	0	0	7	4	0	0	0	0	0	0
GR_19_15	3	0	14	5	0	0	0	0	0	0
GR_19_16	1	0	18	2	0	0	0	0	0	0
GR_19_17	0	2	11	3	0	0	0	0	0	0
GR_19_18	0	0	13	0	0	0	0	0	0	0
GR_19_19	0	0	3	0	0	0	0	0	0	0
GR_19_20	0	0	2	0	0	0	0	0	0	0
GR_19_21	1	0	30	4	0	0	0	0	0	1
GR_19_22	16	0	52	0	0	0	0	0	0	0
GR_19_23	94	0	24	0	0	0	0	0	0	0
GR_19_24	44	0	27	2	0	0	0	0	0	0
MGC_18_01	0	0	0	0	0	0	0	0	0	0

Sample	*Menophyllum* sp.	*Rotiphyllum* sp.	*Rylstonia* sp.	*Vesiculophyllum* sp.	*Zaphrentites* sp.	Rugose coral indeterminate	Colonial coral indeterminate	*Aulopora* sp.	*Cleistopora placenta*	*Syringopora aculeata*
MGC_18_02	0	0	0	0	0	0	0	0	0	0
MGC_18_03	0	0	1	1	0	0	0	0	0	0
MGC_18_04	0	0	3	0	6	0	0	0	0	0
MGC_18_05	0	0	7	0	0	0	0	0	0	0
MGC_18_06	0	0	1	0	0	0	0	0	0	0
MGC_18_07	0	0	0	0	0	0	1	0	0	1
MGC_18_08	0	0	3	2	2	1	0	0	0	1
MGC_18_09	0	0	2	0	4	0	0	0	0	0
MGC_18_10	0	0	0	0	1	0	0	0	0	0
MGC_18_11	11	0	0	0	1	0	0	1	0	0
MGC_18_12	14	0	0	0	0	0	0	0	0	0
MGC_18_13	5	0	0	1	0	2	0	0	2	0
SPC_18_01	0	0	5	0	6	0	0	0	0	0
SPC_18_02	1	0	6	1	2	0	0	0	0	0
SPC_18_03	1	0	8	0	2	0	0	0	0	0
SPC_18_04	0	0	5	0	9	0	0	0	0	0
SPC_18_05	2	0	2	0	6	0	0	2	0	0
SPC_18_06	0	0	0	0	0	0	0	0	0	0
SPC_18_07	0	0	7	0	4	0	0	0	0	0
SPC_18_08	0	0	7	0	1	0	0	0	0	0
SPC_18_09	0	0	7	0	0	0	0	0	0	0
SPC_18_10	0	0	8	0	2	0	0	0	0	0
SPC_18_11	0	0	1	0	3	0	0	0	0	0
SPC_18_12	0	0	1	0	0	0	0	0	0	0
SPC_18_13	0	0	4	0	1	0	0	0	0	0
SPC_18_14	0	0	6	0	6	0	0	1	0	0
SPC_18_15	0	0	5	1	12	0	0	1	0	0
SPC_18_16	0	0	8	2	9	0	0	0	0	0
SPC_18_17	0	0	2	0	1	0	0	0	0	0
SPC_18_18	0	0	0	0	0	0	0	0	0	0
SPC_18_19	4	0	7	5	0	0	0	1	0	0
SPC_18_20	0	0	17	0	5	0	0	0	0	0
SPC_18_21	1	0	0	0	1	0	0	1	0	0
SPC_18_22	1	0	10	1	0	0	0	0	0	0
SPC_18_23	0	0	7	0	0	0	0	1	0	2
SPC_18_24	1	0	6	0	3	0	0	1	1	2

Sample	*Menophyllum* sp.	*Rotiphyllum* sp.	*Rylstonia* sp.	*Vesiculophyllum* sp.	*Zaphrentites* sp.	Rugose coral indeterminate	Colonial coral indeterminate	*Aulopora* sp.	*Cleistopora placenta*	*Syringopora aculeata*
SPC_18_25	4	0	2	4	0	0	0	0	0	1
SPC_18_26	0	2	0	2	1	0	0	0	0	1
SPC_18_27	0	0	4	0	1	0	0	0	0	0
SPC_18_28	0	0	7	0	1	0	0	0	0	1
SPC_18_29	0	0	1	1	3	0	0	1	2	0
SPC_18_30	4	3	5	2	5	0	0	0	0	0
SPC_18_31	2	0	3	2	13	0	0	0	0	0
SPC_18_32	1	0	3	0	4	0	0	0	0	0
SPC_18_33	0	0	7	0	4	0	0	1	1	0

Sample	Proetid trilobite	*Atrypa* sp.	*Axiodeaneia* sp.	*Camarotoechia* sp.	*Chonetes logani*	*Cleiothyridina mitensis*	*Composita humilis*	*Crania blari*	*Crurithyris parva*	*Cyrtina burlingtonensis*
CLR_19_01	0	0	0	1	0	0	2	0	0	0
CLR_19_02	0	0	0	0	0	0	0	0	0	0
CLR_19_03	0	0	0	0	0	0	2	0	0	0
CLR_19_04	0	0	0	2	0	0	0	0	0	0
CLR_19_05	2	0	0	0	0	0	1	0	0	0
CLR_19_06	0	0	0	0	0	0	1	0	0	0
CLR_19_07	0	0	0	0	0	0	0	0	0	0
CLR_19_08	0	0	0	8	0	0	0	0	0	0
CLR_19_09	0	0	0	5	0	0	0	0	0	0
CLR_19_10	0	0	0	0	0	0	3	0	0	0
CLR_19_11	0	0	0	0	0	0	0	1	0	0
GR_19_01	0	3	0	0	0	0	0	0	0	0
GR_19_02	0	1	0	0	0	0	0	0	0	0
GR_19_03	0	0	0	0	0	0	0	0	0	0
GR_19_04	0	0	0	0	0	0	0	0	0	0
GR_19_05	0	7	0	0	0	0	0	0	0	0
GR_19_06	0	1	0	0	0	0	0	0	0	0
GR_19_07	0	0	0	0	0	0	0	0	0	0
GR_19_08	0	0	0	0	0	0	0	0	0	0
GR_19_09	0	1	0	0	0	0	0	0	0	0
GR_19_10	0	2	0	0	0	0	0	0	0	0
GR_19_11	0	1	0	0	0	0	0	0	0	0
GR_19_12	0	1	0	1	3	0	0	0	0	0
GR_19_13	0	5	0	0	0	0	0	0	0	0
GR_19_14	0	4	0	0	0	0	0	0	0	0
GR_19_15	0	0	0	0	0	0	0	0	0	0
GR_19_16	0	1	0	0	0	0	0	0	0	0
GR_19_17	0	2	0	0	0	0	0	0	0	0
GR_19_18	0	5	0	0	0	0	0	0	0	0
GR_19_19	0	0	0	0	0	0	0	0	0	0
GR_19_20	0	15	0	0	0	0	0	0	0	0
GR_19_21	0	1	0	0	0	0	0	0	0	0
GR_19_22	0	1	0	0	0	0	0	0	0	0
GR_19_23	0	0	0	0	0	0	0	0	0	0
GR_19_24	0	0	0	0	0	0	0	0	0	0
MGC_18_01	0	0	0	0	0	0	1	0	0	0

Sample	Proetid trilobite	*Atrypa* sp.	*Axiodeaneia* sp.	*Camarotoechia* sp.	*Chonetes logani*	*Cleiothyridina mitensis*	*Composita humilis*	*Crania blari*	*Crurithyris parva*	*Cyrtina burlingtonensis*
MGC_18_02	1	0	0	0	0	2	1	0	0	0
MGC_18_03	0	0	0	0	0	0	0	0	0	0
MGC_18_04	0	1	0	0	0	0	0	0	0	0
MGC_18_05	0	0	0	0	0	0	1	0	0	0
MGC_18_06	0	1	0	2	0	0	0	0	0	0
MGC_18_07	0	0	0	0	1	0	1	0	0	0
MGC_18_08	0	0	0	0	0	0	0	0	0	0
MGC_18_09	0	2	0	1	3	0	2	0	0	0
MGC_18_10	0	0	0	0	0	0	2	0	0	0
MGC_18_11	0	0	0	0	0	0	0	0	0	0
MGC_18_12	0	0	0	0	0	0	1	0	0	0
MGC_18_13	0	0	0	0	0	0	0	0	0	0
SPC_18_01	0	0	0	0	0	0	0	0	0	1
SPC_18_02	0	0	0	0	0	0	0	0	0	0
SPC_18_03	0	0	0	0	0	0	1	0	0	0
SPC_18_04	0	1	0	0	0	0	0	0	0	0
SPC_18_05	0	0	0	0	0	0	0	0	0	0
SPC_18_06	0	0	0	1	3	0	0	0	1	0
SPC_18_07	0	0	0	0	0	0	0	0	0	0
SPC_18_08	0	0	0	0	0	0	2	0	1	0
SPC_18_09	0	0	0	0	0	1	1	0	0	2
SPC_18_10	0	0	0	0	0	0	0	0	0	0
SPC_18_11	0	1	0	1	0	0	18	0	0	0
SPC_18_12	1	0	0	0	1	0	0	0	0	0
SPC_18_13	0	0	0	0	1	0	0	0	0	0
SPC_18_14	0	0	0	0	0	0	0	0	0	0
SPC_18_15	0	0	0	0	0	0	0	0	0	0
SPC_18_16	0	1	0	0	0	0	0	0	0	0
SPC_18_17	0	0	0	2	0	0	4	1	0	0
SPC_18_18	1	0	0	1	1	0	1	0	1	0
SPC_18_19	0	0	0	0	0	0	1	0	0	0
SPC_18_20	0	0	0	0	0	0	0	0	0	0
SPC_18_21	0	0	1	1	0	2	0	0	0	0
SPC_18_22	0	0	0	0	0	0	0	0	0	0
SPC_18_23	0	0	0	0	0	0	0	0	0	0
SPC_18_24	0	0	0	0	1	0	0	0	0	0

Sample	Proetid trilobite	*Atrypa* sp.	*Axiodeaneia* sp.	*Camarotoechia* sp.	*Chonetes logani*	*Cleiothyridina mitensis*	*Composita humilis*	*Crania blari*	*Crurithyris parva*	*Cyrtina burlingtonensis*
SPC_18_25	0	0	0	0	0	0	0	0	0	0
SPC_18_26	0	0	0	0	1	0	0	0	0	0
SPC_18_27	0	1	0	0	0	0	0	0	0	0
SPC_18_28	0	0	0	0	0	0	0	0	0	0
SPC_18_29	0	0	0	0	0	0	0	0	0	0
SPC_18_30	0	0	0	0	0	0	0	0	0	0
SPC_18_31	0	0	0	0	0	0	0	0	0	0
SPC_18_32	0	0	0	0	0	0	0	0	0	0
SPC_18_33	0	0	0	0	0	0	1	0	0	0

Sample	*Dictyoclostus inflatus*	*Dictyoclostus gallatinensis*	*Dictyoclostus* sp.	*Dielasma utah?*	*Eumetria* sp.	*Hustedia texana*	*Leptaena* sp.	*Linoproductus* sp.	*Neospirifer* sp.	*Nucleospira obesa*
CLR_19_01	0	0	0	0	0	0	0	0	0	0
CLR_19_02	0	0	0	0	0	0	0	0	0	0
CLR_19_03	0	0	0	0	0	0	1	0	0	0
CLR_19_04	0	0	0	0	0	1	0	0	0	0
CLR_19_05	4	0	0	0	0	0	0	0	0	0
CLR_19_06	0	0	0	0	0	0	0	0	0	0
CLR_19_07	2	0	0	0	0	0	0	0	0	0
CLR_19_08	0	0	0	0	0	0	0	0	0	0
CLR_19_09	0	0	0	0	0	0	0	0	0	0
CLR_19_10	1	0	0	0	0	0	0	0	0	0
CLR_19_11	0	0	0	0	0	1	0	0	0	0
GR_19_01	0	0	0	0	1	0	1	0	0	1
GR_19_02	0	0	0	0	0	0	0	0	0	0
GR_19_03	0	0	0	0	0	0	0	0	0	0
GR_19_04	0	0	0	0	0	0	0	0	0	0
GR_19_05	0	0	0	0	0	0	0	0	0	0
GR_19_06	0	0	0	1	0	0	0	0	0	2
GR_19_07	0	0	0	0	0	0	0	0	0	1
GR_19_08	0	0	0	0	0	0	0	0	0	0
GR_19_09	0	0	0	0	0	0	0	0	0	0
GR_19_10	0	0	0	0	0	0	0	2	0	0
GR_19_11	0	0	0	0	0	0	0	0	0	0
GR_19_12	0	0	0	0	0	0	0	0	0	0
GR_19_13	0	0	0	0	0	0	0	0	0	0
GR_19_14	0	0	0	0	0	0	0	0	0	0
GR_19_15	0	0	0	0	0	0	0	0	0	0
GR_19_16	0	0	0	0	0	0	0	0	0	0
GR_19_17	0	0	0	1	0	0	0	0	0	0
GR_19_18	0	0	0	0	0	0	0	0	0	0
GR_19_19	0	0	0	0	0	0	0	0	0	22
GR_19_20	0	0	0	0	0	0	0	0	0	0
GR_19_21	0	0	0	0	0	0	0	0	0	0
GR_19_22	1	0	0	0	0	0	0	0	0	0
GR_19_23	0	0	0	0	0	0	0	0	0	0
GR_19_24	0	0	0	0	0	0	0	0	0	0
MGC_18_01	0	0	0	0	0	0	0	0	0	0

Sample	*Dictyoclostus inflatus*	*Dictyoclostus gallatinensis*	*Dictyoclostus* sp.	*Dielasma utah?*	*Eumetria* sp.	*Hustedia texana*	*Leptaena* sp.	*Linoproductus* sp.	*Neospirifer* sp.	*Nucleospira obesa*
MGC_18_02	0	0	1	0	0	0	0	0	0	0
MGC_18_03	0	0	0	0	0	0	0	0	0	1
MGC_18_04	0	0	0	0	0	0	0	0	0	0
MGC_18_05	0	0	0	0	0	1	0	0	0	0
MGC_18_06	0	0	0	0	0	0	0	0	1	0
MGC_18_07	0	0	0	0	0	0	0	2	0	0
MGC_18_08	0	0	0	0	0	0	0	0	0	0
MGC_18_09	0	0	0	0	0	0	0	0	0	0
MGC_18_10	0	0	0	0	0	0	0	0	0	0
MGC_18_11	0	0	0	0	0	0	0	0	0	0
MGC_18_12	0	0	0	0	0	0	0	0	0	0
MGC_18_13	0	0	0	0	0	0	0	0	0	1
SPC_18_01	0	0	0	0	0	0	0	0	0	0
SPC_18_02	0	0	0	0	0	0	0	0	0	0
SPC_18_03	0	0	0	0	0	0	0	0	1	0
SPC_18_04	0	0	0	0	0	0	0	0	0	0
SPC_18_05	0	0	1	0	0	0	0	0	1	0
SPC_18_06	0	0	0	0	0	0	0	0	0	0
SPC_18_07	0	0	0	0	0	0	0	0	0	0
SPC_18_08	0	0	0	1	1	0	1	0	0	0
SPC_18_09	0	0	2	0	0	0	0	0	1	0
SPC_18_10	0	0	0	1	0	0	0	0	0	0
SPC_18_11	0	0	0	4	0	0	0	0	0	0
SPC_18_12	0	0	1	0	0	0	0	0	0	0
SPC_18_13	0	0	0	0	0	0	1	0	0	0
SPC_18_14	0	0	0	0	0	0	0	0	0	0
SPC_18_15	0	0	0	0	0	0	0	0	0	0
SPC_18_16	0	0	0	0	0	0	0	0	0	0
SPC_18_17	0	0	0	0	1	0	0	0	1	0
SPC_18_18	0	0	0	1	0	1	0	2	0	0
SPC_18_19	0	0	1	0	0	0	0	0	0	0
SPC_18_20	0	0	0	0	0	0	0	0	0	0
SPC_18_21	0	1	0	0	0	0	0	0	0	0
SPC_18_22	0	1	0	1	0	0	0	0	0	0
SPC_18_23	0	0	0	0	0	0	0	1	0	0
SPC_18_24	0	1	4	0	0	0	0	0	0	0

Sample	*Dictyoclostus inflatus*	*Dictyoclostus gallatinensis*	*Dictyoclostus* sp.	*Dielasma utah?*	*Eumetria* sp.	*Hustedia texana*	*Leptaena* sp.	*Linoproductus* sp.	*Neospirifer* sp.	*Nucleospira obesa*
SPC_18_25	0	0	0	0	0	0	0	0	0	0
SPC_18_26	0	0	0	0	0	0	0	1	0	0
SPC_18_27	0	4	0	0	0	0	0	0	0	0
SPC_18_28	0	0	0	0	0	0	0	0	0	1
SPC_18_29	0	0	0	0	0	0	0	3	0	0
SPC_18_30	0	0	0	0	0	0	0	0	0	0
SPC_18_31	0	0	0	0	0	0	0	0	0	0
SPC_18_32	0	0	0	0	0	0	0	0	0	0
SPC_18_33	0	0	0	0	0	0	0	0	0	0

Sample	*Orbinaria* sp.	*Orthotetes* sp.	Orthotetid indeterminate	*Plectospira problematica*	*Productina lodgepolensis*	Productid indeterminate	Productid concentric	*Prospira* sp.	*Punctospirifer subtexta*	*Reticularia* sp.
CLR_19_01	0	0	0	1	0	0	0	0	3	0
CLR_19_02	0	0	0	0	0	0	0	0	0	0
CLR_19_03	0	0	0	0	0	0	1	0	0	0
CLR_19_04	0	0	0	0	0	0	0	1	0	0
CLR_19_05	0	0	0	0	0	0	0	0	0	0
CLR_19_06	0	0	0	0	0	0	0	0	3	0
CLR_19_07	0	0	0	0	0	0	0	0	1	0
CLR_19_08	0	0	0	0	0	0	0	0	0	0
CLR_19_09	0	0	0	0	0	0	0	0	0	0
CLR_19_10	0	0	0	0	0	0	0	0	0	0
CLR_19_11	0	0	0	0	0	0	0	0	3	0
GR_19_01	0	3	0	0	2	0	0	1	0	0
GR_19_02	0	0	0	0	0	0	0	1	0	0
GR_19_03	0	0	0	0	0	0	0	0	0	0
GR_19_04	0	0	0	0	0	0	0	0	0	0
GR_19_05	0	0	1	2	0	0	0	0	0	0
GR_19_06	0	0	0	0	0	0	0	2	0	0
GR_19_07	0	0	0	0	0	0	0	1	0	0
GR_19_08	0	2	0	1	0	0	0	0	0	0
GR_19_09	0	0	0	0	0	0	0	0	0	0
GR_19_10	0	1	0	0	3	0	0	0	0	0
GR_19_11	0	0	0	0	0	0	0	0	0	0
GR_19_12	0	0	0	0	0	0	0	0	0	0
GR_19_13	0	1	0	0	0	0	0	0	0	0
GR_19_14	0	0	0	0	0	0	0	0	0	0
GR_19_15	0	0	0	0	0	0	0	0	0	0
GR_19_16	0	0	0	0	0	0	0	0	0	0
GR_19_17	0	0	0	0	1	0	0	0	0	0
GR_19_18	0	0	0	0	0	0	0	0	0	0
GR_19_19	0	2	0	0	2	0	0	0	0	0
GR_19_20	0	1	0	0	0	0	0	0	0	0
GR_19_21	1	0	0	0	0	0	0	0	0	0
GR_19_22	0	0	0	0	0	0	0	0	0	0
GR_19_23	0	0	0	0	0	0	0	0	0	0
GR_19_24	0	0	0	0	0	0	0	0	0	0
MGC_18_01	0	1	0	0	0	0	0	0	0	0

Sample	*Orbinaria* sp.	*Orthotetes* sp.	Orthotetid indeterminate	*Plectospira problematica*	*Productina lodgepolensis*	Productid indeterminate	Productid concentric	*Prospira* sp.	*Punctospirifer subtexta*	*Reticularia* sp.
MGC_18_02	0	2	0	0	0	0	0	0	0	0
MGC_18_03	0	0	0	0	0	0	0	0	1	0
MGC_18_04	0	1	0	0	0	0	0	0	0	1
MGC_18_05	0	0	0	0	0	0	0	0	0	0
MGC_18_06	0	0	4	0	0	0	0	0	0	0
MGC_18_07	0	0	0	0	0	1	0	0	0	0
MGC_18_08	0	0	0	0	0	1	0	0	0	0
MGC_18_09	0	3	0	0	0	0	0	0	0	0
MGC_18_10	0	0	2	0	1	0	0	0	0	0
MGC_18_11	0	0	1	0	0	0	0	0	0	0
MGC_18_12	0	0	1	0	0	0	0	0	0	0
MGC_18_13	0	0	0	0	0	0	0	0	0	0
SPC_18_01	0	0	0	0	0	0	0	0	0	0
SPC_18_02	0	0	0	0	0	1	0	0	0	0
SPC_18_03	0	0	0	0	0	2	0	0	0	0
SPC_18_04	0	0	0	0	0	1	0	0	0	0
SPC_18_05	0	0	0	0	0	0	0	0	0	0
SPC_18_06	0	0	1	0	3	0	0	0	0	1
SPC_18_07	0	0	0	0	0	1	0	0	1	0
SPC_18_08	0	0	0	0	0	0	0	0	1	0
SPC_18_09	0	0	0	0	0	0	0	0	0	0
SPC_18_10	0	0	0	0	0	0	0	0	1	0
SPC_18_11	0	0	0	0	0	0	0	0	0	0
SPC_18_12	0	1	0	1	0	0	0	0	0	2
SPC_18_13	0	0	0	0	0	1	0	0	1	1
SPC_18_14	0	0	0	0	0	0	1	0	2	0
SPC_18_15	0	0	0	0	0	0	0	0	1	0
SPC_18_16	0	0	0	0	0	2	0	1	0	0
SPC_18_17	0	0	0	1	0	0	0	0	3	0
SPC_18_18	0	0	0	0	0	0	0	0	0	0
SPC_18_19	0	0	0	0	0	0	0	0	0	0
SPC_18_20	0	0	0	0	0	0	0	0	0	0
SPC_18_21	0	0	4	0	0	1	0	0	1	0
SPC_18_22	0	0	3	0	0	1	0	0	0	0
SPC_18_23	0	0	1	0	0	1	0	0	1	0
SPC_18_24	1	0	0	0	1	3	0	0	0	0

Sample	*Orbinaria* sp.	*Orthotetes* sp.	Orthotetid indeterminate	*Plectospira problematica*	*Productina lodgepolensis*	Productid indeterminate	Productid concentric	*Prospira* sp.	*Punctospirifer subtexta*	*Reticularia* sp.
SPC_18_25	0	0	0	0	0	8	0	0	0	0
SPC_18_26	0	0	0	0	0	1	0	0	1	0
SPC_18_27	0	0	2	0	0	0	0	0	0	0
SPC_18_28	0	0	0	0	0	2	0	0	0	0
SPC_18_29	0	0	1	0	0	0	0	0	0	0
SPC_18_30	0	0	0	0	0	0	0	0	0	0
SPC_18_31	0	0	0	0	0	0	0	0	0	0
SPC_18_32	0	0	0	0	0	0	0	0	0	0
SPC_18_33	0	0	0	0	0	1	0	0	0	0

Sample	*Rhipidomella* sp.	Rhynchonellid indet.	*Schellwienella inflata*	*Schizophoria compacta*	*Schuchertella chemungensis*	*Shumardella missouriensis*	*Spirifer centronatus*	*Spirifer grimesi*	Spiriferid indeterminate	*Stenoscisma* sp.
CLR_19_01	0	0	0	0	2	0	0	0	1	0
CLR_19_02	1	0	0	0	2	0	3	0	0	0
CLR_19_03	0	0	0	0	2	0	1	0	0	0
CLR_19_04	0	0	0	0	0	0	0	0	0	0
CLR_19_05	0	0	0	0	2	0	6	0	0	0
CLR_19_06	1	0	0	0	9	0	2	0	0	0
CLR_19_07	1	0	0	0	15	0	1	0	0	0
CLR_19_08	5	0	3	0	6	0	2	0	0	0
CLR_19_09	2	0	0	0	13	0	0	0	0	0
CLR_19_10	1	0	0	0	11	0	2	0	0	0
CLR_19_11	0	0	0	0	0	0	18	0	0	0
GR_19_01	0	0	0	0	0	0	0	3	0	0
GR_19_02	0	0	0	0	0	0	0	0	0	0
GR_19_03	0	0	0	0	0	0	0	0	1	0
GR_19_04	0	0	0	0	0	0	0	0	0	0
GR_19_05	3	0	0	0	0	0	0	1	0	0
GR_19_06	0	0	0	0	0	0	2	6	0	0
GR_19_07	0	0	0	0	0	0	0	0	0	0
GR_19_08	0	0	0	0	0	0	0	0	0	0
GR_19_09	0	0	0	0	0	0	0	0	1	0
GR_19_10	0	0	0	0	0	0	2	0	0	0
GR_19_11	0	0	0	0	0	0	1	0	0	0
GR_19_12	0	0	0	0	0	1	0	0	1	0
GR_19_13	0	0	0	0	0	0	0	0	0	0
GR_19_14	0	0	0	0	0	0	0	0	0	0
GR_19_15	0	0	0	0	0	0	0	0	0	0
GR_19_16	0	0	0	0	0	0	0	0	0	0
GR_19_17	0	0	0	0	0	0	0	0	0	0
GR_19_18	0	0	0	0	0	0	0	0	1	0
GR_19_19	0	0	0	0	0	0	0	1	0	0
GR_19_20	1	0	0	0	0	0	0	0	3	0
GR_19_21	0	0	0	0	0	0	1	0	0	0
GR_19_22	0	0	0	0	0	0	0	0	0	0
GR_19_23	0	0	0	0	0	0	0	0	0	0
GR_19_24	0	0	0	0	0	0	0	0	1	0
MGC_18_01	1	0	0	0	4	0	2	0	0	0

Sample	*Rhipidomella* sp.	Rhynchonellid indet.	*Schellwienella inflata*	*Schizophoria compacta*	*Schuchertella chemungensis*	*Shumardella missouriensis*	*Spirifer centronatus*	*Spirifer grimesi*	Spiriferid indeterminate	*Stenoscisma* sp.
MGC_18_02	1	0	0	0	0	0	0	0	1	0
MGC_18_03	1	0	0	0	2	0	3	0	0	0
MGC_18_04	2	0	0	1	2	0	0	0	0	0
MGC_18_05	0	0	0	0	3	0	0	0	0	0
MGC_18_06	2	0	0	0	7	0	0	0	1	0
MGC_18_07	0	0	0	0	9	0	2	0	2	0
MGC_18_08	1	0	0	0	1	0	0	0	2	0
MGC_18_09	1	0	0	0	4	0	1	0	0	0
MGC_18_10	1	0	0	0	8	0	2	0	1	0
MGC_18_11	0	0	0	0	1	0	0	0	0	0
MGC_18_12	0	0	0	0	0	0	0	0	0	0
MGC_18_13	0	0	0	0	0	0	1	0	0	0
SPC_18_01	0	0	0	0	0	0	0	0	0	0
SPC_18_02	0	0	0	0	0	0	2	0	0	0
SPC_18_03	0	0	0	0	0	0	0	0	1	0
SPC_18_04	0	0	0	0	0	0	1	0	2	0
SPC_18_05	0	0	0	0	1	0	1	0	0	0
SPC_18_06	0	0	0	0	1	0	5	0	0	0
SPC_18_07	0	0	0	0	0	0	0	1	3	0
SPC_18_08	0	0	0	0	0	0	0	0	0	0
SPC_18_09	1	0	0	1	1	0	0	0	2	0
SPC_18_10	0	0	0	0	0	0	0	0	0	0
SPC_18_11	0	0	0	0	0	0	0	0	0	0
SPC_18_12	0	0	0	0	3	0	5	0	0	0
SPC_18_13	0	1	0	0	1	0	2	0	0	0
SPC_18_14	1	0	0	0	0	0	2	0	0	0
SPC_18_15	0	0	0	0	0	0	0	0	0	0
SPC_18_16	0	0	0	0	0	0	0	0	0	0
SPC_18_17	0	1	0	0	3	0	0	0	0	0
SPC_18_18	1	3	0	0	0	1	2	0	0	0
SPC_18_19	0	1	0	0	0	0	1	0	1	1
SPC_18_20	0	0	0	0	0	0	0	0	0	0
SPC_18_21	0	0	0	0	1	0	0	0	0	0
SPC_18_22	0	0	0	0	0	0	2	0	1	0
SPC_18_23	0	0	0	0	0	0	0	0	2	0
SPC_18_24	0	0	0	0	0	0	0	0	1	0

Sample	*Rhipidomella* sp.	Rhynchonellid indet.	*Schellwienella inflata*	*Schizophoria compacta*	*Schuchertella chemungensis*	*Shumardella missouriensis*	*Spirifer centronatus*	*Spirifer grimesi*	Spiriferid indeterminate	*Stenoscisma* sp.
SPC_18_25	1	0	0	0	0	0	1	0	0	0
SPC_18_26	1	1	0	0	0	0	1	0	0	0
SPC_18_27	0	0	0	0	2	0	4	8	0	0
SPC_18_28	0	0	0	0	0	0	2	2	0	0
SPC_18_29	1	0	0	0	1	0	5	0	0	0
SPC_18_30	0	0	0	0	0	0	0	0	0	0
SPC_18_31	0	0	0	0	0	0	0	0	0	0
SPC_18_32	0	0	0	0	2	0	0	0	1	0
SPC_18_33	0	0	0	0	1	0	0	0	1	0

Sample	*Subglobosochonetes norquayensis*	*Torynifer* sp.	Coarse ribbed brachiopod	smooth brachiopod	fine ribbed brachiopod	Ribbed inflated brachiopod	Large astrophid brachiopod massive teeth	*Cheilotrypa* sp.
CLR_19_01	0	0	0	0	0	0	0	0
CLR_19_02	0	0	0	0	0	0	0	0
CLR_19_03	0	0	0	0	0	0	0	0
CLR_19_04	4	0	0	0	0	0	0	0
CLR_19_05	0	0	0	0	0	0	0	0
CLR_19_06	7	0	0	0	0	0	0	0
CLR_19_07	0	0	0	0	0	0	0	0
CLR_19_08	0	0	0	0	0	0	0	0
CLR_19_09	0	0	0	0	0	0	0	1
CLR_19_10	6	0	0	0	0	0	0	0
CLR_19_11	0	0	0	0	0	0	0	0
GR_19_01	0	0	0	0	0	0	0	0
GR_19_02	0	0	0	0	0	0	0	0
GR_19_03	0	0	0	0	0	0	0	0
GR_19_04	0	0	0	0	0	0	0	0
GR_19_05	0	0	0	0	0	0	0	0
GR_19_06	0	0	0	0	0	0	0	0
GR_19_07	0	0	0	0	0	0	0	0
GR_19_08	0	0	0	0	0	0	0	0
GR_19_09	0	0	0	0	0	0	0	0
GR_19_10	0	0	0	0	0	0	0	0
GR_19_11	0	0	0	0	0	0	0	0
GR_19_12	0	0	0	0	0	0	0	0
GR_19_13	0	0	0	0	0	0	0	0
GR_19_14	0	0	0	0	0	0	0	0
GR_19_15	0	0	0	0	0	0	0	0
GR_19_16	0	0	0	0	0	0	0	0
GR_19_17	0	0	0	0	0	0	0	0
GR_19_18	0	0	0	0	0	0	0	0
GR_19_19	0	0	0	0	0	0	0	0
GR_19_20	0	0	0	0	0	0	0	1
GR_19_21	0	0	0	0	0	0	0	0
GR_19_22	0	0	0	0	0	0	0	0
GR_19_23	0	0	0	0	0	0	0	0
GR_19_24	0	0	0	0	0	0	0	0
MGC_18_01	0	0	0	1	2	0	0	2

Sample	*Subglobosochonetes norquayensis*	*Torynifer* sp.	Coarse ribbed brachiopod	smooth brachiopod	fine ribbed brachiopod	Ribbed inflated brachiopod	Large astrophid brachiopod massive teeth	*Cheilotrypa* sp.
MGC_18_02	0	0	1	0	0	0	0	0
MGC_18_03	0	0	0	0	0	0	0	0
MGC_18_04	0	0	0	0	0	0	0	0
MGC_18_05	0	0	0	0	0	0	0	0
MGC_18_06	0	0	0	0	0	0	0	0
MGC_18_07	0	0	0	0	0	0	0	1
MGC_18_08	0	0	0	0	0	1	0	0
MGC_18_09	0	0	0	0	0	0	0	0
MGC_18_10	0	0	0	0	0	0	0	0
MGC_18_11	0	0	0	0	0	0	0	1
MGC_18_12	0	0	0	0	0	0	0	0
MGC_18_13	0	0	0	0	0	0	0	0
SPC_18_01	0	0	0	0	0	0	0	0
SPC_18_02	0	0	0	0	0	0	0	1
SPC_18_03	0	0	0	0	0	0	0	1
SPC_18_04	0	0	0	0	0	0	0	0
SPC_18_05	0	0	0	0	0	0	0	0
SPC_18_06	0	0	0	0	0	0	0	1
SPC_18_07	0	0	0	0	0	0	0	0
SPC_18_08	0	0	0	0	0	0	0	0
SPC_18_09	0	1	0	0	0	0	0	0
SPC_18_10	0	0	0	0	0	0	0	0
SPC_18_11	0	0	0	0	0	0	0	0
SPC_18_12	0	0	0	0	0	0	0	0
SPC_18_13	0	0	0	0	0	0	0	0
SPC_18_14	0	0	0	0	0	0	1	0
SPC_18_15	0	0	0	0	0	0	1	0
SPC_18_16	0	0	0	0	0	0	0	0
SPC_18_17	0	0	0	0	0	0	0	0
SPC_18_18	0	0	0	0	0	0	0	0
SPC_18_19	0	0	0	0	0	0	0	0
SPC_18_20	0	0	0	0	0	0	0	0
SPC_18_21	0	0	0	0	0	0	0	0
SPC_18_22	0	0	0	0	0	0	0	1
SPC_18_23	0	0	0	0	0	0	0	0
SPC_18_24	0	0	0	0	0	0	0	0

Sample	*Subglobosochonetes norquayensis*	*Torynifer* sp.	Coarse ribbed brachiopod	smooth brachiopod	fine ribbed brachiopod	Ribbed inflated brachiopod	Large astrophid brachiopod massive teeth	*Cheilotrypa* sp.
SPC_18_25	0	0	0	0	0	0	0	0
SPC_18_26	0	0	0	0	0	0	0	0
SPC_18_27	0	0	0	0	0	0	0	0
SPC_18_28	0	0	0	0	0	0	0	0
SPC_18_29	0	0	0	0	0	0	1	0
SPC_18_30	0	0	0	0	0	0	0	0
SPC_18_31	0	0	0	0	0	0	0	0
SPC_18_32	0	0	0	0	0	0	0	0
SPC_18_33	0	0	0	0	0	0	0	0

Sample	Fenestrate byrozoan	Rhombopora sp.	Trepostome bryozoan	*Dichocrinus bozemanensis*	*Platycrinites bozemanensis*	Crinoid calyx indeterminate	Platycrinites ossicles	Round crinoid ossicle	Large coarse ribbed crinoid ossicle
CLR_19_01	2	0	1	0	0	0	0	1	0
CLR_19_02	18	1	0	0	0	0	0	1	0
CLR_19_03	5	4	0	0	0	0	0	1	0
CLR_19_04	4	1	0	0	0	8	0	1	0
CLR_19_05	3	1	0	1	0	1	0	1	0
CLR_19_06	0	0	0	0	0	0	0	1	0
CLR_19_07	1	0	0	0	0	0	0	1	0
CLR_19_08	0	0	0	0	0	0	0	1	0
CLR_19_09	1	0	0	0	2	0	0	1	0
CLR_19_10	0	0	0	0	0	0	0	0	0
CLR_19_11	0	0	0	0	0	0	0	1	0
GR_19_01	0	0	0	0	0	0	0	1	0
GR_19_02	0	0	0	0	0	0	0	1	0
GR_19_03	0	0	0	0	0	0	0	1	0
GR_19_04	0	0	0	0	0	0	0	1	0
GR_19_05	0	0	0	0	0	0	0	1	0
GR_19_06	0	0	0	0	0	0	0	1	0
GR_19_07	0	0	0	0	0	0	0	1	0
GR_19_08	0	0	0	0	0	0	0	1	0
GR_19_09	0	0	0	0	0	0	0	1	0
GR_19_10	0	0	0	0	0	0	0	1	0
GR_19_11	0	0	0	0	0	0	0	1	0
GR_19_12	0	0	0	0	0	0	0	1	0
GR_19_13	0	0	0	0	0	0	0	1	0
GR_19_14	0	0	0	0	0	0	0	1	0
GR_19_15	0	0	0	0	0	0	0	1	0
GR_19_16	0	0	0	0	0	0	0	1	0
GR_19_17	0	0	0	0	0	0	0	1	0
GR_19_18	0	0	0	0	0	0	0	1	0
GR_19_19	0	0	0	0	0	0	0	1	0
GR_19_20	0	0	0	0	0	0	0	1	0
GR_19_21	0	0	0	0	0	0	0	1	0
GR_19_22	0	0	0	0	0	0	0	1	0
GR_19_23	0	0	0	0	0	0	0	0	0
GR_19_24	0	0	0	0	0	0	0	0	0
MGC_18_01	0	7	0	0	1	0	0	1	1

Sample	Fenestrate byrozoan	Rhombopora sp.	Trepostome bryozoan	*Dichocrinus bozemanensis*	*Platycrinites bozemanensis*	Crinoid calyx indeterminate	Platycrinites ossicles	Round crinoid ossicle	Large coarse ribbed crinoid ossicle
MGC_18_02	0	0	0	0	0	1	0	1	0
MGC_18_03	0	3	0	0	2	3	0	1	0
MGC_18_04	0	0	0	0	0	1	1	1	0
MGC_18_05	0	1	0	0	0	0	1	1	0
MGC_18_06	0	1	0	0	0	0	1	1	0
MGC_18_07	1	1	0	0	0	0	1	1	0
MGC_18_08	0	0	0	0	0	0	0	0	0
MGC_18_09	0	0	0	0	0	1	1	1	0
MGC_18_10	0	0	0	0	0	0	1	1	0
MGC_18_11	0	4	0	0	0	0	0	1	0
MGC_18_12	0	1	0	0	0	0	0	1	0
MGC_18_13	1	0	1	0	0	0	0	1	0
SPC_18_01	0	0	0	0	0	0	0	1	0
SPC_18_02	0	1	0	0	0	0	0	1	0
SPC_18_03	0	0	0	0	0	0	0	0	0
SPC_18_04	0	0	0	0	0	0	0	1	0
SPC_18_05	0	0	0	0	0	0	0	0	0
SPC_18_06	5	3	0	0	0	0	1	1	0
SPC_18_07	0	0	0	0	0	0	0	1	0
SPC_18_08	0	0	0	0	0	0	1	1	0
SPC_18_09	0	0	0	0	0	0	0	1	0
SPC_18_10	0	0	0	0	1	0	0	1	0
SPC_18_11	0	0	0	0	0	0	0	1	0
SPC_18_12	0	0	0	0	0	0	0	1	0
SPC_18_13	0	0	0	0	0	0	1	1	0
SPC_18_14	0	0	0	0	0	0	0	1	0
SPC_18_15	0	0	0	0	0	0	0	0	0
SPC_18_16	0	0	0	0	0	0	0	0	0
SPC_18_17	0	1	0	0	0	1	1	0	0
SPC_18_18	0	0	0	0	0	0	0	1	0
SPC_18_19	0	0	0	0	0	0	0	0	0
SPC_18_20	0	0	0	0	0	0	0	0	0
SPC_18_21	0	0	0	0	0	1	0	1	0
SPC_18_22	0	0	0	0	0	0	0	0	0
SPC_18_23	0	0	0	0	0	0	0	0	0
SPC_18_24	0	0	0	0	0	0	0	1	0

Sample	Fenestrate byrozoan	Rhombopora sp.	Trepostome bryozoan	*Dichocrinus bozemanensis*	*Platycrinites bozemanensis*	Crinoid calyx indeterminate	Platycrinites ossicles	Round crinoid ossicle	Large coarse ribbed crinoid ossicle
SPC_18_25	0	0	0	0	0	0	0	0	0
SPC_18_26	0	0	0	0	0	0	0	1	0
SPC_18_27	0	0	0	0	0	0	0	1	0
SPC_18_28	0	0	0	0	0	0	0	0	0
SPC_18_29	0	0	0	0	0	0	0	0	0
SPC_18_30	0	1	0	0	0	0	0	1	0
SPC_18_31	0	0	0	0	0	0	0	0	0
SPC_18_32	0	0	0	0	0	0	0	1	0
SPC_18_33	0	0	0	0	0	0	0	1	0

Sample	Spoked crinoid ossicle	Hexagonal crinoid ossicle	Elliptical crinoid ossicle	Star hole crinoid ossicle	*Grammysia welleri*	*Edmondia* sp.	Bivalve indeterminate	Elongate bivalve	*Euomphalus* sp.
CLR_19_01	0	0	1	0	0	0	0	0	0
CLR_19_02	0	0	0	0	0	0	0	0	0
CLR_19_03	0	0	0	0	0	0	0	0	0
CLR_19_04	0	0	1	0	0	0	0	0	0
CLR_19_05	0	0	1	0	0	0	0	0	0
CLR_19_06	0	0	1	0	0	0	0	0	0
CLR_19_07	0	0	0	0	0	0	0	0	0
CLR_19_08	0	0	0	0	0	0	0	0	0
CLR_19_09	0	0	1	0	0	0	0	0	0
CLR_19_10	0	0	0	0	0	0	0	0	0
CLR_19_11	0	0	1	0	0	0	0	0	0
GR_19_01	0	0	1	1	0	0	0	0	0
GR_19_02	0	0	1	0	0	0	0	0	0
GR_19_03	0	0	0	0	0	0	0	0	0
GR_19_04	0	0	1	0	0	0	0	0	0
GR_19_05	0	0	1	0	0	0	0	0	0
GR_19_06	0	0	0	0	0	0	0	0	0
GR_19_07	0	0	1	0	0	0	0	0	0
GR_19_08	0	0	0	0	0	0	0	0	0
GR_19_09	0	0	1	0	0	0	0	0	0
GR_19_10	0	0	1	1	1	0	0	0	0
GR_19_11	0	0	1	0	0	0	0	0	0
GR_19_12	0	0	1	0	0	0	0	0	0
GR_19_13	0	0	1	0	0	0	0	0	0
GR_19_14	0	0	1	0	0	0	0	0	0
GR_19_15	0	0	1	0	0	0	0	0	0
GR_19_16	0	0	1	0	0	0	0	0	0
GR_19_17	0	0	1	0	0	0	0	0	0
GR_19_18	0	0	1	0	0	0	0	0	0
GR_19_19	0	0	0	0	0	0	0	0	0
GR_19_20	0	0	0	0	0	0	0	0	0
GR_19_21	0	0	0	0	0	0	0	0	0
GR_19_22	0	0	0	0	0	0	0	0	0
GR_19_23	0	0	0	0	0	0	0	0	0
GR_19_24	0	0	0	0	0	0	0	0	0
MGC_18_01	0	0	0	0	0	0	0	0	0

Sample	Spoked crinoid ossicle	Hexagonal crinoid ossicle	Elliptical crinoid ossicle	Star hole crinoid ossicle	*Grammysia welleri*	*Edmondia* sp.	Bivalve indeterminate	Elongate bivalve	*Euomphalus* sp.
MGC_18_02	0	0	1	0	0	0	0	1	1
MGC_18_03	0	0	0	0	0	0	0	0	0
MGC_18_04	0	0	0	0	0	0	0	0	0
MGC_18_05	0	0	0	0	3	0	1	0	0
MGC_18_06	0	0	1	0	0	0	0	0	0
MGC_18_07	0	0	0	0	0	0	0	0	0
MGC_18_08	0	0	0	0	0	1	0	0	0
MGC_18_09	0	0	0	0	0	0	0	0	0
MGC_18_10	0	0	1	0	0	0	0	0	0
MGC_18_11	0	0	0	0	0	0	0	0	0
MGC_18_12	0	0	0	0	0	0	0	0	0
MGC_18_13	0	0	1	0	0	0	0	0	0
SPC_18_01	0	0	0	0	0	0	0	0	0
SPC_18_02	0	0	0	0	0	0	0	0	0
SPC_18_03	0	0	0	0	0	0	0	0	0
SPC_18_04	0	0	1	0	2	0	0	0	0
SPC_18_05	0	0	0	0	0	0	0	0	0
SPC_18_06	1	0	1	0	0	0	0	0	0
SPC_18_07	0	0	0	0	0	0	0	0	0
SPC_18_08	0	0	0	0	0	0	0	0	0
SPC_18_09	0	0	1	0	0	0	0	0	0
SPC_18_10	0	0	0	0	0	0	0	0	0
SPC_18_11	0	0	0	0	0	0	0	0	0
SPC_18_12	0	0	1	0	0	0	0	0	0
SPC_18_13	0	0	1	0	0	0	0	0	0
SPC_18_14	0	0	0	0	0	0	0	0	0
SPC_18_15	0	0	0	0	0	0	0	0	0
SPC_18_16	0	0	0	0	0	0	0	0	0
SPC_18_17	1	1	0	0	0	1	0	0	0
SPC_18_18	0	1	0	0	0	0	0	0	0
SPC_18_19	0	0	0	0	0	0	0	0	0
SPC_18_20	0	0	0	0	0	0	0	0	0
SPC_18_21	0	1	1	0	0	0	0	0	0
SPC_18_22	0	0	0	0	0	0	0	0	0
SPC_18_23	0	0	0	0	0	0	0	0	0
SPC_18_24	0	0	0	0	0	0	0	0	0

Sample	Spoked crinoid ossicle	Hexagonal crinoid ossicle	Elliptical crinoid ossicle	Star hole crinoid ossicle	*Grammysia welleri*	*Edmondia* sp.	Bivalve indeterminate	Elongate bivalve	*Euomphalus* sp.
SPC_18_25	0	0	0	0	0	0	0	0	0
SPC_18_26	0	0	0	0	0	0	0	0	6
SPC_18_27	0	0	0	0	0	0	0	0	0
SPC_18_28	0	0	0	0	0	0	0	0	0
SPC_18_29	0	0	1	0	0	0	0	0	1
SPC_18_30	0	0	0	0	0	0	0	0	0
SPC_18_31	0	0	0	0	0	0	0	0	0
SPC_18_32	0	0	0	0	0	0	0	0	0
SPC_18_33	0	0	1	0	0	0	0	0	0

Sample	*Loxonema* sp.	*Platyceras* sp.	*Straparollus* sp.	Cephalopod indeterminate
CLR_19_01	0	0	0	0
CLR_19_02	0	0	0	0
CLR_19_03	0	0	0	0
CLR_19_04	0	1	0	0
CLR_19_05	0	0	0	0
CLR_19_06	0	1	0	0
CLR_19_07	0	0	0	0
CLR_19_08	0	1	0	0
CLR_19_09	0	0	0	0
CLR_19_10	0	1	0	0
CLR_19_11	0	0	0	0
GR_19_01	0	0	0	0
GR_19_02	0	0	0	0
GR_19_03	0	0	0	0
GR_19_04	0	0	0	0
GR_19_05	0	0	0	0
GR_19_06	0	0	0	0
GR_19_07	0	0	0	0
GR_19_08	0	0	0	0
GR_19_09	0	0	0	0
GR_19_10	0	0	0	0
GR_19_11	0	0	0	0
GR_19_12	0	0	0	0
GR_19_13	0	0	0	0
GR_19_14	0	0	0	0
GR_19_15	0	0	0	0
GR_19_16	0	0	0	0
GR_19_17	0	0	0	0
GR_19_18	0	0	0	0
GR_19_19	0	0	0	0
GR_19_20	0	0	0	0
GR_19_21	0	0	0	0
GR_19_22	0	0	0	0
GR_19_23	0	0	0	0
GR_19_24	0	0	0	0
MGC_18_01	0	0	0	0

Sample	*Loxonema* sp.	*Platyceras* sp.	*Straparollus* sp.	Cephalopod indeterminate
MGC_18_02	0	4	3	0
MGC_18_03	0	0	0	0
MGC_18_04	0	0	0	0
MGC_18_05	0	0	0	0
MGC_18_06	0	0	0	1
MGC_18_07	0	0	0	0
MGC_18_08	0	0	0	0
MGC_18_09	0	2	1	0
MGC_18_10	0	0	0	0
MGC_18_11	0	0	0	0
MGC_18_12	0	0	0	0
MGC_18_13	0	0	0	0
SPC_18_01	0	0	0	0
SPC_18_02	0	0	0	0
SPC_18_03	0	0	0	0
SPC_18_04	0	0	0	0
SPC_18_05	1	0	0	0
SPC_18_06	0	0	0	0
SPC_18_07	0	0	0	0
SPC_18_08	1	0	0	0
SPC_18_09	0	0	0	0
SPC_18_10	0	0	0	0
SPC_18_11	0	1	0	0
SPC_18_12	0	1	1	0
SPC_18_13	0	1	0	0
SPC_18_14	0	0	0	0
SPC_18_15	0	0	0	0
SPC_18_16	0	0	0	0
SPC_18_17	0	0	0	0
SPC_18_18	0	3	1	0
SPC_18_19	0	0	0	0
SPC_18_20	0	0	0	0
SPC_18_21	0	2	0	0
SPC_18_22	0	0	0	0
SPC_18_23	0	0	0	0
SPC_18_24	0	0	0	0

Sample	*Loxonema* sp.	*Platyceras* sp.	*Straparollus* sp.	Cephalopod indeterminate
SPC_18_25	0	0	0	0
SPC_18_26	1	0	0	0
SPC_18_27	0	0	0	0
SPC_18_28	0	0	0	0
SPC_18_29	1	0	2	0
SPC_18_30	0	0	0	0
SPC_18_31	0	0	0	0
SPC_18_32	0	0	0	0
SPC_18_33	0	0	0	1

Part 4: R Code to Analyze Data and Produce Figures

```
#add needed libraries
library(vegan)
library(sparcl)
library(cluster)
library(pheatmap)

#read faunal data
data<-read.csv("Lodgepole Faunal Data 2019.csv", row.names=1,
header=TRUE)

#read taxa characters
taxdata<-read.csv("Taxa characters 2019.csv", header=TRUE)


faunalData<-data[, 18:101]
env<-data[, 1:17]

#Cull faunal data to remove rare taxa
culledTaxa<- which(colSums(faunalData)/sum(faunalData) >0.01) #grabs
subset of taxa that are less than 1% of aggregate count
culledFaunalData<-faunalData[ , culledTaxa]
culledTaxProp<-taxdata[culledTaxa, ] #matches taxa property matrix with
my culled matrix

#Culled Faunal Data Transformations
cpropsamp<-decostand(culledFaunalData,"total")
cpropsampmax<-decostand(cpropsamp,"max")

#Culled Faunal Distances
cBraypropsamp<-vegdist(cpropsamp,method="bray",diag=TRUE)
cBraypropsampmax<-vegdist(cpropsampmax, method= "bray", diag=TRUE)

#Culled Faunal Cluster Analysis
cCluster<-agnes(cBraypropsamp, method="ward")
dev.new()
plot(cCluster,which.plots=2,cex=1,hang=-0.1)
par(las = 1, lwd= 2)
plot(cCluster,which.plots=2,cex=1,hang=-0.1, main= "", sub="")

cTaxaData <- t(culledFaunalData)
cTaxaStand <- decostand(cTaxaData, method = "total")
cTaxaStand<- decostand(cTaxaStand, method = "max")
cTaxaDist <- vegdist(cTaxaStand, "bray", diag = TRUE)
cTaxacluster<-agnes(cTaxaDist,method="ward")

dev.new()
plot(cTaxacluster,which.plots=2,cex=1,hang=-0.1, main= "", sub="")

dev.new()
plot(cTaxacluster,which.plots=2,cex=0.8,hang=-0.1)
```

```
#Culled twoway using pheatmap
myBreaks <- seq(0.01, max(cpropsamp), by = .01) # you can set your
breaks to any sequence you want, and they don't have to be the same
length.  You can do this manually too.

myBreaks <- c(0, 0.000001, myBreaks) # here we added a 0 to .000001 bin
to the heatmap, making this bin essentially 0.

myColors <- gray.colors(length(myBreaks) - 1, start= 0.9, end= 0.0) #
here grayscale function to create a vector of colors. 0 equals black
and 1 equals white.  It is important that this vector is one element
less than the myBreaks vector

myColors <- c("white", myColors) # now we can add "white" onto the
vector, this will be the first color bin, which we're going to set to
be (essentially) 0.

pheatmap(cpropsamp) # general function, with no custom colors. Note
that values of '0' get a color on the color bar. This makes it
difficult to distinguish a 0 from a non-zero, but small relative
abundance value
pheatmap(cpropsamp, color = myColors, breaks = myBreaks) # general
function using our breaks. This allows us to set the '0' cells to be
white

pheatmap(cpropsamp, color = myColors, breaks = myBreaks,
clustering_method = "ward") #here we use ward's method using the
argument clustering_method = "ward" and a bray-curstis distance by
specifying the Q and R mode distance matricies

pheatmap(cpropsamp, color = myColors, breaks = myBreaks,
clustering_method = "ward", clustering_distance_rows = cBraypropsamp,
clustering_distance_cols = cTaxaDist, border_color = NA) # here we fed
the function a distance matrix we wanted to use.  myDist and myTaxaDist
both are distance matricies that were made by vegdist (bray-curtis
distances).

#Culled point counts to remove components that are less than 5% of the
aggregate
culledPC<- pointCounts[ , which(colSums(pointCounts) > 5)]

#culledPC Distances
brayCulledPC<- vegdist(culledPC, method="bray", diag = TRUE)
culledPcCluster<-agnes(brayCulledPC, method="ward")

dev.new()
par(las = 1, lwd= 2)
plot(culledPcCluster,which.plots=2,cex=1,hang=-0.1, main= "", sub="")

grains <- t(culledPC)
grainsStand <- decostand(grains, method = "total")
grainsStand <- decostand(grainsStand, method = "max")
grainsDist <- vegdist(grainsStand, method='bray', diag = TRUE)

grainClust<- agnes(grainsDist, method="ward")
```

```
dev.new()
par(las = 1, lwd= 2)
plot(grainClust,which.plots=2,cex=1,hang=-0.1, main= "", sub="")
#two-way cluster of point counts
myBreaks <- seq(0.01, max(culledPC), by = .01) # you can set your
breaks to any sequence you want, and they don't have to be the same
length.  You can do this manually too.

myBreaks <- c(0, 0.000001, myBreaks) # here we added a 0 to .000001 bin
to the heatmap, making this bin essentially 0.

myColors <- gray.colors(length(myBreaks) - 1, start= 0.9, end= 0.0) #
here grayscale function to create a vector of colors. 0 equals black
and 1 equals white.  It is important that this vector is one element
less than the myBreaks vector

myColors <- c("white", myColors) # now we can add "white" onto the
vector, this will be the first color bin, which we're going to set to
be (essentially) 0.

pheatmap(culledPC) # general function, with no custom colors. Note that
values of '0' get a color on the color bar. This makes it difficult to
distinguish a 0 from a non-zero, but small relative abundance value

pheatmap(culledPC, color = myColors, breaks = myBreaks) # general
function using our breaks. This allows us to set the '0' cells to be
white

pheatmap(culledPC, color = myColors, breaks = myBreaks,
clustering_method = "ward") #here we use ward's method using the
argument clustering_method = "ward" and a bray-curstis distance by
specifying the Q and R mode distance matricies

pheatmap(culledPC, color = myColors, breaks = myBreaks,
clustering_method = "ward", clustering_distance_rows = brayCulledPC,
clustering_distance_cols = grainsDist, border_color = NA) # here we fed
the function a distance matrix we wanted to use.  myDist and myTaxaDist
both are distance matricies that were made by vegdist (bray-curtis
distances).


#culled NMDS
cNMDSk1<- metaMDS(cpropsamp, distance = "bray", k=1, trymax = 50,
autotransform = FALSE)
#stress = 0.336

cNMDSk2<- metaMDS(cpropsamp, distance = "bray", k=2, trymax = 50,
autotransform = FALSE)
#stress = 0.200

cNMDSk3<- metaMDS(cpropsamp, distance = "bray", k=3, trymax = 50,
autotransform = FALSE)
#stress = 0.146
```

```
cNMDSk4<- metaMDS(cpropsamp, distance = "bray", k=4, trymax = 50,
autotransform = FALSE)
#stress = 0.114

cNMDSk5<- metaMDS(cpropsamp, distance = "bray", k=5, trymax = 50,
autotransform = FALSE)
#stress = 0.095

dev.new()
barplot(c(0.336, 0.200, 0.146, 0.114, 0.095))

#Pull out sample and taxa scores using 3 dimensions
nms1<-scores(cNMDSk3, display="sites", choices=1)
nms2<-scores(cNMDSk3, display="sites", choices=2)
nms3<-scores(cNMDSk3, display="sites", choices=3)

taxNms1<-scores(cNMDSk3, display="species", choices=1)
taxNms2<-scores(cNMDSk3, display="species", choices=2)
taxNms3<-scores(cNMDSk3, display="species", choices=3)



#Create a new matrix using all point count and environment variables
rownames(env)<-env$Sample.Name
variables<-env[ , c(1,13:17)]

culledPC$Sample.Names<-rownames(culledPC)


library(colorscience)
variables$huedeg<- huedegree(variables$hue)# transforms the Munsell hue
from a category to a number around a unit circle

allvars<- merge(culledPC, variables, by="row.names")
rownames(allvars)<- allvars$Row.names
allvars<- allvars[ , c(2:15, 18, 21, 23)]

#Use the envfit function to correlate environmental variables with
samples in the ordination space
cEnvf12<- envfit(ord = cNMDSk3, env = allvars, choices= c(1,2))

#Samples within the ordination space color coded by systems tract
dev.new()
plot(cNMDSk3, type="n", las=1)
points(nms1[env$Sequence == "LST"], nms2[env$Sequence == "LST"], pch =
21, col= "black", bg= "red", cex= 2)
points(nms1[env$Sequence == "TST"], nms2[env$Sequence == "TST"], pch =
21, col= "black", bg= "dodgerblue", cex= 2)
points(nms1[env$Sequence == "HST"], nms2[env$Sequence == "HST"], pch =
21, col= "black", bg= "gray", cex= 2)
text(x= -1, y= -1, labels = "LST", col= "red", cex=1.7)
text(x= -1, y= 0.5, labels = "TST", col="dodgerblue", cex=1.7)
text(x= 1, y= 0.5, labels= "HST", col="gray", cex=1.7)
```

```
#Samples within ordination space color coded by facies
dev.new()
plot(cNMDSk3, type="n", las=1, xlim=c(-2,2), ylim= c(-2,2))
points(nms1[env$Facies == "DS"], nms2[env$Facies == "DS"], pch = 21,
col= "black", bg= "darkblue", cex= 1.5)
points(nms1[env$Facies == "FS"], nms2[env$Facies == "FS"], pch = 21,
col= "black", bg= "dodgerblue", cex= 1.5)
points(nms1[env$Facies == "OS"], nms2[env$Facies == "OS"], pch = 21,
col= "black", bg= "cyan", cex= 1.5)
text(x= -1, y= -0.2, labels = "Deep Subtidal", col= "darkblue",
cex=1.7)
text(x= 1.5, y= 0, labels = "Foreshoal", col="dodgerblue", cex=1.7)
text(x= 0, y= -1, labels= "Ooid Shoal", col="cyan", cex=1.7)

#Plot of species within ordination space color coded by class
dev.new()
plot(cNMDSk3, type="n", las=1, xlim=c(-2,2), ylim= c(-2,2))
text(taxNms1[culledTaxProp$Class == "Anthozoa"],
taxNms2[culledTaxProp$Class == "Anthozoa"], col= "red4", labels=
culledTaxProp$Abbrev[culledTaxProp$Class == "Anthozoa"])
text(taxNms1[culledTaxProp$Class == "Rhynchonellata"],
taxNms2[culledTaxProp$Class == "Rhynchonellata"], col= "purple",
labels= culledTaxProp$Abbrev[culledTaxProp$Class == "Rhynchonellata"])
text(taxNms1[culledTaxProp$Class == "Strophomenata"],
taxNms2[culledTaxProp$Class == "Strophomenata"], col= "royalblue",
labels= culledTaxProp$Abbrev[culledTaxProp$Class == "Strophomenata"])
text(taxNms1[culledTaxProp$Group == c("bryozoan", "crinoid")],
taxNms2[culledTaxProp$Group == c("bryozoan", "crinoid")], col=
"gray30", labels= culledTaxProp$Abbrev[culledTaxProp$Group ==
c("bryozoan", "crinoid")])

#Biplot of environmental variables within the ordination space
dev.new()
plot(cNMDSk3, type="n", las=1, xlim=c(-2,2), ylim= c(-2,2))
plot(cEnvf12, col= "black")
```

Part 5: Taxonomic Monograph for the lower Madison Group

This is not a complete list of all species identified. Only species for which I was able to get a clear photograph are included.

Plate 1

Crinoids

A. *Dichocrinus bozemanensis* (Sample CLR-19-05)

B. *Platycrinites bozemanensis* (Sample MGC-18-01)

C. *Platycrinites bozemanensis* (Sample CLR-19-05)

D. Recrystallized crinoid (From Milligan Canyon)

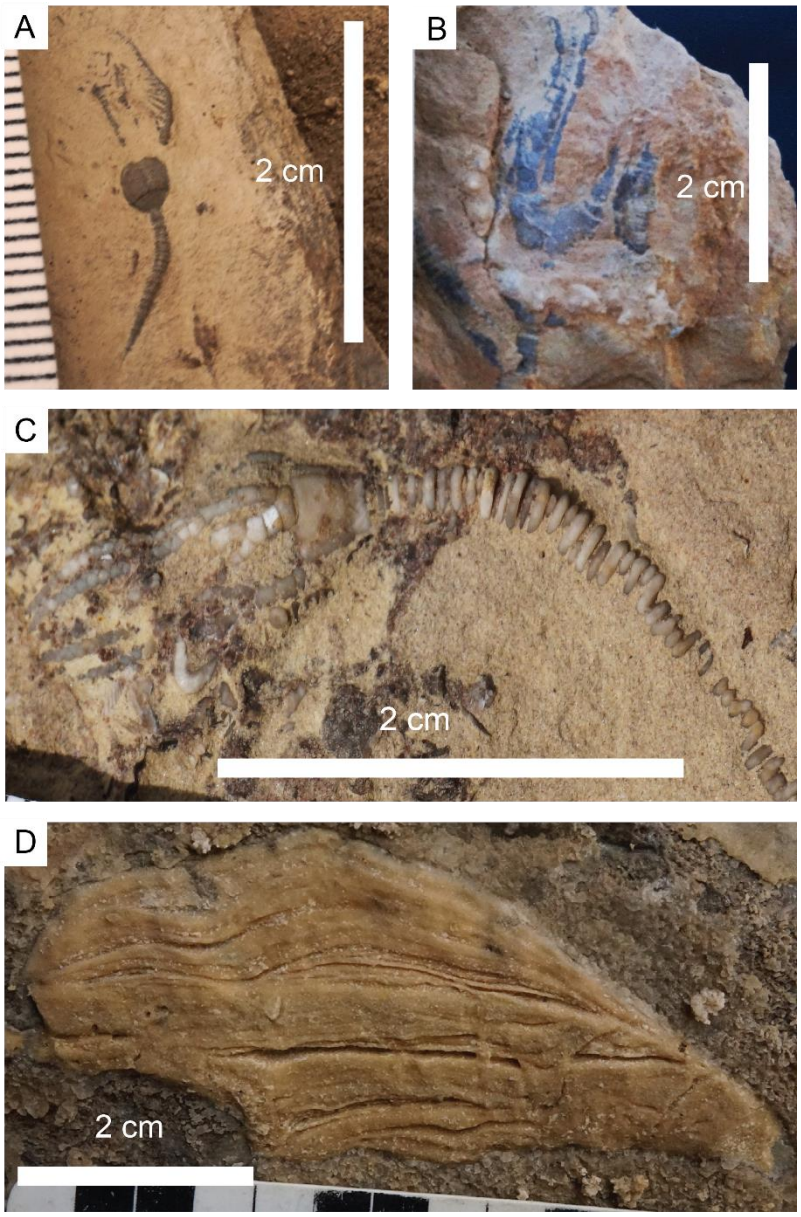

Plate 1

Plate 2

Solitary Corals

A. *Cyathaxonia arcuata* (Gibson Reservoir)

B. *Zaphrentites* sp. (Sappington Canyon)

C. *Rylstonia* sp. cluster (Gibson Reservoir)

D. *Vesiculophyllum* sp. (Milligan Canyon)

E. *Menophyllum* sp. (Gibson Reservoir)

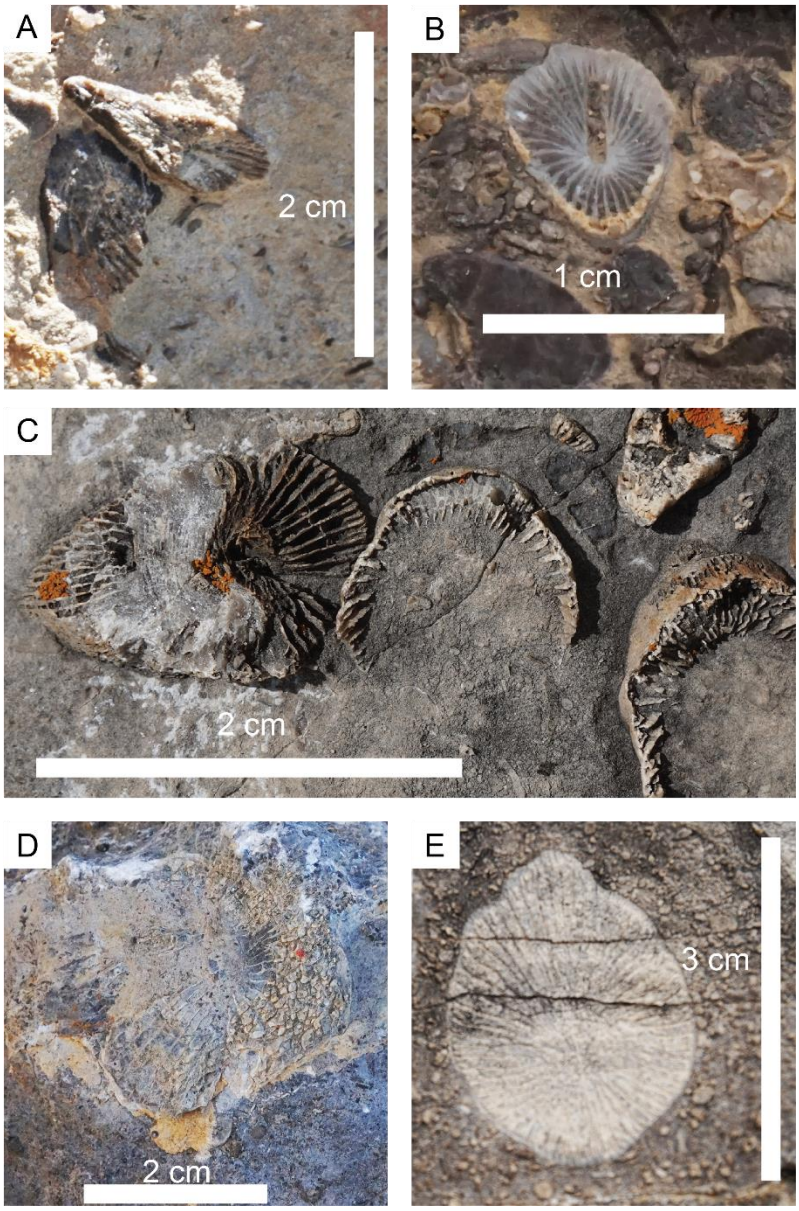

Plate 2

Plate 3

Colonial corals

A. *Cleistopora placenta* (Sample GR-19-09)
B. *Syringopora aculeata* (Milligan Canyon)

Bryozoan

C. Fenestrate Bryozoan
D. Fenestrate Bryozoan (Crystal Lake)

Gastropods

E. *Loxonema* sp. (Sample SPC-18-02)
F. Recrystallized *Straparollus* sp. (Sample MGC-18-09)

Trilobite

G. Proetid trilobite pygidium (Sample CLR-19-05)

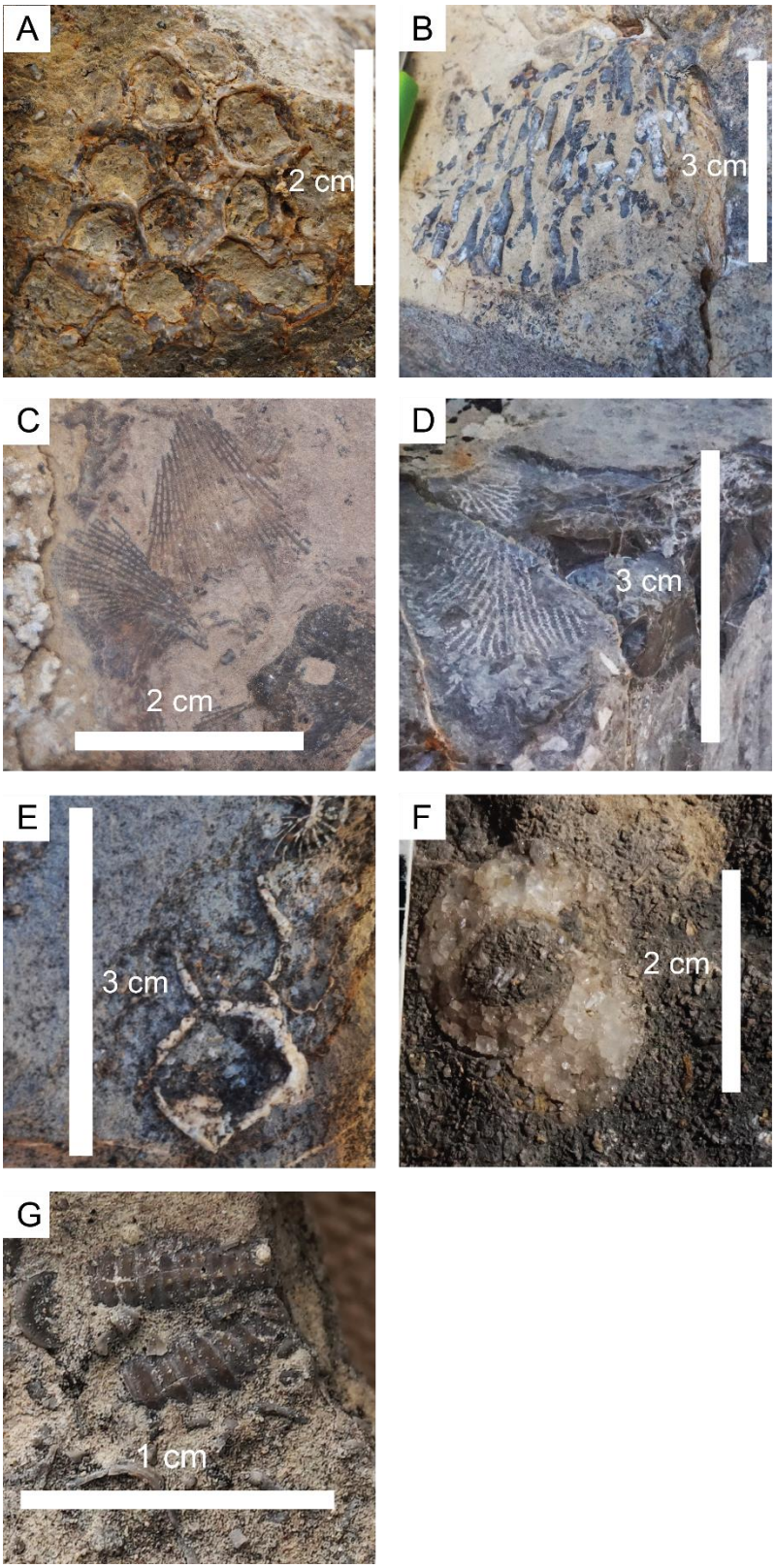

Plate 3

Plate 4
Brachiopods
Spririferids

A. *Spirifer grimsei* (Sample SPC-18-27)
B. *Spirifer centronatus* (Sample SPC-18-05)
C. *Punctospirifer subtexta* (Sample SPC-18-08)

Productids

D. *Productina lodgepolensis* (Sample GR-19-01)
E. *Leptaena* sp. (Sample GR-19-01)

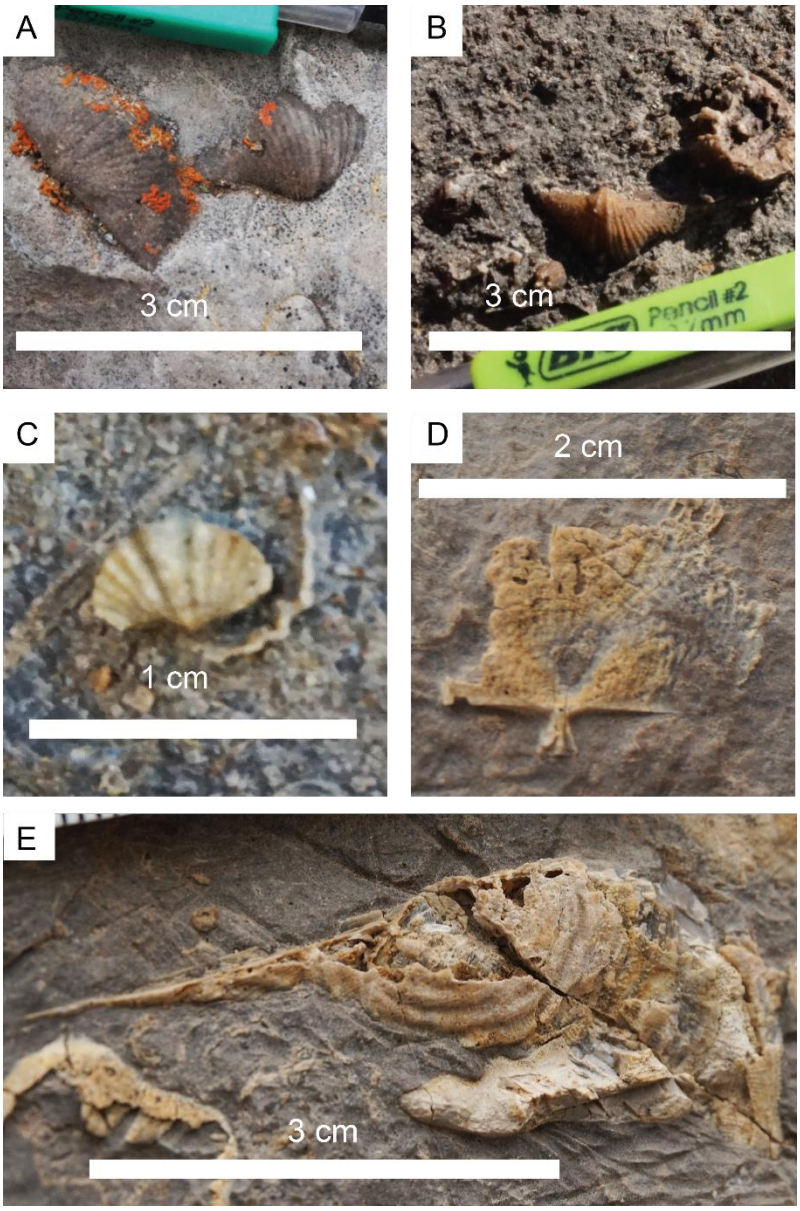

Plate 4

Plate 5
Brachiopods

A. *Orthotetes* sp. (Sample GR-19-19)
B. *Schuchertella chemungensis* (Milligan Canyon)
C. *Composita humilis* (Sample SPC-18-08)
D. *Atrypa* sp? (Sample GR-19-16)
E. *Nucleospira obesa* (Sample MGC-18-13)

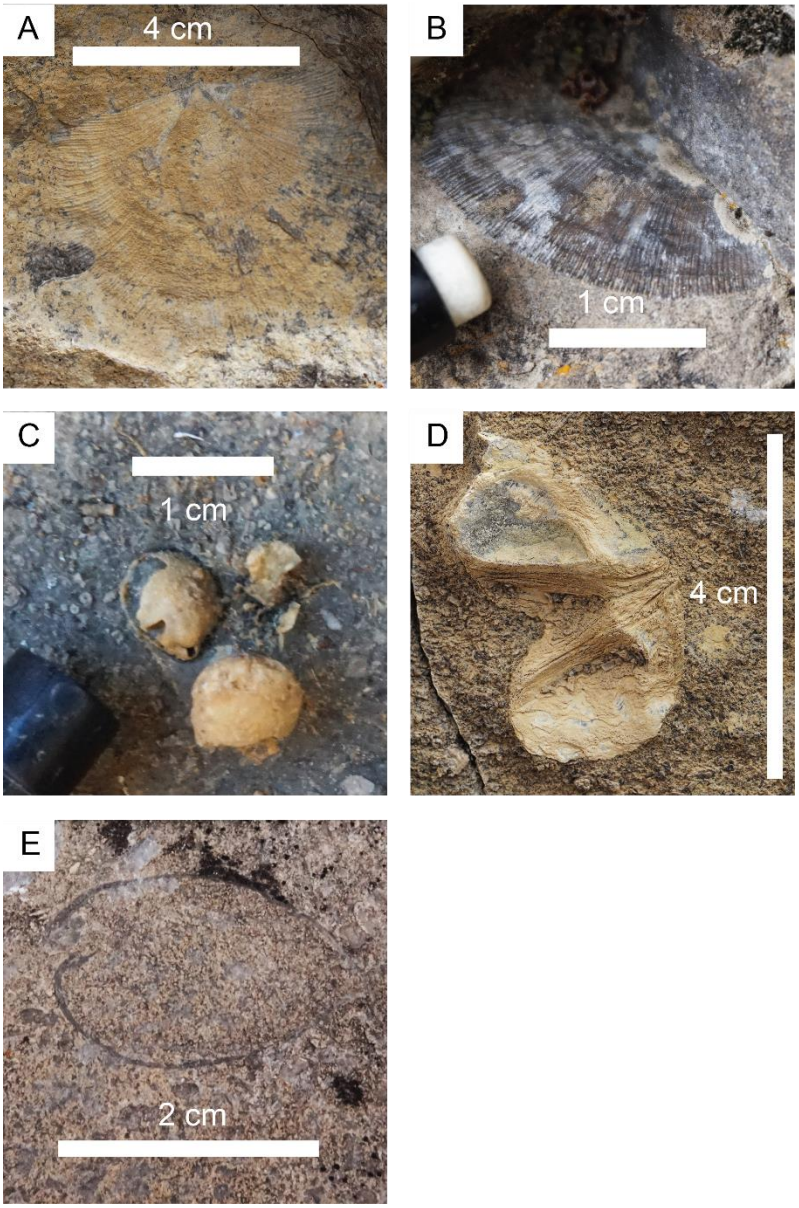

Plate 5